SYNTHESIS AND KINETIC STUDIES OF Pd(II), Pt(II) AND Ru(II) POLYPYRIDINE MONOAQUA COMPLEXES

By

Felicia Tiba B.Sc. (Hons), Natal

A thesis submitted in partial fulfillment of the requirements for the degree of Master of Science in the Faculty of Science, University of Natal, Pietermaritzburg

School of Chemical and Physical Sciences
University of Natal
Pietermaritzburg
October 2003

DECLARATION

I hereby certify that this thesis is the result of my original investigation, which has not been submitted in the fulfillment of any degree in any University.

F.Tiba

We hereby certify that this statement is correct.

Dr D. Jaganyi
(Supervisor)

Dr O. Q. Munro
(Co-Supervisor)

School of Chemical and Physical Sciences
University of Natal
Pietermaritzburg
October 2003

ACKNOWLEDGEMENTS

I would like to express my sincere gratitude to my supervisor Dr D. Jaganyi for his articulated ideas, constant guidance, patience and encouragement throughout the course of this investigation.

I also wish to extended my heartfelt appreciation to:

Dr Q. O. Munro for his invaluable input and assistance with all X-ray structure determinations that are presented in this work.

Mr Martin Watson and Mr Craig Grimmer for their timeous assistance in obtaining and interpreting the NMR spectra reported in this investigation.

Messrs. Dave Crawley, Hashim Desai and Shawn Ball for their considerable technical expertise.

Mr Paul Forder for constructing, assembling and maintaining the vacuum line used during the course of investigation.

Dr C. Southway, Trish Salagaram, and Desigan Reddy for the effort they put into proof-reading this thesis.

National Research Foundation (NRF) and De Beers for financial assistance.

All the research students, whose jovial nature, encouragement and earnest discussions throughout the years were much appreciated.

My family and friends, to whom I am eternally grateful for all their love, patience and guidance. Thank You.

ABSTRACT

The thesis is divided into three parts. The first part looks at the reactivity difference between $[Pt(terpy)(OH_2)]^{2+}$ and $[Pt(bpma)(OH_2)]^{2+}$ where terpy is 2,2':6',2"-terpyridine and bpma is *bis*(2-pyridylmethyl)amine, towards thiols namely, L-cysteine, DL-penicillamine and glutathione. This is followed by a comparative study of $[Pt(bpma)(OH_2)]^{2+}$ and $[Pd(bpma)(OH_2)]^{2+}$. Finally the reactivity differences between $[Ru(terpy)(bipy)(OH_2)]^{2+}$ and $[Ru(terpy)(tmen)(OH_2)]^{2+}$ are reported. Included are the synthesis and characterization of the complexes.

The substitution behaviour of $[Pt(terpy)(OH_2)]^{2+}$ and $[Pt(bpma)(OH_2)]^{2+}$ was studied as a function of entering thiol concentration and temperature. The reactions between the Pt-complexes and DL-penicillamine, L-cysteine and glutathione were carried out in a 0.10 mol dm^{-3} aqueous perchloric acid medium using stopped-flow or conventional UV-Vis spectrophotometry as required. The observed pseudo-first-order rate constants for the substitution reactions are given by $k_{obs} = k_2[thiol] + k_{-2}$. The k_{-2} term represents the reverse solvolysis reaction. This term was found to be zero for Pt^{II}(terpy) which was the most reactive complex. The second-order rate constants, k_2, for the three thiols varied between 0.107±0.001 $M^{-1} s^{-1}$ and 0.517±0.025 $M^{-1} s^{-1}$ for Pt^{II}(bpma) and 10.7±0.7 $M^{-1} s^{-1}$ to 711.9±18.3 $M^{-1} s^{-1}$ for Pt^{II}(terpy), with glutathione being the strongest nucleophile. Analysis of the activation parameters, $\Delta H^{\neq}$ and $\Delta S^{\neq}$, clearly shows that the substitution process is associative in nature.

The second study has looked at the substitution of the coordinated water molecule from $[Pt(bpma)(OH_2)]^{2+}$ and $[Pd(bpma)(OH_2)]^{2+}$ by a series of nucleophiles [Nu] *viz.* TU, DMTU, TMTU and as well as Br^-, Cl^-, SCN^-, and I^- for the Pt^{II}(bpma) complex. The investigation was conducted under pseudo-first-order conditions as a function of concentration of [Nu] as well as temperature for Pt^{II}(bpma) complex using stopped flow spectrophotometry. Reactions involving Pd^{II}(bpma) were done at 10 °C. The observed pseudo-first-order rate constants obeyed the equation $k_{obs} = k_2[Nu]$. The second-order rate

constants, k_2, at 10 °C for the sulfur donor nucleophiles have been found to vary between 70.35 $M^{-1} s^{-1}$ and 223.06 $M^{-1} s^{-1}$ for Pt^{II}(bpma) and (1.24 ± 0.01) x 10^5 $M^{-1} s^{-1}$ to (2.17 ± 0.02) x 10^5 $M^{-1}s^{-1}$ for Pd^{II}(terpy), with DMTU being the strongest nucleophile. The second-order rate constant, k_2, at 25 °C for Pt^{II}(terpy) was found to increase in the following order Cl^- < Br^- < TMTU < SCN^- < TU < DMTU < I^-. This order is in agreement with the polarizability of the nucleophiles, the nucleophilic discrimination factor being 0.38. The temperature studies for Pt^{II}(bpma) suggest that the substitution process is associative in nature.

The third part looked at the reactivities of $[Ru(terpy)(bipy)(OH_2)]^{2+}$ and $[Ru(terpy)(tmen)(OH_2)]^{2+}$ where bipy is 2,2'-bipyridine and tmen is *N,N,N',N'*-tetramethylethylenediamine with three nucleophiles TU, DMTU and CH_3CN. The pK_a values for the complexes were found to be 9.99 and 10.27 for $[Ru(terpy)(bipy)(OH_2)]^{2+}$ and $[Ru(terpy)(tmen)(OH_2)]^{2+}$, respectively. The substitution of water involving the two complexes was studied under pseudo-first order conditions using UV-Visible Spectrophotometry. The pseudo-first-order rate constant fitted the simple rate law $k_{obs} = k_2$ [Nu] + k_{-2}. The k_{-2} term was found to be zero for $[Ru(terpy)(bipy)(OH_2)]^{2+}$ but non-zero for $[Ru(terpy)(tmen)(OH_2)]^{2+}$. The values of the second order rate constants (k_2) for the three nucleophiles were found to be between (1.08 ± 0.02) x 10^{-4} $M^{-1} s^{-1}$ and (15.0 ± 0.27) x 10^{-4} $M^{-1} s^{-1}$ for $[Ru(terpy)(bipy)(OH_2)]^{2+}$ and (0.82 ± 0.04) x 10^{-4} $M^{-1} s^{-1}$ and (21.90 ± 0.69) x 10^{-4} $M^{-1} s^{-1}$ for $[Ru(terpy)(tmen)(OH_2)]^{2+}$. The results suggests that π-back donation accounts for the difference in reactivity.

CONFERENCES AND PUBLICATIONS

The first part of the study has been published. The details of the paper are given in **APPENDIX F.** In addition the third part on Ru(II), was presented at the South African Chemical Institute (SACI), 1-5 July 2002, Port Elizabeth, under the title "Substitution Reaction oF Ru^{II} Polypyridine Mono Aqua Complex" and was voted the best poster.

TABLE OF CONTENTS

LIST OF FIGURES

LIST OF SCHEMES

LIST OF TABLES

LIST OF ABBREVIATIONS AND SYMBOLS

A	associative mechanism
BZZP	benzodiprido[*a:3,2-h:2', 3'-j*]phenazine
bpz	bipyridine
COD	1,5-cyclooctadiene
terpy	2,2':6',2"-terpyridine
D	dissociative mechanism
bpma	bis(2-pyridylmethyl)amine
dppx	7, 8-dimethyldipyridophenazine
DPPZ	dipyrido[3, 2-a: 2', 3'-c]phenazine
DMSO	dimethyl sulfoxide
DMTU	dimethylthiourea
dien	ethylenetriamine
Et	ethyl
EtOH	ethanol
en	ethylenediamine
FDA	United States Food and Drug Administration
HET	2-hydroxoethanethiolate
IR	infrared
Isn	isonicotinamide
k_{obs}	experimental first-order rate constant
k_2	forward second order rate constant
k_{-2}	backward second order rate constant
L	ligand
LFER	linear free energy relationship
M	metal (Pt, Pd or Ru) unless specified
Me	methyl
MC	metal charge
MLCT	metal to charge transfer
NNN	tridentate ligand, bpma or terpy

NMR	nuclear magnetic resonance
NU	nucleophile
NEt_3	trimethylamine
nm	nanometer
phen	1,10-phenanthroline
ppm	parts per million
py	pyridine
pyz	pyrazine
R	substitutes
SAR	Structure Activity Relationships
T	*trans* ligand
TU	thiourea
TMTU	tetramethylthiourea
tpb	trigonal-bipyramidal
tmen	*N,N,N',N'*-tetramethylethylenediamine
UV	ultraviolet
Vis	visible
X	leaving group, unless otherwise specified
Y	incoming ligand (or nucleophile), unless specified
λ	wavelength
ν	frequency
$\Delta S^{\neq}$	entropy of activation
$\Delta H^{\neq}$	enthalpy of activation
$\Delta V^{\neq}$	volume of activation
n^{o}_{pt}	nucleophilicity
I_d	dissociative intermediate
I_a	associative intermediate
μ	ionic strength

CHAPTER ONE

INTRODUCTION

1 INTRODUCTION

PART A Substitution Reactions of Pt(II) and Pd(II) Complexes

1.1 General Background of Square-Planar Complexes

Square-planar complexes are often formed when a metal ion contains eight electrons in its outermost *d* orbitals.[1] Examples of some of these metal ions include Pt(II), Pd(II), Cu(II), Au(III), Rh(I), Ir(I) and Ni(II).[1, 2] These complexes are diamagnetic in nature, that is, they are spin paired. Square-planar complexes of Pt(II) are by far the most stable. As a result the syntheses and reactions of platinum(II) complexes have long been the subject of extensive study.[3]

In general platinum occupies a paramount importance in transition metal-complex chemistry.[4] It may exist in numerous oxidation states (such as 0, +1, +2, +3, +4 and higher) which means that it may react with numerous ligands to form a variety of complexes such as $[Pt^0(COD)_2]$ (COD = 1,5-cyclooctadiene)[4], $[Pt^0(\eta^2\text{-}Ph_2P(X)C{\equiv}CMe)(dcpe)]$ (X = S or O, dcpe = 1,2-bis (dicyclohexylphosphino)ethane)[5], $[Pt^I(Ph_2PCH_2PPh_2)]$[4], $[Pt^{II}(terpy)Cl]Cl$ (terpy = 2,2′;6′,2″-terpyridine)[6], $[Pt^{III}(C_2H_5NH_2)_4Cl]Cl_2.2H_2O$[4], and *cis*-$[Pt^{IV}Cl_4(NH_3)_2]$[7] just to mention a few. The complexes of Pt^0, Pt^{II} and Pt^{IV} are by far the most stable and studied complexes. Platinum complexes in various oxidation states, in particular Pt^{II} and Pt^{IV} (because they form remarkable complexes) have found use in different areas of research such as in catalysis, biochemistry and anticancer studies.[4]

Platinum(II) has the electronic configuration $[Xe]4f^{14}5d^8$. It forms stable complexes with anionic monodentate ligands such as halides, pseudohalides, carboxylate and sulfite and also with neutral donor ligands such as group 14, 15, and 17 donor ligands.[4] Platinum reacts with bidentate ligands such as N-N, P-P, S-S, N-O and P-N to form mononuclear and bridged dinuclear (also known as dimeric or polymeric) complexes. The reaction between platinum(II) and tridentate ligands such as N-N-N, N-P-N, and S-N-S yields mainly mononuclear 4-coordinate planar complexes.[4, 8] The majority of Pt(II) compounds

exhibit a coordination number of four with square-planar geometry although both five- and six-coordinate compounds exist.[9]

The unusual features of Pt(II) d^8 systems include their coordinatively unsaturated character, the ability to undergo nucleophilic attack at the vacant p_z orbital, the ease of formation of π-complexes, hydrido- and Pt-C σ bonded complexes, the tendency to undergo oxidative addition through electrophilic attack at the filled d_z^2 orbital and the ability to undergo reductive elimination.[4] As a result of these properties, Pt(II) d^8 systems are used as catalysts with great success.

Square-planar platinum(II) complexes are relatively kinetically inert compared to the other square-planar complexes, and this feature is of considerable importance in their chemistry.[9] Their inertness allowed them to play a role in the development of coordination chemistry such as studies of geometrical isomerism and reaction mechanism.[10] During the past four decades quantitative studies have been made on platinum(II) systems, with an appreciable effort being devoted to the investigation of the kinetics and mechanisms of their reactions.[3, 11, 12, 13, 14] These studies have resulted in a better understanding of the mechanism of ligand exchange process and the kinetics for different ligands and different geometries.[15] The wealth of data from these studies resulted in the development of the useful rule, the *trans* effect which will be discussed in much detail in the following sections.

The discovery of the square-planar complex *cis*-diamminedichloro-platinum(II) (*cis*-$[Pt(NH_3)_2Cl_2]$) by Rosenberg and colleagues[16], which is one of the three commonly used antitumour drugs, led to interest in the aqueous chemistry of platinum and its binding to polynucleotides.[17] The complex *cis*-$[Pt(NH_3)_2Cl_2]$ is widely known as cisplatin, and is currently used in many hospitals throughout the world in the treatment of ovarian, testicular, and other forms of cancer.[17] Recently it has become apparent that planar Pt(II) compounds are also of interest from a physicist point of view.[15] Complexes such as $[(en)PtCl_2]$ form polymeric species in the solid state through axial metal-metal stacking interactions.[9] The platinum complexes which exhibit these stacking interactions display some unsual conductivity properties.[9, 15]

1.2 Platinum Amine Complexes

The coordination chemistry of platinum amine has been known for more than a century and has fascinated chemists from the very beginning.[15] The amine ligands include ammonia, ethylenediamine (dien), hydrazine and hydroxylamine. The complexes *cis*- and *trans*-$[PtCl_2(NH_3)_2]$ are amongst the oldest known platinum(II) amine complexes. The discovery by Rosenberg around 1968 that the *cis*-isomer has antitumour activity stimulated the synthesis and screening of over 2000 different complexes with different amines and anionic ligands.[10, 17, 18] This has led to a considerable resurgence in interest in Pt(II) chemistry.[18, 19, 20, 21]

Both platinum(II) and (IV) amine complexes have been synthesized and tested for their antitumour activity. Some of these Pt(II) and Pt(IV) complexes have been found to be effective as anticancer agents. The platinum complexes which have shown antitumour activity have been found to have some common structural features, namely neutrality of the compounds and non-leaving groups in a *cis*–configuration.[7]

Studies on the mechanism of action of platinum compounds have suggested that their cytotoxic effects are related to their ability to bind to cellular DNA.[22, 23, 24] It was observed that the platinum antitumour compound undergoes hydrolysis inside the cells, where the Cl^- concentration is much lower than outside the cells, before it can interact with the DNA.[25, 26] Since platinum(IV) complexes are generally slow to undergo substitution reactions, it has been suggested that their ability to kill tumour cells requires reduction to active platinum(II) compounds.[7]

Amongst these novel complexes are platinum compounds which contain α-diimine ligands as a bidentate [bipyridine (bipy), phenanthroline (phen) and ethylenediamine (en)][27, 28, 29, 30, 31] or as a tridentate ligand [2,2':6',2"-terpyridine (terpy) and diethylenetriamine (dien)][6, 32, 33] instead of amine. Although not all of these complexes exhibit antitumour activity they have proved to be very useful models for the first binding step of platinum antitumour compounds to DNA.[16] These complexes are of much interest because of their wide range

of applications.[34] They exhibit both physical as well as biological properties.[27, 35] Structures of some bidentate and tridentate complexes are shown in **Figure 1.1**.

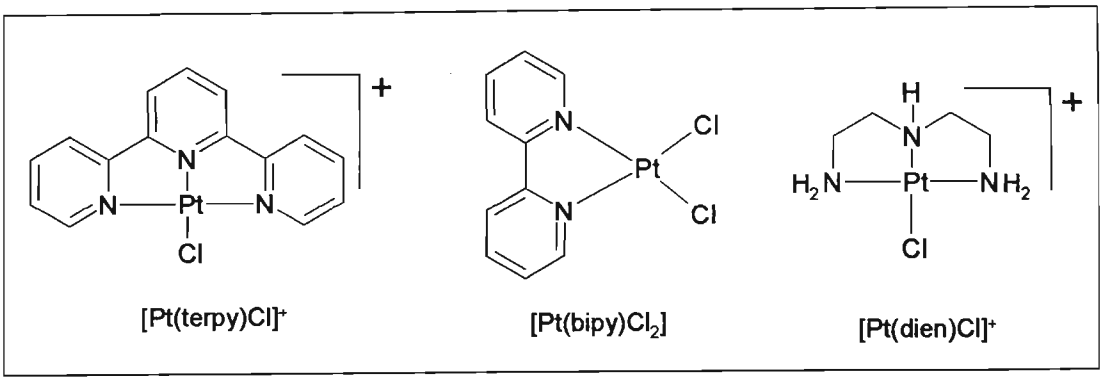

Figure 1.1 *Platinum(II) complexes containing N-donor ligand.*

Complexes such as $[Pt(terpy)(HET)]^+$(HET = 2-hydroxoethanethiolate and terpy = 2,2':6',2"-terpyridine), $[Pt(terpy)Cl]^+$, $[Pt(bipy)Cl_2]$ (bipy = bipyridine) and [Pd(terpy)Cl]Cl have been reported to bind strongly to DNA by intercalation.[36, 37, 38, 39] The mechanism of intercalation has shown that the process depends on various factors such as planarity, aromaticity, and surface tension of the interacting moiety.[40]

The atoms in $[Pt(terpy)(HET)]^+$, $[Pt(terpy)Cl]^+$, $[Pt(bipy)Cl_2]$, [Pd(terpy)Cl]Cl complexes all lie on the same plane. This promotes interaction between the metal and the π orbital of the chelating ligand (terpy), resulting in an extensive charge delocalization in an expanded π system.[6] The degree of charge delocalization in platinum-terpy complexes is higher than in platinum-dien, and -bipy complexes, therefore platinum-terpy complexes are better intercalators. Some types of drug molecules that are known to intercalate are antibiotics, antibacterials, antimalarial, and antitumour substances.[13] Compounds such as platinum(II) terpy complexes have been reported to display cytotoxic activity to human ovarian carcinoma.[41]

The Magnus green salt, which is prepared by mixing $[Pt(NH_3)_4]^{2+}$ and $[PtCl_4]^{2-}$ forms one-dimensional (1D) chain polymers and platinum(II) terpyridines, *e.g. N, S-bis*[(4'-chloro-2,2':6',2"-terpyridine)platinum(II)]-2-mercaptoimidazoltrishexafluorophosphate form parallel stacking with Pt-Pt interaction in the solid state.[41, 42] The 1D solid and parallel

stacking of terpyridine moieties give anisotropic physical properties such as conductivities and optical properties.[15, 42, 43, 44]

Furthermore, platinum(II) complexes containing ligands such as terpyridine and dien are of great interest because of their ability to bind to biological macromolecules.[45, 46] As a result, these types of complex have been used as probes for macromolecules. Tertiary structures of most nucleic acids as well as their functions have been elucidated using these types of complex.[46] Additional properties of platinum(II) complexes which have made them useful as biological macromolecule probes include their inability to form insoluble hydrated oxides at neutral pH, their kinetic stability and their moderate solubility in water.[17] Since the application of platinum compounds in anticancer treatment is so prominent, the interaction of these compounds with DNA has been included in **section 1.5**.

1.3 Substitution Reactions on Square-Planar Complexes

Substitution reactions on four coordinate planar complexes that have been studied systematically are for low-spin d^8 complexes[11], in particular square-planar Pt(II) complexes, because their reactions proceed at more convenient rates than the other square-planar complexes.[10] For example, Au(III) complexes react ~10^3 times faster while Ni(II) and Pd(II) complexes react 10^6-10^5 times more rapidly than their analogous Pt(II) complexes[47, 48], respectively, with exceptions being exchange reactions with CN^- in $[M(CN)_4]^{2-}$ where these relative rates may vary.[10, 49] As a result, little information is known regarding the substitution reactions of these square planar complexes. However, all available data suggest that the mechanistic results for Pt(II) apply generally to square-planar complexes of other elements.[10]

In general, substitution reactions of d^8 transition metals are both of fundamental[2] and practical importance, the latter stemming from applications in catalysis and cancer chemotherapy.[27, 15] The understanding of the mechanisms through which substitution reactions on Pt(II) *cis*-dichlorodiammine square-planar complexes take place is considered as the key step for the understanding of the antitumour activity of most of these complexes.[50]

The substitution reactions concerned with here involve the displacement of one ligand for another on the square-planar coordination sphere as represented by equation (1.1).

$$Pt(T)L_2X + Y \rightarrow Pt(T)L_2Y + X \qquad (1.1)$$

where T is the ligand *trans* to the leaving group X, L are ligands *cis* to the X and Y is the incoming ligand. A square-planar complex consists of two vacant sides, through which the incoming ligand Y can attack the metal centre.[51] The incoming ligand can approach from either side of the plane, that is, above and below the plane of the square-planar substrate.

Due to the low coordination number of Pt(II) complexes, it seems reasonable to expect that the reactions represented by equation (1.1) occur almost entirely by associative pathways.[10] Various studies of these types of reaction (1.1) have proved that this is the case with a few exceptions.[52, 53, 54, 55, 56] These studies have shown that these reactions proceed via associative activated substitution with the formation of trigonal-bipyramidal (tbp) intermediate.[57, 58, 59, 60, 61] A general representation of the stereochemical course of displacement reactions of Pt(II) square-planar complexes is given in **Figure 1.2**.

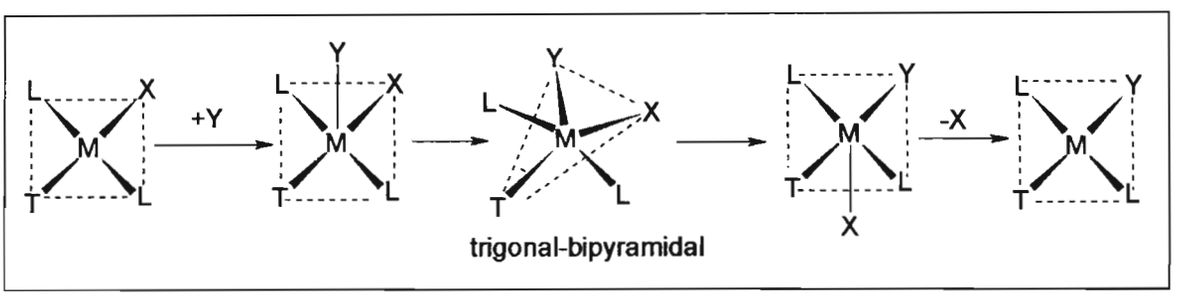

Figure 1.2 *Schematic representation of the attack of* Y *at a planar complex and the tbp five-coordinate structure*

Some of the experimental evidence for associative pathways includes the uniformly negative entropies and volume of activation, including marked dependence of rates on the nature of both entering and leaving groups.[10] The volume of activation, $\Delta V^{\#}$, derived from the pressure dependence of the rate constants[85, 63] and measurements of activation parameters namely, $\Delta H^{\#}$ and $\Delta S^{\#}$, have been used as criteria to distinguish associative and dissociative reaction paths. An associative mechanism is associated with a negative volume of activation, while positive volume of activation implies a dissocative mechanism.[88]

Under normal conditions, substitution reactions at the square-planar complexes have been found to occur with a complete retention of stereochemistry of the initial platinum(II) substrate.[1, 10, 11] Substitution reactions of *trans*-[Pt(T)L_2X] yield a *trans* product and the *cis* isomer gives a *cis* product as shown in **Figure 1.3**.

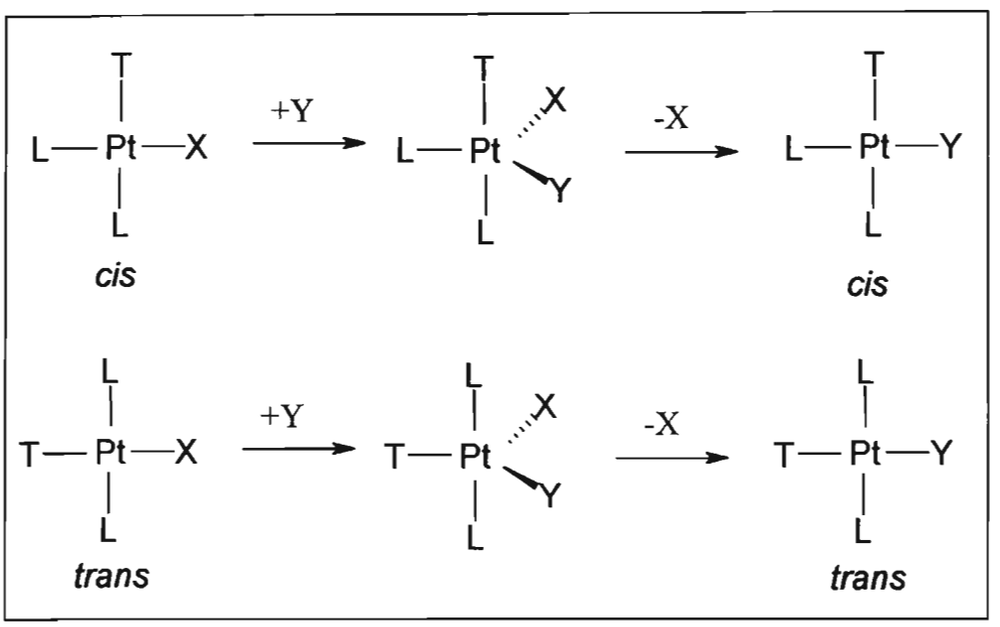

Figure 1.3 *Stereochemistry of square-planar substitution reaction through a trigonal-bipyramidal (tbp) intermediate.*

In the case whereby a substitution reaction on a square-planar complex proceeds via a dissociative mechanism, which involves bond breaking of Pt-X, a three coordinated intermediate is formed. This may at times have a nearly regular planar structure with angles of 120°. When one starts with a *trans*-Pt(II) complex, it may yield a *cis* product.[3] This is because the incoming ligand (Y) can attack the metal centre from adjacent to L or opposite L.

A two-term rate law consisting of a ligand-dependent as well as a ligand-dependent term as shown in equation (1.2) has been observed for most reactions.[1, 3, 4, 11, 63]

$$Rate = (k_1 + k_2[Y])[Pt(T)L_2X] \qquad (1.2)$$

where k_1 and k_2 are first-order and second-order rate constants, respectively. Under pseudo-first order conditions, that is, the concentration of the incoming ligand (Y) is in excess, the experimental first-order rate constant, k_{obs}, is related to the individual rate constants as shown by equation (1.3).[62]

$$k_{obs} = k_1 + k_2[Y] \tag{1.3}$$

A plot of k_{obs} versus [Y] should be linear with an intercept of k_1 for the reagent-independent path and a slope of k_2 for the reagent dependent path. The mechanistic representation of this two-term rate law is illustrated in **Figure 1.4**.

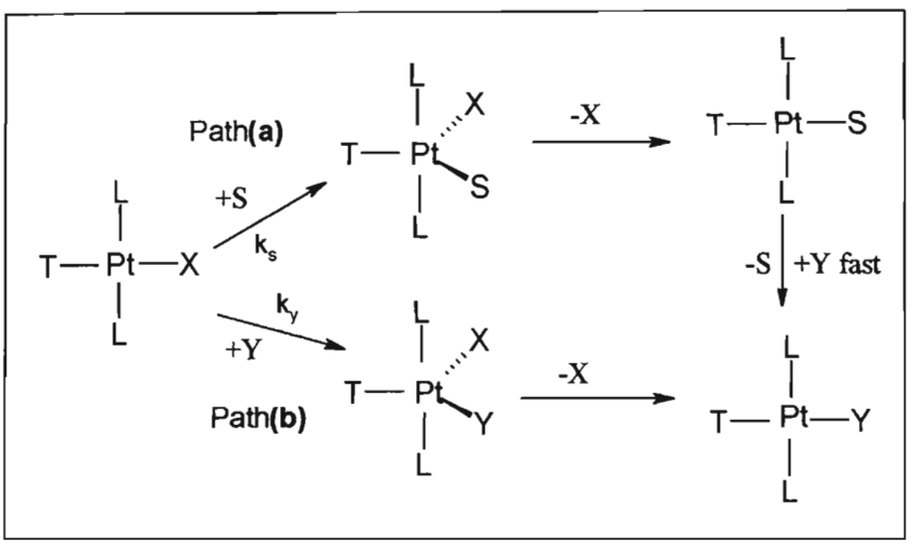

Figure 1.4 *The proposed mechanism representing the two-term rate law for the reaction of a square-planar complex. Path* **(a)** *represents the solvent path (k_s) and path* **(b)** *represents the direct attack on the metal centre by the incoming ligand* (Y).

The ligand independent rate constant k_1 is due to the slow displacement of X by the solvent to form a labile solveto species, which then is rapidly substituted by the nucleophile Y. A direct attack at the metal by the nucleophile Y to displace X is responsible for the ligand dependent term (k_2). It then becomes convenient to designate the solvent path k_1 as k_s and the reagent path k_2 as k_Y, so that equation (1.3) becomes

$$k_{obs} = k_S + k_Y[Y] \tag{1.4}$$

The importance of the two terms depends on various factors such as: spectator ligand(s) (non-labile ligand(s)) [63], incoming ligand (nucleophile)[64], leaving group (X) [65], solvent medium in which the reaction is carried out and the metal centre charge. The importance of these effects depends on the amount of bond formation or bond breaking in the transition state.

The substitution reaction on square-planar complexes can be considered to have a double humped potential energy curve as represented in **Figure 1.5**.[1, 3, 12]

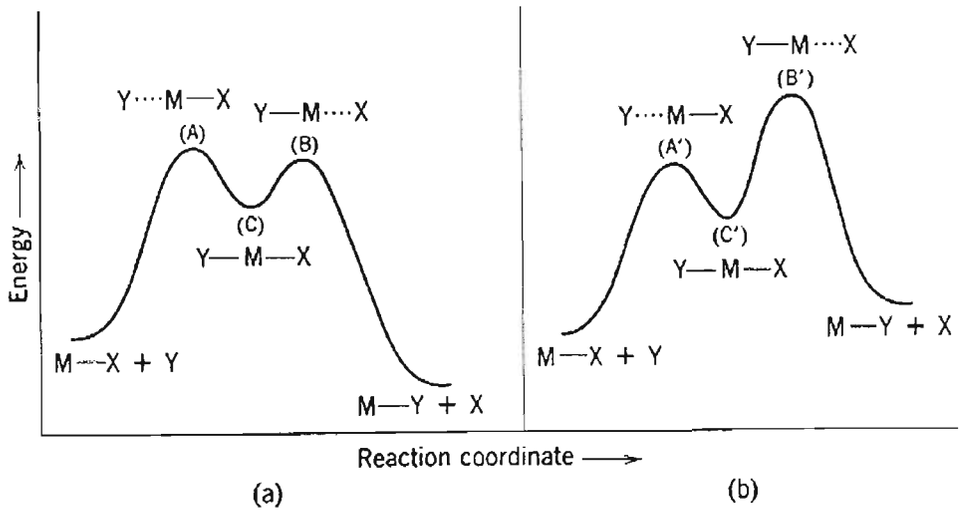

Figure 1.5 *The potential energy curves for the substitution reaction on square-planar complexes involving a reactive intermediate.*

Reaction profile **(a)** represents the reaction whereby the leaving group is readily replaced and for which the rate of substitution is almost independent of the leaving group. This follows because the higher activation energy between the transition states is that of (A). This type of reaction will show a very sharp dependence on the entering nucleophile since bond formation will be the most important with little rupture of the Pt-X bond. Therefore, the nature of X will have a secondary effect on the formation of transition state (A) and will affect the reaction rate only in so far as it is one of the four non-participating ligands.

Reaction profile **(b)** represents the case whereby X is more difficult to displace and the rate of the reaction depends on the nature of the leaving group. This is supported by the fact that now the higher activation energy between the ground state and the transition state

is that of (B). In this case bond breaking would be most important with the reaction rate showing a very large dependence on the leaving group.

Support for the energy profile shown in **Figure 1.5**, where the five-coordinate, trigonal-bipyramidal species is an intermediate, comes from studies that show that the intermediate can exist for a sufficiently long time to undergo pseudo-rotation.[66] In addition, the rate shows dependence on the nature and the concentration of the incoming ligand.

1.4 Factors that Affect the Rate of Ligand Substitution Reactions on Square-Planar Complexes

As already mentioned, the rate of a substitution reaction on square-planar Pt(II) complexes depends on the nature and the concentration of the incoming ligand (Y)[3, 4], the steric effect[67, 68], the solvent in which the reaction is carried out and the spectator ligand. [57, 65, 69] The rate also depends on other factors such as the metal charge[70] and temperature at which the study is conducted. It has been found that the aromaticity of the chelate ring in Pt(II) complexes such as $[Pt(bipy)Cl_2]$ and $[Pt(terpy)Cl]^+$ also affects their reactivity.[3] This section contains a discussion of how some of these factors, namely the spectator ligand(s), the solvent, the leaving group and the incoming group affect the rate of square-planar Pt(II) reactions.

1.4.1 The Spectator Ligand

The rate of substitution of the square-planar complexes has been largely probed by changing the electronic properties such as the σ, π and the steric properties of spectator ligand(s) *trans* or *cis* to the leaving group, especially in the case of the platinum(II) complexes.[71] Various studies on the substitution reactions on Pt(II) indicate that the rate is more sensitive to a ligand *trans* to the leaving group (X) than it is to a ligand(s) *cis* to the leaving group (X).

1.4.1.1 The *trans* Effect

The *trans* effect is a well established concept in platinum(II) chemistry and many ligand substitution reactions have been investigated with regard to this property.[81, 72] The *trans* effect may be defined as the effect of a coordinated group upon the rate of substitution reactions of ligands opposite to it in a metal complex.[2] Since the first observation of a ligand's ability to promote substitution of a ligand trans to it in platinum(II) complexes by Alfred Werner, and the introduction of the concept of the *trans* effect by Chernayev *et al* in 1926, intensive investigations have shown that this effect is a kinetic rather than a thermodynamic phenomenon.[2, 8, 93]

The ability of a ligand T in $[Pt(T)L_2X]$ to promote the rate of substitution of the ligand *trans* to itself decreases as follows:[73, 74, 75, 76]

$$CO, CN^-, C_2H_4 > PR_3, H^- > CH_3 > C_6H_6^-, NO > Br^-, Cl^- > py, NH_3, OH^-, H_2O$$

This is known as the *trans* effect series. This order spans a factor of 10^6 in rate and it holds for all square-planar complexes that have been examined so far.[10] The sources of the *trans* effect are the thermodynamic and kinetic factors.

The thermodynamic factor refers to the weakening of the Pt-X bond in the ground state of the platinum(II) substrate, while the kinetic factor refers to the stabilization of the transition state by the *trans* ligand (T). This effect has been studied extensively by measuring Pt-X bond distances, infrared stretching frequencies and Nuclear Magnetic Resonance (NMR) coupling constants, and it is referred to as the *trans* influence.[72, 77] It is believed that in the absence of multiplicity of the bond, the length of the bond is inversely proportional to its strength. As a result, the longer the bond the weaker it becomes. A decrease in the bond stretching force constant implies that the bond is becoming weak. Alternatively, the kinetic effect is assumed to operate because of better bonding between the M and the T in the transition state. Most explanations regarding this effect have been given by considering square-planar Pt(II) complexes as models. The kinetic effect has been also studied by considering the π and the σ effects.

To rationalize the *trans effect* sequence, different theories such as the *extended Hückel molecular orbital*, *π-bonding*, *crystal field* and *polarization theory* have been applied.[78, 72] *Molecular orbital* (M. O.) theory has been employed to unify the *π-bonding* and *polarization* theories. The following sections discuss the *polarization*, *molecular orbital* and the π-bonding theories.

The π-Bonding Theory

The concept of π-bonding in metal complexes was first introduced by Pauling to account for the shortcomings Ni-C bond in $Ni(CO)_4$ and to account for the large stability of the cyanide complexes of transition metals.[3] The π-bonding theory is mainly concerned with π-bonding ligands such as C_2H_4, CN^-, CO, terpy, and PR_3 and SR_2. This theory suggests that all these ligands tend to stabilize the transition state during a reaction through electron back donation from filled *d* orbitals of the metal to empty π* orbitals of the ligand.[57] This accounts for their high *trans* effect. According to Chatts[11], these ligands possess an empty orbital of π-symmetry that could withdraw charge from the metal and minimize the disturbance produced by the binding of the fifth ligand. Chatts emphasized that removal of charge from the Pt(II) by π-bonding of T will enhance the addition of Y, thereby promoting a more rapid reaction.

Orgeal proposed the π-accepting mechanism using the same reasoning in terms of a molecular orbital-based argument.[3, 11] He showed that the presence of a π-acceptor in the trigonal plane lowers the energy of the five-coordinate transition state or intermediate. This five-coordinate transition state is assumed to have the structure given in **Figure 1.6**.[3]

Figure 1.6 *The proposed structure of the five-coordinate intermediate.*

This mechanism suggests an associative mode of activation for these systems. From various experiments it was proved that reactions of *trans*-Pt(T)L_2X proceed via an associative mechanism.[65, 79]

The Polarization Theory

This theory offers the explanation for the high *trans* effect of ligands such as H^-, alkyl and aryl, which do not have orbitals of π symmetry.[79] Grinberg suggested that the large *trans* effect of T in trans Pt(T)L_2X results from a weakening of the Pt-X bond.[3] He explained this hypothesis in terms of the polarizability of the *trans* ligand T. The electrostatic-polarization theory offers an explanation for the weakening of the Pt-X bond on the basis of charge distribution, as shown in **Figure 1.7**.

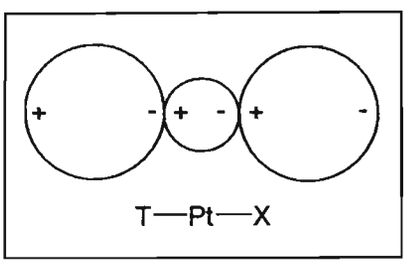

Figure 1.7 *Distribution of charge in induced dipoles in the T-Pt-X coordinate of trans-Pt(T)L_2X.*

The primary charge on Pt(II) induces a dipole in T, which in turn also induces a dipole in the metal. The induced dipole by T from the metal is oriented in such a way as to repel the negative charge in X. As a result, the attraction of X towards Pt(II) is reduced, the Pt-X bond is lengthened and consequently weakened. This theory explains the parallelism between the magnitude of the *trans* influence of T and its polarizability. It also predicts that the effect will be more important if the central metal is polarizable. This prediction is supported by the experimental observation that Pt(II) complexes are more polarizable than their Pd(II) counterparts.[80]

However, this electrostatic theory has several shortcomings. For instance, the induced dipole on Pt(II) should depend on the net charge of T more strongly than on the induced moment, which in turn will be greater if the Pt-T bond is short. This suggests that Cl^- will have a larger *trans* effect than I^-. This is not true, in reality this shortcoming is overcome

by taking covalent bonding into consideration. The covalent bonding has been accounted for in the *M. O. theory*.[3]

The Molecular Orbital Theory for π- and σ-Effects

The Molecular Orbital (M. O.) theory offers the best explanation of the π and σ-bonding of square-planar complexes. The M. O. diagram of $PtCl_4^{2-}$ is simplified in **Figure 1.8**.[3] The most stable orbitals are σ bonding and are located mainly on the four chlorine groups, followed by the π-bonding orbitals, both of which are present in the four chlorine groups.

The antibonding partners of these σ- and π-bonding orbitals, namely σ^* and π^* are the next in order of stability, and are derived from the 5d atomic orbitals of Pt(II). They consist of the four relatively stable MO's with the probable order of stability being π_{xz}^*, π_{yz}^*, σ_{z^2} * *and* π_{xy}^*, and the relatively unstable $\sigma_{x^2-y^2}^*$ orbital. The p_z valence orbital which is not involved in σ bonding, and the antibonding orbitals σ_s^*, σ_x^* and σ_y^* exist at higher energies.

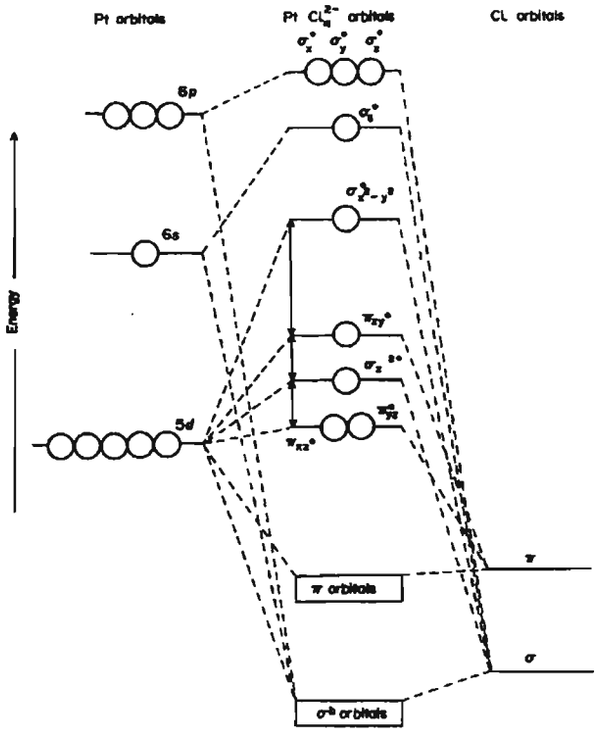

Figure 1.8 *The M. O. diagram of* $[PtCl_4]^{2-}$.

Making use of this type of bonding scheme, σ and π trans effects can be explained as follows:

a) σ *trans* effect. Taking the geometries of the atomic orbitals into consideration, of the four metal valence orbitals ($d_{x^2-y^2}$, *s*, p_x and p_y) used in σ bonding in a square planar complex, only the *p* orbitals have *trans* directional properties. This implies that the *trans* ligand T and the leaving group X in *trans*-Pt(T)L_2X must share the same σ_x orbital in the overall M.O. arrangements. It follows that a strong σ-bonding ligand T will take on the larger share of the bonding σ_x M.O. leaving a much smaller share for X as illustrated in **Figure 1.9**.

(a) **(b)**

Figure 1.9 *The σ bonding of L-Pt-X, using the σ_x M.O.* **(a)** *The σ-bond strengths of L and X are about equal.* **(b)** *The σ-bond strength of L is much greater than that of X.*

This means that the Pt-X bond is weakened, as was also predicted by the polarization theory. Such a result is expected to lead to an increased rate of replacement of X regardless of the mechanism of the substitution reaction. According to Langford and Gray[3,4,11] the increase in the stabilization of the transition state of the trigonal bipyramidal intermediate results from more orbitals being available for σ-bonding. Only one p orbital, that is, p_x is used to bond the *trans* ligand L-Pt-X on the *x*-axis of the square-planar complex. As a result, addition of the incoming ligand (Y) to form a trigonal-bipyramidal intermediate from above the *xy* plane causes X to move down out of the plane as shown in **Figure 1.10**.

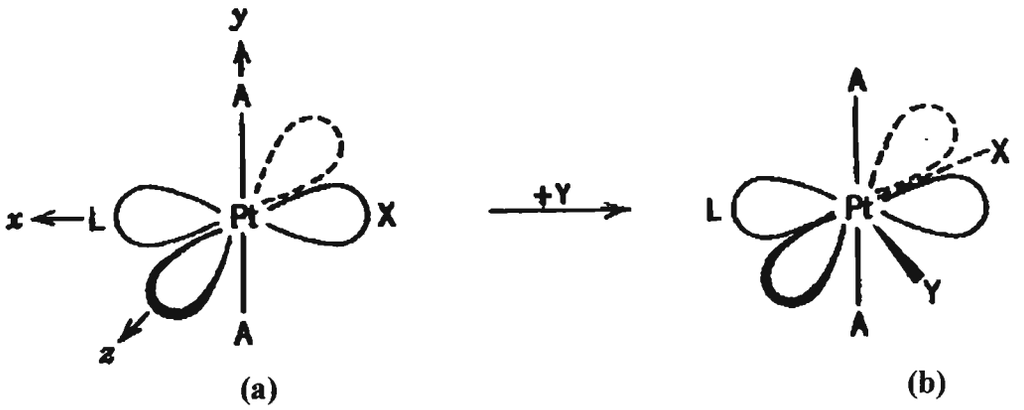

Figure 1.10 *The σ-trans effect due to a stabilization of the trigonal bipyramidal intermediate. Only one p orbital is available for σ bonding of two ligands in* **(a)** *and p orbitals are suitable for σ bonding in* **(b)**.

This trigonal plane now consists of p orbitals namely, p_x and p_z suitable for bonding. A good σ-bonding ligand such as H^- and CH_3^- can use the extra p character to form the σ structure in the trigonal bipyramid which have high *trans* effects.

b) π *trans* effect. Ligands such as C_2H_4, CO and CN^-, which form strong π bonds may also be explained in terms of M. O. theory. In a square-planar complex only three M.O.'s, the π_{xz}^*, π_{yz}^* and π_{xy}^* have proper π-bonding. The formation of the trigonal bipyramidal transition state involves the π-interaction of four M.O.'s of correct symmetry namely, π_{xz}^*, π_{yz}^* and π_{xy}^*, and $\pi_{x^2-y^2}^*$. All of these orbitals are shared in π bonding by the *trans* ligand(s) T, the leaving group X, and the incoming group Y in the trigonal plane. Therefore, the trigonal bipyramidal transition state would be greatly stabilized if T is capable of bonding to the π^* orbitals.

The bonding of T to the π^* orbitals results in delocalization of electronic charge to the ligands and lowering of the system's energy. Since there are more filled π^* orbitals in the transition state than in the ground state, the transition state is stabilized to the greater extent. The net effect of a good π-acceptor ligand L is to lower the activation energy of the reaction. The contribution of σ and π bonding abilities is determined by the nucleophilic

discrimination factor that will be discussed later.[81] This theory rates the *trans*-ligands as follows:

σ-effect:

$$H^- > PR_3 > SCN^- > I^- > CH_3^-, CO, CN^- > Br^- > Cl^- > NH_3 > OH^-$$

π-effect:

$$C_2H_4, CO > CN^- > CN^- > NO_2^- > SCN^- > I^- > Br^- > Cl^- > NH_3 > OH^-$$

The *trans* effect has found potential use in synthesis of various platinum compounds. **Scheme 1.1** illustrates the use of the *trans* effect in synthesis of *cis*- and *trans*-isomers of $[Pt(NH_3)NO_2Cl_2]$ from $[PtCl_4]^{2-}$, NH_3 and NO_2^-.[10, 11]

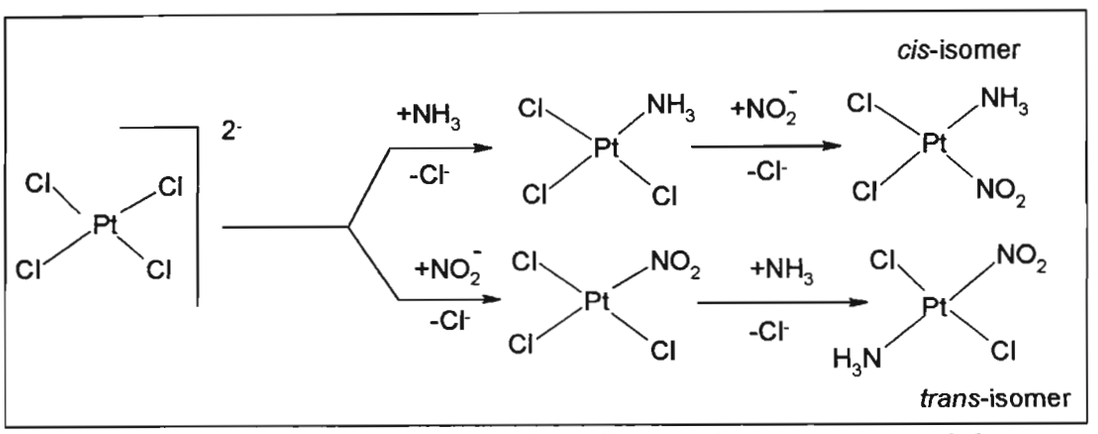

Scheme 1.1 *Utilization of the trans ability effect in the preparation of the cis- and trans-isomer of* $[Pt(NH_3)NO_2Cl_2]$.

The scheme indicates that the order of addition of reagents can influence the product geometry in reactions. The combination of the *trans* effect, incoming group and the leaving group led to the observed products in these reactions. These reactions also indicate the greater *trans* ability effect of chloride over ammonia and of nitrite over chloride. The *trans* effect has also been applied to explain the differing chemical behaviour of *cis* and *trans* isomers of $[PtL_2X_2]$. The *cis*-$[Pt(NH_3)_2Cl_2]$ reacts with thiourea (TU) to give $[Pt(TU)_4]Cl_2$, whereas the *trans* isomer gives $[Pt(TU)_2]Cl_2$.[4]

1.4.1.2 The *cis* Effect

For square-planar complexes the *trans* effect dominates the *cis* effect.[78, 82 89] The *cis* effect becomes important if the *cis* ligands are bulky because of their proximity to the site of replacement.[10] For example, the rate of substitution of chloride from *cis*-$[Pt(PEt_3)_2LCl]$

with pyridine when L = Cl^-, $C_6H_6^-$ and CH_3^- was observed to increase in the following order: Cl^- (1.7×10^2 s^{-1}) < $C_6H_6^-$ (3.8×10^2 s^{-1}) < CH_3^- (6.0×10^2 s^{-1}).[1] The sequence for the *cis* effect for various ligands was observed to be as follows:[89]

$$NO_3^- > CH_3CO_2^- > Cl^- > Br^- > py > I^- > PR_3 > CO, H^-$$

Cattalini *et al*[83] studied the kinetic displacement of the chloride in the $[Pt(Me_2SO)(en)Cl]^+$ and $[Pt(NH_3)(en)Cl]^+$ (Me_2SO = dimethylsulfoxide, en = ethylenediamine) by various incoming groups in aqueous solution at 25 °C. They found that these complexes have similar reactivity, with the Me_2SO complex being at least one order of magnitude more labile than that of ammonia. Further, they pointed out that the greater *cis* effect stems from the greater nucleophilic discrimination factor of the complexes which will be discussed in greater detail later.

1.4.2 The Steric Effect

Studies of the effect of the steric factors on the rate of reaction of platinum(II) complexes have played a major role in determining the mechanism of their substitution reactions.[84] Recently, interest in kinetic studies of sterically hindered square-planar complexes have increased since the discovery of factors that may cause the mechanism mode of square-planar Pt(II) complexes to change from an associative mechanism to a dissociative mechanism.[85, 86] Massive steric hindrance is thought to be a way of stabilizing a three-coordinate d^8 state thereby favouring a dissociative mechanism.[85]

It has been observed from various studies that the rate of aquation or water exchange on aquated platinum (II) complexes is a factor of 10^5-10^6 lower than the palladium(II) analogue. van Eldik *et al*[87] have demonstrated that the rate of the substitution reaction of water from $[Pd(R_5dien)H_2O]^{2+}$ complexes may be decreased by at least four orders of magnitude to match that of their platinum analogues in going from R = H to R = Et by introduction of steric hindrance. The substitution reactions of $[Pd(dien)Cl]^+$ with various nucleophiles are 10^5 times faster than reactions of the corresponding $[Pd(X\text{-}dien)Cl]^+$

where X = Et_4 or $MeEt_4$.[99] These observations point to the fact that the rate of substitution on Pd(II) can be decreased by introduction of steric effects on the substrate.

There is little information regarding the studies of steric effects on platinum(II) complexes due to the fact that the systems become extremely slow. Complexes such as *trans* or *cis*-[$Pt(PEt_3)_2RX$] where R = alkyl or aryl and X is the halogen have been investigated to determine the steric effect on both the rate of substitution and the mode of mechanism.[99] It was found that the *cis* complex underwent a *cis* to *trans* isomerization in methanol which proceeded via a dissociative asynchronous mechanism whereby the Pt-X breaking step was the rate-determining step.[100]

1.4.3 Incoming Group Effect (Y)

The nature and the concentration of the incoming ligand Y have been found to have an effect on the rate of substitution of square-planar complexes. It has been mentioned already that under pseudo-first order conditions, the experimental first-order rate constant k_{obs} depends on the concentration of the incoming ligand. The dependence of the rate constant on the entering ligand supports the fact that square-planar reactions proceed via an associative mechanism. The sensitivity of [$Pt(T)L_2X$] substrate on the incoming ligand is given in terms of nucleophilicity of the incoming ligand ($n_{pt}^{\ o}$) defined by equation (1.5).

$$n_{pt}^{\ o} = \log\left(\frac{k_y}{k_s}\right)_o \qquad (1.5)$$

where k_y is the second order rate constant ($M^{-1}\ s^{-1}$) for a given nucleophile and k_s is the first order rate constant (s^{-1}). About 30 years ago a standard nucleophilicity scale was introduced based on the rate of substitution reactions of chloride in the neutral standard substrate *trans*-[$Pt(py)_2Cl_2$] with various nucleophiles in methanol at 30 °C.[88, 89] Since then much of the kinetic data for platinum complexes have been rationalized in terms of equation (1.5).

It was observed from various investigations that the nucleophilicity of the incoming ligand n_{pt}^{0} depends on one or a combination of the following factors: the steric hindrance, biphilicity of the ligand, and charge effect. [88, 89] Ligands such as thiourea, SCN^- and $SeCN^-$ which are biphilic[90] were found to be less reactive toward cationic platinum(II) complexes than predicted. However, these nucleophiles may be more reactive than predicted for the corresponding dianionic substrate.[96] This is due to the effect of charge on the π-basicity of platinum and the degree of back donation to these nucleophiles in the transition state.

Plots of log k_y for other Pt(II) complexes against n_{pt}^{o} with a wide range of nucleophiles yields linear free energy relationships (LFER).[1] Such a LFER is given by equation (1.6).

$$\log k_y = s n_{pt}^{o} + \log k_s \qquad (1.6)$$

The slope *s* depends on the complex and is called the *nucleophilic discrimination factor*. If the value of *s* is large it implies that the rates of reaction are very sensitive to the nature of the entering group.[4] The intercept *log* k_s is the measure of the *intrisic reactivity*. A large negative intercept is the case whereby the solvent rate constant it too small to detect. A low value of the *intrisic reactivity* is associated with very fast reactions and hence a high *nucleophilic discrimination factor*.

1.4.4 Leaving Group Effect (X)

In order to monitor the effect of the leaving group on the rate of substitution, one needs to keep the *cis* and the *trans* effect constant. If the rate of substitution of X from the metal complex inversely parallels the M-X bond strength, this implies that there is a certain amount of M-X bond rupture in the transition state. Therefore, it is important to assess the ease of replacement of X from the metal complex. The reactions of substitution of various X from $[Pt(dien)X]^+$ with pyridine in aqueous solution indicate that the rate increases in the following order as X is changed:[91]

$$CN^- < NO_2^- < SCN^- < N_3^- <<< I^- < Br^- < Cl^- < H_2O < NO_3^-$$

This order is similar to the inverse of the *trans* effect. The spread in rates of approximately 10^6 in this series of reactions shows that the leaving group has a major effect on the rate of reaction, indicating that considerable Pt-X bond breaking is involved in forming the transition state. The same order was found for the reactions of $[Pd(terpy)X]^+$ and $[Pd(dien)X]^+$ with the same incoming ligands at 25 °C.[92] Further, this series illustrates that strongly bound ligands such as CN^-, NO_2^-, dissociate more slowly from the trigonal bipyramidal intermediate.

1.4.5 The Solvent Effect

It has been mentioned above that the rate law of a square-planar substitution reaction consists of two-terms: a term (k_1) which results from the attack at the Pt(II) centre by the solvent to form a solveto species which is readily attacked by the nucleophile to form the product, and a second term (k_2) resulting from the direct attack at the Pt(II) centre by a nucleophile to yield a product. The importance of these terms depends on the solvent in which the reaction is carried out. Early kinetic studies on substitution reactions of square-planar complexes have shown the importance of the solvent effect.[93]

If a reaction is performed in a coordinating solvent, such as DMSO, the path which involves the solveto species becomes important. Palmer and co-workers[94] have reported the substitution of *cis* and *trans* bromomesitylbis(triethylphosphine)platinum(II) with thiourea in methanol, ethanol, dimethylsulfoxide and acetone at 30 °C. They have found that the rate of substitution in ethanol for the *trans* isomer was dominated by the k_2 term, whereas for the *cis*-isomer, the k_1 term was more dominant in DMSO.

1.5 The Biological Importance of Pt(II) Complexes

During the course of an investigation on the growth of *Escherichia coli* bacteria under the influence of an electric field, in the early 1960's [14], Rosenberg and colleagues discovered cisplatin (*cis*-$[PtCl_2(NH_3)_2]$), a now widely-established antitumour drug **Figure 1.11**.[7,95, 96, 97, 98, 99, 106]

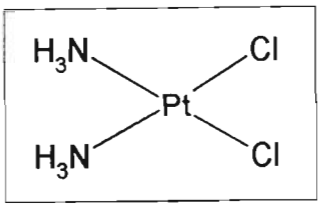

Figure 1.11 *Structure of cis-diamminedichloro platinum(II) (cis-[Pt(NH$_3$)$_2$Cl$_2$]).*

The investigation involved the generation of an electric field between two inert platinum electrodes immersed in an aqueous solution of NH_4Cl as an electrolyte in the presence of *Escherichia coli* bacteria. Under these experimental conditions, they observed no bacterial division, instead there was a strong filament growth of the bacteria to 300 times its normal length.[14, 7] Thus cell division was inhibited while cell growth was unaffected.[9]

Initially, it was thought that the electric field was responsible for the filament growth. However, subsequent experiments proved that the filamentous growth was not caused by the electric field, but by the presence of a small amount of Pt(IV) compounds in the solution.[15] Amongst these compounds were *cis*-$PtCl_4(NH_3)_2$ and $[PtCl_6]^{2-}$.[9, 15] These compounds formed from the Pt electrodes and the corroding NH_4Cl under the influence of an electric field. Complexes *cis*-$PtCl_4(NH_3)_2$ and $[PtCl_6]^{2-}$ have been shown to inhibit cell growth, the former having a small inhibitory effect on the growth rate and the latter being very effective at low concentrations (approximately 10 ppm).[9] From microbiological studies, it turned out that the complex *cis*-$[PtCl_2(NH_3)_2]$ was the most active species responsible for the growth of the filament.[14, 15]

Various platinum complexes such as *cis*-bis(ammine)platinum(II) and *cis*-platinum(IV) complexes were also found to induce filamentous growth in bacteria. Even though these *cis*-platinum complexes were observed to induce filamentous growth, their *trans* isomers were found to be inactive. The *trans* complexes have been reported to suppress bacterial growth at high concentrations.[14]

Due to the fact that cisplatin suppressed cell division without killing the bacteria it was deduced that it was capable of inhibiting the rapid growth of tumour cells.[14] The antitumour activity of cisplatin and other platinum complexes such as *cis*-$[PtCl_4(NH_3)_2]$, $[Pt(en)Cl_4]$, $[PtCl_2(en)]$ and $[PtCl_4(en)]$ which also induce filamentous growth in bacteria

were subsequently tested on animal tumours and found to be active towards tumours such as sarcoma 180 in Swiss white mice.[14, 15]

Following the successful animal testing cisplatin was introduced for clinical trial in 1971.[7, 100] In 1978 cisplatin was approved by the United State Food and Drug Administration (FDA) for clinical use as a treatment for testicular and ovarian cancer.[14, 15, 101, 102] Currently, cisplatin is a commonly used antitumour drug.[7] About 30,000 patients in the USA are cured each year using the drug[15], generating annual sales worth 500 million U.S. dollars.[7, 103] This drug has also been found to be successful in the treatment of cervical carcinoma, lymphoma, osteosarcoma, melanoma, bladder carcinoma and neuroblasta cancer.[7, 15]

Although cisplatin may be highly effective in the treatment of ovarian and testicular cancers, severe toxic side effects have limited its use.[24, 25, 104] The most dominant side effects include nausea, vomiting, bone marrow toxicity, neurotoxicity and renal toxity.[15, 105] The other problems associated with its use are: certain malignant tumours become resistant to it, its low solubility in aqueous solution and the fact that it is administered intravenously.[95, 100, 106] All these problems are inconvenient to patient treatment and have led to its limitation in clinical use.

Thousands of novel platinum(II) and (IV) complexes have been synthesized and their antitumour activity assayed with the hope of reducing some of the problems associated with cisplatin.[7, 107, 108] The thinking relating to platinum(IV) complexes is that their kinetics are much slower than those of platinum(II), hence they can be administered orally since they are not likely to be degraded too early in the gastrointestinal tract.[106] The development of these novel platinum drugs leads to an alteration of the pharmacokinetics of cisplatin by replacing the labile chlorides by other leaving group ligands, and extending the ligand ammine group to a series of cyclic or acyclic alkyl ammines.[109, 110] This resulted in a second generation of antitumour platinum complexes.

Examples of these second generation antitumour platinum complexes include complexes such as carboplatin (diammine[1,1-cyclobutanedicarboxylato(2-)]-*O,O'*-platinum(II)) which displays similar antitumour activity as cisplatin with less toxicity.[7] Because of its lower toxicity it is widely used for the treatment of ovarian tumours and certain lung

carcinomas.[7, 101] However, due to its lower solubility and stability, this drug is still administered intravenously.[106] These shortcomings led to searches for better platinum antitumour complexes with lower toxicity, greater stability and a different mode of administration.

The structure of carboplatin and some of the second generation antitumour complexes namely, lobaplatin [(1,2-di(aminomethyl)cyclobutane-platinum(II)lactate], spiroplatin [(aqua(1,1-bis(aminomethyl)cyclohexane)(sulphato)-platinum(II)], and iproplatin [*cis*-dichloro-*trans*-dihydroxydi(iso-propylammine)-platinum(IV)] are given in **Figure 1.12**.

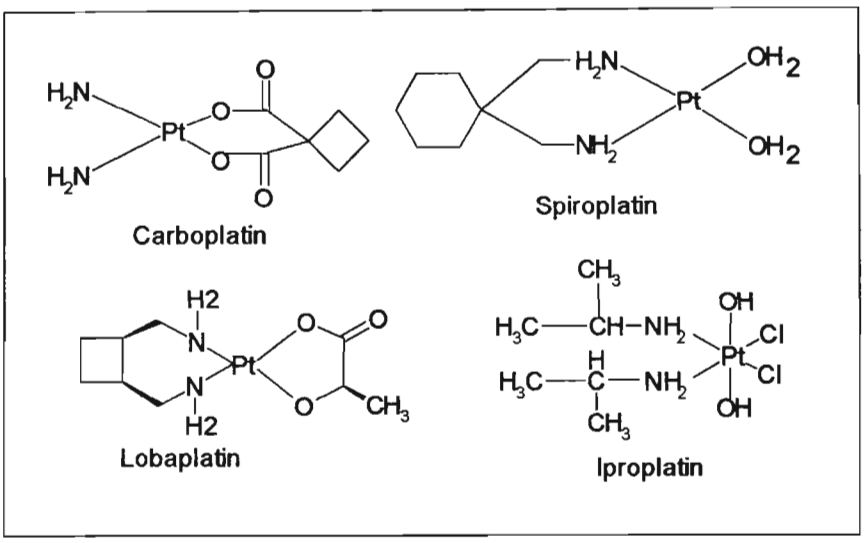

Figure 1.12 *Structures of some platinum antitumour complexes.*

Lobaplatin has shown positive activity in treating larger cell carcinomas in lung, stomach, breast, and ovarian cancers while spiroplatin was found to be inferior in humans.[95]

The early research linked the antitumour activity to the structures of the complexes. Clare and Hoeschele developed structure-activity relationships (SAR) based on the new platinum drug complexes.[7] The SAR required that for the platinum complex to have antitumour properties it had to exhibit the following structural features:[5, 9, 15, 70, 96, 107, 111]

a) The two amine groups must have *cis*-geometry with a general formula $[Pt(X_2)(Am)_2]$ for Pt(II) and $[Pt(X_2)(Y_2)(Am)_2]$ for Pt(IV) complexes with X and Y as the other ligands.

b) The ligand X had to be an anion preferably consisting of groups that have intermediate binding strength to Pt(II), for example Cl^-, SO_4^{2-} but not ClO_4^- or NO_3^- because of their highly toxic nature. Furthermore, X had to have a weak *trans* effect to avoid labilizing the amine. Complexes with inert leaving groups were generally regarded to be inactive. In the case of Pt(IV), the Y group was often preferred to be OH^-.

c) The amine group, in the form of a monodentate or bidentate ligand, had to have at least one N-H moiety. The requirement for the N-H moiety is not fully understood. However, it is thought to be responsible for the hydrogen bonding interactions towards DNA.

The SAR dominated the development of novel platinum drugs complexes for about 20 years.[7] Since then, a number of platinum(II) antitumour complexes which violate the SAR requirement have been reported, for example, platinum organoamides containing pyridine ligands and complexes containing bis(imidazole)ligands have shown that it is not a necessity to have hydrogen bonding interaction for platinum antitumour drugs to be active.[70, 111]

Furthermore, although the *trans*-$[Pt(NH_3)_2Cl_2]$ (transplatin) has been found to be therapeutically inactive, it has been observed that when the ammine is changed to a planar ligand such as pyridine or quinoline, the cytotoxicity of the *trans* geometry was observed to increase drammatically in comparison to that of both *cis* and *trans* isomers of $[Pt(NH_3)_2Cl_2]$.[107, 112] For example, platinum(IV) compounds with the *trans* configuration, *trans, trans, trans*-$[Pt(NH_3)(c\text{-}C_6H_{11}NH_2)Cl_2(OH)_2]$ also known as JM-335 was tested to be antitumour active.[106]

Recently the search for new antitumour platinum compounds has been based on dinuclear platinum compounds of the general formula $[\{PtCl_n(NH_3)_{3-n}\}_2(\mu\text{-}H_2N(CH_2)_x(NH_2)]^{2(2-n)+}$ where n = 0 - 3, x = 4 – 9. These have been found to be active against cell lines resistant to cisplatin.[95, 113, 114, 115] Trinuclear and tetranuclear platinum complexes are also known.[7] Qu and co-workers[116] have reported the synthesis and characterization of trinuclear platinum complexes consisting of three *cis*-Pt(ammine)$_2$ units linked together in a linear manner. These complexes have been shown to interact with DNA.[113]

As the search for new platinum antitumour drugs with high antitumour activity and less toxicity compared to cisplatin continues, intensive effort is also devoted towards the understanding of the mechanism of action of anticancer activity of cisplatin and new complexes.

1.5.1 The Mechanism of Antitumour Activity of Cisplatin

The working mechanism of cisplatin has been studied intensively by chemists as well as biologists, biochemists and medical researches over the last decade.[5, 15, 14] Various methods such as UV-visible spectrophotometry and Nuclear Magnetic Resonance (NMR)[117] have been employed to monitor the interaction of the platinum complexes with DNA. Evidence pointed out that the antitumour activity of cisplatin is related to its ability to bind to DNA.[24, 96, 98, 118, 119]

In general there are a variety of binding sites available to heavy metals on DNA.[14] Metals may covalently bind to the negative charge of the DNA bases such as purine and pyrimidine, while planar molecules such as $[Pt(terpy)(HET)]^+$ can intercalate between DNA bases.[14, 17] Cisplatin has been shown to have bifunctional binding modes with DNA whereby it cross-links between two bases on opposite strands of the DNA helix, DNA-protein cross links or intrastrand cross link between two bases on the same DNA strand as shown in **Figure 1.13**.[14]

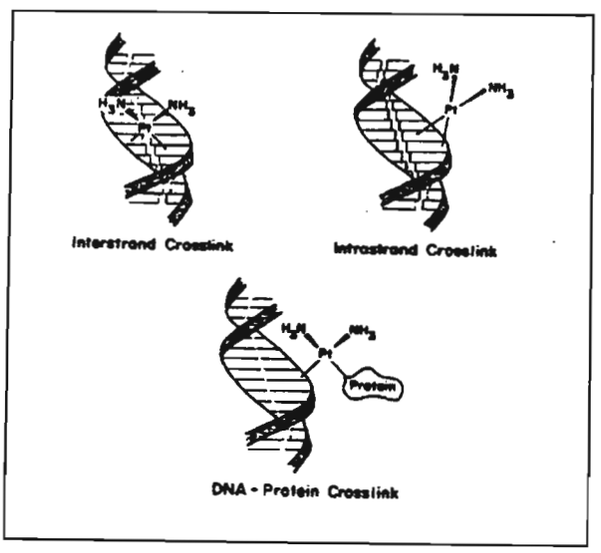

Figure 1.13 *Bifunctional binding modes of cisplatin with DNA.*

These modes of interactions have been thought to be responsible for cisplatin antitumour activity.

From *in vitro* and *in vivo* experiments it has been found that the binding of cisplatin to DNA proceeds through a sequential replacement of coordinated water by N7 atoms of guanines or adenine to form 1,2 intrastrand (GG) cross-link in 60-65 % as the major adduct.[97, 111, 117, 120, 121, 122, 123] As a result the therapeutic effect of cisplatin is believed to depend on the formation of the GG intrastrand cross-link.[124] The schematic diagram representing the binding process of cisplatin to DNA is given in **Figure 1.14**.[117]

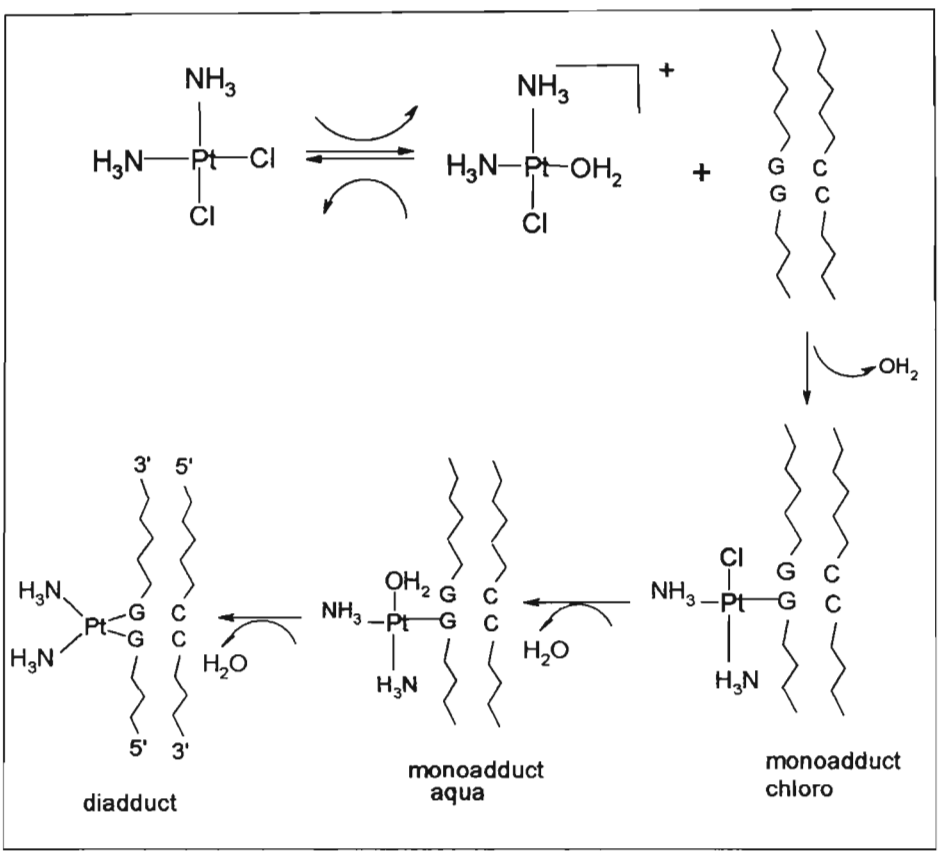

Figure 1.14 *Schematic presentation of assumed mechanism for cisplatin-DNA interactions.*

It has been suggested that when cisplatin is administered into the blood it may not be the active species, rather it is converted over a period of time to the actual drug. In aqueous solution cisplatin undergoes hydrolysis whereby the two chloride ions which are very labile are displaced by solvent molecules according to equations (1.7) and (1.8).

$$cis\text{-}[Pt(NH_3)_2Cl_2] \underset{k_{-1}}{\overset{k_1}{\rightleftharpoons}} cis\text{-}[Pt(NH_3)_2Cl(H_2O)]^+ + Cl^- \quad (1.7)$$

$$cis\text{-}[Pt(NH_3)_2Cl(H_2O)]^+ \underset{k_{-2}}{\overset{k_2}{\rightleftharpoons}} cis\text{-}[Pt(NH_3)_2(H_2O)_2]^{2+} + Cl^- \quad (1.8)$$

Martin and Lee[15] highlighted that at high pH and Pt-concentration, hydrolysis of *cis*-$[PtCl_2(NH_3)_2]$ can lead to the formation of dinuclear and trinuclear hydroxo-bridged Pt-species as shown in **Figure 1.15**. Under biological conditions these hydroxo-bridged species rarely form, and since water is a much better leaving group than chloride or hydroxo, the aqua species are suspected to be the most likely to react with the DNA.[14]

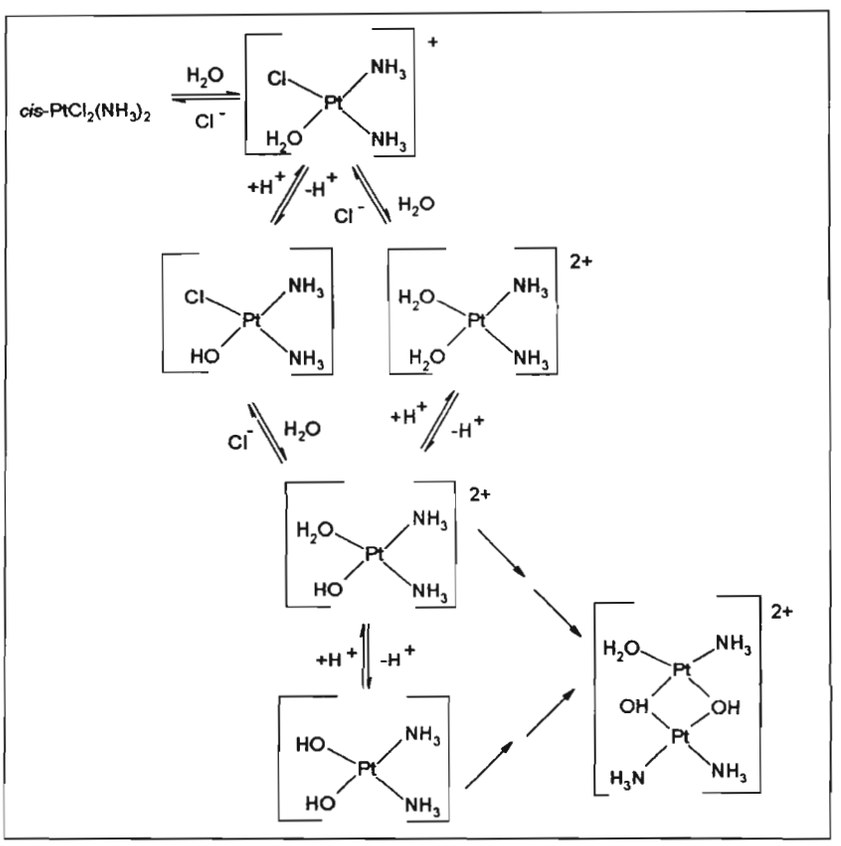

Figure 1.15 *Hydrolysis scheme of cisplatin.*

The process of hydrolysis is more favoured inside the cells than outside the cells. This results from the fact that at high pH, in aqueous solution cisplatin will loose Cl^- and an aqua and/or hydroxo ligand becomes coordinated. Outside the cell there is high concentration of Cl^- (approximately 100 mM, whereas inside the cell the $[Cl^-]$ is about 4 mM) [14, 25], and as a result hydrolysis is largely prohibited.[15]

The *in vitro* kinetic experiments have shown that the first step towards the binding of cisplatin with the DNA is first order with a rate constant corresponding to the hydrolysis of *cis*-$[Pt(NH_3)_2Cl_2]$ to *cis*-$[PtCl(NH_3)_2(OH_2)]^+$.[117] Hence, hydrolysis of cisplatin is the rate-determining step, controlling the time dependence of platinum binding to DNA.[14, 15, 71, 64] The rate constants for the first and second hydrolyses as represented by equations (1.7) and (1.8) have been determined to be $k_1 = 2 \times 10^{-5}$ and $k_2 = 3 \times 10^{-5}$ s^{-1}, respectively.[14]

The formation of a diadduct from the interaction of the Pt-complex and DNA causes a distortion of the double helix, which leads to the disruption of the cellular replication.[14] Studies on the binding mode of transplatin to DNA, revealed that *trans*-$[Pt(NH_3)_2Cl_2]$ has a different DNA binding mode from that of cisplatin. Transplatin forms the 1,3 intrastrand (GNG) cross-link, which tends to rearrange to form the bifunctional interstrand adduct as shown in **Figure 1.16**. This is thought to be responsible for the therapeutic inactivity of transplatin. [125]

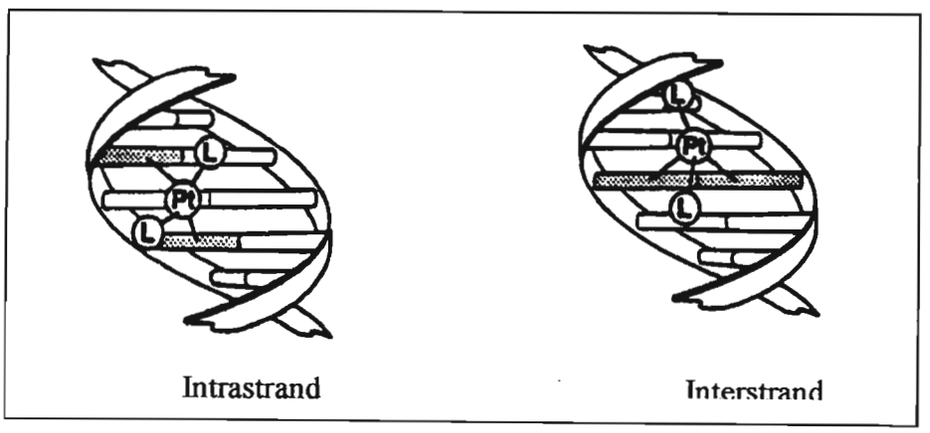

Figure 1.16 *The cross-link adducts of the trans-$[Pt(NH_3)_2Cl_2]$-DNA interaction.*

Therefore, the antitumour activities of a large number of *trans* compounds reported, which are active *in vitro* and *in vivo* could be accounted for by the isomerization of the *trans* compounds to an active *cis* isomer.[7, 14]

1.5.2 The Interaction of Pt(II) Complexes with S-donor Ligands

Due to the widespread use of transition metal complexes containing metal-sulfur bonds in biology, environment and industry, a fundamental understanding of the general chemistry

of such complexes has been the focus of investigations over the past decade.[126, 102] It has been reported that when cisplatin is administered into the blood by injection or infusion it tends to interact with the sulfur donors present in the cell before it reaches the target species (DNA). This process is illustrated in **Figure 1.17**.[120]

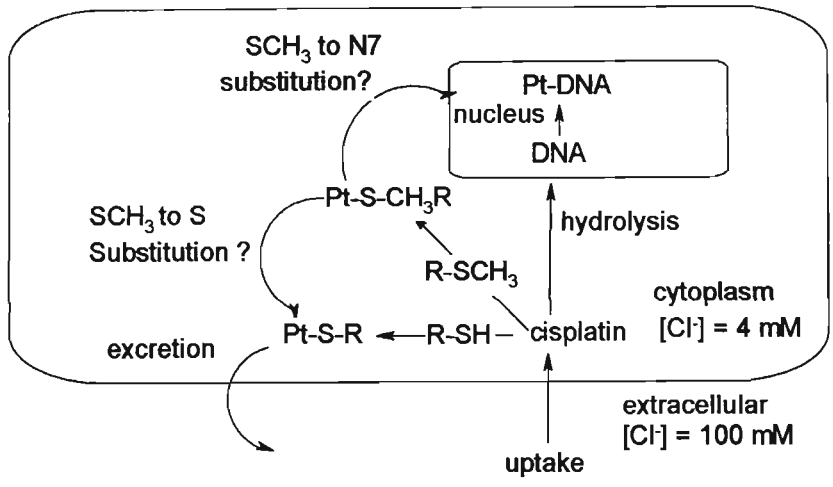

Figure 1.17 *The proposed pathway mechanism of cisplatin in vivo.*

In general S-donor ligands have a high affinity for platinum, and the Pt-S bond is relatively inert.[127] Therefore, it is expected that the reactivity of the platinum complexes with the sulfur donors will be greater than their reactivity with the nitrogen donor ligands such as adenine and guanosine. Cisplatin has been observed to react with sulfur containing biomolecules such as methionine, cysteine and glutathione to yield Pt-S products. The accumulation of these Pt-S products *in vivo* is believed to be responsible for the toxicity of cisplatin.[98, 128] The interaction between cisplatin and sulfur donors is believed to deactivate the drug before reaching the targeted DNA.

Although the interaction of the platinum compounds with the sulfur donor biomolecules has been associated with negative phenomena such as resistance and toxicity in antitumour treatment,[80] recently Reedjik[121] highlighted the importance of Pt-sulfur interaction. He suggested that such interaction could serve as a drug reservoir for platination at DNA. He further proposed two pathways towards platination of DNA. The pathways involve direct nucleophilic displacement of platinum from the sulfur by the guanine-N7 group or the spontaneous release of the platinum from the sulfur followed by the reaction with DNA.

To understand the above mentioned pathways several studies were carried out using complexes of the type $[M(NNN)Cl]Cl$, $[M(NNN)H_2O]^{2+}$ [where M is Pt or Pd and NNN denotes diethylenetriamine, terpy or bis(2-pyridylmethyl)amine] and [Pt(en)Cl]Cl.[80, 129] The complex [Pt(dien)Cl]Cl was preferentially used for these studies because it is readily available and forms relatively stable complexes with S-donor ligands.[105]

Competitive intramolecular and intermolecular studies between Pt-S of the protein bound such as cysteine and methionine residue and Pt-N mainly that of guanine–N7 bonding have been investigated.[130] Most of these studies were conducted using molecules such as S-adenosyl-L-homocysteine (SAH), S-guanosyl-L-homocysteine (SGH), methionine, methylated glutathione (GSMe), and S-methyl-glutathione (GS-Me) as the sulfur donor ligands and guanosine 5'-monophosphate (5'-GMP) as the N-donor ligand. The relatively easily available ligands such as SAH and SGH were chosen by Lempers for intramolecular studies while GS-Me and 5'-GMP were used as models for intermolecular studies.[121] **Figure 1.18** contains structures of some of these S and N donors ligands namely, SGH, SAH and GSMe. The other sulfur donors have been applied as N7-containing models for DNA.[121]

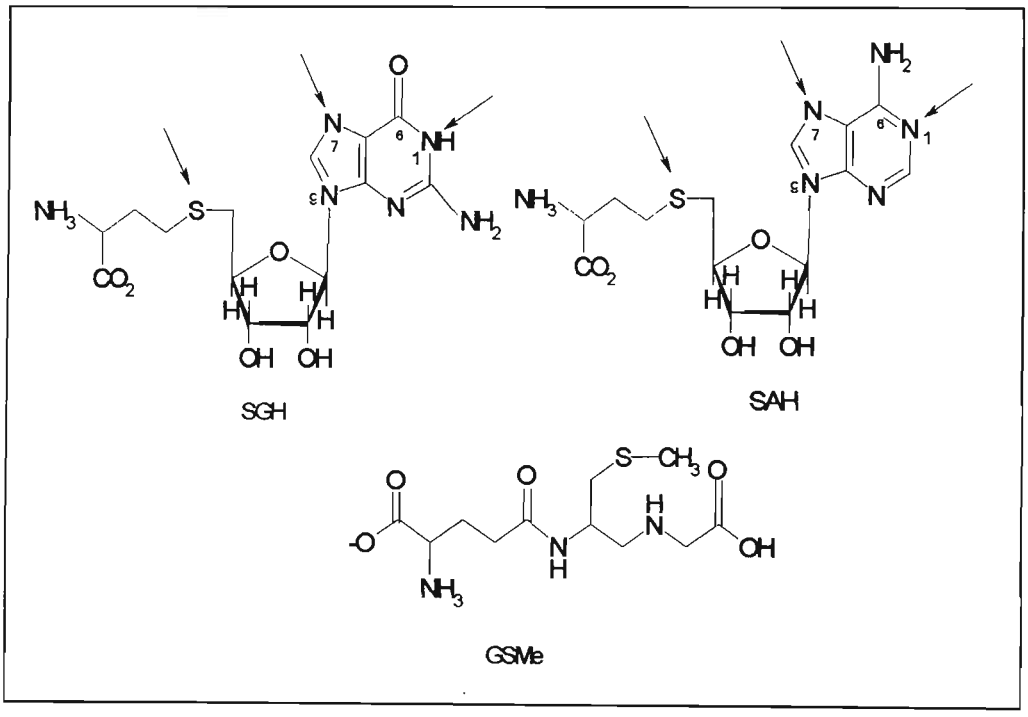

Figure 1.18 *Structures of SAH, SGH and GSMe.*

Reedjik and co-workers[129, 17] have investigated a number of reactions between $[Pt(dien)Cl]^+$ and $[Pt(dien)OH_2]^{2+}$ with glutathione (GSH), 5'-GMP and GS-Me. They found that the reaction of $[Pt(dien)Cl]^+$ with GSH occurred via a two-step reaction. The first step involves the reaction of the mononuclear unit $[Pt(dien)Cl]^+$ to the sulfhydryl group forming **(1)** in **Scheme 1.2**, and the second step involves the binding of the second mononuclear unit $[Pt(dien)Cl]^+$ to **(1)** forming a dinuclear sulfur diplatinum complex **(2)** in **Scheme 1.2**.

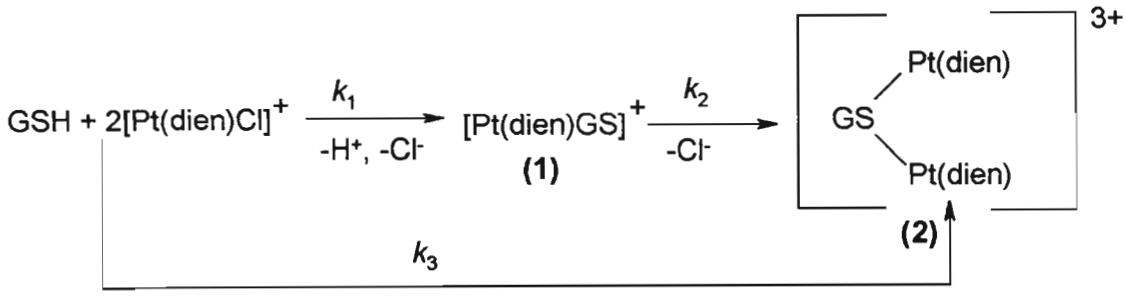

Scheme 1.2 *Reaction mechanism between the [Pt(dien)Cl]Cl and the GSH.*

This reaction was observed also to be pH dependent. The Pt complex has been shown to have a high affinity for the sulfhydryl group over the pH ranges of 2 to 12. At pH less than 7, the rate of the second platinum binding is fast compared to the first platinum binding step. At pH greater than 7 the rate constant of the first platinum binding step was observed to be faster than the second one. The reaction of SAH with an equivalent of [Pt(dien)Cl]Cl was also shown to be pH dependant. At pH less than 7, SAH platinated at the sulfur atom only to form $[Pt(dien)(SAH\text{-}S)]^{2+}$. However, this product isomerizes quickly to form $[Pt(dien)(SAH\text{-}N)]^+$ at pH greater than 7, with a half life, $t_{1/2}$, of ten minutes. When SAH was made to react with two equivalents of [Pt(dien)Cl]Cl at a pH in the range from 2 to 6.5, a dinuclear complex was also formed $[\{Pt(dien)\}_2(SGH\text{-}S,N7)]^{4+}$.

From these studies it was concluded that even if the platinum drug complexes react with the sulfur donor of a protein bound molecule, the N7 atom of the guanine intramolecularly replaces the sulfur atom in the platinum-sulfur adduct.[80] Reedjik *et al*[120] mentioned that this type of indirect DNA platination is limited to platinum-thioether adducts since platinum-thiolate adducts were shown to be unreactive towards the N-7 atom of guanine.

1.5.3 The Antitumour Protection Groups

As already mentioned, the major problem with the use of cisplatin is its toxicity, in particular its nephrotoxicity. The *cis*-Pt bonds to the sulfhydryl groups of the cysteine residue result in the deactivation of certain enzymes. This is the source of the nephrotoxicity of cisplatin.[121, 80] This problem was reduced by using the cisplatin analogue carboplatin, which unfortunately also has clinical limitations.

In order to reduce the toxicity of the platinum antitumour drugs, the so called "rescue agents or protecting groups" have been developed. These compounds contain sulfur donors, and are co-administrated with the antitumour drug without affecting the drug antitumour activity.[4, 27, 30, 47] Examples of these protecting groups include sodium diethyldithiocarbamate (Naddtc), sodium thiosulfate (STS), and thiourea (TU) as shown in **Figure 1.19**.[105]

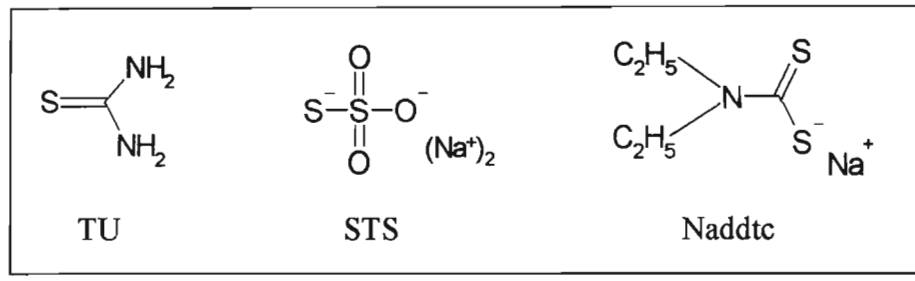

Figure 1.19 *Some protecting groups for the platinum antitumour drugs.*

The study by Allu *et al* [131] involving rats proved that both *trans*- and *cis*-Pt complexes do bind to thiol groups of proteins. They showed that the addition of 2-mercaptoethanol prevented the binding process but did not reverse it. This outcome led Borch and Pleasants[121] to suggest that the sulfur compounds shown in **Figure 1.19** (*i.e.* the rescue agent) might play a role in reducing the toxicity of Pt-complexes in the treatment of tumour cells. The protective effects of these compounds are due to the prevention or reversal of Pt-S adducts in proteins.

Reactions of these rescue agents with Pt(II) complexes have been reported.[7, 27, 132]. The rate constants for the reaction of $[Pt(dien)Cl]^+$ with Naddtc, thiourea and STS were found to decrease in the order: Naddtc > thiourea > STS. The result supports the findings that Naddtc is the most effective rescue agent. It is documented that STS reduces

nephrotoxicity, between the period of 1 hour prior and 0.5 hour after cisplatin administration, while Naddtc is effective between 1-4 hours after administration.

PART B Substitution Reactions of Ru(II) Polypyridine Complexes

1.6 The General Chemistry of Ruthenium Complexes

Ruthenium belongs to Group 8 in the periodic table along with osmium and iron. It has [Kr] $4d^7$ $5s^1$ electronic configuration. Although, ruthenium is rare, it is the least expensive of the platinum group metals (PGM)[9], the other PGM's being platinum, osmium, palladium, iridium and rhodium. Furthermore, it is commercially available in several forms. The chemistry of ruthenium more closely resembles that of osmium than that of iron.[10]

Ruthenium forms complexes of different oxidation states and geometries with various ligands. Examples of some of these complexes include $[Ru^0(CO)_5]$, $[Ru^{II}HCl(PPh_3)_2]$, and $[Ru^{III}(terpy)Cl_3]$ and KRu^VF_6 with geometries of trigonal bipyramidal for the first and second complex and octahedral for the last two complexes.[10] Synthesis of most of these complexes begins with $[(NH_3)_6Ru]Cl_3$ or $RuCl_3{\cdot}3H_2O$ which is actually a soluble mixture of Ru(III) and Ru(IV) complexes rather than a pure Ru(III) complex.[9]

In aqueous solution only Ru(II) and Ru (III) predominate, and the most stable complexes are those containing N-donor ligands.[9] As a result the coordination chemistry of ruthenium complexes containing nitrogen donor ligands such as terpyridine, bipyridine, and ammonia has received much attention over the past decades. Most of these complexes have found potential use in various areas such as in the development of several branches of chemistry, for example, in photophysics and photochemistry, [133, 134] electrochemistry,[135, 136, 137] electron transfer[138, 139] and in establishment of the *trans*-labilizing order for ligands (L) in octahedral complexes[9]. Some of the ruthenium complexes such as *cis*-$[Cl_2(NH_3)_4Ru^{III}]Cl_2$ and (HIm)[*trans*-$(Im)_2Cl_4Ru^{III}$] (Im is imidazole) have shown a direct correlation between cytotoxicity and DNA binding and hence are representative of ruthenium ammine anticancer compounds.[140]

Most ruthenium(II) complexes containing polypyridine ligands such as terpy, bipy and phen are associated with strong metal to ligand charge transfer (MLCT), charge transfer absorptions and long lived excited states.[141] As a result, ruthenium(II) polypyridine complexes have been used as chromophores for the study of photoinduced electron and energy transfer in molecular assembles and signaling subunits.[142, 143]

Recently, ruthenium(II) complexes containing polypyridine ligands such as $[Ru(phen)_3]^{2+}$ (phen = phenathroline), $[Ru(bipy)(dppx)]^{2+}$ (dppx = 7, 8-dimethyldipyridophenazine) and bipy = bipyridine) and $[Ru(bipy)_2DPPZ]$ (DPPZ = dipyrido[3,2-a:2',3'-c]phenazine) have been reported to act as "molecular light switches".[144, 145, 146] In aqueous solution the luminescence of these complexes was completely quenched, whereas in the presence of DNA they gave an intensive luminescence.

Dinuclear ruthenium(II) polypyridine complexes such as $[\{Ru(phen)_2(\mu\text{-HAT})\}_2]$ where HAT is 1,4,5,8,9,12-hexaazatriphenylene have also been found to enhance the luminescence slightly in the presence of DNA and the luminescence was increased intensively in the presence of denatured DNA. As a result these kinds of complex have found application as probes for the structure of denatured DNA.

Ruthenium(II) polypyridine complexes have also proven useful as precursors for high valent oxo complexes, which in turn are potent and efficient oxidants.[147, 148, 149, 150] Ruthenium high valent oxo complexes such as $[Ru(terpy)(bipy)O]^{2+}$ have been shown to be capable of oxidizing most organic substrates[151] such as olefins to epoxides[152], polyfunctional molecules such as carbohydrates[153, 154] and alcohols to corresponding aldehydes. It has been long established that most high valent oxo transition metal complexes are capable of acting as oxidants, common examples include MnO_4^-, RuO_4^- and CrO_3.[155]

The laboratory efficiency of these oxidants is hampered mainly by their lack of selectivity, which results in poor product yield and also by their impractical use as catalysts.[156] For example, to oxidize alcohols to their corresponding aldehydes or ketones without any further oxidations to carboxylic acids, the reagents required are extremely dangerous or harmful *e.g.* CrO_3 and in other cases high temperature, strong acids or bases are required to facilitate the oxidation process. High valent ruthenium polypyridine oxo complexes

offer several advantages towards oxidation of hydrocarbons. These include: high selectivity in the reactions and the reactions are easy to carry out and can be conducted under mild conditions.[157, 158]

Thorp and colleagues[159] have also demonstrated the ability of the oxoruthenium complex $[Ru(terpy)(bipy)O]^{2+}$ to act as an efficient DNA cleavage reagent. They have reported that the cleavage reaction can be carried by direct treatment of DNA with the active oxo form or it can be performed by electrolysis at a certain pH and potential. The cleavage of DNA using $[Ru(terpy)(bipy)O]^{2+}$ is summarized in **Figure 1.20**[159] below.

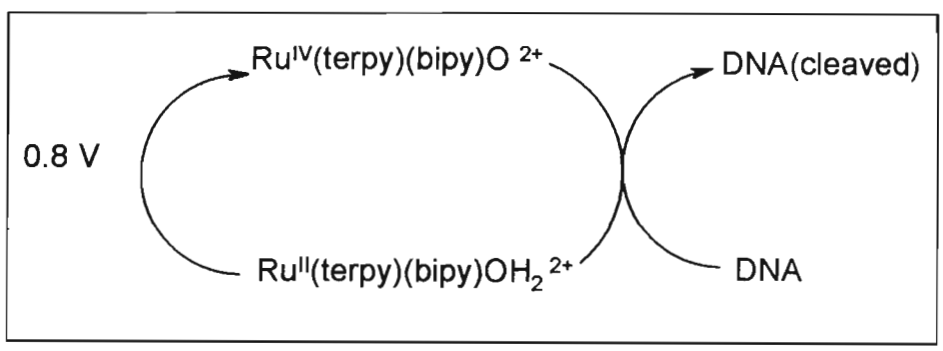

Figure 1.20 *Catalytic electrolysis reaction for the cleavage of DNA with* $[Ru(terpy)(bipy)O]^{2+}$.

In order for DNA cleavage to take place there must be excess Ru(II) present. The other ruthenium polypyridine oxo complexes which have been shown to cleave DNA are $[Ru(terpy)(tmen)O]^{2+}$ (tmen = *N,N,N',N'*-tetramethylethylenediamine), $[Ru(terpy)(pyz)O]^{2+}$ (pyz = pyrazine) and $[Ru(terpy)(phen)O]^{2+}$ (phen = phenathroline).[159]

Some ruthenium(II) polypyridine complexes have found use as probes for nucleic acid structure and sites and in the understanding of the mechanism of action of the ruthenium antitumour drugs with DNA.

1.7 Substitution Reactions on Octahedral Complexes

The octahedral geometry is by far the most common ligand arrangement in six-coordinate chemistry.[11] This geometry is the favoured arrangement for the d^3 and low-spin d^6 configuration. It is also very common for other configurations of d-block metal ions such

as d^4 and d^9. The octahedra of the d^4 and d^9 do show distortion towards tetragonal due to Jahn-Teller distortion or towards trigonal prism due to the presence of bidentate ligands such as oxygen and sulfur donor ligands.[11] These kinds of distortions can exert a profound effect upon the reactivity of the system.

Due to the different geometries expected for the six-coordinated complexes, and the different oxidation states different modes of substitution reactions can be expected. However, the bulk of information on octahedral substitution reactions points out that these reactions involve mostly an intermediate mechanism (I_d).[1, 11] Recently it has been found that the associative mode of activation may be possible for a range of geometries for such transition states.[11]

Various theories have been applied to explain the reactivity trend of octahedral complexes. These include the valence bond, crystal field and molecular orbital theory.[11, 160] The valence bond theory is based on the energy difference between the t_{2g} and e_g orbitals of the metal ion. The metal ion that is labile is described as the one containing an empty low energy t_{2g} orbital or at least one electron in a high energy e_g orbital.

The crystal field theory is based on the calculation of the energies of valence d-orbitals of possible transition states for the substitution reactions. The crystal field stabilization energy (CFSE) for the ground state and the intermediate are calculated and their difference is determined which gives the crystal field activation energy (CFAE) for the particular reaction. The CFSE calculation suggests that the order of reactivity is in the order: (d^4, d^9) > (d^2, d^7) > (d^1, d^6) > (d^0, d^5, d^{10}) > (d^3, d^8).

The molecular orbital model is concerned with the extent to which the ligand based orbitals are stabilized and metal based orbitals are destabilized as a result of overlap for both the ground state and the transition state. In the case where there is no π-interaction with suitable ligand orbitals, there is no disturbance of the extent of σ-bonding resulting from the interaction of occupational metal based orbital with the π-symmetry. In the case where the occupational metal based orbital interacts with the σ-symmetry, the stability of the complex becomes reduced owing to the antibonding character of these orbitals.

Substitution reactions of the octahedral transition complexes cannot be comprehensively defined as they are for square-planar complexes. The most information gathered regarding substitution reactions at an octahedral metal centre is for Co(III), Cr(III) and Ni(II) complexes.[1] It is well accepted that substitution reactions on octahedral complexes do not possess a nucleophilic discrimation that equals that found in the associative reactions of square-planar d^8 metal complexes.[11]

Under pseudo first-order reactions, for the reactions under neutral conditions the rate is dependent on the concentration of the entering ligand (L) at low ligand concentration and independent at higher concentration of (L). These two conditions can be described by equations (1.9) and (1.10).

$$M\text{-}H_2O \underset{k_{-1}}{\overset{k_1}{\rightleftharpoons}} M + H_2O \qquad (1.9)$$

$$M + L \overset{k_2}{\rightleftharpoons} M\text{-}L \qquad (1.10)$$

These equations give the following rate law (1.11)

$$rate = \frac{k_1 k_2 [M - H_2O][L]}{k_{-1}[H_2O] + k_2[L]} \qquad (1.11)$$

The term $k_{-1}[H_2O]$ is constant since the reactions are carried out in water. The mechanism described by equation (1.9) and (1.10) is a dissociative mechanism. In the case of an interchange dissociative mechanism, equations (1.9) and (1.10) can be represented by equations (1.12) and (1.13) and it follows that the rate law is given by (1.14).

$$M\text{-}H_2O + L \overset{K}{\rightleftharpoons} M\text{-}H_2O, L \qquad (1.12)$$

$$M\text{-}H_2O, L \overset{k}{\rightleftharpoons} M\text{-}L, H_2O \qquad (1.13)$$

$$rate = \frac{k_1 K[M - H_2O][L]}{1 + k_2[L]} \qquad (1.14)$$

Most substitution reactions on octahedral transition metal complexes have been reported to depend on the spectator ligands that surround the metal centre, the leaving group X, and the charge of the metal ion.[1] The dependence of the rate on the leaving group is enough evidence that substitution reactions on the octahedral complexes favour a dissociative mechanism over an associative mechanism. Furthermore, the activation parameters are frequently consistent with a dissociative mechanism.

It has been found that an increase in the charge on the complex leads to a decrease in the rate of substitution, while steric crowding increases the rate of the reaction and that the rates for the different leaving groups correlate with the bond strength. The effect of the incoming ligand L on the rate of the reaction is less significant than in the case of square-planar complexes. Unlike in the case for square-planar complexes the kinetic *trans* effect for the octahedral complexes is not fully understood, with the exceptions of chromium(III) and rhodium(III).[161] The kinetic *trans* effects for these two metal ions based on the data obtained for the aquation of coordinated aquachlororhodium(III) and aquachlorochromiun(III) complexes was observed to follow an order:

$$OH_2 < NH_3 < Cl^- < Br^- < I^-$$

It is clear that there is limited information concerning the substitution reactions of octahedral complexes when compared to that of square-planar complexes.

1.8 Substitution Reactions of Ruthenium Complexes

The most studied substitution reactions of ruthenium complexes involve those complexes with ruthenium in oxidation states (II) and (III), in particular Ru(II).[162] Most studies regarding the substitution reactions of Ru(II) deal with complexes of the type $[Ru(NH_3)_5X]^{2+}$.[163, 164] The second order rate constants for the substitution reaction of $[Ru(NH_3)_5X]^{2+}$ where $X = H_2O$ with various neutral ligands at 25 °C has been found to fall in the range between 2.7 to 302 x 10^{-3} $M^{-1}s^{-1}$.[165, 166]

Taube and co-workers have shown that substitution reactions of ruthenium(II) complexes proceed via a dissociative interchange mechanism.[167, 168] An attempt to enhance the lability of the water molecule in $[Ru(NH_3)_5OH_2]^{2+}$ was made by replacing one of the ammine ligands with a new ligand L to form $[Ru(NH_3)_4L(OH_2)]^{2+}$, where L represents CO, N_2, isonicotinamide (isn), pyridine (py), CN^- or SO_3^{2-}. Isied and Taube[169] have reported the rate of substitution of the water molecule from *cis*- and *trans*-$[Ru(NH_3)_4L(OH_2)]^{2+}$ with isonicotinamide. Their results revealed that these reactions follow a dissociative mechanism, and that for both the *cis* and the *trans* complexes, the second order rate constant, increased from 10^{-6} to 10^{-1} M^{-1} s^{-1} in the following L order: CO < N_2 < isn < py.

In general the reactivity and stability of the transition metal complexes depend on the oxidation state of the metal as well as the stereoelectronic properties of the ligand around the metal centre.[170] Davies and Mullins[171] have studied the conjugation effect of ligands such as terpy, bipy and phen on the rate of substitution of X from complexes such as $[Ru(terpy)(bipy)X]^+$ and $[RuX_2bipy_2]$ (X = Cl^- or Br^-) in aqueous solution. They found that the substitution reactions of these complexes occur via extremely rapid formation of the aquaamines. Furthermore it has been found that the substitution of the aqua group by NO_2^- and N_3^- occurs by a measurably slow process at room temperature and the reactions were not base catalysed.

Allen and colleagues have also reported the rate of substitution of the water molecule from *cis* and *trans*-$[Ru(NN)_2(H_2O)X]^{2+}$ where NN denotes bipy or phen and X = SO_2, PPh_3, H_2O, CH_3CN and CO. [172] For both the *trans* and *cis* isomers, the second-order rate constants for the substitution of water by acetonitrile were found to depend on the type of X ligand with the order of reactivity being: SO_2> PPh_3 > H_2O > CH_3CN > CO. No specific *trans* effect was noted, but the rate constants for substitution in the *cis* isomers were found to be greater than those for substitution in the corresponding *trans* isomers by a factor of 10.

Studies looking at the ligand steric effects by Bessel and co-workers [170] on ruthenium(II) polypyridine complexes of the form $[Ru(H_2O)(NN)(terpy)]^{2+}$ where NN = 2,2'-bipyridine (bipy), 1,10-phenathroline (phen), 4,7-dimethyl-1,10-phenathroline (4, 7-Me_2phen), 2,9-dimethyl-1,10-phenathroline (2,9-Me_2phen), 2,2'-biquinoline (biq) and 6,6'-dichloro-2,2'-

bipyridine (6,6'-Cl_2bipy) and terpyridine(terpy) have been carried out. The rate constants for the substitution of the aqua ligand using acetonitrile were determined for $[Ru(H_2O)(NN)(terpy)]^{2+}$ and a series of $[Ru(H_2O)(bipy)_2(PR_3)]^{2+}$, where R = Me, Et, *p*-$C_6H_4F$, C_6H_5, *p*-$C_6H_4CH_3$, *p*-$C_6H_4OCH_3$ at 25 °C. The steric effect of $[Ru(H_2O)(NN)(terpy)]^{2+}$ was determined by using the same equation used for $[Ru(H_2O)(bipy)_2(PR_3)]^{2+}$ complexes in determining the cone angles of the six bidentate bipyridyl ligands (NN), hence these cone angles represented the first quantitative estimates of steric ligand effects for bidentate bipyridyl ligands.

A remarkable increase in the rate of substitution of Ru(II) by a factor of 1.9×10^{7} was reported recently by Huynh *et al.*[167] The ruthenium (II) complex investigated contained what is known as "scorpion ligands" namely poly(pyrazol-1-yl)alkanes and poly(pyrazol-1-yl)borates which can act as tridentate or bidentate ligands.

1.9 The Biological Importance of Ru(II) Complexes

Due to the fact that ruthenium is a platinum group metal and in its lower oxidation states exhibits a high affinity for nitrogen ligands, it was suggested that some of its complexes may exhibit antitumour activity.[9] Ruthenium amine antitumour drug complexes such as $[Cl_2(NH_3)_4Ru^{III}]Cl_2$ and (HIm)[*trans*-$[(Im)_2Cl_4Ru^{III}]$ have since been discovered. The advantages in using transition-metal ions other than platinum include additional coordination sites, change in oxidation state, alterations in ligand affinity and substitution kinetics and lastly photodynamic approaches to therapy.[140]

Various ruthenium(II) complexes have been synthesized and screened for their antitumour activity. Complexes such as the α-isomer of the dichlorobis(2-phenylazopyridine)ruthenium(II), α-$[Ru(azpy)_2Cl_2]$ have shown remarkably high cytoxicity against a series of human tumour cell lines.[173] The complex mer-$[Ru(terpy)Cl_3]$ where (terpy = 2,2':6',2"-terpyridine) has also been found to exhibit antitumour activity midway between that of cisplatin and carboplatin in the L120 cell line and is cytotoxic against human cervix carcinoma.[140]

There is evidence that indicates that the coordination of ruthenium amine complexes to nucleic acids could be occuring in a fashion similar to that of diamineplatinum complexes.[9] The ultimate target for antitumour active ruthenium complexes is reported to be DNA as it is in the case of antitumour-active platinum complexes.[140]

1.9.1 Interactions of Ru(II) Complexes with DNA

Studies regarding the interaction of DNA with inert transition metal complexes were investigated by a number of researchers in the hope of developing new probes for three dimensional nucleic acid structure (*i.e.* sequence and conformations) and sites, DNA mediated electron transfer, understanding the mechanism of action of antitumour ruthenium drugs and new therapeutic agents.[174, 175, 176, 177]. Ruthenium(II) polypyridine complexes such as $[Ru(phen)_3]^{2+}$, $[Ru(bipy)_3]^{2+}$, $[Ru(phen)_2BZZP]^{2+}$, $[Ru(bipy)_2DPPZ]^{2+}$ and $[Ru(bpy)_2(dppx)]^{2+}$ where BZZP, DPPZ and dppx stand for (benzodipyrido[*a:3,2-h:2',3'-j*]phenazine), (dipyrido[3,2-a:2',3'-c]phenazine) and (7,8-dimethyldipyridophenazine) respectively, have proven to be useful substrates.

The ability of $[Ru(phen)_3]^{2+}$ to bind to DNA was recognized first by Barton and her colleagues.[176] They have since proposed two ways in which this complex can bind to DNA, namely; by intercalation which causes the DNA duplex to unwind or by surface interaction. In general most of the ruthenium complexes containing α-diimine type ligands have been shown to bind to DNA by intercalation.[178] When ruthenium complexes containing planar aromatic ligands bind to DNA, they have various advantages. These include:

1) the ease with which the metal can be attached to the ligand in a controlled manner.
2) strong visible absorbance, due to localized MLCT.
3) luminescent characteristics, in particular their strong fluorescence
4) perturbation on binding to the DNA.

The binding of $[Ru(phen)_3]^{2+}$ to the DNA double helix is associated with an increase in the luminescence, which is thought to result from the emission due to MLCT of the excited state decaying with two different lifetime states. One of these emissions is due to intercalation (2 μs) process while the second one is from the surface bound (0.6 μs). The

binding constant of $[Ru(phen)_3]^{2+}$to calf thymus DNA was measured to be 6.2 x 10^3 M^{-1}. Although a large amount of work has been reported regarding the binding mode of $[Ru(phen)_3]^{2+}$ to DNA either by intercalative or surface interaction, the binding mode of this complex to DNA is not yet fully understood.[179]

Novel ruthenium(II) polypyridine complexes have been synthesized and characterized in terms of their binding to DNA. Of remarkable interest were complexes of the type $[Ru(NN)_2X]^{2+}$ where NN denotes bidentate phen or bipy and X denotes the ligands DPPZ or DPP (2,3-di-2-pyridylpyrazine). These complexes were observed to act as molecular light switches.[145, 180, 181] In aqueous solution the luminescence of the complexes was completely quenched.[182] In the presence of the DNA these complexes showed an intense luminescence.

The binding constants for these complexes to DNA are in the range of approximately 10^6 M^{-1}. They also bind to DNA by intercalation with the DPPZ ligand intercalating between the stacked base pairs. Further, these complexes have been shown to be capable of promoting oxidative DNA damage. Electron transfer reactions with DNA are essential since they provide a way of characterizing oxidative damage to the double helix. This process requires a proper stacking of the π-orbitals of the heterocyclic nucleobases. When the DNA π arrays are properly stacked, it mediate the guanine oxidation at sites 200 Å from a remotely bound oxidant[183, 184]

Like the diamineplatinum anticancer compounds, the complex *trans*-$[Cl_4(Im)_2Ru]^-$ undergoes stepwise aquation by sequential loss of two chlorides at an initial rate of 9.6 x 10^{-6} s^{-1} at 25 °C, which is accompanied by a drop in pH which may be due to proton loss from the corresponding aqua complexes.[140] For some ruthenium complexes such as cis-$[Cl_2(Me_2SO)_4Ru]$ which has been shown to inhibit both primary tumour growth and metastases of B16 melanoma in mice, the substitution rates for the chloride were found to be similar to those of cisplatin and hence the mechanism of action of this complex is thought to be similar to that of cisplatin.[140]

1.10 Aims of the Project

This project is divided into three parts having three different aims as shown below:

Part (i)

The high affinity of platinum compounds for sulfur atoms and their biological importance has attracted lots of interest among chemists, biochemists, biologists and medical researchers. Questions such as 'why does cisplatin reach guanine-N7 with competing S-donor ligands available in the cell?' have been asked. The early papers focused on the negative phenomena resulting from the interaction between Pt-metal and sulfur containing biomolecules. These phenomena include aspects such as resistance and toxicity in the antitumour treatment. However, in search for an answer to the above question sulfur-containing compounds are currently under investigation as "protecting agents" to ameliorate the side effects of platinum therapy. These include compounds such as glutathione, cysteine, penicillammine, S-2-(3-(aminopropyl)amino)ethylphosphorothioic acid, sodium diethyldithiocarbamate and WR-2721 which is already registered in a number of European countries. Therefore, understanding the interactions between the platinum complexes and sulfur-containing biomolecules is of crucial importance from a biological and medical point of view. The first aim of this project was to synthesize and characterize two platinum complexes namely, $[Pt(terpy)(OH_2)]^{2+}$ and $[Pt(bpma)(OH_2)]^{2+}$, investigate their substitution reactions with the following sulfur donor ligands, L-cysteine, DL-Penicillamine and glutathione, and to compare their reactivities.

Part (ii)

In most textbooks dealing with inorganic reaction mechanisms the rates of water exchange on aquated metal ions are used to demonstrate that the reactivity of many platinum(II) complexes is a factor of 10^5-10^6 lower than that of the corresponding palladium(II) complexes. This reactivity difference can strongly depend on the co-ordination environment, as well as on the nature of the entering and leaving ligands. The objectives of this part of the project were to synthesize and characterize $[Pd(bpma)(OH_2)]^{2+}$, then investigate the substitution reactions of $[Pd(bpma)(OH_2)]^{2+}$ using stopped flow technique with the following nucleophiles, TU, DMTU and TMTU. The reactivity of this palladium complex was then compared with that of $[Pt(bpma)(OH_2)]^{2+}$ studied in part (ii) using the

same nucleophiles. The underlying aim was to compare their reactivities and to try and understand how the π-back bonding present on the co-ordinated ligand will influence the reactivity.

Part (iii)

Ruthenium(II) polypyridine complexes are a potential basis for the development of new families of non-radioactive luminescent probes for DNA sequences. Their development depends on the knowledge and understanding of their reactivity as well as the nature of their binding to DNA. It was therefore the aim of this point of the project to synthesize and characterize Ru(II) polypyridine complexes namely, $[Ru(terpy)(bipy)(OH_2)](ClO_4)_2$ and $[Ru(terpy)(tmen)(OH_2)](ClO_4)_2$ and then to investigate their substitution kinetics with the following nucleophiles: acetonitrile, DMTU and TU for the purpose of elucidating the reaction mechanism.

REFERENCES

1) J. D. Atwood, *Inorganic and Organometallic Reaction Mechanisms*, 2nd Edition, Wiley – VCH, Inc, New York, **1997**, 43, 57, p 80-81.

2) R.G. Wilkins, *Kinetics and Mechanism of Reactions of Transition Metal Complexes*, 2nd Edition, New York, **1991**, p 232.

3) F. Basolo and R. G. Pearson, *Mechanisms of Inorganic Reactions, A study of Metal Complexes in Solution*, 2nd Edition, John Wiley and Sons, Inc., **1967**, p 351, p 406.

4) U. Belluco, *Organometallic and Coordination Chemistry of Platinum*, Academic Press, London, **1974,** p 1, p 5, p 20.

5) M. Bennett, L. Kwan, A. D. Rae, E. Wenger and A. C. Willis, *J. Chem. Soc., Dalton Trans.*, **2002**, 226.

6) G. Annibale, L. Cattalini, A. Cornia, A. Fabretti, and F. Guidi, *Inorganic Reaction Mechanisms*, **2000**, *2(3)*, 185.

7) E. Wong and C. M. Giandomenico, *Chem. Rev.*, **1999**, *99*, 2451.

8) B. Pitteri, G, Marangoni and L. Cattalini, *Polyhedron*, **1995**, *17-18*, 2331.

9) H. Sigel, *Metal ions in biological systems, metal complexes as anticancer agents*, M. Dekker, **1980**, 9, 11, 64, 241-2.

10) F. A. Cotton, G. Wilkinson, *Advanced Inorganic Chemistry*, 5th Edition, John Wiley & Sons, New York, **1988**, 919.

11) M. L. Tobe, *Inorganic Reaction Mechanisms*, Addison Wesley Longman Limited, New York, **1999**, 71.

12) J. K. Burdett, *Inorg. Chem.*, **1977**, *16*, 12.

13) E. L. J. Breet, R. van Eldik, *Inorg. Chem.*, **1984**, *23*, 1865.

14) S. E. Sherman and S. J. Lippard, *Chem. Rev.*, **1987**, 1153.

15) J. Reedjik, A M. J. Fichtiger-Schepman, A.T. van Oosterom and P. van de Putte, *Structure and Bonding, Platinum Ammine Coordination Compounds as Anti-Tumour Drugs, Molecular Aspects of the Mechanism of Action*, **1987**, *67*, 53.

16) M. I. Djuran, E. L.M. Lempers and J. Reedjik, *Inorg. Chem.*, **1991**, *30*, 2648.

17) S. J. Lippard, *Acc. Chem. Res.*, **1978**, 211.

18) S. E. Miller, K. J. Gerard, and D. A. House, *Inorg. Chim. Acta.*, **1991**, *190*, 135.

19) S. Al-Baker, and J. C. Dabrowiak, *Inorg. Chem.*, **1987**, *26*, 613.

20) T. G. Appleton, R. D. Berry, C. A. Davis, J. R. Hall, and H. A. Kimli, *Inorg. Chem.*, **1984**, *23*, 3514.

21) A. W. Roszak, O. Clement and E. Buncel, *Acta Cryst*, **1996**, *C25*, 1645.

22) E. L. M. Lempers and J. Reedjik, *Inorg. Chem.*, **1990**, *29*, 217.

23) A. Passini and M. Moroni, *J. Chem. Soc., Dalton Trans.*, **1997**, 1093.

24) J. Teuben, S. S. G. E. van Boom and J. Reedjik, *J. Chem. Soc., Dalton Trans.*, **1997**, 3979.

25) S. J. Berners-Price, T. A. Frenkiel, U. Frey, J. D. Ranford, and P. J. Sadler, *J. Chem. Soc., Chem. Commun.*, **1992**, 789.

26) R. Romeo, A. Grassi, and L. M Scolaro, *Inorg. Chem.*, **1992**, *31*, 4383.

27) U. Fekl and R. van Eldik, *Eur. J. Inorg. Chem.* **1998**, 389 (is there a comma after R)

27) H. Yip, L. Cheng, K. Cheung, and C. Che, *J. Chem. Soc. Dalton Trans.* **1993**, 2933.

29) M. Cusumano, M. L. Di Pietro and A. Giannetto, *Chem. Commun.*, **1996**, 2527.

30) K. R. Koch, C. Sacht and C. Lawrence, *J. Chem. Soc. Dalton Trans.*, **1998**, 689.

31) J. G. Collins, R. M. Rixon and J. R. Aldrich-Wright, *Inorg Chem.* **2000**, *39*, 4377.

32) F. P. Cavasino and C. Sbrizilo, *J. Chem. Soc., Faraday Trans.1*, **1989**, *85(12)*, 4237.

33) L.E. Erickson, H. L. Erickson, and T. Y. Meyer, *Inorg.Chem.*, **1987**, *26*, 997.

34) T. G. Applenton, R. D. Berry, C. A. Davis, J. R. Hall and H. A. Kimlin, *Inorg. Chem*, **1984**, *23*, 3514.

35) S. Cosar, M. B. L. Janik, M. Flock, E. Freisinger, E. Farkas and B. Lippert, *J. Chem. Soc., Dalton Trans.*, **1999**, 2329.

36) K. W. Jennette, J. T. Gill, J. A. Sadownick, and S. J. Lippard, *J. Am. Chem. Soc.*, **1976**, 6159.

37) M. Howe-Grant, K. C. Wu, W. R. Bauer and S. J. Lippard, *Biochemistry*, **1976**, *15(19)*, 4339.

38) C. Che, M. Yang, K. Wong, H. Chan and W. Lam, *Chem. Eur. J.* **1999**, *5*, 3350.

39) G. Arena, L. M. Scolaro, R. F. Pasternack and R. Romeo, *Inorg. Chem.*, **1995**, *34*, 2994.

40) M. Cusumano, M. L. Di Pietro, and A. Giannetto, *Inorg. Chem.*, **1999**, *38*, 1754.

41) G. Lowe, S. A. Ross, M. Probert and A. Cowley, *Chem. Commun.*, **2001**, 1288.

42) K. Wang, M. Haga, H. Monjushiro, M. Akiba and Y. Sasaki, *Inorg. Chem.*, **2000**, 39, 4022.

43) R. Büchner, C. T. Cunningham, J. S. Field, R. J. Haines, D. R. McMillin and G. C. Summerton, *J. Chem. Soc., Dalton Trans.*, **1999**, 711.

44) T. Cheung, K. Cheung, S. Peng, and C. Che, *J. Chem. Soc., Dalton Trans.*, **1996**, 1645.

45) J. F. Michalec, S. A. Bejune, and D. R. McMillan, *Inorg. Chem.*, **2000**, *39*, 2708.

46) J. G. Collins, R. M. Rixon, and J. R. Aldrich-Wright, *Inorg. Chem.*, **2000**, *39*, 4377.

47) M. Schmülling and R. van Eldik, *J. Chem. Soc., Dalton Trans.*, **1994**, 1257.

48) M. Schumülling, A. D. Ryabov and R. van Eldik, *J. Chem. Soc., Chem. Commun.*, **1992**, 1609.

49) S. Elmroth, Z. Bugarčić and L.I. Elding, *Inorg. Chem.*, **1992**, *31*, 3551.

50) N. De Barrios, G. González, A. Grandas, M. Martinez and V. Moreno, *Inorganic Reaction Mechanisms*, **1999**, *1*, 205.

51) D. Katakis, G. Gordon, *Mechanisms of Inorganic Reactions*, New York, **1987**, 191.

52) S. Lanza, D. Minniti, P. Moore, J. Sachinidis, R. Romeo, M. L. Tobe, *Inorg. Chem.*, **1984**, *23*, 4428.

53) G. Alibrandi, G. Bruno, S. Lanza, D. Minniti, R. Romeo, and M. L. Tobe, *Inorg. Chem.*, **1987**, *26*, 185.

54) U. Frey, L. Helm, A. E. Merbach, and R. Romeo, *J. Am. Chem. Soc.*, **1989**, *111*, 8161.

55) D. Minniti, G. Alibrandi, M. L. Tobe, and R. Romeo, *Inorg. Chem.*, **1987**, **26**, 3956.

56) M. Schmülling and R. van Eldik, *Chem. Ber./Recueil.*, **1997**, *130*, 1791.

57) R. Romeo, M. R Plutino, L. M. Scolaro, S. Stoccoro and G. Minghetti, *Inorg Chem.*, **2000**, 4749.

58) F. P. Cavasino, C. Sbrizilo, M. Cusumano, and A. Giannetto, *J. Chem. Soc., Faraday Trans.1*, **1989**, *85(12)*, 4237.

59) R Romeo, A. Grassi, and L M Scolaro, *Inorg. Chem.*, **1992**, *31*, 4383.

60) G. Albrandi, D. Minnitti, L. M. Scolaro, R. Romeo, *Inorg. Chem*, **1989**, *28*, 1939.

61) L. Canovese, L. Cattalini and P. Uguagliati, *J. Chem. Soc., Dalton Trans.*, **1990**, 867.

62) H. Hohmann, B. Hellquist and R. van Eldik., *Inorg. Chim. Acta.*, **1991**, *188*, 25.

63) M. Kotowski, D. A. Palmer and H. Kelm., *Inorg. Chem.*, **1979**, *18*, 2555.

64) R. Romeo, G. Arena, L. M. Scolaro, M. R. Plutino, G. Bruno and F. Nicoló, *Inorg. Chem*, **1994**, *33*, 4029.

65) D. Jaganyi, A. Hofmann and R. van Eldik, *Angew. Chem.*, **2001**, *113*, 1730.

66) M. Mikola, K. D. Klika, A. Hakala, and J. Arpalahti, *Inorg. Chem.*, **1999**, *38*, 571.

67) L. Casanovese, M. L. Tobe and L. Cattalini, *J. Chem. Soc., Dalton Trans.*, **1985**, 27.

68) B. Bruno, G. Marangoni, L. Cattalini, and L. Cattalini, *J. Chem. Soc., Dalton Trans.*, **1994**, 3539.

69) B. Bruno, G. Marangoni, L. Cattalini, and T. Bobbo, *J. Chem. Soc., Dalton Trans.*, **1995**, 3853.

70) L. Cattalini, A. Orio, and M. Nicolini, *J. Am. Chem. Soc.*, **1966**, *88*, 5734.

71) R. Romeo, M. R. Plutino, L. M. Scolaro, S. Stoccoro, and G. Minghetti, *Inorg. Chem*, **2000**, *39*, 4749.

72) S. S. Zumdahl and R. S. Drago, *J. Am. Chem. Soc.*, **1968**, 6670.

73) L. E. Orgel, *J. Inorganic and Nuclear Chemistry*, **1956**, *2*, 137.

74) S. Otto, and L. I. Elding, *J. Chem. Soc., Dalton Trans.*, **2002**, 2354.

75) L. G. Vanquickenborne, J. Vranckx, and C. Görller-Walrand, *J. Am. Chem. Soc.*, **1974**, 4122.

76) J. K. Burdett, *Inorg. Chem.*, **1977**, *16*, 12.

77) M. L. Tobe and A. T. Treadgold, *J. Chem. Soc., Dalton Trans.*, **1998**, 2347.

78) R. B. Jordan, *Reaction Mechanisms of Inorganic and Organometallic Systems*, Oxford University Press, New York, **1991**, 58, 60.

79) M. Schülling, D. M. Grove, G. van Koten, R. van Eldik, N. Veldman, and A. L. Spek, *Organometallics*, **1996**, 15, 1384.

80) Z. D. Bugarčić, G. Liehr and R. van Eldik, *J. Chem. Soc., Dalton Trans.*, **2002**, 951.

81) N. Kuznik and O. F. Wendt, *J. Chem. Soc., Dalton Trans.*, **2002**, 3074.

82) J. K. Burdett, *Inorg. Chem.*, **1977**, 16, 12.

83) M. Bonivento, L. Cattalini, G. Marangoni, G. Michelon, A. P. Schwab, and M. L. Tobe, *Inorg. Chem.*, **1980**, *19*, 1743.

84) R. J. Mureinik and W. Robb, *Inorg. Chim. Acta*, **1971**, 333.

85) R. van Eldik, D. A. Palmer and H. Kelm, *Inorg. Chem.*, **1979**, 18, 572.

86) E. L. J. Breet and R. van Eldik, *Inorg. Chem.*, **1984**, 23, 1865.

87) M. Schmülling, A. D. Ryabov, and R. van Eldik, *J. Chem. Soc., Chem. Comm.*, **1992**, 1609.

88) R. Romeo, M. R. Plutino, L. M. Scolaro, S. Stoccoro, *Inorg. Chim. Act*a, **1997**, 225.

89) L. Cattalini, G. Chessa, G. Marangoni, B. Pitteri, and E. Celon., *Inorg. Chem.*, **1989**, *28*, 1944.

90) R. Romeo, and M. Cusumano, *Inorg. Chim Acta.*, **1981**, *49*, 167.

91) U. Belluco, R. Ettorre, F. Basolo, R. G. Person and A. Turco, *Inorg. Chem.*, **1966**, *5*, 591.

92) M. Cusumano and G. Guglielmo, *Inorg. Chim. Acta.*, **1978**, *27*, 197.

93) R. Romeo, G. Arena, L. M. Scolaro, M. R. Plutino, *Inorg. Chim. Acta.*, **1995**, *240*, 81.

94) D. A. Palmer, R. Van Eldik, and H. Kelm, *Z. anorg. allg. Chem*, **1980**, *468*, 77.

95) B. K. Keppler, *Metal Complexes in cancer Chemotherapy*, John Wiley & Sons, **1993**, 1.

96) M. J. Bloemink, H. Engelking,S. Karentzopoulos, B. Krebs, and J. Reedjik, *Inorg. Chem.*, **1996**, *35*, 619.

97) F. Gonnet, F. Reeder, J. Kozelka and J. Chottard, *Inorg. Chem.*, **1996**, *35*, 1653.

98) B. V. Petrovic, M. I. Djuran and Z. D. Bugarčić, *Metal-Based Drugs*, **1999**, *6*, 355.

99) D. V. Deubel, *J.Am.Chem.Soc.*, **2002**, *124*, 5834.

100) L. R. Kelland, S. Y. Sharp, C. F. O'Neill, F. I. Raynaud, P. J. Beale, I. R. Judson, *J. Inorg. Biochem.*, **1999**, *77*, 1111.

101) E. R. Jamieson and S. J. Lippard, *Chem Rev.*, **1999**, 2467.

102) Z. D. Bugarčić and B. V. Djordjević, *Monatshefte für Chemie.*, **1998**, *129*, 1267.

103) D. V. Deubel, *J. Am. Chem. Soc.*, **2002**, *124*, 5834.

104) K. Lemma, T. Shi, and L. I. Elding, *Inorg Chem.*, **2000**, *39*, 1728.

105) K. Lemma, S. K. C. Elmroth and L. I. Elding, *J. Chem. Soc., Dalton Trans.*, **2000**, 1281.

106) E. G. Talman, W. Brüning, J. Reedjik, A. L. Spek, and N. Veldman, *Inorg. Chem.*, **1997**, *36*, 854.

107) J. Yoo, J. Kim, Y. S. Sohn and Y. Do, *Inorg. Chim. Acta.*, **1997**, *263*, 53.

108) U. Bierbach, M. Sabat and N. Farrell, *Inorg. Chem.*, **2000**, *39*, 1882.

109) S. Shamsuddin, J. W. van Hal, J. L. Stark, K. H. Whitmire, and A. R. Khokhar, *Inorg. Chem.*, **1997**, *36*, 5969.

110) S. Shamsuddin, M. S. Ali and A. R. Khokhar, *J. Coord. Chem.*, **2000**, *49*, 291.

111) M. J. Bloemink, R. J. Heertebrij, J. Ireland, G. B. Deacon, J. Reedijk, *JBIC.*, **1996**, *1*, 278.

112) M. V. Beusichem and N. Farrell. *Inorg. Chem.*, **1992**, *31*, 634.

113) E. Schuhmann, J. Altman, K. Karaghiosoff and W. Beck, *Inorg. Chem.*, **1995**, *34*, 2316.

114) N. Farrell, S.G. de Almeida, *J. Am.Chem. Soc.*, **1988**, *110*, 5018.

115) N. Farrell and Y. Qu, *Inorg. Chem.*, **1989**, *28*, 3416.

116) Y. Qu and N. Farrell, *J. Am. Chem. Soc.*, **1991**, *113*, 4851.

117) J. Kozelka, F. Legendre, F. Reeder, J. Chottard, *Coord. Chem. Rev.*, **1999**, *190*, 61.

118) D.P. Bancroft, C.A. Lepre and S. J. Lippard, *J. Chem. Soc., Dalton Trans.*, **1990**, *112*, 6850.

119) S.T. Cham, C. I. Diakos, L. T. Ellis, D. R. Fenton, V. P. Munk, B. A. Messerle, and T. W. Hambley, *J. Chem. Soc., Dalton Trans.*, **2001**, 2769.

120) J. Teuben, M. R Zubiri, and J. Reedijk, *J. Chem. Soc., Dalton Trans.*, **2000**, 369.

121) J. Reedjik, *Chem. Rev.*, **1999**, 2499.

122) V. Monjardet-Bas, M. Elizondo-Riojas, J. Chottard, and J. Kozelka, *Angew. Chem. Int. Ed.* **2002**, *41*, 2998.

123) F. Gonnet, J. Kozelka and J. Chottard., *Angew. Chem. Int. Engl.*, **1992**, *31(11)*, 1483.

124) Z. Guo, Y. Chen, E. Zang and P. J. Sadler, *J. Chem Soc., Dalton Trans.*, **1997**, 4107.

125) U. Bierbach and N. Farrell, *Inorg. Chem.*, **1997**, *36*, 3657.

126) A. K. Fazlur-Rahman and J. G. Verkade, *Inorg. Chem.*, **1992**, *31*, 2064.

127) Z. D. Bugarčić, B. V. Djordjević, *Monatshefte für Chemie.*, **1998**, 1267.

128) A. Pasini, C. Fiore, *Inorg. Chim. Acta.*, **1999**, *285*, 249.

129) M. I. Djuran, E. L.M. Lempers and J. Reedjik, *Inorg. Chem.*, **1991**, *30*, 2648.

130) S. S. G. E. van Boom, and J. Reedjik, *J. Chem. Comm.*, **1993**, 1397.

131) J. L. Allu, A. C. Rice, L. A. Tebbets, *Biochemistry.*, **1997**, *16*, 627.

132) J. F. Perez-Benito, C. Arias and E. Amat, *New J. Chem.*, **1995**, *19*, 1089.

133) T. Yukuta, I. Mori, M. Kurihara, J. Muzutani, K. Kubo, S. Furusho, K. Matsumura, N. Tamai, and H. Nishihara, *Inorg. Chem.*, **2001**, *40*, 4986.

134) J. A. Treadway, G. F. Strouse, R. R. Ruminski and T. J. Meyer, *Inorg. Chem.*, **2001**, *40*, 4508.

135) W.R. Murphy, K. J. Takeuchi, and T. J. Meyer, *J. Am. Chem. Soc.*, **1982**, *104*, 5817.

136) W.R. Murphy, K. J. Takeuchi, M. H. Barley, and T. J. Meyer, *Inorg. Chem.*, **1986**, *25*, 1041.

137) T. J. Meyer, *J. Electrochem. Soc.*, **1984**, 221C.

138) S. Delaney, M. Pascaly, P. K. Bhattacharya, K, Han, and J. K. Borton, *Inorg. Chem.*, **2000**, *7*, 1966.

139) E. D. A. Stemp, M. R. Arkins, J. K. Borton, *J. Am. Chem. Soc.*, **1997**, *119*, 2921.

140) M. J. Clarke, F. Zhu and D. R. Frasca, *Chem. Rev.*, **1999**, *99*, 2511.

141) K. R. Barqawi, A. Llobet and T. J. Meyer, *J. Am. Chem. Soc.*, **1988**, *110*, 7751.

142) B. J. Coe, D. W. Thompson, C. T. Culbertson, J. R. Schoonover, and T. J. Meyer, *Inorg. Chem.*, **1995**, *34*, 3385.

143) N. D. McClenagham, F. Barigelletti, B. Maubert and S. Camagna, *Chem. Commun.*, **2002**, 602.

144) A. E. Friedman, J. Chambron, J. Sauvage, N. J. Turro, and J. K, Barton, *J. Am. Chem. Soc.*, **1990,** *112*, 4960.

145) A. Greguric, I. D. Greguric, T. W. Hambley, J. R. Aldrich-Wright and J. G. Collins, *J. Chem. Soc., Dalton Trans.*, **2002**, 849.

146) C. G. Coates, L. Jacquet, J. J. McGarvey, S. E. J. Bell, A. H. R. Al-Obaidi, and J. M. Kelly, *J. Am. Chem. Soc.*, **1997**, *119*, 7130.

147) N. C. Fletcher and F. R. Keene, *J. Chem. Soc., Dalton Trans.*, **1998**, 2293.

148) S. A. Adeyemi, D. Dovletoglou, A. R. Guadalupe and T. J. Meyer., *Inorg. Chem.*, **1992**, *31*, 1375.

149) C. Che, K. Wong, W. Leung and C. Poon., *Inorg. Chem.*, **1986**, *25*, 345.

150) L. K. Stultz, R. A. Binstead, M. S. Reynold, and T. J. Meyer, *J. Am. Chem. Soc.*, **1995**, *117*, 2520.

151) C. Che, T. Lai and K. Wong, *Inorg. Chem.*, **1987**, *26*, 2289.

152) G. M. Coia, K. D. Kemadis and T. J. Meyer, *Inorg. Chem.*, **2000**, *39*, 2212.

153) K. Kalynasundaram and M. K. Nazeerudin, *Inorg. Chem.*, **1990**, *29*, 1888.

154) M. S. Reynolds, T. J. Meyer, *J. Am. Chem. Soc.*, **1995**, *117*, 2520.

155) B. A. Moyer, M. S. Thompson, and T. J. Meyer., *J. Am. Chem. Soc.*, **1980**, 2310.

156) K. J. Takeuchi, M.S. Thompson, D. W. Pipes, and T. J. Meyer, *Inorg. Chem.*, **1984**, *23*, 1845.

157) M. S. Thompson and T. J. Meyer, *J. Am. Chem. Soc.*, **1982**, *104*, 5070.

158) M. E. Mormion, K. J. Takeuchi, *J. Chem. Soc., Dalton Trans.*, **1988**, 2385.

159) N. Grover, H. H. Thorp, *J. Am. Chem. Soc.*, **1991**, *113*, 7030.

160) R. B. Jordan, *Reaction Mechanisms of Inorganic and Organometallic Systems*, New York, Oxford University Press, **1991**, 67-70.

161) F. Galsbøl, L. Mønsted, and O. Mønsted., *Acta Chemica. Scandinavica*, **1992**, 46, 43.

162) F. M. Foley, F. R. Keene and J. G. Collins, *J. Chem. Soc., Dalton Trans.*, **2001**, 2968.

163) P. Byabartta, J. Dinda, P. K. Santra, C. Sinha, K. Pannerselvam, F. L. Liao and T. Lu, *J. Chem. Soc., Dalton Trans.*, **2001**, 2825.

164) R. E. Sheperd, and H. Taube, *Inorg. Chem.*, **1973**, *12*, 1392.

165) L. Dozsa, J. E. Sutton and H. Taube., *Inorg. Chem.*, **1982**, *21*, 3997.

166) J. F. Ojo, O. Olubuyide, and O. Oyetunji, *J. Chem. Soc., Dalton Trans.*, **1987**, 957.

167) M. V. V. Huynh, J. Smyth, M. Weltzler, B. Mort, P. K. Gong, L. M. Witham, D. L. Jameson, D. K. Geiger, J. M. Lasker, M. Charepoo, M. Gornikiewicz, J. M. Cintron, G. Imahori, R. R. Sanchez, A. C. Marschilok, L. M. Krajkowski, D. G. Churchill, M. R. Churchill, and T. K. Taukechi, *Angew. Chem.*, **2001**, *113*, 4601.

168) R. E. Shepherd, H. Taube, *Inorg. Chem.*, **1973**, *12*, 1392.

169) S. S. Isied, and H. Taube, *Inorg. Chem.*, **1976**, *12*, 3070.

170) C. A. Bessel, J. A. Margarucci, J. H. Acquaye, R. S. Rubino, J. Crandall, A. J. Jircitano and K. J. Takeuchi, *Inorg Chem.*, **1993**, *32*, 5779.

171) N. R. Davies and T. L. Mullins, *Aust. J. Chem.*, **1967**, *20*, 657.

172) L. R. Allen, P. P. Craft, B. Durham and J. Walsh, *Inorg. Chem.*, **1987**, 26, 53.

173) A. C. G. Hotze, M. E. T. Broekhuisen, A. H. Velders, H. Kooijman, A. L. Spek, J. G. Haasnoot and J. Reedjik, *J. Chem. Soc., Dalton Trans.*, **2002**, 2809.

174) I. Greguric, J. R. Aldrich-Wright, and J. G. Collins, *J. Am. Chem. Soc.*, **1997**, *119*, 3621.

175) I. Hag, P. Lincoln, D. Suh, B. Norden, B. Z. Chowdhry, and J. B. Chaires, *J. Am. Chem. Soc.*, **1995**, *117*, 4788.

176) Y. Xiong, X. He, X. Zou, J. Wu, X. Chen, L. Ji, R. Li, J. Zhou, and K. Yu, *J. Chem. Soc., Dalton Trans.*, **1999**, 19.

177) F. M. Foley, F. R. Keene, and J. G. Collins, *J. Chem. Soc., Dalton Trans.*, **2001**, 2968.

178) P. Byabartta, J. Dinda, P. K. Santra, C. Sinha, K. Panneerselvam, F. L. Liao and T.Lu., *J. Chem. Soc., Dalton Trans.*, **2001**, 2825.

179) P. Lincoln, A. Broo and B. Nordén, *J. Am. Chem. Soc.*, **1996**, 118, 2644.

180) A. E. Friedman, J. Chambron, J. Sauvage, N. J. Turro and J. K. Barton, *J. Am. Chem Soc.*, **1990**, 112, 4960.

181) C. G. Coates, L. Jacquet, J. J. McGarvey, S. E. J. Bell, A. H. R. Al-Obaidi, and J. M. Kelly, *J. Am. Chem. Soc.*, **1997**, 119, 7130.

182) E. Tuite, P. Lincoln, and B. Norden, *J. Am. Chem. Soc.*, **1997**, 119, 239.

183) D. Ly, S. Sanii, G. B. Schuster, *J. Am. Chem. Soc.*, **1999**, 121, 9400.

184) S. R. Rajski, S. Kumar, R. J. Roberts and J. K. Borton, *J. Am. Chem. Soc.*, **1999**, 121, 5615.

CHAPTER TWO

THEORY

2. KINETIC THEORY

2.1 Introduction

The aims of studying chemical kinetics are:

(i) to determine experimentally the rate of a reaction and its dependence on parameters such as concentration, temperature, and catalysts; and

(ii) to understand the mechanism of a reaction, that is, the number of steps involved and the nature of the intermediates formed.

In general, a kinetic study begins with the collection of data of concentration versus time of a reactant or product. This can be accomplished by determining the time dependence of some variable that is proportional to concentration, such as absorbance or NMR peak intensity. The next step is to fit the concentration-time data to some model that will allow one to determine the rate constant, if the data fits the model.

This section gives a brief summary of some of the integrated rate laws that were relevant in this study. It also contains a section that describes two types of instrument used to study the substitution reactions of the complexes investigated.

2.2 Integrated Rate Expressions

2.2.1 Irreversible First-Order Reactions

Most reactions are either first order or are executed under conditions that approximate first order. For a first order reaction,

$$A \xrightarrow{k_1} \text{Product} \qquad (2.1)$$

the rate of reaction is given by

$$\frac{d[P]}{dt} = -\frac{d[A]}{dt} = k_1[A]_t \tag{2.2}$$

Upon rearrangement

$$-\frac{d[A]}{[A]_t} = k_1 dt \tag{2.3}$$

Integrating between t = 0 ($[A]_o$) to t = t ($[A]_t$), one obtains

$$\int_{[A]_o}^{[A]_t} \frac{d[A]}{[A]_t} = -\int_0^t k_1 dt \tag{2.4}$$

$$\ln\frac{[A]_t}{[A]_o} = -k_1 t \tag{2.5}$$

or

$$\ln[A]_t = -k_1 t + \ln[A]_o \tag{2.6}$$

or

$$[A]_t = [A]_o e^{-k_1 t} \tag{2.7}$$

where $[A]_0$ and $[A]_t$ are concentrations at time t = 0 and t = t respectively. A plot of $\ln[A]_t$ versus t results into a straight line with a slope equal to the rate constant ($-k_1$) in s^{-1}.

The advantage of a first-order rate law is that any physical parameter that is proportional to concentration, *viz.* absorbance, volume, pressure, conductivity, *etc.*, can be used directly to measure the first-order rate constant.

2.2.2 Reversible First-Order Reactions

Some reactions do not go to completion, *i.e.* equilibrium is reached

$$A \underset{k_2}{\overset{k_1}{\rightleftharpoons}} P \tag{2.8}$$

The rate law for this reaction is

$$\frac{d[P]}{dt} = -\frac{d[A]}{dt} = k_1[A]_t - k_2[P]_t \tag{2.9}$$

At time t = 0, $[P]_o = 0$, and $[A]_t = [A]_o$

Therefore

$$[P]_t = [A]_o - [A]_t \tag{2.10}$$

substituting (2.10) into (2.9) gives

$$-\frac{d[A]}{dt} = k_1[A]_t - k_2([A]_o - [A]_t) \tag{2.11}$$

At equilibrium the net reaction rate is equal to zero. Applying this to equation (2.11) and introducing the equilibrium expressions

$$-\frac{d[A]}{dt} = 0 = k_1[A]_{eq} - k_2([A]_o - [A]_{eq}) \tag{2.12}$$

implies that

$$[A]_o = \frac{k_1 + k_2}{k_2}[A]_{eq} \tag{2.13}$$

Substitution of (2.13) into (2.11) leads to

$$-\frac{d[A]}{dt} = (k_1 + k_2)([A]_t - [A]_{eq}) \tag{2.14}$$

Separation of the variables gives

$$\frac{d[A]}{([A]_t - [A]_{eq})} = -(k_1 + k_2)dt \tag{2.15}$$

on integration

$$\int_{[A]_o}^{[A]_t} \frac{d[A]}{([A]_t - [A]_{eq})} = -(k_1 + k_2)\int_o^t dt \tag{2.16}$$

leads to

$$\ln\left(\frac{[A]_t - [A]_{eq}}{[A]_0 - [A]_{eq}}\right) = -(k_1 + k_2)t \tag{2.17}$$

or

$$\ln([A]_t - [A]_{eq}) = -(k_1 + k_2)t + \ln([A]_o - [A]_{eq}) \tag{2.18}$$

A plot of $\ln([A]_t - [A]_{eq})$ against t will give a straight line of slope $-(k_1 + k_2)$.

To determine the individual values of k_1 and k_2, one must evaluate the equilibrium constant,

$$K_{eq} = \frac{[P]_{eq}}{[A]_{eq}} = \frac{k_1}{k_2} \tag{2.19}$$

with the observed rate constant

$$k_{obs}=(k_1+k_2) \tag{2.20}$$

2.2.3 Second Order Reactions

Second order kinetics plays an important role in the reactions of complex ions. Two types of second order reactions exist. The first type is when the rate is second order with respect to one of the reactants and zero-order with respect to the second reactant. The second type that is considered in this section is a reaction that is first order with respect to both reactants.

$$A+B \xrightarrow{k_2} \text{Product} \tag{2.21}$$

The rate equation can be written as

$$\frac{d[P]}{dt}=-\frac{d[A]}{dt}=-\frac{d[B]}{dt}=k_2[A]_t[B]_t \tag{2.22}$$

Separating the variables leads to

$$\frac{d[A]}{[A]_t[B]_t}=-k_2dt \tag{2.23}$$

To integrate this equation, it is desirable to simplify equation (2.23) by substituting $\frac{1}{[A]_t[B]_t}$ with $\frac{1}{([A]_0-[B]_0)}\left\{\frac{1}{[B]_t}-\frac{1}{[A]_t}\right\}$ so equation (2.23) becomes

$$\frac{1}{([A]_o-[B]_o)}\left\{\frac{1}{[B]_t}-\frac{1}{[A]_t}\right\}d[A]=-k_2dt \tag{2.24}$$

Through integration of equation (2.24) one obtains

$$\frac{1}{([A]_o - [B]_o)} \ln \frac{[B]_o[A]_t}{[A]_o[B]_t} = k_2 t \qquad (2.25)$$

Thus one needs to know the concentration of A and B, initially and at any time t, *i.e.* $[A]_o$, $[B]_o$, $[A]_t$ and $[B]_t$ in order to determine the second order rate constant k_2 (M^{-1} s^{-1}). This is in most kinetic experiments very complicated and time consuming. Second order reactions are usually studied under pseudo-first-order conditions, *i.e.* one of the reactants is selected in large excess such that its concentration remains constant during the reaction.

When $[B]_0 >> [A]_0$ (at least a 10 fold excess) equation (2.22) can be written as

$$\begin{aligned} -\frac{d[A]}{dt} &= k_2[A]_t[B]_t \\ &= k_2[A]_t[B]_o \\ &= k_{obs}[A]_t \end{aligned} \qquad (2.26)$$

with $k_{obs} = k_2[B]_o$.

The rate is now a first-order expression and k_{obs} can be determined in the usual way. A plot of k_{obs} (s^{-1}) versus $[B]_o$ will be linear with a slope of k_2 (M^{-1} s^{-1}).

2.2.4 Reversible Second Order Reactions

A reaction starting from A and B which does not go to completion but reaches equilibrium can be written as:

The forward reaction is second-order, the reverse reaction is first-order, which means that the reaction

$$A + B \underset{k_{-2}}{\overset{k_2}{\rightleftharpoons}} C \qquad (2.27)$$

will have a mixed order behavior. This

difficulty is usually overcome by selecting pseudo first-order conditions for the forward reaction, *viz.* $[B]_o >> [A]_o$. The treatment of the equation then becomes similar to that of a reversible first-order reaction.

The rate of formation of C can be expressed as

$$-\frac{d[A]}{dt} = -\frac{d[B]}{dt} = \frac{d[C]}{dt} = k_2[A]_t[B]_t - k_{-2}[C]_t \tag{2.28}$$

Applying the mass balance:
At any time t

$$[A]_t = [A]_o - [C]_t \text{ and } [B]_t = [B]_o - [C]_t \tag{2.29}$$

and at equilibrium

$$[A]_e = [A]_o - [C]_e \text{ and } [B]_e = [B]_o - [C]_e \tag{2.30}$$

Also at equilibrium the rates of the two opposing reactions becomes equal, that is,

$$-\frac{d[A]}{dt} = k_2[A]_e[B]_e - k_{-2}[C]_e = 0 \tag{2.31}$$

this implies that

$$k_2[A]_e[B]_e = k_{-2}[C]_e \tag{2.32}$$

But $[C]_t = [A]_o - [A]_t$ and $[C]_e = [A]_o - [A]_e$

Therefore, (2.32) becomes

$$k_2[A]_e[B]_e = k_{-2}([A]_o - [A]_e) \tag{2.33}$$

resulting in

$$k_{-2}[A]_0 = k_2[A]_e[B]_e + k_{-2}[A]_e \tag{2.34}$$

Substituting for $[C]_t$, followed by replacement of $k_{-2}[A]_o$ from (2.34) gives

$$-\frac{d[A]}{dt} = k_2[A]_t[B]_t - k_2[A]_e[B]_e - k_{-2}[A]_e + k_{-2}[A]_t \tag{2.35}$$

Substitution of $[B]_t$ and $[B]_e$ in equation (2.34) and approximating that $k_2[A]_t[A]_0 \approx k[A]_e[A]_o$ and $k_2[A]_t^2 \approx k_2[A]_e^2$ leads to

$$\begin{aligned} -\frac{d[A]}{dt} &= k_2[A]_t[B]_o - k_2[A]_e[B]_o - k_{-2}[A]_e + k_{-2}[A]_t \\ &= \left(k_2[B]_o + k_{-2}\right)\left([A]_t - [A]_e\right) \end{aligned} \tag{2.36}$$

Separation of the variables and integration gives

$$\int_{[A]_o}^{[A]_t} \frac{d[A]}{\left([A]_t - [A]_e\right)} = -\left(k_2[B]_o + k_{-2}\right)\int_o^t dt \tag{2.37}$$

which results in

$$\begin{aligned} \ln\left(\frac{[A]_t - [A]_e}{[A]_0 - [A]_e}\right) &= -\left(k_2[B]_0 + k_{-2}\right)t \\ &= -k_{obs}\,t \end{aligned} \tag{2.38}$$

with $k_{obs} = k_2[B]_0 + k_{-2}$. Thus a plot of k_{obs} versus $[B]_o$ will be a straight line with a slope of k_2 and an intercept of k_{-2}. The ratio k_2/k_{-2} represents the equilibrium constant K, and can be checked thermodynamically.

Many reactions exhibit a two term rate law which can either be due to a reversible process as outlined above, or to two parallel reaction paths of which one is independent of $[B]$.

2.2.5 Pre-Equilibrium with Parallel Reactions-(One Acid-Base Equilibrium)

Many reaction rates are affected by the pH of the solution. The modification of the rate as the pH is changed is due to the formation of different species with different reactivities. A plot of observed or intrinsic rate constant resembles the profile for an acid base titration curve. Typical examples are the aqua and hydroxy complexes. The rate law and the general reaction scheme is written as:

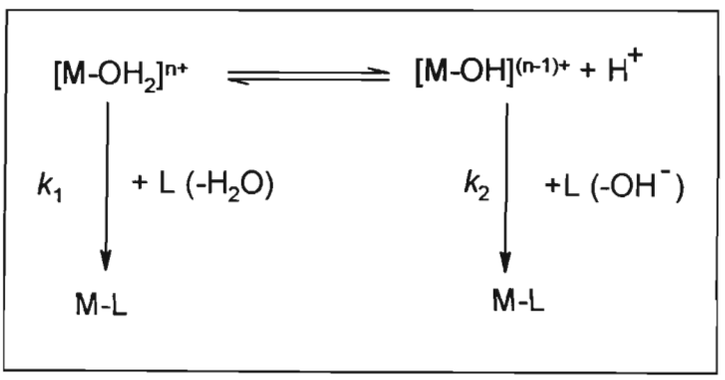

***Scheme 2.1**. A general reaction scheme representing one-acid base equilibrium.*

It follows that

$$\frac{d[M-L]}{dt} = -\frac{d[M-OH_2]}{dt} = -\frac{d[M-OH]}{dt} = k_1[M-OH_2][L] + k_2[M-OH][L]$$

$$= -\frac{d[M-OH_2 + M-OH]}{dt} = k_1[M-OH_2][L] + k_2[M-OH][L] \qquad (2.39)$$

Applying the mass balance law it follows that

$$K_a = \frac{[M\text{–}OH][H^+]}{[M\text{–}OH_2]} \tag{2.40}$$

$$[M\text{–}OH_2] = \frac{([M\text{–}OH_2]+[M\text{–}OH])[H^+]}{([H^+]+K_a)} \tag{2.41}$$

$$[M\text{–}OH] = \frac{([M\text{–}OH_2]+[M\text{–}OH])}{[H^+]+K_a} \tag{2.42}$$

Substituting (2.41) and (2.42) into (2.40) results in

$$-\frac{d([M\text{–}OH_2]+[M\text{–}OH])}{dt} = \left\{\frac{k_1[H^+]+k_2K_a}{[H^+]+K_a}\right\}[L]([M\text{–}OH_2]+[M\text{–}OH]) \tag{2.43}$$

and

$$k_{obs} = \left\{\frac{k_1[H^+]+k_2K_a}{[H^+]+K_a}\right\}[L] \tag{2.44}$$

Considering the limits of equation (2.44)

At low $[H^+]$

$$k_{obs} = k_2[L] \tag{2.45}$$

and at high $[H^+]$

$$k_{obs} = k_1[L] \tag{2.46}$$

2.3 Substitution Mechanism of Square Planar Complexes

Square planar complexes have two "open" positions.[7] The incoming ligand can approach from either side of the plane. The typical mechanism is associative, but a dissociative process involving the substitution of *cis*-PtR_2S_2 (R = Me, ph; S = SMe_2, $S(O)Me_2$) has been reported[1, 2, 3, 4]

2.3.1 Associative Mechanism

The rate law governing substitution in planar complexes usually consists of two terms, one first-order in the metal complex (M) alone and the other first-order in both M and the entering group L.[8]

Associative mechanism can be represented as:

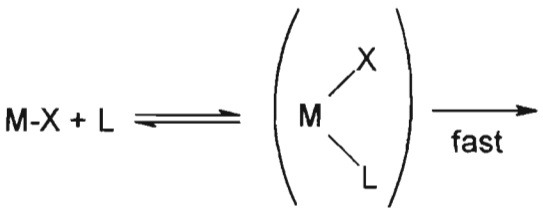

(2.47)

Assuming steady state for the intermediate

$$-\frac{d[M-X]}{dt} = k_2[M][L] + k_{-2}[M] \qquad (2.48)$$

Under pseudo-first-order conditions, experimental first order rate constant, k_{obs}, is given by

$$-\frac{d[M-X]}{dt} = k_{obs}[M] \qquad (2.49)$$

with

$$k_{obs} = k_2[L] + k_{-2} \qquad (2.50)$$

A plot of k_{obs} against $[L]$ will have a slope k_2 and an intercept k_{-2} that represents the back reaction.

The rate and the mechanism, among other things, depend also on the solvent. The rate law for square-planar substitution reactions where the rate-determining step is solvolytic will include a term that is independent of the entering nucleophile.

Therefore the mechanism involving the solvent (s) attack can be represented as:

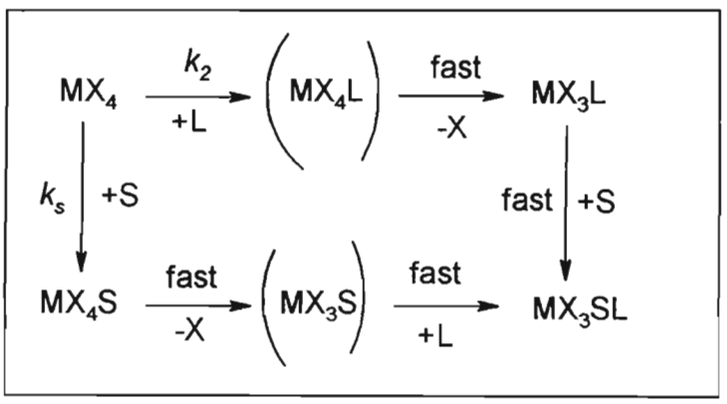

Scheme 2.2 *Associative mechanism for ligand (L) as well as solvent (S) attack on a square-planar complex.*

The rate of the reaction can be expressed as

$$-\frac{d[MX_4]}{dt} = k_2[L][MX_4] + k_s[S][MX_4] = (k_2[L] + k_s[S])[MX_4] \tag{2.51}$$

where

$$k_{obs} = k_s[S] + k_2[L] \tag{2.52}$$

Since $[S]$ represents the concentration of the solvent which is the reaction medium, the term $k_s[S] = k_s'$

Therefore

$$k_{obs} = k_s' + k_2[L] \qquad (2.53)$$

Depending on the relative nucleophilicity of the solvent and the entering ligand, the observed rate law may be dependent or independent of the ligand. A large value of k_s' relative to k_2 is observed in solvents capable of coordinating strongly to the metal. In solvents that are poor coordinators, the k_2 value dominates.[5]

2.3.2 Dissociative Mechanism

The primary evidence for a dissociative mechanism (D) is:

(i) positive values for the activation volume
(ii) independence of the rate on the nature of the entering group
(iii) identical rates for substitution and solvent exchange and
(iv) positive values for the entropy of activation.

Dissociation of ligands from square-planar complexes is important and relatively common in ligand redistribution reactions of square-planar complexes.[6]

The dissociative mechanism is represented in **Scheme 2.3**.

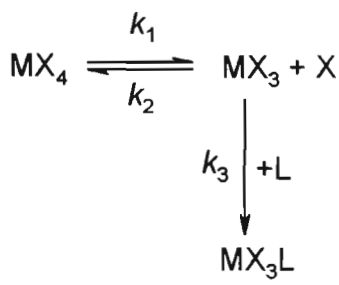

Scheme 2.3 *Dissociative pathways for substitution on a square-planar complex.*

$$-\frac{d[MX_4]}{dt} = \frac{d[MX_3L]}{dt} = \frac{k_1k_3[MX_4][L]}{k_2[X]+k_3[L]} \qquad (2.54)$$

This mechanism is also true for octahedral complexes. Other mechanisms are the interchange mechanisms. These are dissociative interchange (I_d) and associative interchange (I_a) where there is no definite evidence of an intermediate. In the transition state for (I_d) there is a large degree of bond-breaking to the leaving group and a small amount of bond making to the entering group. The rate is more sensitive to the nature of the leaving group. In the case of (I_a), the bond to the entering group is largely made while the bond to the leaving group is essentially unbroken. The mechanisms discussed are presented in schematic form in **Figure 2.1**.[8]

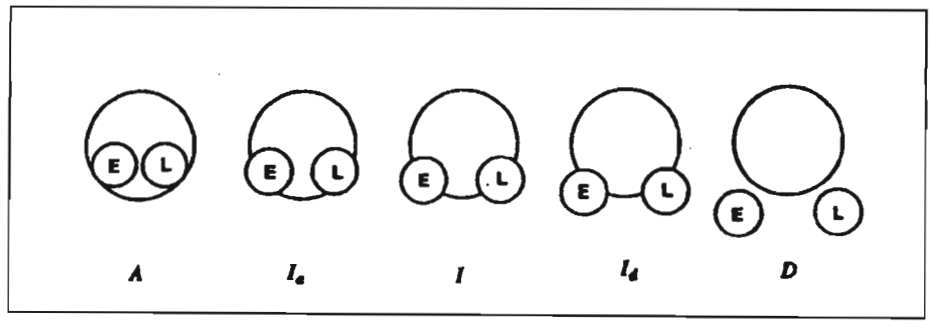

Figure 2.1 *Schematic representation of the associative (A), interchange associative (I_a), interchange (I), interchange dissociative (I_d) and dissociative (D) mechanism.*

2.4 Temperature Dependence of Rate Constants

The rate law is very useful in assigning a mechanism for a reaction, but other data are also beneficial, activation parameters are usually essential. A reaction's activation parameters are derived from the temperature dependence of its rate constant. The relationship can be derived from empirical relationships or from the absolute reaction rate theory.

2.4.1 Arrhenius Equation

Rates of chemical reactions are affected by temperature in several ways. The most common is that observed by Arrhenius

$$k = A\exp\left(-\frac{E_a}{RT}\right) \tag{2.55}$$

which can be expressed also as

$$\ln k = -\frac{E_a}{RT} + \ln A \tag{2.56}$$

where k is the rate constant, A is the Arrhenius pre-exponential factor, E_a is the activation energy, R is the gas constant, and T is the temperature in Kelvin. A plot of $\ln k$ versus $1/T$ gives a straight line graph with slope equal to $-E_a/R$ and intercept equal to $\ln A$.

The Arrhenius equation is still widely used in certain areas of kinetics and the complex systems where the measured rate constant is thought to be a complex composite of specific rate constants.

2.4.2 Transition-State Theory

In case of absolute reaction rate theory, the activated complex is in equilibrium with the reactants A and B.

$$A + B \rightleftharpoons^{K^{\neq}} \underset{\text{activated complex}}{(A\text{----}B)^*} \longrightarrow A{-}B \tag{2.57}$$

The rate of reaction can be written as

$$\begin{aligned} -\frac{d[A]}{dt} &= \frac{k_b T}{h}[A--B]^{\neq} \\ &= \frac{k_b T}{h} K^{\neq}[A][B] \end{aligned} \tag{2.58}$$

where k_b is Boltzman's constant and h is Planck's constant. Experimentally the second-order rate constant k_2 can be equated to

$$k_2 = \frac{k_b T}{h} K^{\neq} \tag{2.59}$$

But the Gibbs energy of activation, $\Delta G^{\neq}$ can be expressed as

$$\Delta G^{\neq} = -RT \ln K^{\neq} = \Delta H^{\neq} - T\Delta S^{\neq} \tag{2.60}$$

Substituting equation (2.60) into (2.59) gives

$$\begin{aligned} k_2 &= \frac{k_b T}{h} \exp\left(-\frac{\Delta G^{\neq}}{RT}\right) \\ &= \frac{k_b T}{h} \exp\left(-\frac{\Delta H^{\neq}}{RT}\right) \exp\left(\frac{\Delta S^{\neq}}{R}\right) \end{aligned} \tag{2.61}$$

Rearranging and taking the logarithm results in

$$\begin{aligned} \ln\left(\frac{k_2}{T}\right) &= -\frac{\Delta H^{\neq}}{RT} + \left[\ln\left(\frac{k_b}{h}\right) + \frac{\Delta S^{\neq}}{R}\right] \\ \ln\left(\frac{k_2}{T}\right) &= -\frac{\Delta H^{\neq}}{RT} + \left(23.8 + \frac{\Delta S^{\neq}}{R}\right) \end{aligned} \tag{2.62}$$

and a plot of $\ln(k_2/T)$ versus $1/T$ gives $\Delta H^{\neq}$ from the slope as the enthalpy of activation and entropy of activation, $\Delta S^{\neq}$ from the intercept. The plot is known as an Erying plot.

2.4.3 Volume of Activation

The volume of activation is a supplement to the enthalpy and entropy of activation obtained by measuring the variation of the rate constant with pressure.

$$\frac{d(\ln k)}{dP} = -\frac{\Delta V^{\neq}}{RT} \qquad (2.63)$$

The volume of activation ($\Delta V^{\neq}$) is a measure of the compressibility difference between the ground state and transition state. The $\Delta V^{\neq}$ changes with mechanism as $\Delta S^{\neq}$: a positive value indicates a dissociative mechanism and a negative value indicates an associative mechanism.[8]

2.5 Instrumentation

Reactions in solution make up a very large proportion of the chemical reactions whose kinetics have been subjected to detailed investigation. The classical methods of following the progress of such reactions involve chemical analysis by volumetric or gravimetric procedures. This approach gives reliable results if the reaction is slow, with a half-life in excess of an hour. The second group of methods, which are more convenient and applicable in the study of fast reactions, are physical methods. These involve the measurement of some physical property of the reaction mixture, which changes as the reaction proceeds. Currently, large proportions of chemical kinetic studies are carried out by monitoring a physical property of the reaction mixture. This has been made possible by the availability of sophisticated computer-driven laboratory instruments.

The various techniques that are usually employed to study the kinetics of a reaction include the flow methods (*e.g.* stopped-flow, continous flow and quenched flow), UV-Visible spectrophotometry, Nuclear Magnetic Resonance (NMR) spectrophotometry, and use of non-spectrophotometric techniques such as measurements of the conductivity of the reaction mixture at some time interval. The preference of one technique over the other depends on the rate of the reaction being investigated.

The kinetic studies of very fast reactions, such as those involving palladium complexes can be made using flow techniques. The choice of the flow technique depends on the half-life of the reaction. The stopped-flow technique is used to study systems that have a half-life of up to 10^{-3} s.[7] For even faster reactions, the temperature jump method can be used to investigate reactions with a half-life of up to 10^{-7} s while flash photolysis can go down to 10^{-12} s.

Slow reactions can easily be followed using UV-Visible spectrophotometry. The following two sections give a short summary of the general principles of stopped-flow and UV-Visible techniques, since these were employed in the current investigation.

2.5.1 Stopped-Flow technique

The stopped-flow technique is the most popular of the flow methods. It is widely used in the investigation of reactions with a half-life of between 10^{0}-10^{-3} s.[7, 8] A schematic diagram of a stopped-flow is shown in **Figure 2.2**.[9]

The apparatus is designed for the study of a reaction between two substances in solution. From the two reservoirs, the syringes A and B are filled with their respective solutions and the system is left to equilibrate at the desired temperature. To start the reaction, the solutions are forced out of their syringes by concerted pressure on the plungers, into the mixing chamber. This is designed in such a way that jets of the two solutions impinge on one another and give very rapid mixing within 0.001 s.[9]

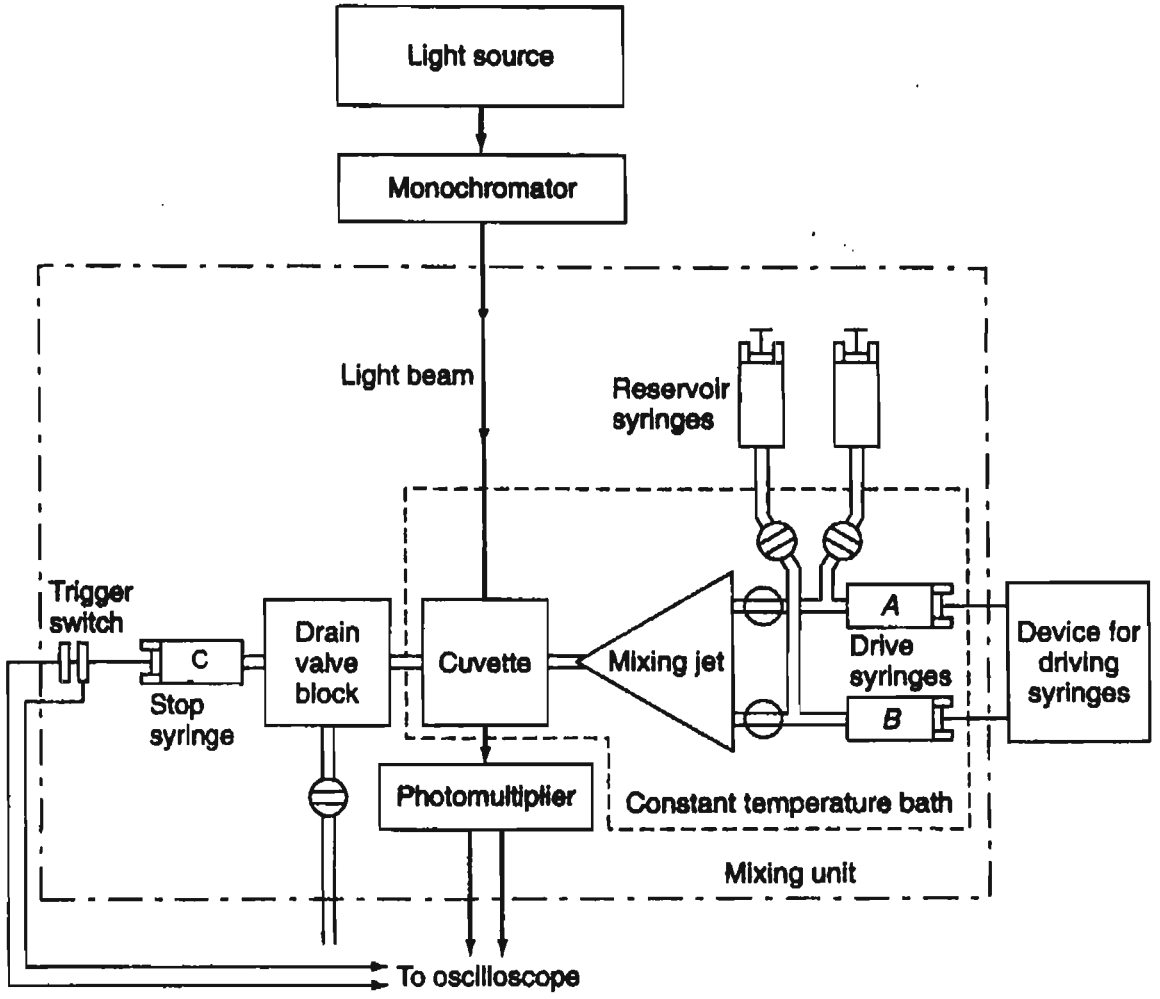

Figure 2.2 *Schematic diagram of stopped flow apparatus.*

From this mixing chamber the solution passes at once into the reaction cuvette; alternatively, the two solutions may be combined inside the reaction chamber. The reaction mixture passes on to the stop syringe C. When the plunger of the latter reaches its stop, this both arrests the flow of the mixing solutions and triggers the recorder. At this point onwards, the amount of light, at the wavelength setting of the monochromator, transmitted through the mixed solution in the cuvette, will undergo changes as the reaction proceeds in the now static mixed solution. A photomultiplier unit converts this transmitted light into an electric current and a signal is fed to the computer over an appropriate time interval. The kinetic data is then processed to evaluate the pseudo-first-order rate constant.

2.5.2 UV-Visible Spectrophotometry technique

UV-Visible spectroscopy is a sensitive technique; it can detect samples of low concentrations in the range of 10^{-4} to 10^{-6} M.[7] The basic units of spectroscopic equipment are the radiation source, the sample container, the monochromator, the detector and the detector output-measuring instrument. Prisms or gratings are normally used as the monochromator. The type of prism used depends on the region of electromagnetic spectrum. For the UV-Visible region, glass prisms are normally used. The eye, photographic plate and photoelectric cells are used as detectors for the visible region, while the last two are also employed for the ultra-violet region. **Figure 2.3** shows a schematic diagram representing the optical system of a typical photoelectric spectrophotometer.[10]

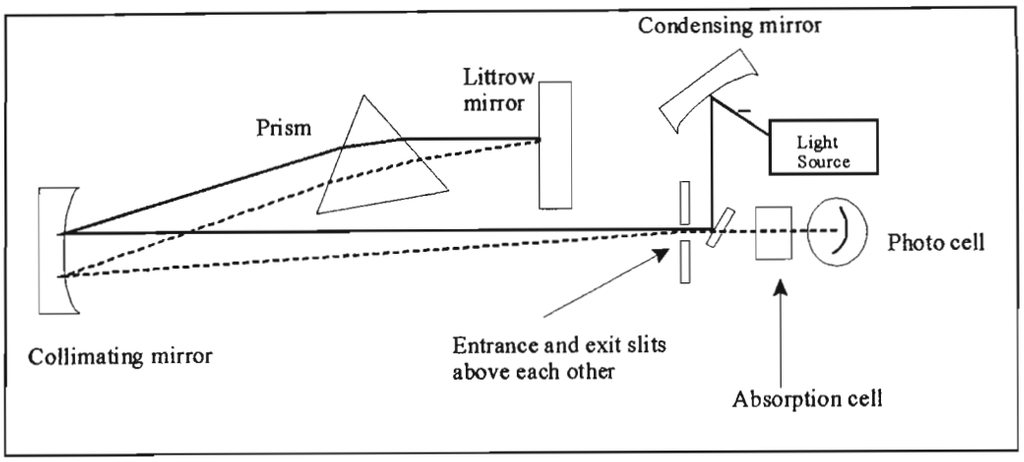

Figure 2.3 *Schematic diagram of a UV-Visible spectrophotometer.*

A substitution reaction that is slow and not able to be monitored using a stopped-flow technique can be monitored by means of UV-Visible spectrophotmetry using tendum cuvettes. UV-Visible scans are recorded at set time intervals immediately after mixing the reactants. A typical set of scans is shown in **Figure 2.4**.

The rate constant for this reaction can be obtained by on line least squares fit of the observed absorbance versus time trace at wavelengths A, B or C, since there is noticeable change in the absorbance over a period of time. The reactions can also be monitored at different temperatures by connecting a thermostat instrument to the UV-Visible instrument.

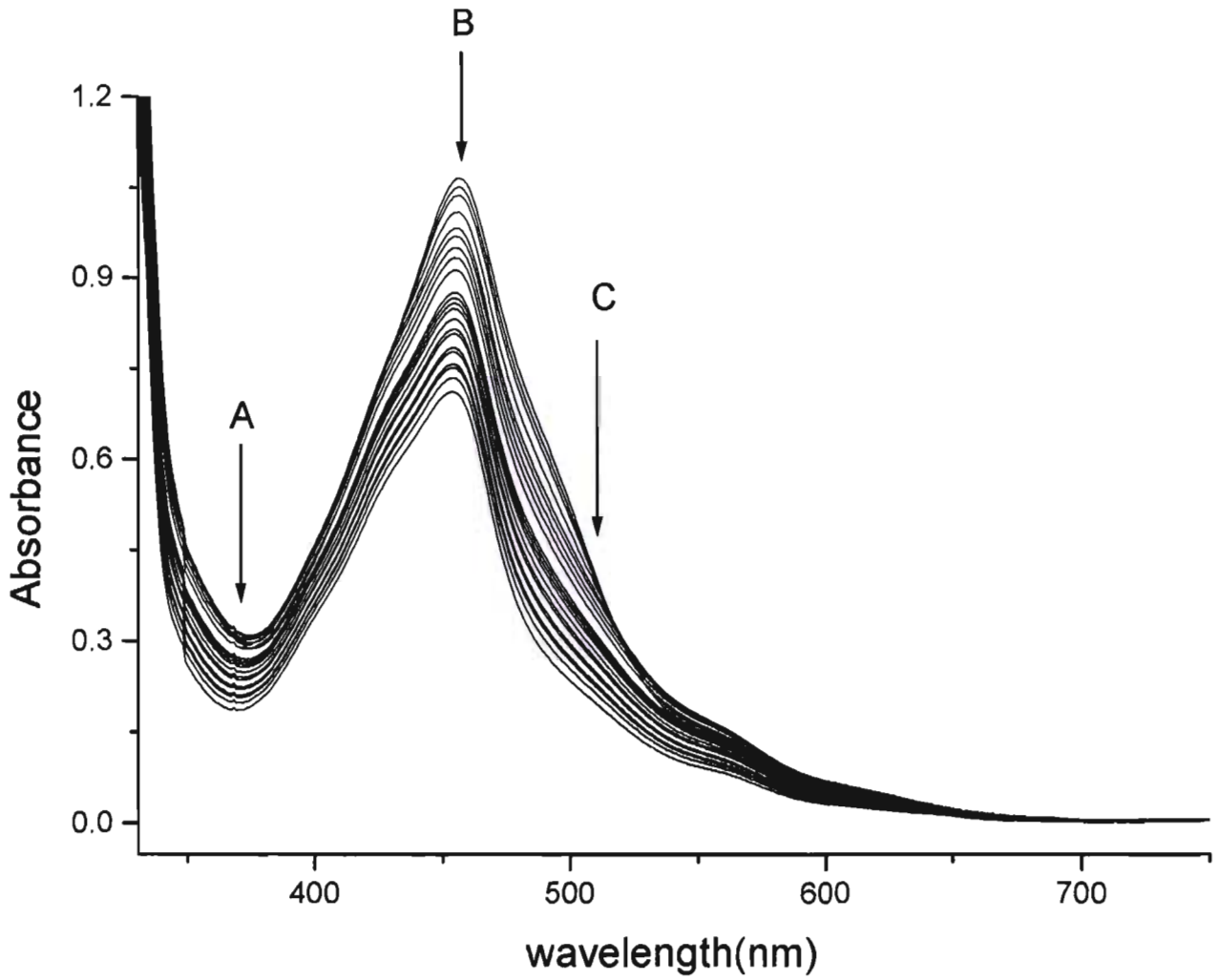

Figure 2.4 *UV-Vis scans for the reaction of* $[Ru(terpy)(bipy)(OH_2)](ClO_4)_2$ *with dimethylthiourea, recorded at 1 hour interval in aqueous medium at 25 °C.*

It is possible to analyze changes in the concentration of specific reactants or products, from absorbance changes in the reaction mixture by using the Beer-Lambert Law given in equation (2.64).

$$A = \log_{10} \frac{I_0}{I_t} = \varepsilon c l \qquad (2.64)$$

where A is the optical absorbance, c is the molar concentration, l is the path length and ε is the molar absorption coefficient. The intensity of the transmitted light, I_t, and the incident light, I_0, are converted into absorbance by taking the log function of the ratio.

REFERENCES

1) G. Alibrandi, G. Bruno, S. Lanza, D. Mittini, R. Romeo, and M. L. Tobe, *Inorg. Chem.*, **1987**, *26*, 185.

2) U. Frey, L. Helm, A. E. Merbach and R. Romeo, *J. Am. Chem. Soc.*, **1989**, 8161.

3) S. Lanza, D. Minniti, P. Moore, J. Sachinidis, R. Romeo, M. L. Tobe, *Inorg. Chem.*, **1984**, *23*, 4428.

4) M. Schumülling and R. van Eldik, *Chem. Ber./ Recueil.*, **1997**, *130*, 1791.

5) R. G. Pearson, H. B. Gray and F. Basolo, *J. Am. Chem. Soc.*, **1960**, *82*, 787.

6) R. L. Rominger, J. M. Mcfarland, J. R. Jeitler, J. S. Thompson and J. D. Atwood, *J. Coord. Chem.*, **1994**, *31*, 7.

7) D. Katakis, G.Gordon, "*Mechanisms of Inorganic Reactions*", John Wiley & Sons, New York, **1987**, p 99.

8) R. G. Wilkins, *Kinetics and Mechanism of Reactions of Transition Metal Complexes*, 2nd Edition, VCH Verlagsgesellschaft mbH, New York, **1991**, p 201, 232.

9) K. J. Laider, J. H. Meiser, *Physical Chemistry*, 3rd, Houghton Mifflin Company, Boston, **1999**, 380.

10) C. N. R. Rao, "*Ultra-Violet and Visible Spectrophotometry, Chemical Applications*", 2nd Edition, London, **1967**, p 7.

CHAPTER THREE

EXPERIMENTAL

3 EXPERIMENTAL

PART A Synthesis of Square Planar Pt(II) and Pd(II) Complexes

The ligands, *bis*(2-pyridylmethyl)amine (bpma), and 2,2:6',2"-terpyridine (terpy) and nucleophiles, *viz*. NaI, NaBr, NaSCN, thiourea (TU), 1,3-dimethyl-2-thiourea (DMTU) and 1,1,3,3-tetramethyl-2-thiourea (TMTU) were purchased from Aldrich and used without further purification. The thiol nucleophiles, *viz*. glutathione, DL-penicillamine and L-cysteine, were also purchased from Aldrich and stored at +4 °C. The metal complexes, K_2PtCl_4 and $PdCl_2$ used in synthesis and the buffer solutions used in calibration of the pH meter were purchased from Merck. All the solvents and other chemicals were of highest purity and were used as received. Ultra pure water (MODULAB water purification system) was used in synthesis and in kinetic and spectroscopic measurements. The purity of the complexes was checked by using a Carlo Erba Elemental Analyser 1106 and NMR spectroscopy (Bruker Advance DPX 300).

3.1 Synthesis of Platinum(II) Terpyridine Monoaqua Complex $[Pt(terpy)(OH_2)](BF_4)_2$

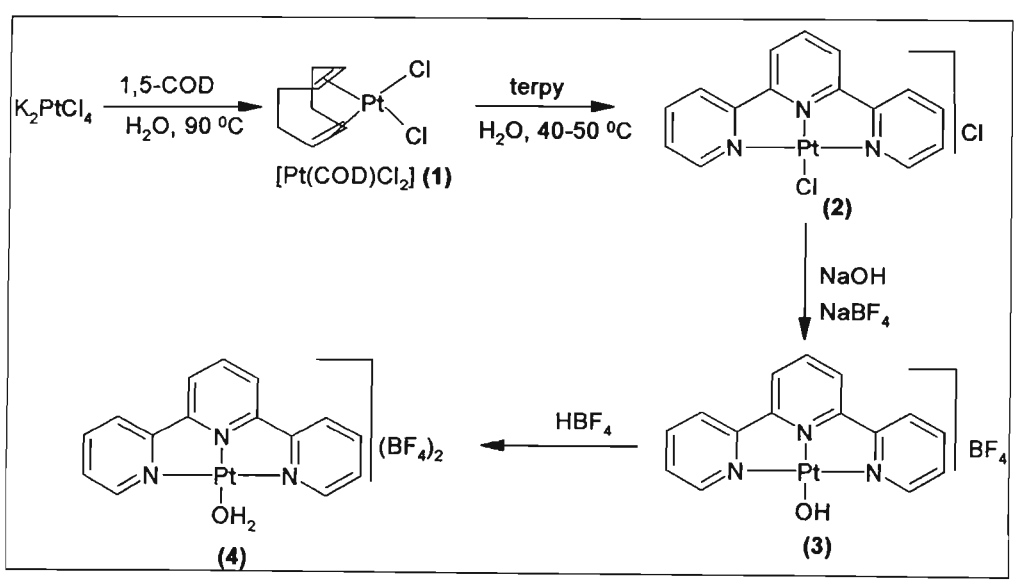

Scheme 3.1 *Synthetic steps in preparing* $[Pt(terpy)(OH_2)](BF_4)_2$.

Synthesis of $[Pt(terpy)(OH_2)](BF_4)_2$ was achieved in four steps. The first step involved the preparation of dichloro(1,5-cyclooctadiene)platinum(II) $[(COD)PtCl_2]$**(1)**[1] which was used as the starting material in the second step to form $[Pt(terpy)Cl]Cl.2H_2O$ **(2)**.[2] The complex $[Pt(terpy)Cl]Cl.2H_2O$ **(2)** was then converted into $[Pt(terpy)OH]BF_4$ **(3)**[3] and finally to $[Pt(terpy)(OH_2)]BF_4$**(4)**[4] the target complex. Complexes **(1)** and **(2)** were used in the subsequent reactions without further purification since they matched the physical description from the literature.[1, 2] Complex **(3)** was characterized by CHN microanalysis before being used in the final step. The final aqua complex **(4)** was also characterized by means of CHN microanalysis.

3.1.1 Dichloro(1,5-cyclooctadiene)platinum(II) [(COD)PtCl$_2$] (1)

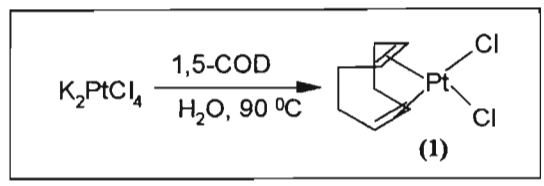

(1)

Potassium tetrachloroplatinate, K_2PtCl_4 (2.18 x 10^3 mg, 5.23 mmol) was dissolved in 55 mL of water and filtered. To the resultant deep red solution was added 35 mL glacial acetic acid and 1,5-cyclooctadiene(COD) (2.1 mL, 17 mmol). The resultant mixture was vigorously stirred and maintained at 90 °C on a steam bath for approximately 30 minutes. During this period the deep red solution changed colour to pale yellow and fine yellow crystals were deposited. To enhance further precipitation of the product the volume of the mixture was reduced under reduced pressure to approximately 10 mL. The fine yellow crystals were collected by filtration and washed in succession with 50 mL portions of water, ethanol and ether. The product was dried in an oven at 100 °C for an hour to afford the desired product. This product was used in the next step of the synthesis without any further purification.

Yield 1.75 g (4.68 mmol, 88 %)

3.1.2 [Pt(terpy)Cl]Cl.2H_2O (2)

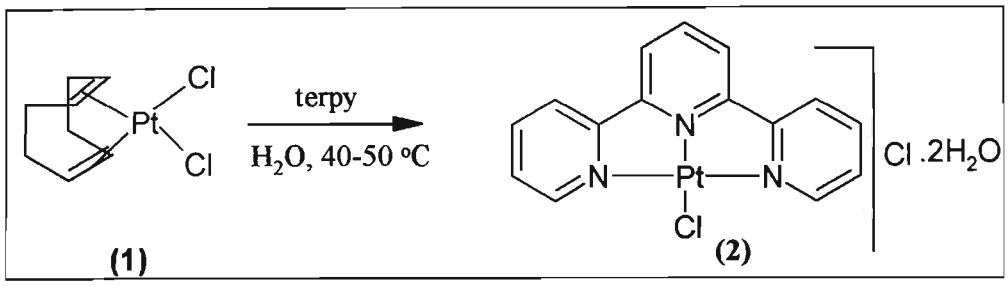

To a stirred suspension of [Pt(COD)Cl_2] **(1)** (500 mg, 1.34 mmol) in 30 ml of water, was added (312.9 mg, 1.34 mmol) of terpy. The mixture was stirred and warmed to 45-50 °C. After approximately 15 minutes, the suspended metal complex completely dissolved to afford a clear, red-orange solution. The solution was cooled to room temperature and then filtered to remove any unreacted [Pt(COD)Cl_2] **(1)**. The filtrate was then evaporated under reduced pressure and a red-orange solid was obtained. This solid was collected and washed thoroughly with diethyl ether and air-dried.

Yield 647 mg (1.21 mmol, 90%).

Microanalysis Found: C, 33.52; H, 2.72; N, 7.74.

Calc. For $C_{15}H_{15}N_3PtCl_2O_2$: C, 33.66, H, 2.77; N, 7.85.

3.1.3 [Pt(terpy)OH]BF_4 (3)

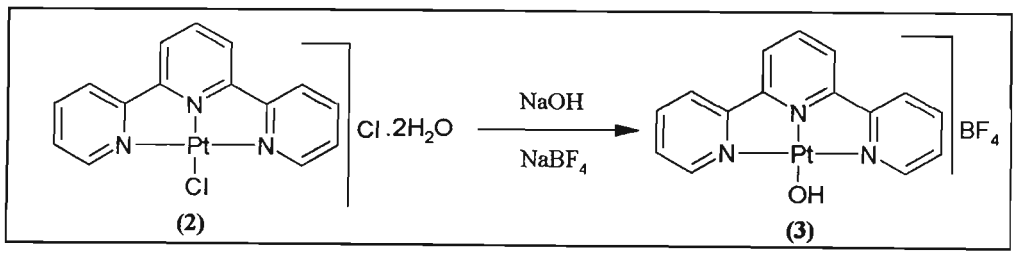

Complex **(2)** (510 mg, 0.95 mmol) was dissolved in 200 mL of water. To this was added NaOH (10 mL, 6 M) and the mixture warmed to 40 °C with stirring for 30 minutes. Upon the dropwise addition of concentrated $NaBF_4$ to the mixture, a bright orange precipitate

was seen to form. Crystallization was completed with the addition of excess $NaBF_4$. The precipitate was then collected by filtration and dried at 50 °C.

Yield 462 g (0.87 mmol, 92 %).

Microanalysis: Found: C, 33.82 %; H, 2.20 %; N, 7.88 %.

Calc. For $C_{15}H_{12}N_3BF_4OPt$: C, 33.74 %; H, 2.10 %; N, 7.92 %.

3.1.4 [Pt(terpy)(OH$_2$)](BF$_4$)$_2$ (4)

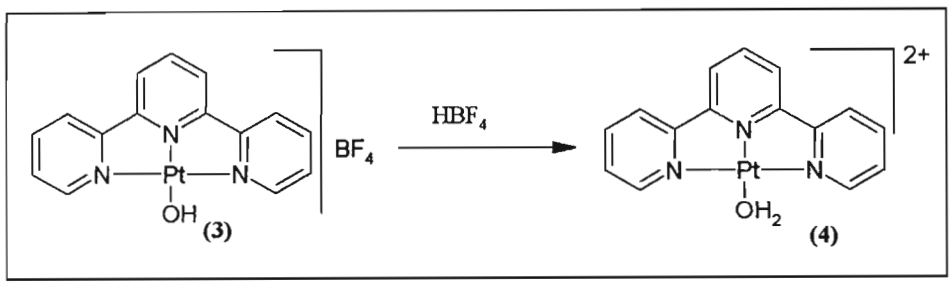

To a clear, orange solution of **(3)** (350 mg, 0.66 mmol) in 20 mL of water was added dropwise 5 mL of HBF_4 (0.15 M). This mixture was stirred for approximately 10 minutes, and then taken to dryness on a rotary evaporator to afford an orange, microcrystalline solid, which was dried *in vacuo* over P_2O_5.

Yield 315 mg (0.51 mmol, 77 %).

Microanalysis Found: C, 29.60; H, 2.18; N, 7.34.

Calc. For $C_{15}H_{13}N_3B_2F_8OPt$: C, 29.06; H, 2.10; N, 6.8.

3.2 Synthesis of Platinum *bis*(2-pyridylmethyl)amine Monoaqua Complex [Pt(bpma)(OH$_2$)](ClO$_4$)$_2$

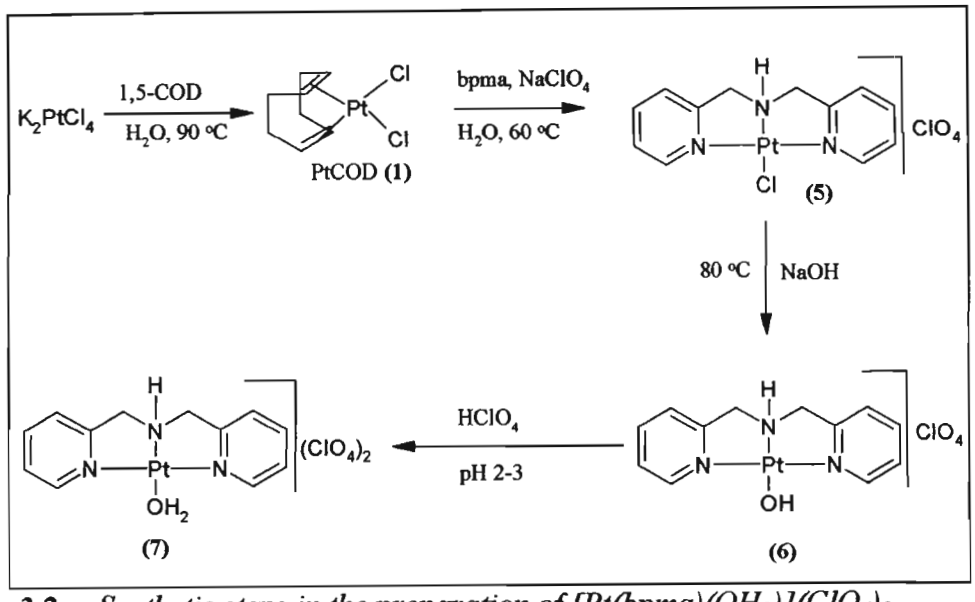

Scheme 3.2 *Synthetic steps in the preparation of [Pt(bpma)(OH$_2$)](ClO$_4$)$_2$.*

The complex [Pt(bpma)(OH$_2$)](ClO$_4$)$_2$ was prepared by following the same procedure as described for [Pt(terpy)(OH$_2$)](BF$_4$)$_2$ with slight modifications.[5] The complex [Pt(bpma)OH](ClO$_4$) **(6)** was characterized by ^{1}H-NMR and CHN microanalysis.

3.2.1 [Pt(bpma)Cl]ClO$_4$ (5)

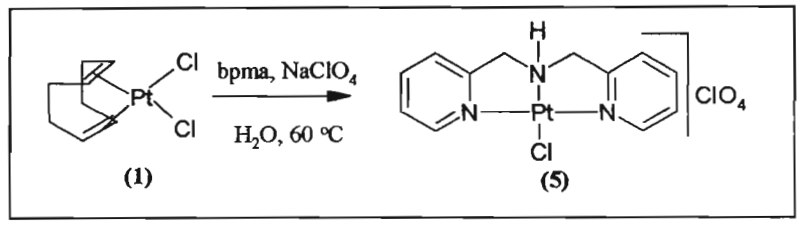

To a suspension of Pt(COD)Cl$_2$ **(1)** (52 mg, 0.14 mmol) in water (30 mL) was added *bis*(2-pyridylmethyl)amine (28 mg, 0.14 mmol). The pH of the mixture was adjusted to 3.5 by the careful addition of concentrated HCl. The temperature of the mixture was raised to 60 °C and maintained whilst stirring until the solution became clear. This was then filtered before adding 2 mL of a saturated NaClO$_4$ solution. A yellow precipitate of [Pt(*bis*(2-pyridylmethyl)amine)Cl]ClO$_4$ was formed and was collected on a sintered glass

filter. This was carefully washed with small amounts of water, ethanol and ether, and dried *in vacuo*, to afford the desired product.

Yield: 21 mg (0.04 mmol, 29 %).

Microanalysis Found: C, 27,50; H, 2.55; N, 7.62

Calc. For $C_{12}H_{13}N_3O_4Cl_2Pt$: C, 27,22; H, 2.46; N, 7.94

3.2.2 [Pt(bpma)OH](ClO$_4$) (6)

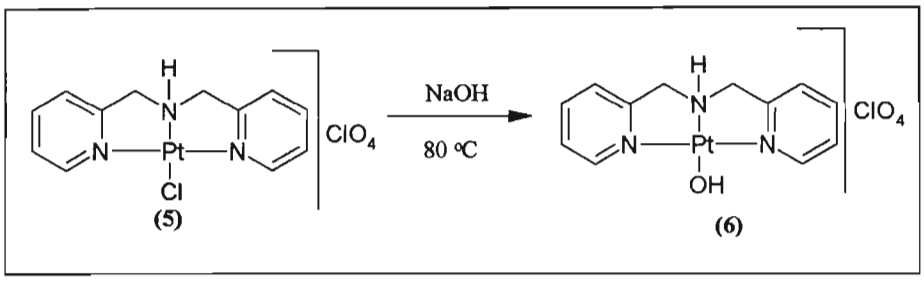

A sample of **(5)** (216 mg, 0.41 mmol) was dissolved in hot water (50 mL). To the clear solution was added NaOH (5 mL, 0.1 M). The solution changed colour from yellow to green. This was then followed by heating the solution to 80 °C. This temperature was maintained for 20 minutes while stirring before it was refrigerated overnight to give the desired yellow precipitate. The product was filtered off, washed carefully with small amounts of water and dried *in vacuo* to afford [Pt(*bis*(2-pyridylmethyl)amine)OH]ClO_4.

Yield: 159 mg (0.31 mmol, 80%).

Microanalysis Found: C, 28.2; H, 2.85; N, 8.49

Calc. For $C_{12}H_{14}N_3O_5ClPt$: C, 28.2; H, 2.75; N, 8.2

3.2.3 [Pt(bpma)(OH$_2$)](ClO$_4$)$_2$ (7)

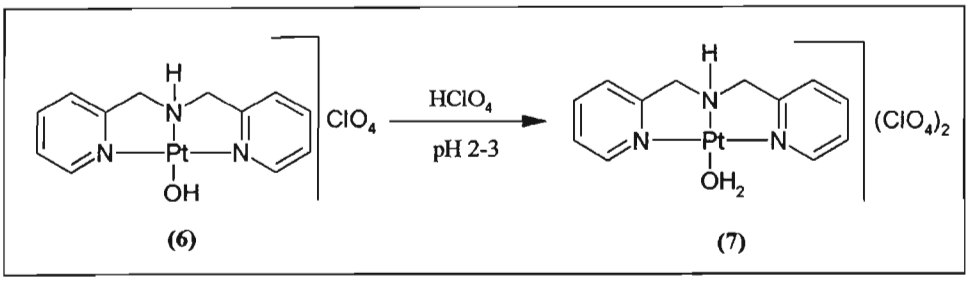

Finally to prepare **(7)**, a known amount of the hydroxo complex **(6)** was dissolved in aqueous solution of pH 2-3, adjusted using $HClO_4$. This solution whose concentration is known was then used for kinetic study. This procedure can also be used to obtain $[Pt(terpy)(OH_2)]^{2+}$ in solution from $[Pt(terpy)OH]^{+}$.

3.3 Synthesis of Palladium bis(2-pyridylmethyl)amine Monoaqua Complex [Pd(bpma)(OH$_2$)](ClO$_4$)$_2$

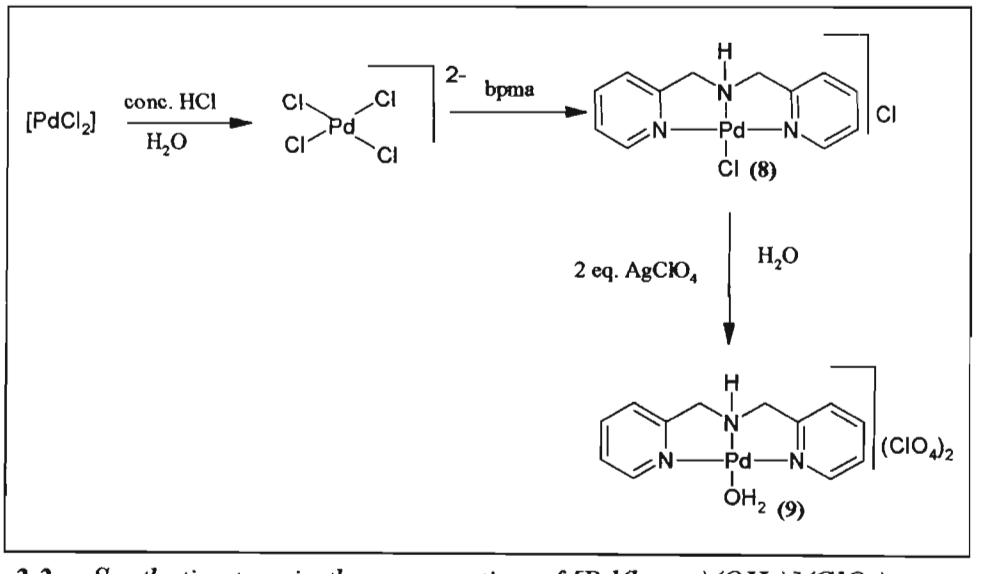

Scheme 3.3 *Synthetic steps in the preparation of [Pd(bpma)(OH$_2$)](ClO$_4$)$_2$.*

Synthesis of $[Pd(bpma)(OH_2)](ClO_4)_2$ was carried out according to the method available in literature.[6] The chloro complex [Pd(bpma)Cl]Cl which is an intermediate compound in the synthesis of the aqua complex product was characterized using CHN microanalysis.

3.3.1 [Pd(bpma)Cl]Cl. H_2O (8)

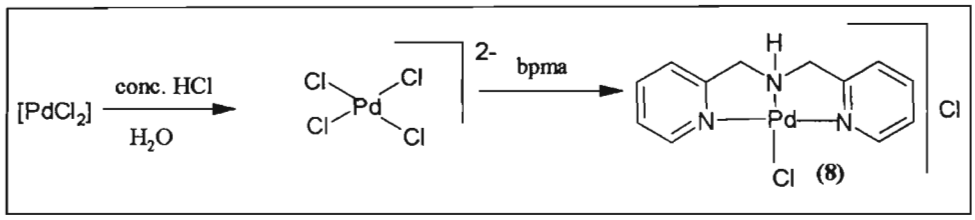

$PdCl_2$ (75.2 mg, 0.424 mmol) was added to a mixture of water (10 mL) and concentrated HCl (3 mL). The resulting mixture was refluxed until the entire solid had dissolved. The resulting clear solution of $[PdCl_4]^{2-}$ was filtered and warmed to 50 °C. This was followed by dropwise addition of a solution of bis(2-pyridylmethyl)amine (84.4 mg, 0.350 mmol) in methanol (10 mL). The pH of the solution was carefully adjusted to between 5.0-5.5 by the addition of aqueous sodium hydroxide. This resulted in a clear, bright yellow solution that was filtered and allowed to stand at room temperature. The bright yellow crystals that precipitated from the filtrate were collected by filtration, washed with cold water and diethyl ether and air-dried. The yellow powder was recrystallised from a minimum amount of 0.1 M HCl at 40-50 °C. The bright yellow needles that formed, were collected by filtration, washed with water and diethyl ether, and the product was air-dried.

Yield 150 mg (0.380 mmol, 90 %).

Microanalysis Found: C, 36.54; H, 3.78; N, 10.58.

Calc. For $C_{12}H_{13}N_3PdCl_2O$: C, 36.52; H, 3.29; N, 10.65.

3.3.2 $[Pd(bpma)(OH_2)](ClO_4)_2$ (9)

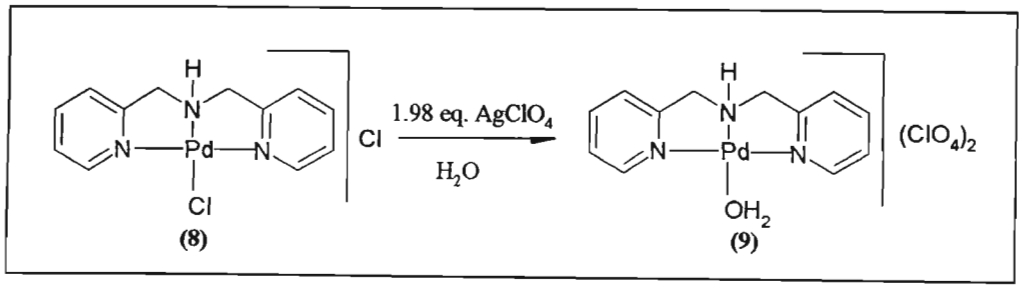

The chloro complex **(8)** (36.4 mg, 0.0922 mmol) was dissolved in water (200 mL, pH = 3 ($HClO_4$)) to obtain a solution of 4.62 x 10^{-4} M concentration. $AgClO_4$ (38.3 mg, 0.1849 mmol) was then added to the solution, the mixture was maintained at 40 °C while stirring for 16 hours in the dark. The AgCl precipitate formed was filtered off using a Millipore unit fitted with a 0.1 μm pore membrane filter. This is important so as to ensure that the final solution was free of Ag^+ ions and that the chloro complex has completely been converted into the aqua species. The ionic strength of the filtrate collected was adjusted to 0.1 M using $NaClO_4$ for the kinetic investigation.

PART B Synthesis of Octahedral Ru(II) Polypyridine Monoaqua Complexes

The materials used were purity grade and were used without further purification. The metal salt, $RuCl_3 \cdot 3H_2O$, 2,2'-bipyridine (bipy), *N,N,N',N'*-tetramethylethylenediamine (tmen), thiourea (TU), 1,3'-dimethyl-2-thiourea (TMTU) and 2,2:6',2"-terpyridine (terpy) were all purchased from Aldrich Chemical Company. Ultrapure water (MODULAB water purification system) was used for all aqueous studies and syntheses. $MgSO_4$ and KBr were dried in an oven at 100 °C overnight before use. The purity of the complexes was checked using NMR (Varian Unity Inova 500 MHz spectrometer using solvent as an internal reference), and Infrared spectrometry (Perkin-Elmer Spectrum One FTIR Spectrophotometer)[1]. Microanalyses were carried out at the following Universities: University of Natal (Durban), University of the Western Cape, University of Erlangen-Nurnberg (Germany), and at Galbraith Laboratories (USA). UV-Vis spectra were recorded using a Varian Cary 100 Spectrophotometer.

---

[1] **Note:** *The Infrared bands were not assigned due to the lack of information relating to the stretching modes of ruthenium(II) polypyridine complexes. The literature searched include* (i) K. Nakamoto, "*Infrared and Raman Spectra of Inorganic and Coordination Compounds*", 3rd Edition, John Wiley & Sons, New York, **1979**. (ii) E. W. Abel, F. G. A. Stone, G. Wilkinson, "*Comprehensive Organometallic Chemistry II*", Pergamon Press, Oxford, **1995** (ii) "*Dictionary of Organometallic Compounds*", Chapman and Hall, London, **1984**.

Synthetic methods for preparations of $[Ru(terpy)(bipy)(OH_2)](ClO_4)_2$ and $[Ru(terpy)(tmen)(OH_2)](ClO_4)_2$ are described below.

3.4 Synthesis of Ruthenium Terpyridine Bipyridine Monoaqua Complex $[Ru(terpy)(bipy)(OH_2)](ClO_4)_2$

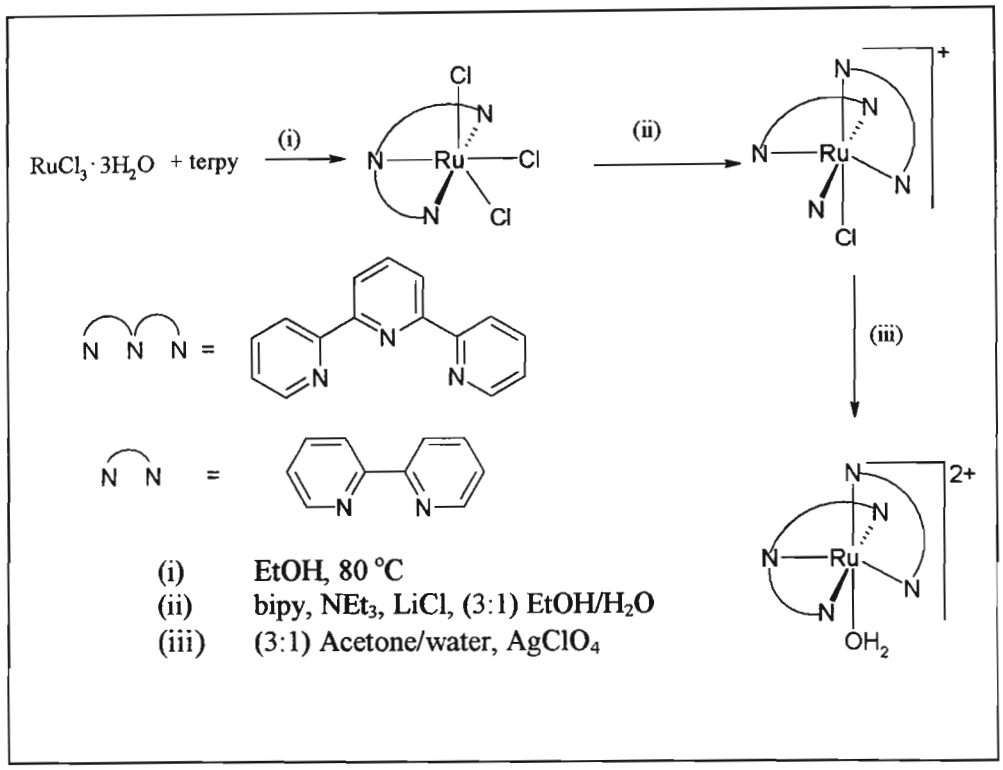

Scheme 3.4 *Synthetic steps in preparation of* $[Ru(terpy)(bipy)(OH_2)](ClO_4)_2$.

The synthesis of this complex was executed in three steps as shown in **Scheme 3.4**. The first step involved the preparation of the $Ru^{III}(terpy)Cl_3$ complex following the method described in the literature.[7] Due to the insolubility of the complex in most organic solvents, this complex was used in the next step without any further purification.

The complex $[Ru(terpy)Cl_3]$ was reduced in the next step from Ru(III) to Ru(II) in the presence of a reductant, namely NEt_3.[8, 9] In the presence of the bidentate ligand, *viz.* bipy, a complex [Ru(terpy)(bipy)Cl]Cl was formed.[10] Finally, the desired product, $[Ru(terpy)(bipy)(OH_2)](ClO_4)_2$, was obtained from the metathesis reaction of [Ru(terpy)(bipy)Cl]Cl with a silver salt, *e.g.* $AgClO_4$.

CAUTION: *perchlorate salts are hazardous because of the possibility of their explosion. They should be prepared in small amounts and stored appropriately.*

3.4.1 [Ru(terpy)Cl$_3$] (10)

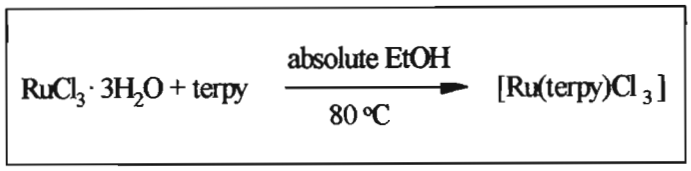

To a solution of $RuCl_3 \cdot 3H_2O$ (~150 mg) in absolute EtOH (125 mL) was added an equivalent amount of terpy. The resultant mixture was heated under reflux for 3 hours with vigorous stirring. After this time the mixture was allowed to cool to room temperature. The precipitate that formed was collected by filtration through a Büchner funnel. The precipitate was washed with a small amount of cold absolute ethanol, followed by diethyl ether and dried *in vacuo*.

Yield **(10)** 0.1435 g (0.627 mmol, 52 %) brown precipitate

This complex matched the description reported by Sullivan *et al.*[8] The infrared spectrum for this complex is given in APPENDIX B, Figure B.1. Due to insolubility of this complex in most of the organic solvent, NMR analysis of this complex was not done.

3.4.2 [Ru(terpy)(bipy)Cl]Cl (11)

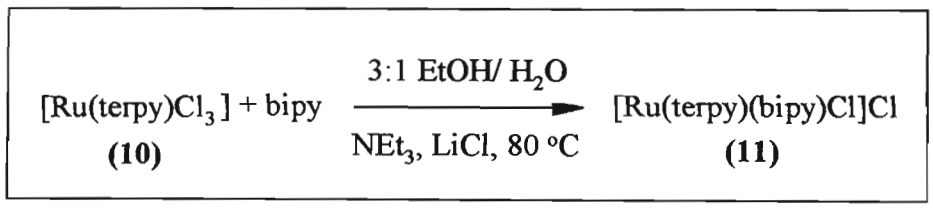

A quantity of about 100 mg of **(10)** was reacted with an equimolar amount of bipy and refluxed for 4 hours in 75 mL of (3:1) $EtOH/H_2O$ containing ~6 molar equivalents of LiCl and an equimolar amount of NEt_3. The mixture was filtered while hot through a sintered glass funnel to remove any unreacted starting material. The volume of the filtrate was reduced under reduced pressure to approximately 10 mL.

A dark reddish precipitate of [Ru(terpy)(bipy)Cl]Cl was seen to form. Further precipitation was induced by cooling overnight at *ca.* +4 °C in the fridge. The precipitate was collected by filtration and washed with a small amount of ethanol followed by diethyl ether and dried *in vacuo*.

Yield **(11)** 0.1990 g (0.317 mmol, 70 %)

This complex was characterized using NMR and infrared spectroscopy. The proton NMR spectrum for this complex along with the infrared spectrum are given in **APPENDIX A**, **Figures A.1** and **APPENDIX B**, **Figure B.2**.

3.4.3 [Ru(terpy)(bipy)(OH_2)]ClO_4 (12)

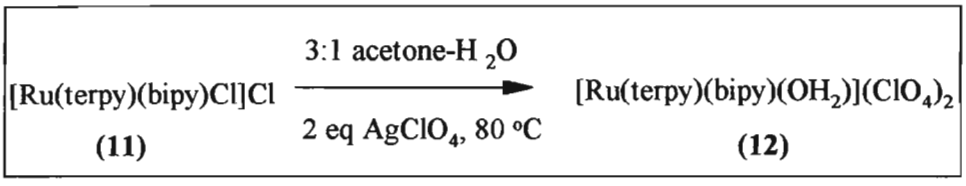

A sample of **(11)** (50 mg, 0.080 mmol) was heated under reflux with two equivalents of $AgClO_4$ (33 mg, 0.160 mmol) for 1 hour in 20 mL of (3:1) acetone/H_2O solution. The AgCl precipitate that formed was filtered using a Millipore Filtration system fitted with 0.1 μm pore membrane filter. The filtrate was concentrated *in vacuo* to obtain brown-black crystals. The crystals were collected by filtration, washed with a small amount of cold water and then dried *in vacuo*.

Yield 25 mg (0.035 mmol, 44 %).

Microanalysis Found: C, 42.29; H, 2.61; N, 9.65.

Calc. for $C_{25}H_{21}N_5O_9RuCl_2$: C, 42.44; H, 2.99; N, 9.9.

UV-Vis (H_2O)[2] [λ_{max}/nm(ε, $M^{-1}cm^{-1}$)]: 475 (8.74×10^3) b, 312 (3.32×10^4) b, 288 (3.42×10^4) b, 231 (2.40×10^4) sh

[2] b = broad, sh = shoulder

3.5 Synthesis of Ruthenium Terpyridine *N,N, N',N'*-tetramethylethylenediamine Monoaqua Complex $[Ru(terpy)(tmen)(OH_2)](ClO_4)_2$

The synthesis of this complex was accomplished by following the method described by Che *et al.*[11] This method is similar to the method described above for the synthesis of the $[Ru(terpy)(bipy)(OH_2)]^{2+}$, except that the reductant used for this reaction was ethylene glycol instead of NEt_3. Ethylene glycol has a very high boiling point (195 °C). At this temperature $Ru^{III}(terpy)Cl_3$ is reduced to Ru(II) and in the presence of a bidentate ligand such as tmen, the complex $[Ru(terpy)(tmen)Cl]^+$ is formed.

3.5.1 $[Ru(terpy)(tmen)Cl]ClO_4$ (13)

$$[Ru(terpy)Cl_3] + tmen \xrightarrow[195\ ^oC]{ethylene\ glycol} [Ru(terpy)(tmen)Cl]^+$$

(10) **(13)**

A sample of **(10)** (479.2 mg, 1.09 mmol) and tmen (5.3 mL, 34.81 mmol) was refluxed together in ethylene glycol (0.72 mL, 12.88 mmol) for 4 hours. The initial brownish-black solution becomes a dark purple after this time. The mixture was allowed to cool to room temperature. To this mixture 5 mL of ethanol was added. A saturated solution of $NaClO_4$ (10 mL) was added to the mixture until a purple precipitate was observed. The precipitate was collected by filtration through a Büncher funnel, washed with little amount of ice-cold water followed by diethyl ether and dried *in vacuo* for an hour.

Yield 355.9 mg (0.608 mmol, 56 %)

UV-Vis (CH_2Cl_2)[3] $[\lambda_{max}/nm(\varepsilon, M^{-1}cm^{-1})]$: 563 ($3.05 \times 10^3$) sh, 380 ($300 \times 10^3$) b, 326 ($2.19 \times 10^4$) b, 281 ($2.71 \times 10^4$) b

Microanalysis Found: C, 43.05; H, 4.85; N, 11.70.

Calc. for $C_{21}H_{27}N_5O_4RuCl_2$: C, 43.08, H, 4.73; N, 11.80.

[3] b = broad, sh = shoulder

The infrared spectrum of this complex is given in **APPENDIX B, Figures B.3**.

3.5.2 [Ru(terpy)(tmen)(OH_2)](ClO_4)$_2$ (14)

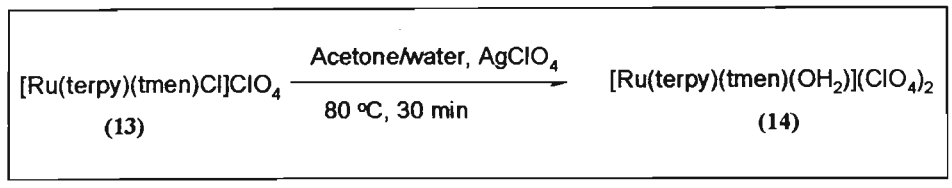

Sample **(13)** (150 mg, 0.256 mmol) and $AgClO_4$ (52.5 mg, 0.256 mmol) were refluxed in acetone-water (3:1) (10 mL) for 30 minutes. The AgCl precipitate was filtered using a Millipore unit fitted with a 0.1 μm pore membrane. The volume of the filtrate was reduced to about 2.5 mL, and about 1 g of $NaClO_4$ was added. The dark purple reddish microcrystalline precipitate that formed was filtered off, washed with a little ice-cold water, and dried *in vacuo*.

Yield 56.9 mg (0.0852 mmol, 33 %)

Microanalysis Found: C, 38.20 H, 4.82; N, 10.89.

Calc. for $C_{21}H_{29}N_5O_9RuCl_2$: C, 37.78; H, 4.38; N, 10.49.

3.6 Synthesis of Ruthenium Terpyridine Triaqua Complex [Ru(terpy)(OH_2)$_3$](ClO_4)$_2$

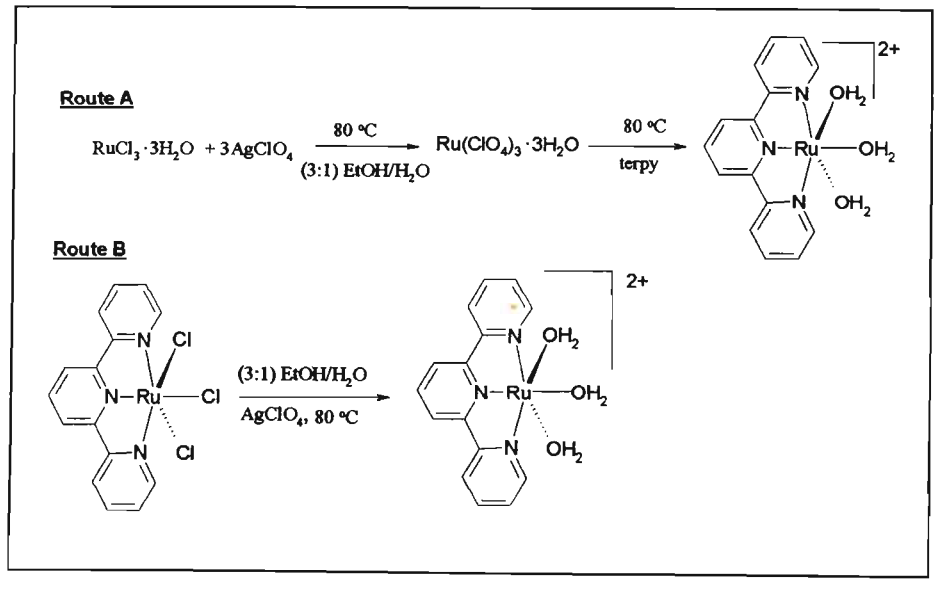

Scheme 3.5 *Synthetic approaches in the synthesis of [Ru(terpy)(OH_2)$_3$](ClO_4)$_2$.*

Two different approaches, **Route A** and **Route B**, were used for the synthesis of ruthenium terpyridine triaqua complex. Both approaches are represented in **Scheme 3.5**.

Route A involved the metathesis of the chloride ions from $RuCl_3 \cdot 3H_2O$ with $AgClO_4$ to obtain $Ru(ClO_4)_3 \cdot 3H_2O$, which was reacted with terpy in aqueous ethanol solution to form $[Ru(terpy)(OH_2)_3](ClO_4)_2$.

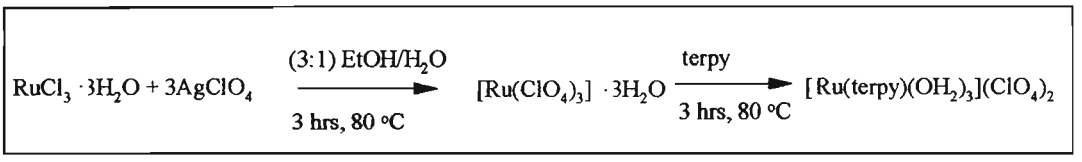

A sample of 100 mg of $RuCl_3 \cdot 3H_2O$ was refluxed with an equivalent quantity of $AgClO_4$ (*i.e.* mole ratio 1:3) in (3:1) $EtOH/H_2O$ solution for 1 hour. The AgCl precipitate was filtered off using a Millipore unit fitted with a 0.1 μm pore membrane filter. To the filtrate an equivalent amount of terpy was added and the mixture further refluxed for 3 hours. This mixture was taken to dryness using a rotary evaporator under reduced pressure.

Crude Yields $[Ru(terpy)(OH_2)_3](ClO_4)_2$ **(15)** 114.9 mg

NMR spectrum along with the infrared spectrum for the isolated complex is given in **APPENDIX A, Figures A.3** and **APPENDIX B, Figures B.4**.

Route B involved the removal of the three chloride ions from $[Ru(terpy)Cl_3]$ **(10)** using an equivalent quantity of $AgClO_4$ in aqueous ethanol solution to form the desired product.

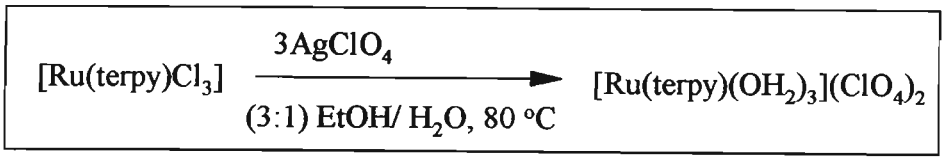

To a solution of **(10)** (100 mg) in (3:1) $EtOH/ H_2O$ was added three equivalents of $AgClO_4$ and the resulting mixture refluxed for 3 hours. The AgCl that precipitated out was filtered using a Millipore filtration system to obtain a clear solution of the desired product. The solution was taken to dryness using the rotary evaporator under reduced pressure.

Crude Yield $[Ru(terpy)(OH_2)_3](ClO_4)_2$ **(16)** 8.1 mg

3.7 X-Ray Structure Determination of $[Ru(terpy)(bipy)Cl]ClO_4$, $[Ru(terpy)(tmen)(CH_3CN)](ClO_4)_2$ and $[Ru(terpy)_2](ClO_4)_2$

During the attempt of synthesizing the complex $[Ru(terpy)(bipy)(OH_2)]^{2+}$ from the metathesis of $[Ru(terpy)(bipy)Cl]Cl$ with silver perchlorate, the complex $[Ru(terpy)(bipy)(Cl)]ClO_4$ was isolated. To check that the ligands had attached to the metal, single crystals suitable for X-ray analysis were grown for $[Ru(terpy)(bipy)Cl]ClO_4$, $[Ru(terpy)(tmen)(CH_3CN)](ClO_4)_2.CH_3CN$ and $[Ru(terpy)_2](ClO_4)_2$. These were obtained by vapour diffusion of diethyl ether into CH_3CN solutions of the complex $[Ru(terpy)(bipy)Cl]ClO_4$, **(14)** $[Ru(terpy)(tmen)(OH_2)](ClO_4)_2$ and the isolated **(16)** $[Ru(terpy)(OH_2)_3](ClO_4)_2$ complex following **Route B** (see **section 3.6**) respectively. Dark red needle-like crystals having approximate dimensions of 0.45 x 0.45 x 0.35 mm^3 $\{[Ru(terpy)(bipy)Cl]ClO_4\}$, 0.05 x 0.40 x 0.40 mm^3 $\{[Ru(terpy)(tmen)(CH_3CN)](ClO_4)_2.CH_3CN\}$ and of dimensions 0.40 x 0.15 x 0.05 mm^3 $\{[Ru(terpy)_2](ClO_4)_2$ were used to collect X-ray diffraction data. The photograph for the single crystal of $[Ru(terpy)_2](ClO_4)_2$ used is given in **Figure 3.1 (a)** along with an example of the observed diffraction pattern **(b)** (photograph parallel to the crystal b-axis).

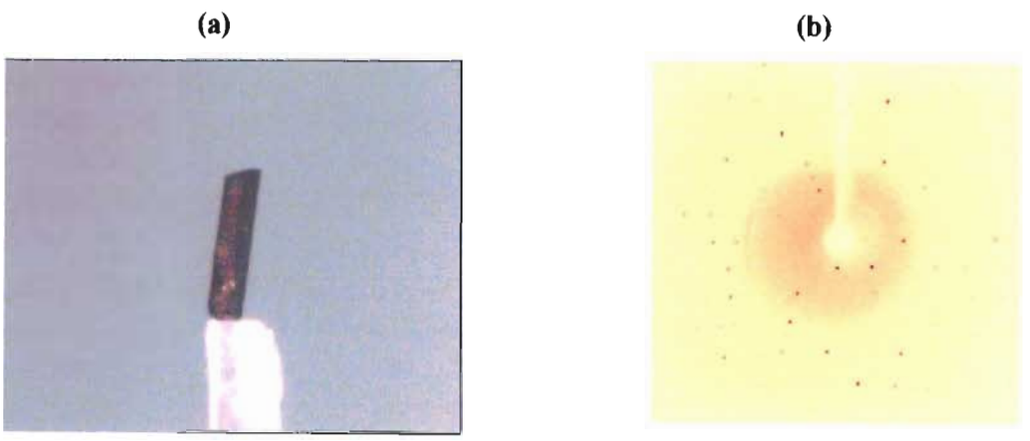

Figure 3.1 Single X-ray crystal photograph **(a)** used to collect X-ray data and **(b)** diffraction pattern observed for $[Ru(terpy)_2](ClO_4)_2$.

The X-ray data for $[Ru(terpy)(bipy)Cl]ClO_4$ were collected using ω-2θ scans with an

Enraf-Nonius CAD4-Turbo diffractometer at 20 °C. The structure was solved in the triclinic space group $P\bar{1}$ by automated Patterson methods and subsequent difference Fourier syntheses (SHELXS-97).[9] Refinement of F^2 was carried out by full matrix least-squares techniques (SHELXL-97).[10] Anisotropic thermal parameters were used for all non-hydrogen atoms. Hydrogen atoms were included in the refinement cycle at calculated positions, riding on their carrier atoms. Geometric calculations and the ORTEP[11] illustration were effected with WINGX.[12]

The X-ray data for $[Ru(terpy)(tmen)(CH_3CN)](ClO_4)_2.CH_3CN$ and $[Ru(terpy)_2](ClO_4)_2$ were collected on an Oxford Diffraction Xcalibur 2 CCD diffractometer with graphite monochromated Mo-Kα radiation (2.8 kW) at 20 °C and –173 (1) °C respectively. The unit cell dimensions were obtained from a least squares fit of reflections in the range $3.98 < \theta < 31.89°$ for $[Ru(terpy)(tmen)(CH_3CN)](ClO_4)_2.CH_3CN$ and $3.75 < \theta < 31.87°$ for $[Ru(terpy)_2](ClO_4)_2$. Lorentz, scan speed scaling and overlap corrections were applied during data reduction with the program CrysAlis RED.[12] The data were corrected for absorption effects using MULTISCAN.[13] The structures of $[Ru(terpy)(tmen)(CH_3CN)](ClO_4)_2.CH_3CN$ and $[Ru(terpy)_2](ClO_4)_2$ were solved in the monoclinic space group $P2_1/c$ and triclinic space group $P\bar{1}$ using direct methods (SHELXS-97)[14] and refined anistropically (SHELXS-97)[15] to a final R_1 of 12.8 % and 4.9 % respectively. The programs ORTEP,[16] WINGX,[17] Mercury 1.1[18] and Oscail[19] were used for data analysis and graphics.

Final parameter listings of the thermal parameters, bond distances, bond and torsion angles are given in **APPENDIX C**. Crystal data and summarized experimental procedures are given in **Table 3.1**, **3.2** and **3.3** for $[Ru(terpy)(bipy)Cl]ClO_4$, $[Ru(terpy)(tmen)(CH_3CN)](ClO_4)_2.CH_3CN$ and $[Ru(terpy)_2](ClO_4)_2$ respectively.

Table 3.1 Crystal *Data for [Ru(terpy)(bipy)Cl]ClO$_4$.*

Empirical Formula	$C_{25}H_{19}Cl_2N_5O_4Ru$	
Formula Weight	625.42	
T(K)	293(2)	
Wavelength	0.71073 Å	
Crystal system	Triclinic	
Space group	$P\bar{1}$	
Unit cell dimension	a = 9.121(2) Å	α = 101.14(4) °
	b = 12.777(6) Å	β = 97.41(3) °
	c = 13.353(7) Å	γ = 107.36(2) °
Volume	1428.0 (11) Å^3	
Z	2	
Density (calculated)	1.455 Mg/m^3	
Absorption coefficient	0.774 mm^{-1}	
F(000)	628	
Crystal size	0.45 x 0.45 x 0.35 mm^3	
θ range for data collection	2.39 to 24.97°	
Index ranges	-1<=h<=10, -15<=k<=14, -15<=l<=15	
Reflections collected	6124	
Independent reflections	4993 [R(int) = 0.0168]	
Completeness to θ = 24.97°	99.7 %	
Absorption correction	None	
Max. and min. transmission	0.7735 and 0.7222	
Refinement method	Full-matrix least-squares on F^2	
Data / restraints / parameters	4993 / 0 / 334	
Goodness–of–fit on F^2	1.127	
Final R indices [I > 2σ(I)]	R_1[a] = 0.0480, wR_2[b] = 0.1633	
R indices (all data)	R_1 = 0.0515, wR_2 = 0.1697	
Largest diff. peak and hole	1.885 and –0.849 e Å^{-3}	

Table 3.2 Crystal data for $[Ru(terpy)(tmen)(CH_3CN)](ClO_4)_2$.

Identification code	$[Ru(terpy)(tmen)(CH_3CN)](ClO_4)_2$	
Empirical formula	$C_{23}H_{30}Cl_2N_6O_8Ru$	
Formula weight	690.50	
Temperature	293(2) K	
Wavelength	0.71073 Å	
Crystal system	Monoclinic	
Space group	$P2_1/c$	
Unit cell dimensions	a = 32.050(6) Å	α = 90°
	b = 9.966(2) Å	β = 99.56(2)°
	c = 20.498(6) Å	γ = 90°
Volume	6456(3) $Å^3$	
Z	8	
Density (calculated)	1.421 Mg/m^3	
Absorption coefficient	0.701 mm^{-1}	
F(000)	2816	
Crystal size	0.40 x 0.40 x 0.05 mm^3	
θ range for data collection	3.98 to 31.90°	
Index ranges	-47<=h<=47, -14<=k<=14, -29<=l<=23	
Reflections collected	57385	
Independent reflections	20607 [R(int) = 0.0657]	
Completeness to θ = 25.00°	99.5 %	
Absorption correction	Numerical	
Max. and min. transmission	0.9658 and 0.7668	
Refinement method	Full-matrix least-squares on F^2	
Data / restraints / parameters	20607 / 716 / 731	
Goodness-of-fit on F^2	1.045	
Final R indices [I>2σ(I)]	R_1 = 0.1045, wR_2 = 0.3011	
R indices (all data)	R_1 = 0.1532, wR_2 = 0.3352	
Largest diff. peak and hole	2.222 and -1.902 e $Å^{-3}$	

Table 3.3 *Crystal data for $[Ru(terpy)_2](ClO_4)_2$*

Empirical formula	$C_{30}H_{22}Cl_2N_6O_8Ru$	
Formula weight	702.51	
Temperature	100(2) K	
Wavelength	0.71073 Å	
Crystal system	Triclinic	
Space group	P $\bar{1}$	
Unit cell dimensions	a = 9.514(3) Å	α= 69.75(4)°
	b = 16.932(11) Å	β= 82.83(2)°
	c = 20.156(6) Å	γ = 83.01(4)°
Volume	3012(2) $Å^3$	
Z	4	
Density (calculated)	1.549 Mg/m^3	
Absorption coefficient	0.744 mm^{-1}	
F(000)	1416	
θ range for data collection	3.75 to 31.87°	
Index ranges	-13<=h<=14, -17<=k<=24, -29<=l<=29	
Reflections collected	30287	
Independent reflections	18298 [*R*(int) = 0.0475]	
Completeness to θ = 31.87°	88.4 %	
Max. and min. transmission	0.9637 and 0.7551	
Refinement method	Full-matrix least-squares on F^2	
Data / restraints / parameters	18298 / 0 / 775	
Goodness-of-fit on F^2	0.919	
Final R indices [I>2σ(I)]	$R_1^{(a)}$ = 0.0493, $wR_2^{(b)}$ = 0.1053	
R indices (all data)	R_1 = 0.0910, wR_2 = 0.1212	
Largest diff. peak and hole	2.342 and -1.234 e $Å^{-3}$	

(a) $R_1 = \sum \left| |F_0| - |F_c| \right| / \sum |F_0|$ (based on *F*)

(b) $wR_2 = \left[\sum_w (|F_0^2 - F_c^2|)^2 \right] / \left[\sum_w (F_0^2)^2 \right]^{1/2}$ (based on F^2)

$$w = q / \left[(\sigma F_0)^2 + (a * P)^2 + (b * P) + d + e * \sin(\theta) \right]$$

PART C Preparation of the complex and nucleophile solutions

3.8 Complex Solutions

3.8.1 $[Pt(terpy)(OH_2)](BF_4)_2$ and $[Pd(bpma)(OH_2)](ClO_4)_2$

The acidity of the terpy complex was not investigated, only the substitution reactions using thiols nucleophiles were carried out. These reactions were done at pH = 1, due to the acidity of the thiols. For kinetic investigation the complex solution was prepared by dissolving (1.340 mg, 13.4 mmol) of $[Pt(terpy)(OH_2)](BF_4)_2$ in pH 1 ($HClO_4$) solution to give a concentration of 2.50×10^{-5} M, while maintaining ionic strength at 0.1 M. The bpma concentration complex solution 4.6×10^{-4} M was prepared as described in **section 3.3.2**. The pH of the solution was adjusted to 1 using $HClO_4$ for thermodynamic and kinetic investigations involving thiols. In case of the other substitution studies the pH was adjusted to 3 and ionic strength made up to 0.1 M using $NaClO_4$.

3.8.2 $[Pt(bpma)(OH_2)](ClO_4)_2$

To investigate the acidity of this complex 5.11 mg (1.00×10^{-2} mmol) of $[Pt(bpma)(OH)](ClO_4)$ was dissolved in 200 mL of ultra pure water of pH 1 ($HClO_4$) to give a final concentration of 5.00×10^{-5} M and ionic strength of the solution was therefore 0.1 M. For kinetic studies using thiol nucleophiles, the complex solution was prepared by dissolving (26.25 mg, 5.137×10^{-2} mmol) in 100 mL of ultra pure water of pH 1 ($HClO_4$) to give a final concentration of 5.137×10^{-4} M and the ionic strength of the solution was therefore 0.1 M. In case of substitution kinetics involving other non-biological nucleophiles a concentration of 5.0×10^{-5} M of the complex (10.2 mg, 1.996 mmol) was prepared in an aqueous medium of pH 2. The ionic strength of this solution was made up to 0.1 M using $NaClO_4$.

3.8.3 [Ru(terpy)(bipy)(OH_2)](ClO_4)$_2$

Two sets of solutions were prepared for thermodynamic and kinetic investigations. The complex solution used for the thermodynamic investigation was prepared by dissolving [Ru(terpy)(bipy)(OH_2)](ClO_4)$_2$ (5.95 mg, 0.0084 mmol) in a pH 1 solution of $HClO_4$. The concentration of the solution was calculated to be 8.40×10^{-5} M. For kinetic studies the concentration of the complex was doubled compared to that used for thermodynamic studies. The complex solution was prepared in a pH 4 solution of $HClO_4$. The ionic strength was adjusted to 0.1 M using $NaClO_4$ solution to obtain a final concentration of 1.68×10^{-4} M.

3.8.4 [Ru(terpy)(tmen)(OH_2)](ClO_4)$_2$

Two sets of solutions were also prepared for thermodynamic and kinetic investigations. The complex solution used for the thermodynamic investigation was prepared by dissolving [Ru(terpy)(tmen)(OH_2)](ClO_4)$_2$ (12.0 mg, 1.80×10^{-3} mmol) in a pH 1 solution of $HClO_4$. The concentration of the solution was calculated to be 7.19×10^{-5} M. For kinetic studies the complex solution was prepared by dissolving [Ru(terpy)(tmen)(OH_2)](ClO_4)$_2$ (5.6 mg, 8.39×10^{-3} mmol) in pH 3 solution to afford a concentration of 8.39×10^{-5} M. The ionic strength was adjusted to 0.1 M using $NaClO_4$.

3.9 Nucleophile Solutions

Solutions of appropriate nucleophiles were prepared by dissolving known amounts in the same medium as used for the metal complex. Since perchlorate ion is a non-coordinating ion with respect to these metal complexes, $HClO_4$ and $NaClO_4$ were used to adjust the pH of the solutions and to maintain the ionic strength of 0.1 M respectively. Nucleophile concentrations were of the order 10, 20, 30, 40 and 50 times the concentration of the metal complex. In the case of the ruthenium complex the initial concentration of the nucleophile was 500 times that of the complex.

3.10 pH Titration

It was important to determine the pH range within which successful kinetic studies could be carried out. The reason for this is that the complexes being investigated are aqua complexes and therefore there is a possibility of the hydroxo complex being formed at higher pH's which would have complicated the study. The titration study also provided information regarding the dissociation of the water molecule through the determination of the pK_a value.

pK_a values for complexes $[Pt(bpma)(OH_2)]^{2+}$ and $[Pd(bpma)(OH_2)]^{2+}$ were found by pH titration. The literature pK_a value for $[Pt(terpy)(OH_2)]^{2+}$ has been reported to be 4.6.[5] The substitution reaction of a water molecule in $[Pt(terpy)(OH_2)]^{2+}$ and $[Pt(bpma)(OH_2)]^{2+}$ with the thiols was carried out at pH 1. This is due to the fact that the first pK_a for cysteine, DL-penicillamine and glutathione at 25 °C is approximately 2, while that of $[Pt(terpy)(OH_2)]^{2+}$ and $[Pt(bpma)(OH_2)]^{2+}$ was determined to be 4.6 and 5.49 respectively.

A solution of the metal complex was prepared as described in **section 3.8.** The pH and ionic strength of the aqueous solution were maintained at 1 and 0.1 M respectively. To avoid carrying out absorbance correction due to dilution, a large volume of *ca* 200 mL of the complex solution was used. The solution was then titrated with NaOH solution. A further precaution was taken in order to prevent dilution when changing the pH of the solution from 1 to 2. This was achieved by the addition of crushed NaOH pellets.

For every titrated solution, a UV-Vis scan was recorded at 25 °C, using the Varian UV-Visible Cary 100 Spectrophotometry. The pH of the solution was measured using a Jenway 4330 pH meter and a combination Jenway glass electrode that had been calibrated using standard buffer solutions at pH 4.0, 7.0 and 10.0 (Merck). To avoid precipitation of $KClO_4$ in the pH electrode, the KCl solution inside the electrode was replaced with a 3 M NaCl. It was found that dipping the electrode into the metal complex solution for a length of time resulted in the precipitation of the complex as a chloro compound due to the substitution of water by the chloride ions from the electrode. Due to this all pH measurements were determined outside the stock solution, by sampling approximately 1.0 mL aliquots of the stock solution into specially designed narrow vials. The pH electrode

3.12 Kinetic Measurements

The wavelength at which there was the biggest change in the absorbance as determined in **section 3.11** was selected for kinetic studies. Ligand substitution reactions were performed under pseudo-first order conditions with the nucleophiles being present in at least 10-fold excess over the metal complexes. Kinetic studies for fast reactions were monitored using an Applied Photophysics SX. 18MV Stopped-flow ASVD instrument coupled to an on-line data acquisition system. Slow reactions were monitored spectrophotometrically by collecting repetitive spectrum scans of the reaction mixture or by monitoring the kinetic reaction at a specific wavelength using a Varian UV-Visible Cary 100 Spectrophotometer. This was equipped with a cell holder thermostated by a Varian Peltier temperature programmer. The cuvette used was a 0.8 cm tandem quartz Suprasil cell. The temperature was controlled with an accuracy of ± 0.05 and 0.1 °C for the UV-Vis and stopped-flow instruments respectively. All reactions were followed for at least 6 half-lives.

All kinetic runs were best described by a single exponential equation. The observed pseudo-first order rate constants, k_{obs}, were calculated using the on-line non-linear least square fit of exponential data to equation (3.2).

$$A_t = A_o + (A_o - A_\infty)\exp(-k_{obs}t) \qquad (3.2)$$

where A_o, A_t, and A_∞ represents the absorbance of the reaction mixture initially, at time t and at the end of the reaction respectively. Kinetic traces from UV-Vis spectrophotometry were analyzed using the first-order exponential decay equation of Origin 50 version 5.0, a data analysis and technical graphics software.

3.12.1 Kinetic Studies Using Stopped-Flow Spectrophotometry

The instrument lamp was warmed for *ca* 1 hour prior to analysis. The sample syringes and reaction chamber were cleaned several times with ultra pure water followed by the aqueous medium used to dissolve the complex and the nucleophiles under investigation. The instrument was then zeroed before scanning. The sample syringes were rinsed with

the complex and the nucleophile solutions before filling them and letting them equilibrate at the desired temperature. The monochromator was then set to a pre-determined wavelength as described in **section 3.11**. The reactants were then forced into the reaction chamber followed by analysis. Once time base was established, *i.e.* the time required for the completion of the reaction, consecutive runs were made automatically, the number of runs depended on the reproducibility of the data but these were not less than six. The observed rates were then recorded followed by the necessary calculations.

The above procedure was carried out for all the concentration dependence studies of the nucleophiles at 25 °C. Temperature dependence studies on the rate constant were also conducted in the same manner at temperatures of 20, 30, 35 and 40 °C. Each of the reported constants is an average of six kinetic runs.

3.12.2 Kinetic Studies Using UV-Visible Spectrophotometry

Both temperature and concentration dependence studies were carried out using tendum cuvettes. Equal volumes of the complex and the nucleophile were placed in each compartment of the cuvettes and allowed to equilibrate to the desired temperature before mixing. The UV-Visible Cary 100 Spectrophotometer was set at a specific wavelength predetermined as indicated in **section 3.11**. The instrument was zeroed before reaction was monitored by using the kinetic run programme. This programme was employed in the investigation involving $[Pt(bpma)(OH_2)]^{2+}$ with cysteine and DL-penicillamine. Substitution reactions of $[Ru(terpy)(bipy)(OH_2)]^{2+}$ and $[Ru(terpy)(tmen)(OH_2)]^{2+}$ were monitored through repeated scans from 800 to 190 nm. The data collected was imported into Origin 5.0 programme and absorbance versus time graphs plotted. These were then analyzed using a first-order exponential decay equation. The rate constants obtained were pseudo rate constants since the concentrations of the nucleophiles were not less than 10-fold that of the complex. A minimum of three kinetic runs were recorded under all conditions and the reported rate constants represent the mean values.

REFERENCES

1) G. M. Whitesides, *J. Am. Chem. Soc.*, **1976**, *98*, 6521.

2) G. Annibale, *Polyhedron*, **1995**, *14*, 451.

3) D. R. McMillian, *Inorg. Chem.*, **1994**, *33*, 722.

4) M. Cattabriga, *J. Chem. Soc., Dalton Trans.*, **1999**, 3877.

5) A. Hofmann, D. Jaganyi, Q. O. Munro, G. Leihr and R. van Eldik, *Inorg. Chem.*, **2003**, 42, 1688.

6) Z. D. Bugarčić, G. Leihr and R. van Eldik, *J. Chem. Soc., Dalton Trans.*, **2002**, 951.

7) F. P. Dwyer, H. A. Goodwin, F. C. Gyarfas, *Aust. J. Chem.*, **1963**, *16*, 42.

8) B. P. Sullivan, J. M. Calvert, and T. J. Meyer, *Inorg. Chem.*, **1980**, *19*, 1404.

9) C. Cheng, J. G. Goll, G. A. Neyhart, T. W. Welch, P. Singh and H. Thorp, *J. Am. Chem. Soc.*, **1995**, *117*, 2970.

10) K. J. Takeuchi, M. S. Thompson, D. W. Pipes and T. J. Meyer, *Inorg. Chem.*, **1984**, *23*, 1845.

11) C. Ho and C. Che, *J. Chem. Soc., Dalton Trans*, **1990**, 967.

12) P. J. McArdle, *Appl. Cryst.*, **1995**, *28*, 65-65.

13) MULTISCAN— R. H. Blessing, *Acta Cryst*, **1995**, *A51*, 33-38.

14) G. M. Sheldrick, *Acta Cryst.*, **1990**, *A46*, 467-473.

15) G. M. Sheldrick, T. R. Schneider, *"SHELXL: High-Resolution Refinement", Methods in Enzymology*, Macromolecular Crystallography Part B, Eds. C.W.Carter & R. M. Sweet., **1997**, *277*, 319-343.

16) L. J. Farrugia, *J. Appl. Cryst.*, **1997**, *30*, 565.

17) L. J. Farrugia , *J. Appl. Cryst*, **1999**, *32*, 837-838.

18) Mercury 1.1—Cambridge Crystallographic Data Centre, 12 Union Road, Cambridge CB2 1EZ, United Kingdom, **2002**.

19) P. McArdle, *J. Appl. Cryst.*, **1995**, *28*, 65.

CHAPTER FOUR

RESULTS AND DISCUSSION

4 RESULTS AND DISCUSSION

4.1 Synthesis

In this section only the synthetic results of the complexes whose kinetic studies were investigated will be discussed. Discussion concerning the other complexes reported in the experimental section will be given in **APPENDIX E**.

4.1.1 Synthesis of Square-Planar Pt(II) and Pd(II) Complexes

The complex $[Pt(terpy)(OH_2)](BF_4)_2$ **(4)** was isolated in a very high yield (77 %). The other complexes, $[Pd(bpma)(OH_2)](ClO_4)_2$ **(9)** and $[Pt(bpma)(OH_2)](ClO_4)_2$ **(7)** were prepared in solution form from $[Pd(bpma)Cl]Cl.H_2O$ and $[Pt(bpma)OH]^+$ complexes respectively. The complexes $[Pd(bpma)Cl]Cl.H_2O$ and $[Pt(bpma)OH]^+$ were also isolated in high yields, 90 and 80 % respectively. The CHN microanalysis results of $[Pt(terpy)(OH_2)]^{2+}$, $[Pd(bpma)Cl]Cl.H_2O$ and $[Pt(bpma)OH]^+$, showed that the complexes were of high purity.

4.1.2 Synthesis of Ru(II) Polypyridine Complexes

The reaction of $RuCl_3.3H_2O$ with terpyridine yields $[Ru(terpy)Cl_3]$ in a satisfactory yield of 52 %. This complex was used in the next step of synthesis without any further purification as described in the literature.[1] Synthesis of the complexes $[Ru(terpy)(bipy)Cl]ClO_4$ and $[Ru(terpy)(bipy)(OH_2)]^{2+}$ following a modified method described by Meyer *et al* gave yields of 70 % and 44 %, respectively.[1] Single crystals suitable for X-ray analysis for $[Ru(terpy)(bipy)Cl](ClO_4)$ were obtained by vapour diffusion of diethyl ether into acetonitrile solution of the complex. An ORTEP drawing of $[Ru(terpy)(bipy)Cl](ClO_4)$ with the atom-labelling scheme is shown in **Figure 4.1.**

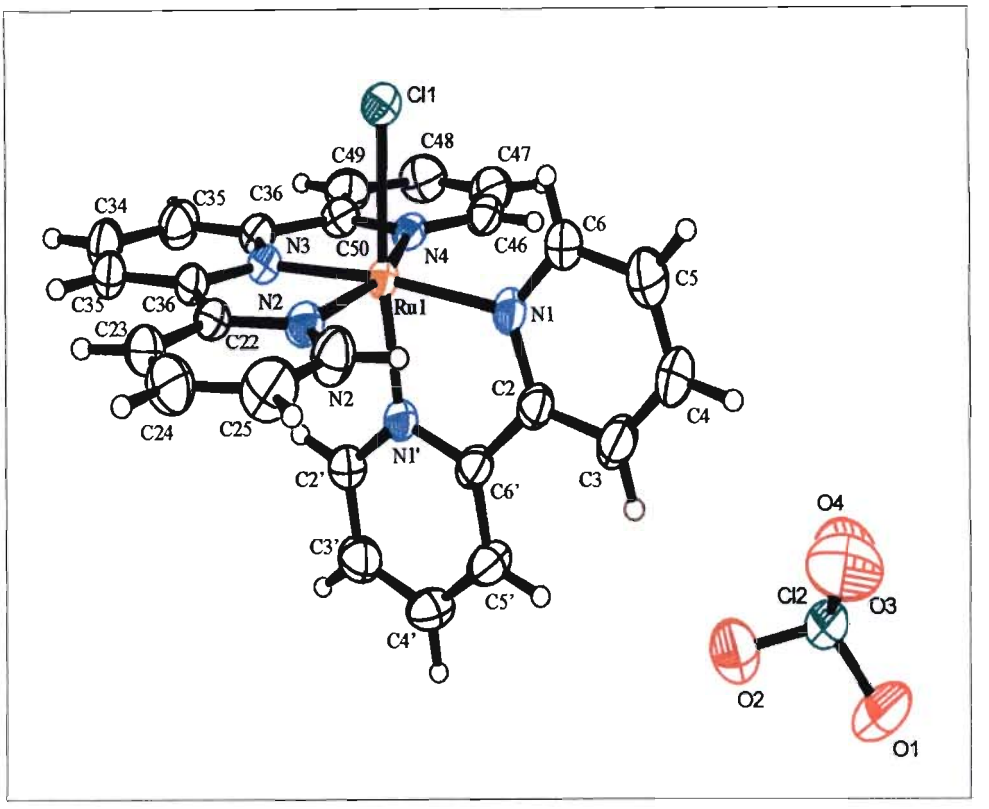

Figure 4.1 *An ORTEP diagram depicting the X-ray structure of [Ru(terpy)(bipy)Cl]ClO_4.*

The complex [Ru(terpy)(bipy)Cl]ClO_4 crystallizes in the triclinic crystal system (space group $P\bar{1}$). The unit cell dimensions are given in **Table 3.1 (Chapter 3)**. A list of interatomic distances, angles and other crystallographic data are listed in **Appendix C**, **Tables C1-C5.**

The complexes [Ru(terpy)(tmen)Cl]ClO_4 and [Ru(terpy)(tmen)(OH_2)](ClO_4)$_2$ were also isolated in yields of 56 % and 33 % following the method described by Ho and Che.[2] Single crystals suitable for X-ray analysis were also obtained for [Ru(terpy)(tmen)(CH_3CN)](ClO_4)$_2$ from slow diffusion of diethyl ether into an acetonitrile solution of [Ru(terpy)(tmen)(OH_2)](ClO_4)$_2$ with diethyl ether. An ORTEP drawing of [Ru(terpy)(tmen)(CH_3CN)](ClO_4)$_2$ with the atom-labelling scheme is shown in **Figure 4.2**.

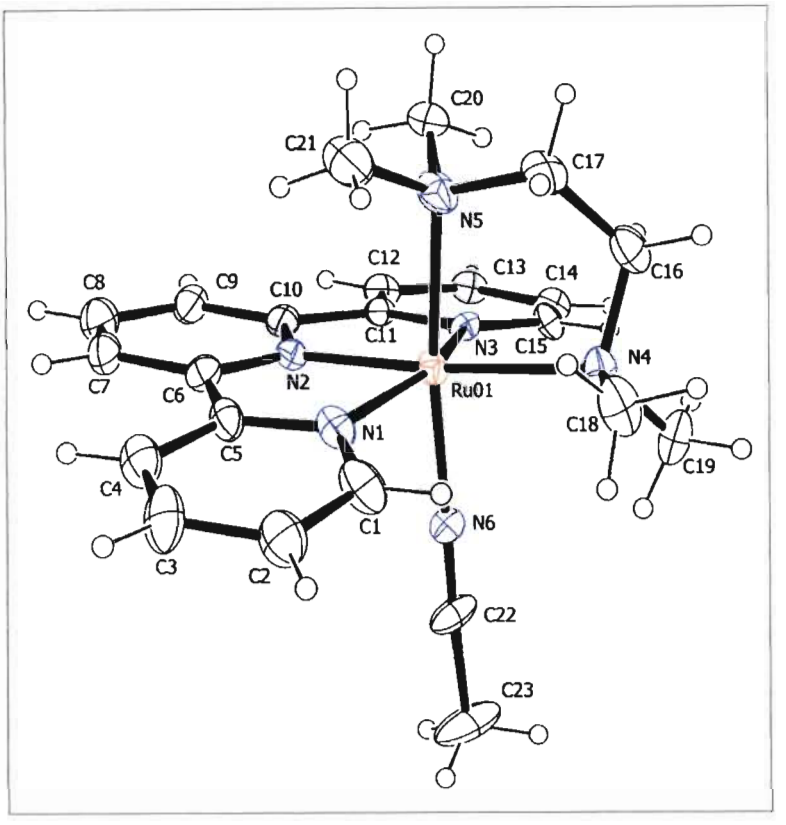

Figure 4.2 *ORTEP diagram depicting the X-ray structure of one of the independent molecules of [Ru(terpy)(tmen)(CH$_3$CN)](ClO$_4$)$_2$ (40 % ellipsoid probabilities). The perchlorate ions have been omitted for clarity.*[1]

The complex [Ru(terpy)(tmen)(CH$_3$CN)](ClO$_4$)$_2$ crystallized in the monoclinic crystal system (space group $P2_1/c$). The unit cell dimensions are given in **Table 3.2 (Chapter 3)**. From **Table 3.2**, the *R*-factor R_1 exceeds 10 % due to the poor quality of the crystal (as evidenced by the high internal *R*-value for the data set). Moreover, two moderately disordered CH$_3$CN solvent molecules were present in the asymmetric unit. The had to be treated using PLATON's SQUEEZE algorithm to remove the diffuse electron density from the data such that a stable refinement was possible.

[1] **Note**: *Disordered solvent molecules (non-coordinated) were removed using PLATON's SQUEEZE algorithm. All H atoms were calculated using a riding model (HFIX 23, 33, 43 commands in SHELXL97).*

Two independent Ru(II) complexes with the general formula $[Ru(terpy)(tmen)(CH_3CN)](ClO_4)_2$ were found in the asymmetric unit. A list of interatomic distances, angles and other crystallographic data are listed in **Appendix C**, **Tables C6-C8**. This crystal structure has been included to serve as confirmation that the complex of interest was synthesized in high purity. This is also confirmed by CHN analysis.

4.2 Kinetic Studies of Square Planar Pt(II) and Pd(II) Complexes

4.2.1 pH Titration

When solutions of $[Pt(bpma)(OH_2)]^{2+}$ **(7)** and $[Pd(bpma)(OH_2)]^{2+}$ **(9)** prepared by dissolving a known amount of the complex in aqueous solution of pH 1.0 and $\mu = 0.1$ M ($HClO_4$) were titrated using an aqueous solution of NaOH, shifts in the absorption maxima were observed. Such shifts correspond to the formation of the analogous hydroxo complexes, namely $[Pt(bpma)OH]^+$ and $[Pd(bpma)OH]^+$. The titration reaction of the complex solutions with NaOH can be presented in the general form by equation (4.1).

$$[M(NNN)(OH_2)]^{2+} + OH^- \underset{+H^+}{\overset{-H^+}{\rightleftharpoons}} [M(NNN)OH]^- + H_2O \qquad (4.1)$$

where M = Pt or Pd and NNN denotes bpma. Upon addition of a small amount of $HClO_4$ to the titrated solution of the complex at a certain pH, reversibility of the titration was observed. An isosbestic point was maintained proving that only two species, *i.e.* the hydroxo and the aqua species were present in the solution, and were in equilibrium as represented by equation (4.1).

The UV-Vis spectra recorded during the titration are given in **Figures 4.3** and **4.4** for complexes **(7)** and **(9)** respectively. The UV-Vis spectra **Figures 4.3** and **4.4** are characterized by more than one isosbestic point. This is an indication that the simple equilibrium as shown in equation (4.1) exists. In addition, the baselines for all the curves

are intact, which implies that there was no formation of a precipitate during titration or a change in the structure of the complex over the pH range investigated.

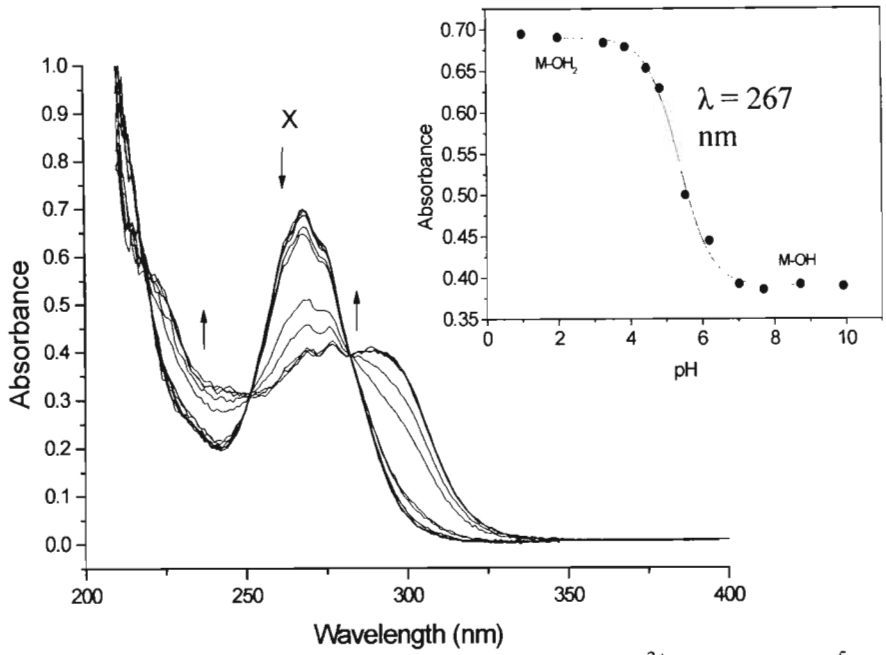

Figure 4.3 *UV-Visible Spectra for $[Pt(bpma)(OH_2)]^{2+}$ (4.93×10^{-5} M), μ = 0.1 M ($HClO_4$); pH range of 1 - 9.92, T = 25 °C. Inset is the plot of absorbance versus pH at the specified wavelength.*

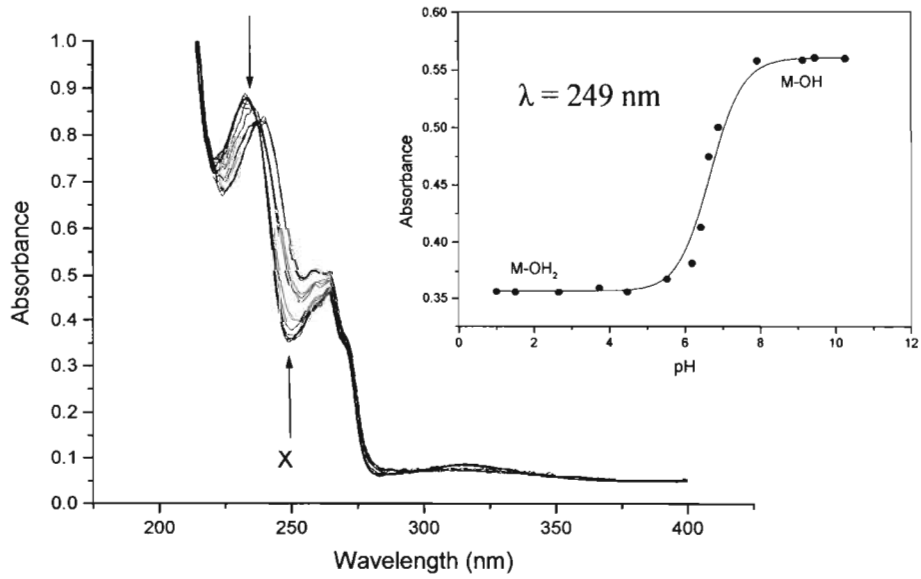

Figure 4.4 *UV-Visible Spectra for $[Pd(bpma)(OH_2)]^{2+}$ (1.00×10^{-4} M), μ = 0.1 M ($HClO_4$); pH range of 1-12, T = 25 °C. Inset is the plot of absorbance versus pH at the specified wavelength.*

The wavelengths where there was a significant spectral change as indicated in the Figure by X were chosen for the absorbance versus pH plot. These are shown as insets in Figures **4.3** and **4.4**. The pK_a values were determined to be 5.49 ± 0.08 and 6.67 ± 0.067 for $[Pt(pbma)(OH_2)]^{2+}$ and $[Pd(bpma)(OH_2)]^{2+}$ respectively.

The pK_a plots (Insets), indicate that within the pH range of 1- 4.5 and 1- 3.5, the complexes **(7)** and **(9)** exist in complete aqua form and after pH 9 as hydroxo species. Therefore the substitution reactions of coordinated water from these complexes were performed within these pH ranges.

4.2.2 Substitution Reactions of Pt(II) Complexes, $[Pt(terpy)(OH_2)]^{2+}$ and $[Pt(bpma)(OH_2)]^{2+}$ with Thiols

The substitution of the coordinated water molecule with thiol nucleophiles (Nu), namely, L-cysteine, glutathione and DL-penicillamine, from the complexes $[Pt(NNN)OH_2]^{2+}$, where NNN = terpy **(4)** or NNN = bpma **(7)** in acidic aqueous media of pH 1.0 and μ = 0.1 M ($HClO_4$) can be represented by equation (4.2).

$$[Pt(NNN)(OH_2)]^{2+} + Nu \underset{k_{-2}}{\overset{k_2}{\rightleftharpoons}} [Pt(NNN)Nu]^{2+} + H_2O \qquad (4.2)$$

These reactions were investigated at pH = 1, due to the fact that the biological thiols under investigation are highly susceptible to hydrolysis. The literature acid dissociation constants defined in **Scheme 4.1** reported at 25 °C and μ = 1.0 M for these thiols are pK_{a1} = 1.9, pK_{a2} = 8.10 and pK_{a3} = 10.1 for L-cysteine and pK_{a1} = 1.9, pK_{a2} = 7.92 and pK_{a3} = 10.5 for DL-penicillamine.[3] The dissociation constants for the glutathione reactions measured at 25 °C and μ = 0.2-0.55 M were determined to be pK_{a1} =2.05, pK_{a2} = 3.40 and pK_{a3} = 8.74 and pK_{a4} = 9.49.[4]

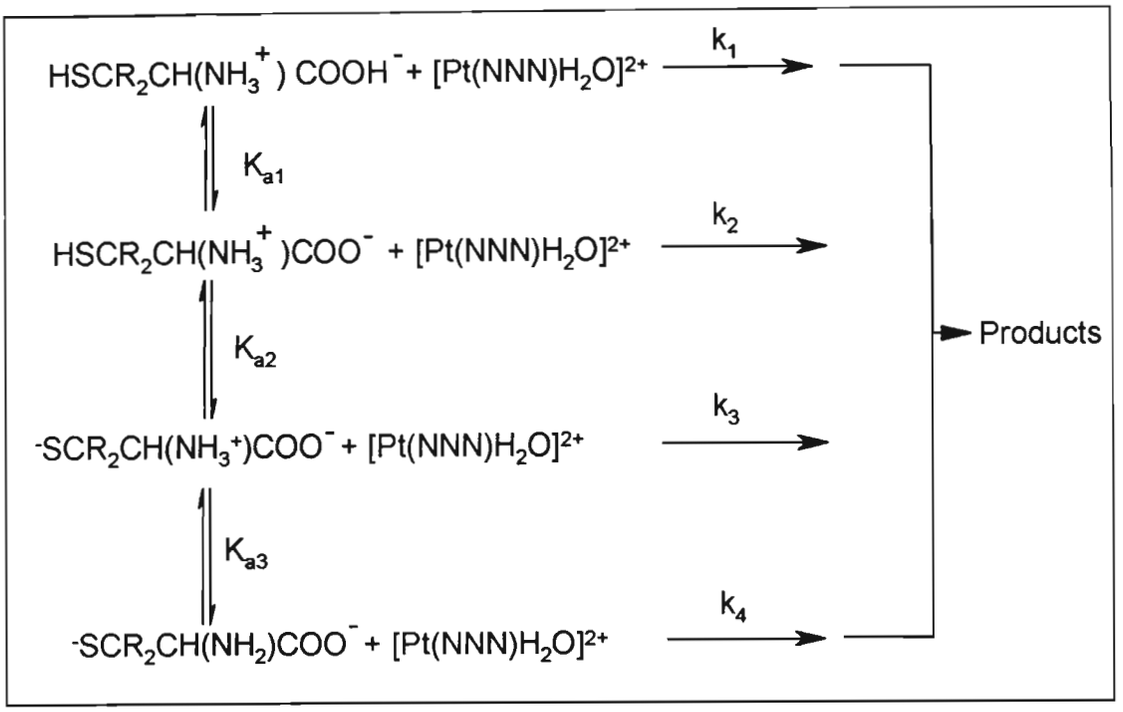

Scheme 4.1 *Acid dissociation scheme for biological thiols, L-cysteine (R= H) and (R = Me) DL-penicillamine.*

The mechanism depicted in **Scheme 4.1** gives the second order overall rate constant defined by equations (4.3) for L-cysteine and DL-penicillamine [3]

$$k_2 = \left\{ \frac{k_1[H^+]^3 + k_2K_{a1}[H^+]^2 + k_3K_{a1}K_{a2}[H^+] + k_4K_{a1}K_{a2}K_{a3}}{[H^+]^3 + K_{a1}[H^+]^2 + K_{a1}K_{a2}[H^+] + K_{a1}K_{a2}K_{a3}} \right\} \qquad (4.3)$$

and for glutathione[3], the second order overall rate constant is given by

$$k_2 = \left\{ \frac{k_1[H^+]^4 + k_2K_{a1}[H^+]^3 + k_3K_{a1}K_{a2}[H^+]^2 + k_4K_{a1}K_{a2}K_{a3}[H^+] + k_5K_{a1}K_{a2}K_{a3}K_{a4}}{[H^+]^4 + K_{a1}[H^+]^3 + K_{a1}K_{a2}[H^+]^2 + K_{a1}K_{a2}K_{a3}[H^+] + K_{a1}K_{a2}K_{a3}K_{a4}} \right\} \qquad (4.4)$$

At pH = 1, $[H^+] >> K_a$ the thiols are fully protonated and the reaction pathways denoted by k_2, k_3, k_4, and k_5 are not significant. Therefore, kinetic studies of $[Pt(bpma)(OH_2)]^{2+}$ and $[Pt(terpy)(OH_2)]^{2+}$ were conducted at pH = 1.

4.2.3 Kinetic Trials

To determine the optimum wavelength for substitution reactions, kinetic trials were carried out as stated in **section 3.11**. An example of the UV-Vis spectra obtained for the substitution of water from $[Pt(terpy)(OH_2)]^{2+}$ with L-cysteine at 25 °C is given in **Figure 4.5**. The Figure shows the scan before mixing, immediately after mixing and 5 minutes after mixing. It can be seen that the last two scans overlap. The wavelength chosen for kinetic study in this case was 341 nm. Since the reaction was complete in less than 16 minutes, the stopped flow technique was used. The other thiols investigated were DL-penicillamine and glutathione. The wavelength chosen for these two were 240 and 340 nm respectively using the stopped flow technique.

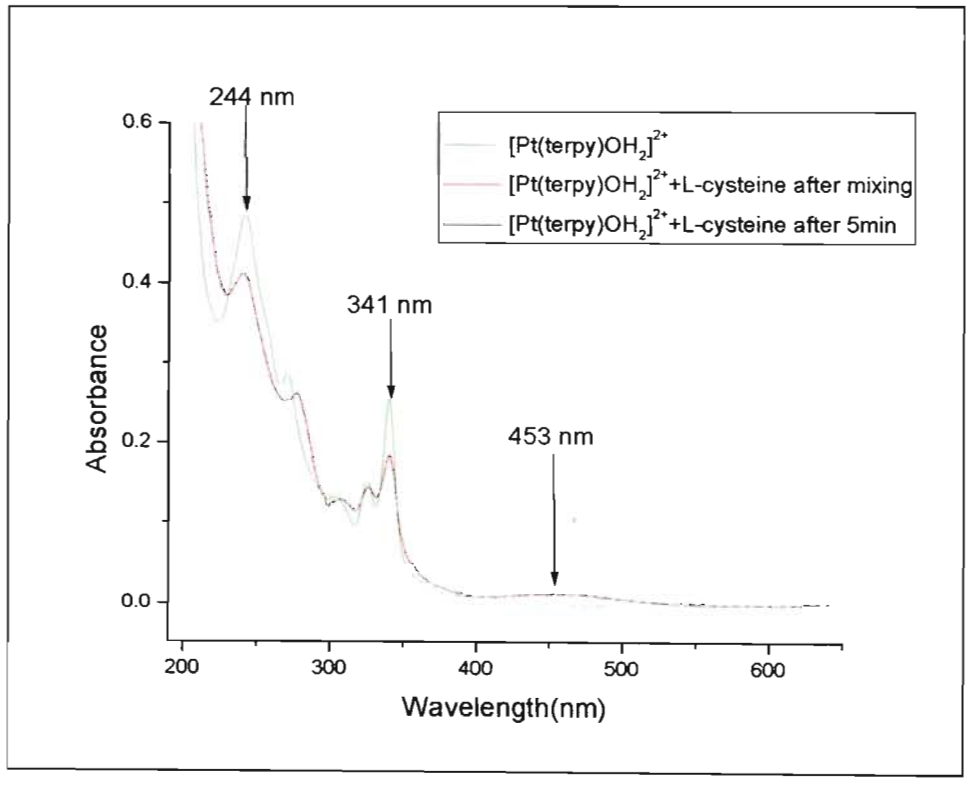

Figure 4.5 *UV-visible scans for the reaction of $[Pt(terpy)(OH_2)]^{2+}$ with L-cysteine recorded after mixing and 5 minutes after mixing.*

The other complex which was reacted with thiols was $[Pt(bpma)(OH_2)]^{2+}$. The substitution reactions using L-cysteine and DL-penicillamine were slow and as a result

UV-Visible spectrophotometry was used. Reactions with glutathione were fast enough to be followed using the stopped flow technique. The wavelengths chosen for this complex were 300, 266 and 240 nm for L-cysteine, DL-penicillamine and glutathione respectively.

4.2.4 Concentration Dependence Study for $[Pt(terpy)(OH_2)]^{2+}$ and $[Pt(bpma)(OH_2)]^{2+}$

In order to determine second order rate constants, k_2, concentration dependence studies were carried out. To ensure that the reactions proceeded to completion, pseudo first order conditions were maintained. This was achieved by varying the concentration of the nucleophile from 10 to 50 times the concentration of the complex, in increments of 10 times. The reactions were allowed to take place and a typical kinetic trace obtained from the stopped flow for the reaction of $[Pt(terpy)(OH_2)]^{2+}$ with DL-penicillamine is shown in **Figure 4.6**.

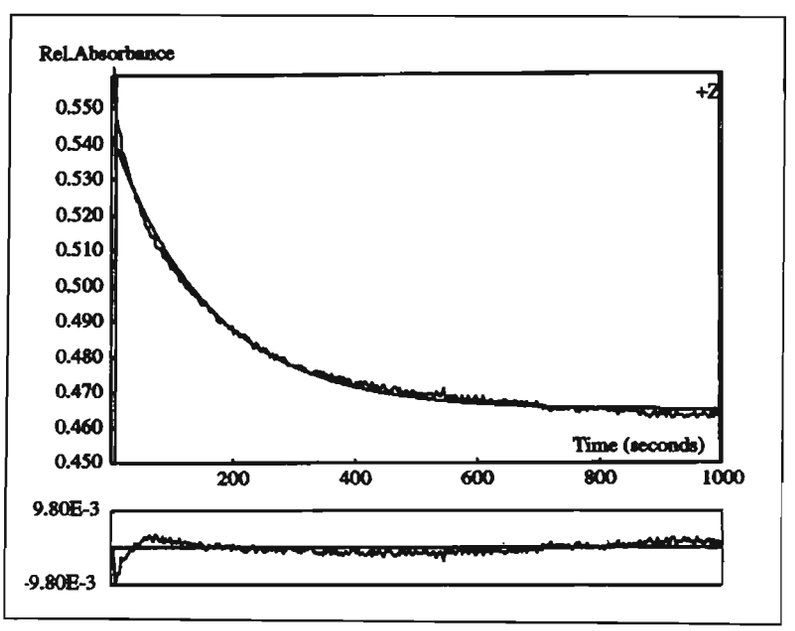

Figure 4.6 *A stopped flow kinetic trace recorded for the reaction of (3.38 x 10^{-5} M) $[Pt(terpy)(OH_2)]^{2+}$ with (1.69 x 10^{-3} M) DL-penicillamine at 240 nm and T = 25 °C.*

Pseudo first order rate constants, k_{obs}, were calculated from the single exponential kinetic traces, by non-linear least-square fit[5] of experimental data to:

$$A_t = A_o + (A_o - A_\infty)\exp(-k_{obs}t) \qquad (4.5)$$

where A_o, A_t, and A_∞ represent absorbances of the reaction mixture initially, at time t and at the end of the reaction respectively. The accuracy of the fit is shown below the graph. The exponential decay curves obtained in the case of $[Pt(bpma)(OH_2)]^{2+}$ with the thiols were also subjected to the same treatment but the k_{obs} were calculated using Origin 5.0 software.

Since the kinetic traces for the substitution reactions of the co-ordinated water by thiols followed single exponentials, it suggests that the substitution reactions are first-order in both the thiols and Pt(II) complexes. The analysis of the kinetic data showed that the pseudo-first order rate constants, k_{obs}, that were an average of six kinetic runs for the fast reactions and four for the slow reactions, were linearly dependent upon thiol concentration, according to the two-term rate law,

$$k_{obs} = k_2[thiol] + k_{-2} \qquad (4.6)$$

This is in accordance with the usual two-term rate law for nucleophilic substitution at a square-planar d^8 metal complex.[6] As represented in equation (4.6), k_2 denotes a second-order rate constant for the forward reaction which involves the direct substitution of the water molecule and k_{-2} represents a first order rate constant for the backward reaction whereby the water molecule replaces the coordinated nucleophile attached to the metal centre to form the aqua complex.

Hence from equation (4.6), plots of k_{obs} against the concentration of the thiols were plotted. These are shown in **Figure 4.7 (a)** and **(b)** for $[Pt(terpy)(OH_2)]^{2+}$ and

$[Pt(bpma)(OH_2)]^{2+}$ respectively. Straight line plots with zero intercepts were obtained for the substitution reactions involving $[Pt(terpy)(OH_2)]^{2+}$ with all the thiols, while small noticeable intercepts were obtained for the substitution of water from $[Pt(bpma)(OH_2)]^{2+}$ for all the thiols. This implies that for the terpy complex, the backward reaction as shown in equation (4.6), whereby the water molecule displaces the coordinated thiol to form the original aqua complex, is not effective, *i.e.* $k_{-2} \approx 0$. This means that equation (4.2) can be written as:

$$[Pt(NNN)(OH_2)]^{2+} + \text{thiol} \xrightarrow{k_2} [Pt(NNN)\text{thiol}]^{(2-n)+} \qquad (4.7)$$

implying that equation (4.6) becomes

$$k_{obs} = k_2[\text{thiols}] \qquad (4.8)$$

The values of k_2, obtained by least-square analysis, are tabulated in **Table 4.1.**

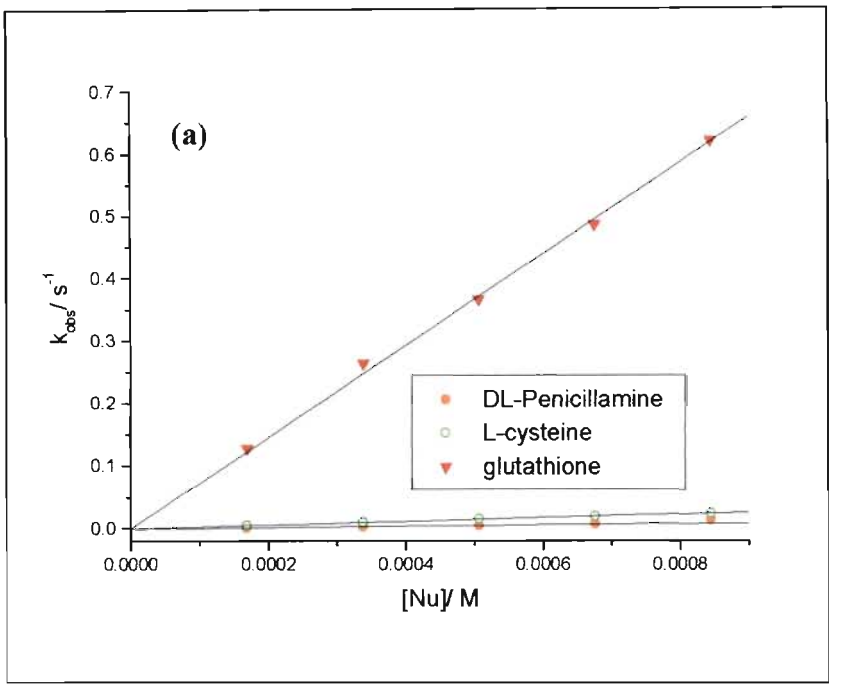

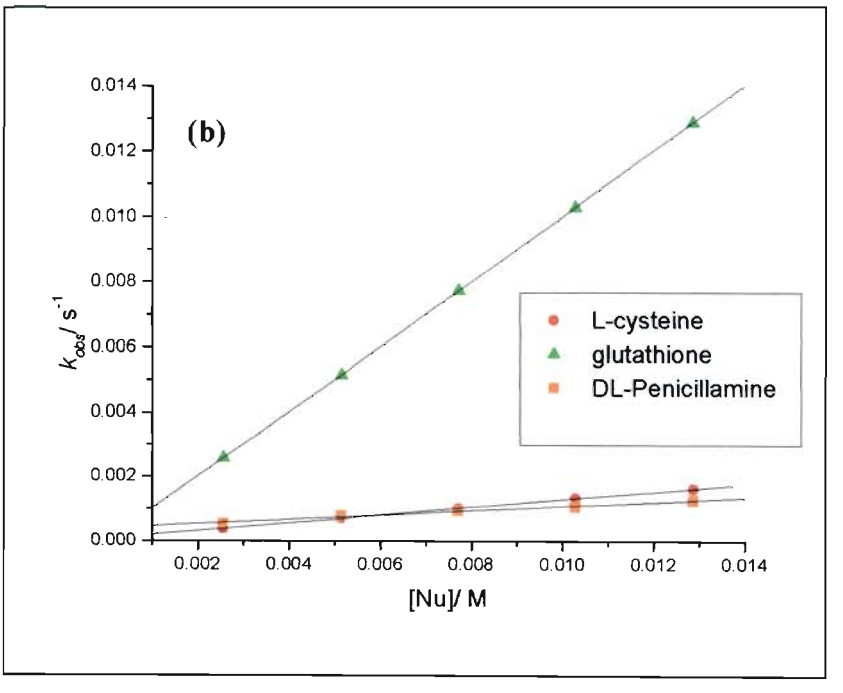

Figure 4.7 *Concentration dependence plots of k_{obs} on the concentration of the incoming thiols at 25 °C, for* **(a)** *$[Pt(terpy)(OH_2)]^{2+}$ = 4.96 x 10^{-5}M and* **(b)** *$[Pt(bpma)(OH_2)]^{2+}$ = 4.94 x 10^{-5} M; pH 1.0 ($HClO_4$).*

4.2.5 Temperature Dependence Study

To determine the activation parameters namely, the entropy $\Delta S^{\neq}$ and enthalpy $\Delta H^{\neq}$, temperature dependence studies were performed. In these studies the concentration of the thiols was fixed at 30 times the concentration of the complex for the reactions that did not show any y-intercept (*i.e.* the reactions of $[Pt(terpy)(OH_2)]^{2+}$ with the three thiols) in the concentration dependence study when plotting k_{obs} versus concentration. In the case of the reactions that did show a y-intercept, the temperature dependence was carried out at each concentration. This included the reactions of $[Pt(bpma)(OH_2)]^{2+}$ with the three thiols investigated.

The temperature was varied from 20 to 40 °C in increments of 5 °C. The stopped flow technique was applied in the reactions of $[Pt(terpy)(OH_2)]^{2+}$ with L-cysteine and glutathione as well as for those of $[Pt(bpma)(OH_2)]^{2+}$ with glutathione. The other reactions of $[Pt(terpy)(OH_2)]^{2+}$ with DL-penicillamine at 20 °C and those of $[Pt(bpma)(OH_2)]^{2+}$ with L-cysteine and DL-penicillamine were too slow for the stopped flow technique, as a result UV-Visible spectrophotometry was used instead.

Plots showing the effect of temperature on rates of reaction between $[Pt(bpma)(OH_2)]^{2+}$ and DL-penicillamine, glutathione and L-cysteine are shown in **Figure 4.8 (a), (b)** and **(c)** respectively. The slope of the linear plot gave the required k_2 value at the respective temperature. In the case of $[Pt(terpy)(OH_2)]^{2+}$ this value was obtained by dividing the average k_{obs} value by the concentration of the thiols which was a fixed term. All the k_{obs} in these studies were an average of 6 in case of stopped flow and 4 in case of UV-Vis study.

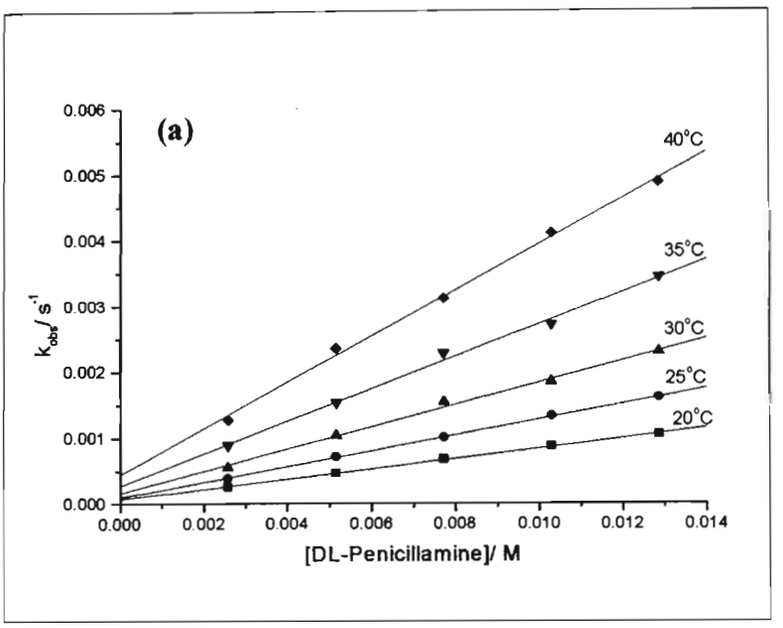

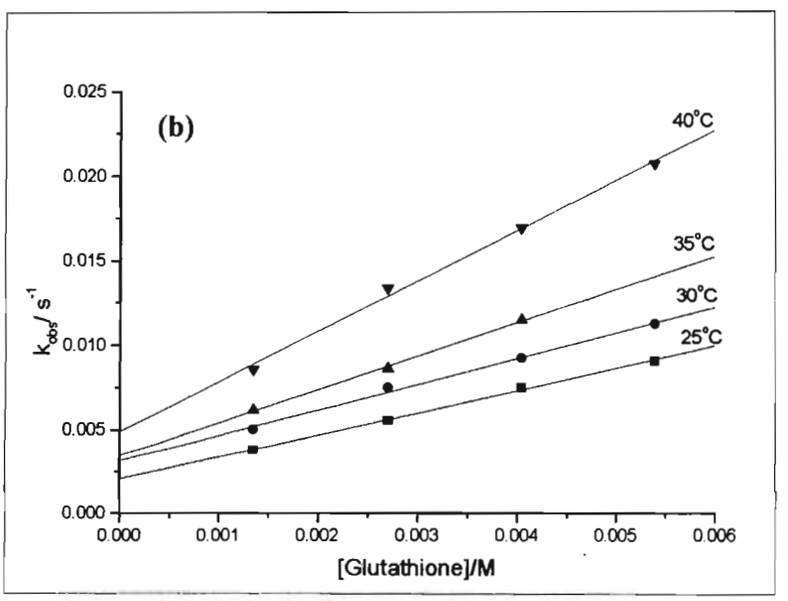

Figure 4.8 *Plots of observed pseudo-first order constants versus [DL-penicillamine]* **(a)** *and [glutathione]* **(b)** *for the reaction between* $[Pt(bpma)(OH_2)]^{2+}$ *= 4.94 x* 10^{-5} *M, pH 1.0 (*$HClO_4$*).*

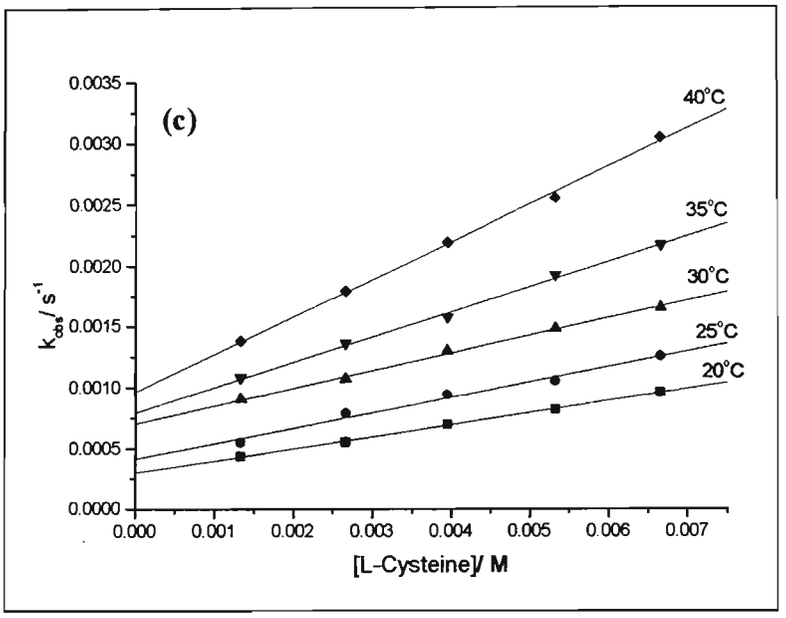

Figure 4.8(c) *Plots of observed pseudo-first order constants versus [L-cysteine] and for the reaction between* $[Pt(bpma)(OH_2)]^{2+}$ *= 4.94 x* 10^{-5} *M, pH 1.0* ($HClO_4$).

Activation parameters namely, $\Delta H^{\#}$ and $\Delta S^{\#}$ corresponding to these reactions were determined from the Erying plots based on the obtained second order rate constants k_2 for each thiol. The graphs which involved plotting $\ln(k_2/T)$ against $(1/T)$ were drawn and these are shown for $[Pt(terpy)(OH_2)]^{2+}$ in **Figure 4.9 (a)** and $[Pt(bpma)(OH_2)]^{2+}$ in **Figure 4.9 (b)** respectively.

Entropy was obtained from the intercept {intercept = 23.8 + ($\Delta S^{\#}$ / R)} and enthalpy from the slope {slope = ($-\Delta H^{\#}$ / R)} where R is the gas constant. The values obtained are listed in **Table 4.1** along with their standard deviations. Included in the table are equilibrium constants K for $[Pt(bpma)(OH_2)]^{2+}$ as well as the second order rate constant, k_2, values obtained from the linear dependence of k_{obs} on the concentration of the thiol nucleophiles.

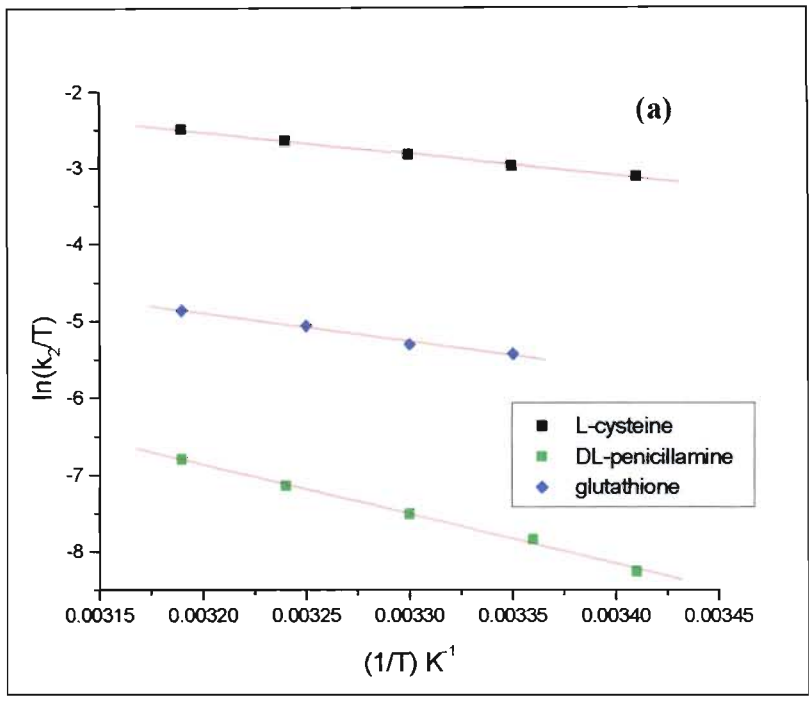

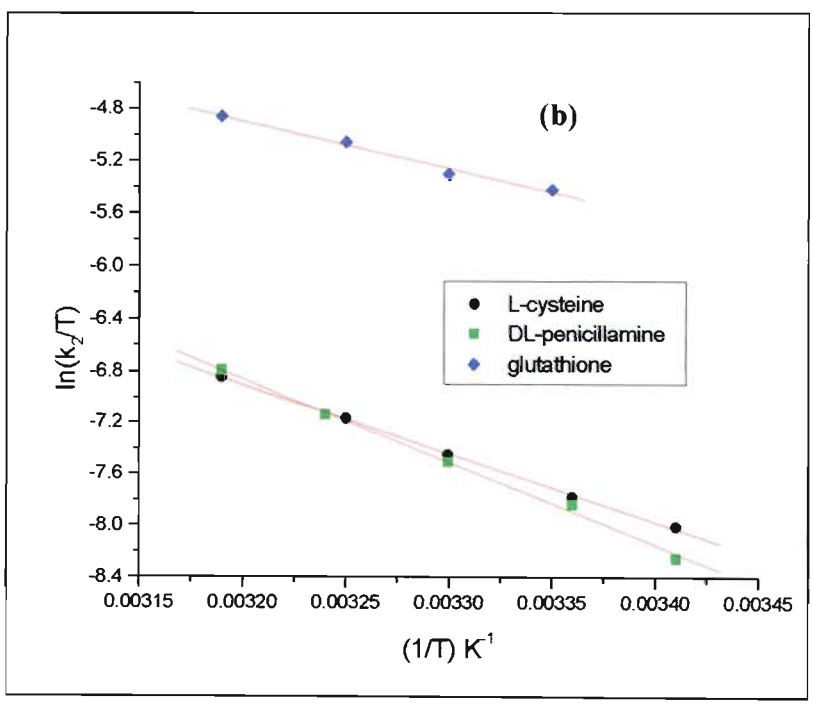

Figure 4.9 *Erying plots for the reactions of* $[Pt(terpy)(OH_2)]^{2+}$ **(a)** *and* $[Pt(bpma)(OH_2)]^{2+}$ **(b)** *with different thiols.*

Table 4.1 *Rate constants recorded at 25 °C and activation parameters for the reaction between the complexes $[Pt(terpy)OH_2]^{2+}$ and $[Pt(bpma)(OH_2)]^{2+}$ with biological thiols at pH 1.0 ($HClO_4$)*

Complex + Thiol	k_2^{298} /$M^{-1}s^{-1}$	k_{-2}^{298} /s^{-1}	$\Delta H^{\neq}_2$ /kJ mol^{-1}	$\Delta S^{\neq}_2$ /J K^{-1} mol^{-1}	*K*/M
$[Pt(terpy)OH_2]^{2+}$					
DL-Penicillamine	10.7±0.7		42±2	-83±8	
L-Cysteine	29.7±0.2		23.7±0.9	-143±3	
L-Glutathione	712±18		17.5±0.8	-132±3	
$[Pt(bpma)OH_2]^{2+}$					
DL-Penicillamine	$(1.07\pm0.01)\times10^{-1}$	$(9.9\pm1.3)\times10^{-5}$	53±2	-86 ±5	1083
L-Cysteine	$(1.25\pm0.03)\times10^{-1}$	$(4.2\pm0.4)\times10^{-4}$	44±1	-115±4	300
L-Glutathione	$(5.17\pm0.25)\times10^{-1}$	$(4.2\pm0.2)\times10^{-4}$	31±3	-141±8	1246
$[Pd(terpy)OH_2]^{2+*}$					
DL-Penicillamine	$(4.52\pm0.01)\times10^{3}$		28±1	-80±3	
L-Cysteine	$(6.32\pm0.02)\times10^{3}$		32±1	-67±1	
L-Glutathione	$(4.45\pm0.02)\times10^{4}$		16±1	-102±1	
$[Pd(bpma)OH_2]^{2+*}$					
DL-Penicillamine	$(8.37\pm0.02)\times10^{2}$		35±2	-70±4	
L-Cysteine	$(1.13\pm0.01)\times10^{3}$		36±1	-66±3	
L-Glutathione	$(5.45\pm0.04)\times10^{3}$		36±1	-54±3	

*are literature values for $[Pd(terpy)(OH_2)]^{2+}$ and $[Pd(bpma)(OH_2)]^{2+}$.[7]

4.2.6 Reactivity of $[Pt(terpy)(OH_2)]^{2+}$ versus $[Pt(bpma)(OH_2)]^{2+}$

This study has managed to compare the reactivity of the two platinum complexes $[Pt(terpy)(OH_2)]^{2+}$ and $[Pt(bpma)(OH_2)]^{2+}$ using L-cysteine, DL-penicillamine and glutathione thiols as the nucleophiles. The comparison is seen clearly from **Table 4.1**, in which the corresponding reactivity of $[Pt(bpma)(OH_2)]^{2+}$ is compared with that of $[Pt(terpy)(OH_2)]^{2+}$; the latter complex reacts 10^2-10^3 faster with the same thiols. This difference in reactivity has also been observed when nucleophiles other than the thiols used in this study were used.[8] Similar behaviour in reactivity has also been observed in the displacement of a water molecule from the palladium analogues namely $[Pd(terpy)(OH_2)]^{2+}$ and $[Pd(bpma)(OH_2)]^{2+}$ using the same thiols.[7]

The difference in the rate of substitution is a reflection of the individual complex structure. The structures of the two complexes investigated are shown in **Scheme 4.2**. The scheme shows that the difference between these complexes is the fact that the platinum terpy complex consists of an additional pyridyl ring, which is *trans* to the leaving group (H_2O) while in the case of the platinum bpma complex the leaving group is *trans* to hydrogen bonded to the middle nitrogen.

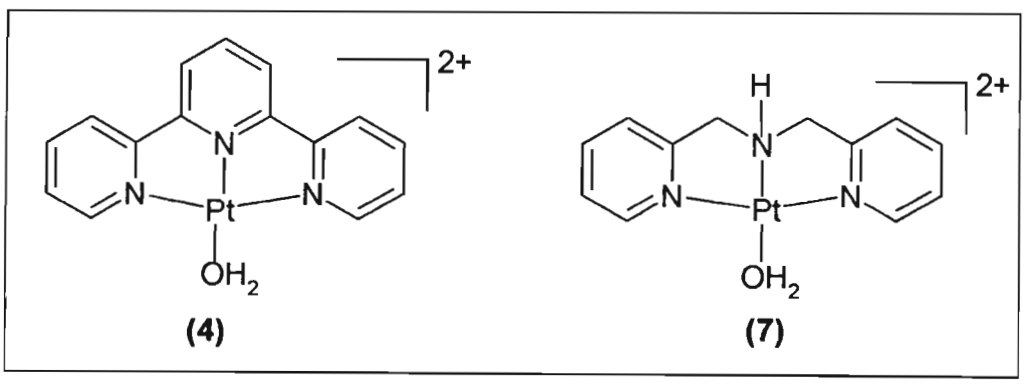

Scheme 4.2 *Structures of the complexes investigated; $[Pt(terpy)(OH_2)]^{2+}$ **(4)** and $[Pt(bpma)(OH_2)]^{2+}$ **(7)**.*

The enhanced reactivity of $[Pt(terpy)(OH_2)]^{2+}$ can be largely attributed to extensive conjugation of the aromatic system around the Pt-metal.[8] Hence, the flow of electron

density away from the d_{xz} metal orbital into the aromatic antibonding π^* orbitals due to the π-back donation is more widely spread in the case of $[Pt(terpy)(OH_2)]^{2+}$ than in $[Pt(bpma)(OH_2)]^{2+}$. This increases the electrophilicity of the metal centre by making it more positive, resulting in easier attack by the incoming nucleophile. In addition, $[Pt(terpy)(OH_2)]^{2+}$ is likely to stabilize the trigonal-bipyramidal transition state much better than $[Pt(bpma)(OH_2)]^{2+}$ through the delocalisation of the negative charge facilitating new bond formation. The high lability of the metal-terpy system has also been reported in the case of $[Pd(terpy)Cl]^+$ [9] and $[Pt(terpy)Cl]^+$.[10, 11, 12] The effect is similar to that of $[Pt(terpy)(OH_2)]^{2+}$ and has been described as being due to the electronic communication between the aromatic system and the metal d_{xz} orbital.

A comparison of $[Pt(terpy)(OH_2)]^{2+}$ and $[Pt(bpma)(OH_2)]^{2+}$ with $[Pd(terpy)(OH_2)]^{2+}$ and $[Pd(bpma)H_2O]^{2+}$ shows that in changing the spectator ligand from (bpma) to (terpy), the reactivity increased by a factor of 10^2-10^3 for Pt(II) metal but only by a factor of 5-8 for Pd(II) metal when the same nucleophiles are used.[7] This difference in reactivity points to the fact that the aromatic terpy ligand increases the lability of the Pt(II) metal more than Pd(II) metal. This is because of the fact that platinum metal is a softer centre than palladium metal and as a result it is more sensitive to the electronic communication between the metal and the coplanar aromatic conjugation system. Hence the lability of the platinum terpy complex is much greater than that of the palladium terpy complex.

The second order rate constants, k_2, for $[Pt(terpy)(OH_2)]^{2+}$ listed in **Table 4.1** are similar to ones reported by Burgarčić *et al.*[7] Looking at the two complexes investigated, the order of reactivity of the thiols is also the same:

glutathione > L-cysteine >> DL-penicillamine

i.e. glutathione being the most reactive while DL-penicillamine the least.

The reactivity difference can be explained by considering the structural properties of these ligands such as the steric effects and the neighbouring interaction effect (anchimeric effect). The structures of the thiols are as shown in **Scheme 4.3**.

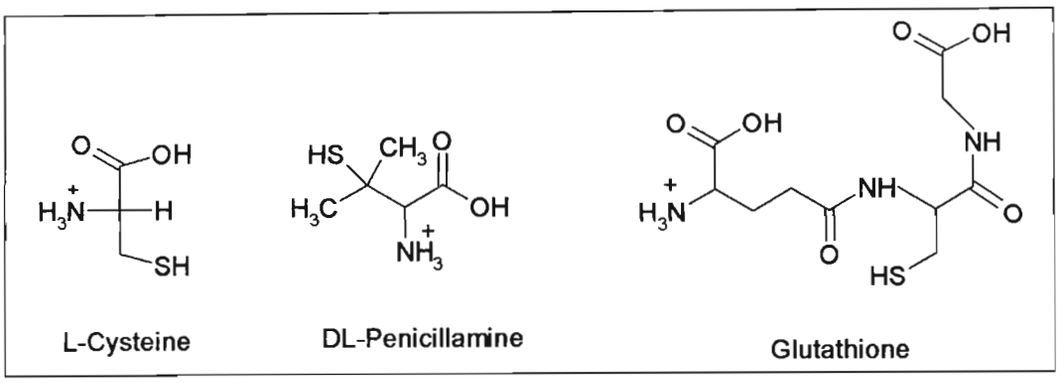

Scheme 4.3 *Structures of the three thiols used as nucleophiles.*

Considering the steric effects of the thiols, DL-penicillamine is more sterically hindered than L-cysteine due to the presence of the two methyl groups bonded to the carbon next to the sulfur atom. Therefore one would expect the reactivity of DL-penicillamine with the two complexes to be lower compared with that of L-cysteine. This is what is observed in **Table 4.1** for both complexes. When glutathione is compared to the other two nucleophiles, it is the bulkiest and therefore would be expected to be the least reactive. However, the results show the opposite.

This unexpected reactivity points to the existence of an anchimeric effect (neighbouring interaction effect). This feature probably arises from hydrogen bonding interactions between the incoming thiols and the leaving water molecule during the transition state, with a net reduction in the activation energy barrier of the substitution reaction. This neighbouring group effect has also been observed in other reactions involving $[Pd(H_2O)_4]^{2-}$ with monodentate acetate, propionate, glycolate carboxylic acid and $[Pt(H_2O)_4]^{2-}$ with thioglycolic acid. [3, 12, 13] In general, the anchimeric effect has been observed to play a role in most organic reactions.[14] This same effect was reported to operate in the formation of Pt(II) chelates.[15] The lower reactivity of DL-penicillamine can

be linked to the presence of the two methyl groups attached to the α-carbon centre causing steric hindrance.

The stability constants {K = k_2/k_{-2}} for the $[Pt(bpma)(OH_2)]^{2+}$ complex show that the thiol products that result from the substitution of water are quite stable. The sensitivity of the reaction on the nature of the incoming group is an indication that these reactions proceed via an associative mode of activation. This is supported by the large and negative values of $\Delta S^{\neq}$ for the forward reactions. The enthalpy values follow the trend of substitution indicating that glutathione goes through the smallest energy barrier and DL-penicillamine the highest, accounting for the trend of the k_2 values.

In conclusion, the results of this study have shown that the substitution reactions of the two platinum complexes, $[Pt(terpy)(OH_2)]^{2+}$ and $[Pt(bpma)(OH_2)]^{2+}$ proceed via an associative mechanism. Furthermore, the study has managed to compare the reactivity of these two platinum(II) complexes. The results have shown that $[Pt(terpy)(OH_2)]^{2+}$ complex is more reactive than $[Pt(bpma)(OH_2)]^{2+}$. This difference in reactivity is mainly because of the extended π-conjugation of the aromatic system around the Pt(terpy) metal centre. The thiols investigated, L-cysteine, glutathione and DL-penicillamine were observed to have a high affinity for the platinum(II) complexes. The order of reactivity was found to be: glutathione > L-cysteine > DL-penicillamine. This difference is mainly due to the steric hindrance in the case of the DL-penicillamine and due to the anchimeric effect in the case of glutathione, which overcompensates the steric effect when compared to L-cysteine. Therefore, bulkiness and solvation of the entering nucleophile play a major role. It can therefore be said that compounds that contain a sulfhydryl group, if co-administered in platinum anticancer therapy may play a role in the reduction of side effects.

4.3 Reactions of $[M(bpma)(OH_2)]^{2+}$ (M = Pt or Pd) with I^-, Br^-, Cl^-, SCN^-, TU, DMTU and TMTU.

The rates of substitution of the coordinated water molecule from $[Pd(bpma)OH_2]^{2+}$ using TU, DMTU and TMTU and from $[Pt(bpma)(OH_2)]^{2+}$ with TU, DMTU, TMTU Cl^-, Br^-, I^- and SCN^- as the incoming nucleophiles [Nu] were studied under pseudo-first-order conditions using a stopped-flow technique. The reactions were carried out in aqueous media of pH 2-3 ($NaClO_4$). At the chosen pH the complexes were 100 % in the aqua form (see **section 4.2.1**). Reactions involving the palladium complex were performed at 10 °C because they were too fast to be followed at 25 °C. Because of this no temperature dependence studies were carried out. In the case of the platinum complex the temperature was varied between 20 and 40 °C in increments of 5 °C. The substitution reactions performed can be represented in general by equation (4.9).

$$[M(bpma)(OH_2)]^{2+} + Nu \underset{k_{-2}}{\overset{k_2}{\rightleftharpoons}} [M(bpma)Nu]^{2+} + H_2O \qquad (4.9)$$

M = Pt or Pd

Kinetic trials as described in **section 4.2.3** were done so as to determine the optimum experimental conditions. From these trials the wavelengths tabulated in **Table 4.2** were chosen for kinetic studies involving both complexes $[Pt(bpma)(OH_2)]^{2+}$ and $[Pd(bpma)(OH_2)]^{2+}$. The concentrations of the complexes were 5.0×10^{-5} M and 4.62×10^{-4} M for Pt(II) and Pd(II) respectively. All the reactions were studied at constant ionic strength μ = 0.1 M ($NaClO_4$). Substitution reactions of $[Pd(bpma)(OH_2)]^{2+}$ were only investigated for TU, DMTU and TMTU. This is because the spectral changes between the complex and the other nucleophiles were too small for stopped flow analysis.

Table 4.2 *Optimum wavelengths chosen for kinetic studies.*

Nucleophile	$[Pd(bpma)(OH_2)]^{2+}$ λ (nm)	$[Pt(bpma)(OH_2)]^{2+}$ λ (nm)
TU	380	300
DMTU	390	300
TMTU	390	330
Br^-		290
Cl^-		268
I^-		267
SCN^-		268

Typical UV-Visible spectra for the reactions of $[Pt(bpma)(OH_2)]^{2+}$ and $[Pd(bpma)(OH_2)]^{2+}$ with different concentrations of NaCl and TMTU respectively are shown in **Figure 4.10 (a)** and **(b)**. The scans clearly show that when NaCl and TMTU nucleophiles are used as incoming ligands a major change in absorbance is observed around 268 and 390 nm for Pt(II) and Pd(II) complexes respectively.

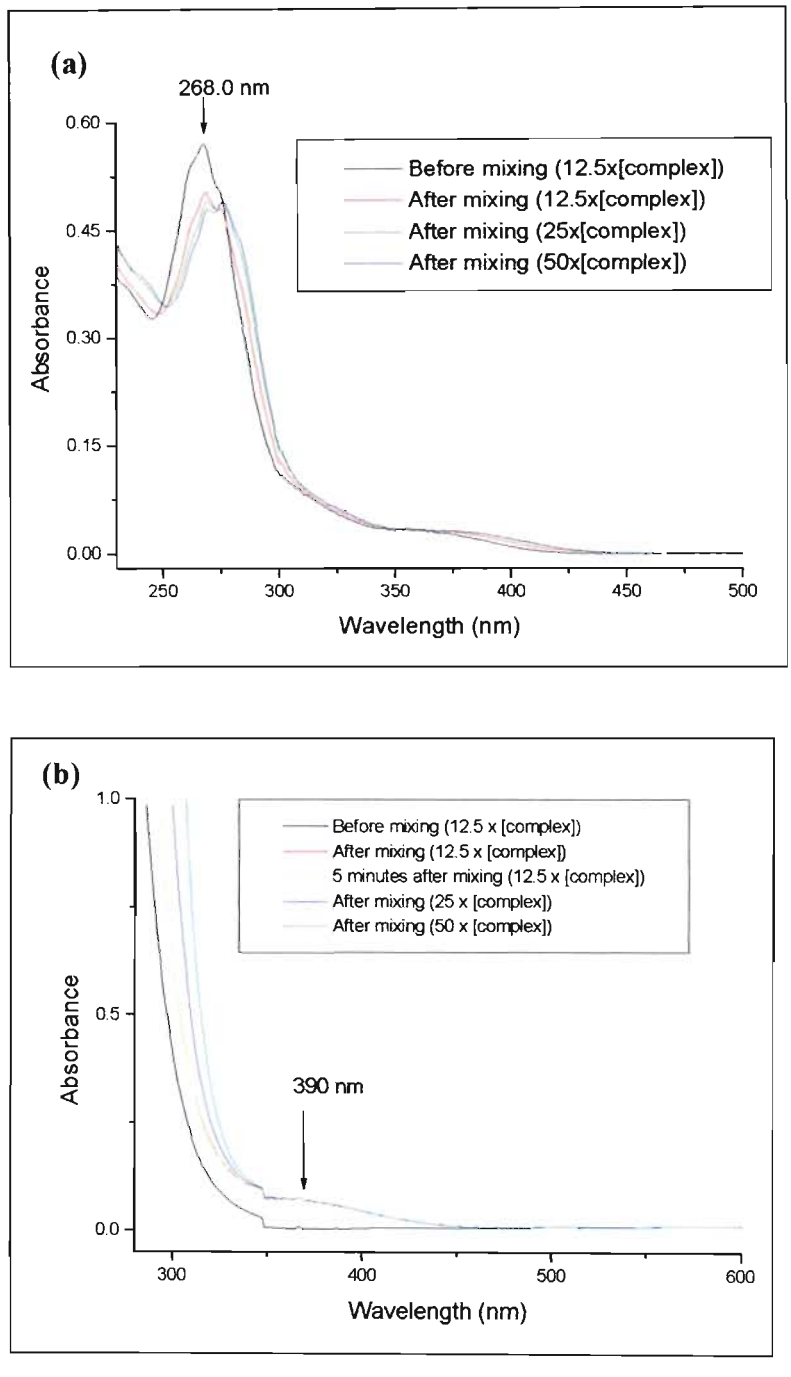

Figure 4.10 *The UV-Visible spectra for the reaction of* **(a)** $[Pt(bpma)(OH_2)]^{2+}$ *with NaCl at pH 2 solution and* **(b)** $[Pd(bpma)(OH_2)]^{2+}$ *with TMTU in pH 3 solution at 25 °C.*

4.3.1 Concentration Dependence Study for $[M(bpma)(OH_2)]^{2+}$ (M = Pt or Pd)

The second order rate constants, k_2, were determined by carrying out concentration dependence studies under pseudo-first order conditions by varying the concentration of the nucleophile from 10 to 50 times that of the complexes. The stopped flow kinetic traces for the reactions that can be represented by equation (4.5) were found to fit single exponentials. This is an indication that the reactions were first-order in both the concentration of the nucleophile and the complexes. Representative samples of the kinetic traces obtained for the reaction involving $[Pt(bpma)(OH_2)]^{2+}$ and $[Pd(bpma)(OH_2)]^{2+}$ with thiourea are given in **Figure 4.11 (a)** and **(b)** respectively.

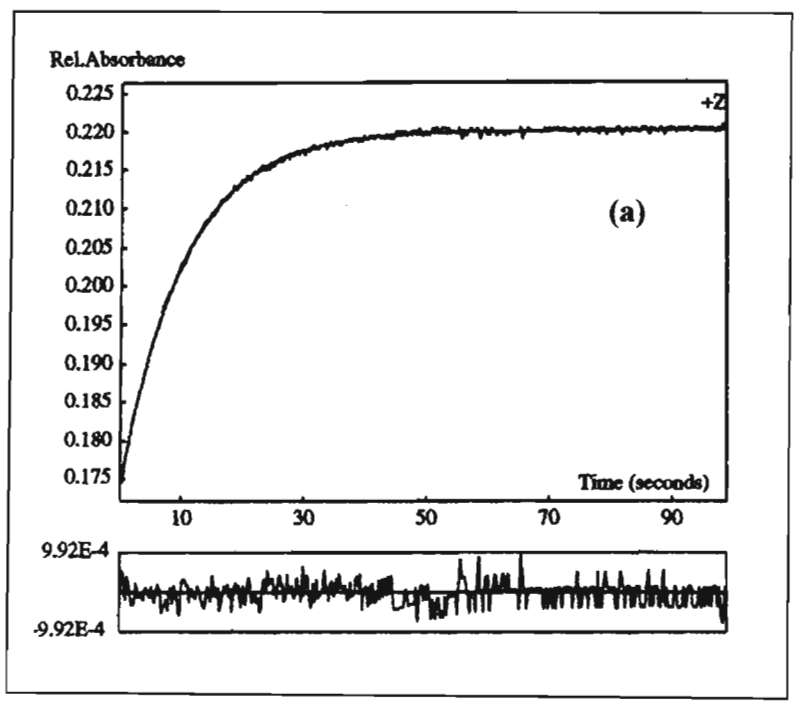

Figure 4.11(a) *Stopped flow kinetic traces for the reaction of thiourea (TU) with* $[Pt(bpma)(OH_2)]^{2+}$ *at 25 °C.*

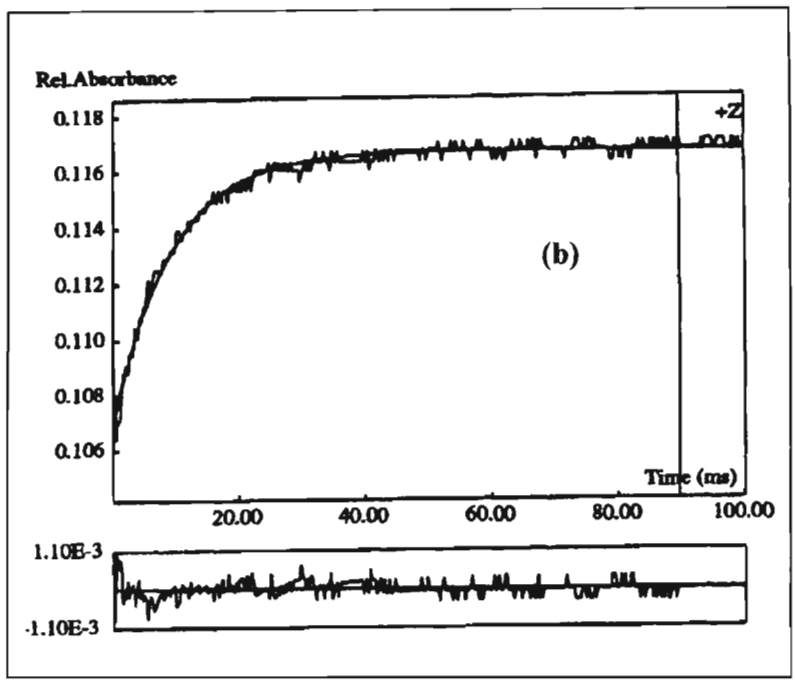

Figure 4.11(b) *Stopped flow kinetic trace for the reaction of thiourea (TU) with* $[Pd(bpma)(OH_2)]^{2+}$ *at 10 °C.*

Straight line plots with zero intercept were obtained when the observed pseudo first-order rate constants, k_{obs}, were plotted against the concentrations of the incoming nucleophiles. The graphs obtained are given in **Figure 4.12 (a)** and **(b)** for Pt(II) and Pd(II) complexes respectively. Since the linear plots had zero intercept, it can be concluded that the backward reaction did not exist. Therefore, $k_{-2} \approx 0$, and equation (4.9) can be represented as:

$$[Pt(NNN)OH_2]^{2+} + Nu^{n-} \xrightarrow{k_2} [Pt(NNN)Nu]^{(2-n)+} + H_2O \qquad (4.10)$$

It therefore follows that the two-term rate law given by equation (4.6) can be expressed as:

$$k_{obs} = k_2[Nu] \qquad (4.11)$$

The k_2 values obtained from the slope of the different plots are summarized in **Table 4.3**.

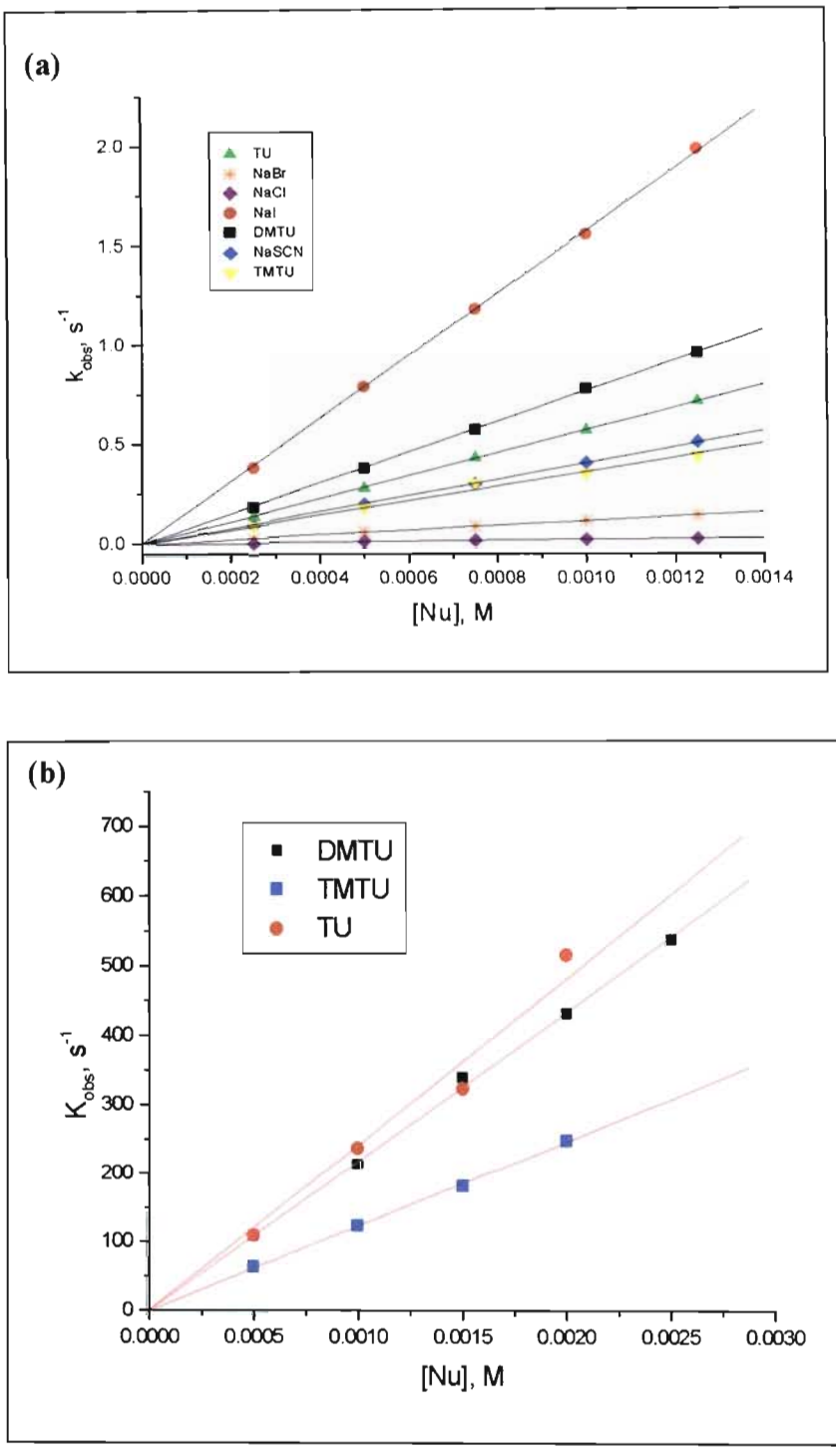

Figure 4.12 *Plots of k_{obs} versus [Nu] for* **(a)** *$[Pt(bpma)(OH_2)]^{2+}$ (5.0×10^{-5} M) at 25 °C and* **(b)** *$[Pd(bpma)(OH_2)]^{2+}$ (4.62×10^{-4} M) at 10 °C. pH = 2-3 ($HClO_4$), μ = 0.1 M.*

4.3.2 Temperature Dependence Studies

Temperature dependence studies for the purpose of determining the activation parameters, $\Delta H^{\neq}$ and $\Delta S^{\neq}$, were only done for $[Pt(bpma)(OH_2)]^{2+}$ with TU, DMTU, TMTU, I^-, Br^-, SCN^- and Cl^- at temperatures 15, 20, 25, 30, 35 and 40 °C. These studies were not carried out for $[Pd(bpma)(OH_2)]^{2+}$ due to the fact that the reactions involving this complex were extremely fast even at 10 °C. As a result it was difficult to analyze the kinetic traces.

The corresponding Erying plots for Pt(II) complex based on the second order rate constants, k_2, for all the nucleophiles investigated were plotted and are given in **Figure 4.13**.

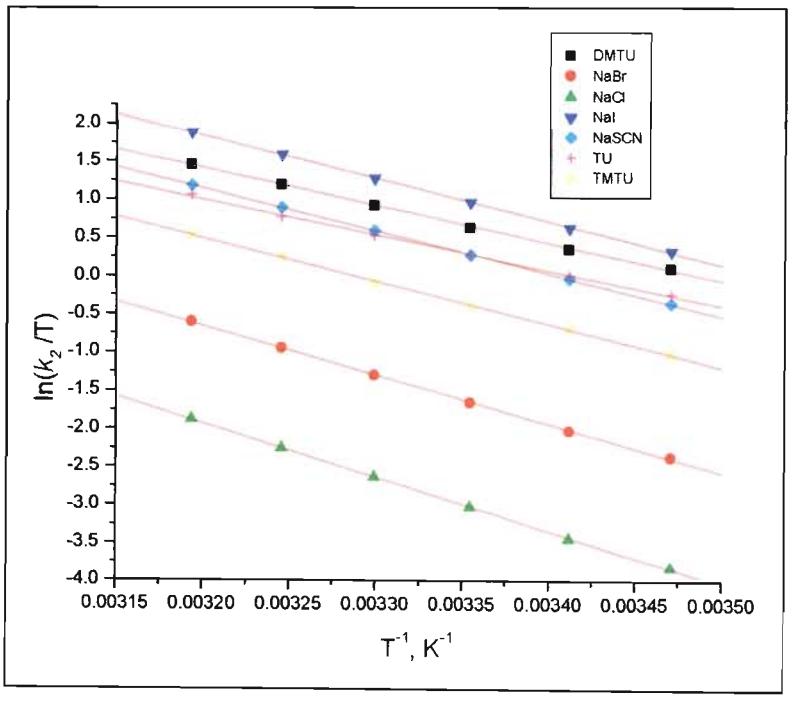

Figure 4.13 *Temperature dependence plots for the reaction of* $[Pt(bpma)(OH_2)]^{2+}$ *with various nucleophiles.*

Using the slope and the y-intercept, $\Delta H^{\neq}$ and $\Delta S^{\neq}$ values for each nucleophile were calculated. These values with the associated second order rate constants, k_2, at 25 °C are tabulated in **Table 4.3**. In order to compare the reactivities of the Pt(II) and Pd(II) complexes, the k_2 values should have been determined at the same temperature. This was not done, but a correction was achieved by converting k_2 for $[Pt(bpma)(OH_2)]^{2+}$ at 25 °C to 10 °C using the linear equations (equation 4.12) from the Erying plots of TU, DMTU and TMTU assuming that the linearity exists down to 10 °C.

$$\ln\left(\frac{k_2}{T}\right) = m\left(\frac{1}{T}\right) + c \qquad (4.12)$$

The symbols m and c in equation (4.12) are the slope and the intercept whose values are known for the respective nucleophiles. The resulting k_2 values that were calculated for 10 °C are included in **Table 4.3.**

Table 4.3 *Second order rate constants, (k_2), and activation parameters for the reaction of $[Pt(bpma)(OH_2)]^{2+}$ and $[Pt(bpma)(OH_2)]^{2+}$ with various nucleophiles in aqueous solution of pH 2-3 ($HClO_4$), μ = 0.1 M ($NaClO_4$).*

	k_2^{283} /$M^{-1}s^{-1}$	k_2^{298} /$M^{-1}s^{-1}$	$\Delta H^{\neq}_2$ /kJ mol^{-1}	$\Delta S^{\neq}_2$ /J K^{-1} mol^{-1}
$[Pt(bpma)(OH_2)]^{2+}$				
TU	162.1	405 ± 3	38.7 ± 0.8	-66 ± 3
DMTU	223.0	570 ± 2	41.1 ± 0.7	-55 ± 2
TMTU	70.3	180 ± 5	46.9 ± 0.6	-44 ± 2
I^-	267.4	788 ± 4	47.1 ± 0.5	-32 ± 2
Br^-	17.4	57.0 ± 0.3	53.2 ± 0.6	-33 ± 2
Cl^-	3.9	9.6 ± 0.1	60.9 ± 0.4	-22 ± 1
SCN^-	137.4	384 ± 2	46.4 ± 0.2	-40 ± 1
$[Pd(bpma)(OH_2)]^{2+}$				
TU	$(2.12 \pm 0.05)\times10^5$			
DMTU	$(2.17 \pm 0.02)\times10^5$			
TMTU	$(1.24 \pm 0.01)\times10^5$			

4.3.3 Reactivity

In general the reactivity of many Pt(II) complexes is a factor of 10^5-10^6 lower than that of the corresponding Pd(II) complexes.[16, 17, 18, 33] For instance, the rate of solvent exchange for $[Pd(H_2O)_4]^{2+}$ is 10^6 times faster than for $[Pt(H_2O)_4]^{2+}$. This reactivity is largely influenced by the co-ordination environment and the nature of the incoming nucleophile. Basolo[19], Romeo[20, 21, 22] and van Eldik[23] have shown that introduction of the metal-carbon bond strongly stabilizes the *trans* position for a substitution reaction through the σ-effect. When four metal-carbon bonds are involved, the difference in reactivity between Pt(II) and Pd(II) disappears.[24] The other route which has been used is to slow down the rate of

reaction of Pd(II) to approach that of Pt(II) through the introduction of steric hindrance.[25, 26, 27]

Investigations looking specifically at the role of the π-effect in substitution reactions has received less attention because of the difficulty of separating it from that of the strong σ-effect. Recently, Jaganyi *et al*,[8, 28] showed that it is possible to separate the two electronic effects. In this part of the study a comparison is being made between Pt(II) and Pd(II) so as to shed light on the role of the π-effect on the reactivity of the two metal centres.

Platinum is a softer centre than palladium, therefore it is more sensitive to electronic communication between the metal and the chelate ring than is palladium. This behaviour has also been observed for the reactions of $[Pd(terpy)(OH_2)]^{2+}$ and $[Pt(terpy)(OH_2)]^{2+}$ with thiols as nucleophiles.[7]

From this study, a comparison of the reactions between $[Pd(bpma)(OH_2)]^{2+}$ and $[Pt(bpma)(OH_2)]^{2+}$ with nucleophiles TU, DMTU and TMTU at 10 °C has been managed. The values of the second order rate constants, k_2, given in **Table 4.3** clearly indicate that the reactivity of $[Pd(bpma)(OH_2)]^{2+}$ is higher than that of $[Pt(bpma)(OH_2)]^{2+}$ by at least three orders of magnitude. The reactivity difference points to the metal properties since the spectator ligand and the leaving group are the same in both complexes. The σ-effect in both cases is also the same.[28]

In this case the reactivity difference between $[Pd(bpma)(OH_2)]^{2+}$ and $[Pt(bpma)(OH_2)]^{2+}$ is 10^3 instead of the 10^5-10^6 seen in earlier studies.[16, 17, 18, 33] This increase in reactivity of Pt(II) can be explained in terms of π-back bonding due to the two *cis* pyridyl rings. The presence of the pyridine group increases the electrophilicity of the metal centre by accepting back donation of electron density from the metal centre. This reduces the electron density on the metal making it more positive. This has an effect of lowering the energy of π*-orbitals and resulting in an enhanced reactivity towards the incoming nucleophiles. Apart from making the metal centre more electrophilic, the chelate stabilizes the trigonal-bipyramidal intermediate by withdrawing the electrons from the

incoming nucleophile. The explanation given should apply to both metals, but this seems not to be the case when one looks at the lowering of the reactivity difference between the two complexes investigated.

The second order rate constants (k_2) given in **Table 4.3** show that the reactivity of the nucleophiles towards the complexes follows the order TMTU < TU< DMTU for the platinum-bpma complex and TMTU < TU ≈ DMTU for the palladium complex.

The trends can be explained in terms of the steric and the inductive effects of the nucleophiles. The order of decreasing steric hindrance for these three nucleophiles is as follows: TMTU < DMTU < TU. Theoretically, it would be expected that TU would be a better nucleophile towards the metal centre, followed by DMTU and TMTU would be the least reactive nucleophile because of the degree of its steric hindrance due to the four methyl groups bonded to the nitrogen. However, the trends point out that DMTU is a much better nucleophile than TU. The reason for this behaviour is the inductive effect introduced by the two methyl groups in the case of DMTU, which overcompensate the steric effect. In the case of the palladium complex the reactivities of TU and DMTU are practically equal, this implies that the inductive effect is still playing a role. However its effect is of less significance in this case because of the nature of the metal centre as already explained above.

The order of the reactivity with respect to the substitution of water from $[Pt(bpma)(OH_2)]^{2+}$ with halides, namely Cl^-, Br^- and I^-, seems to increase with the polarizability of the halide. The polarizabilities of the halides are 2.18×10^{-24}, 3.05×10^{-24} and 4.7×10^{-24} cm^3 for Cl^-, Br^-, and I^- respectively.[29] Iodine is the most polarized halide and can be classified as a softer ligand compared to the rest. Soft nucleophiles (polarizable) favour soft substrates and hard ligands (nonpolarizable) prefer hard substrates.[30] Since platinum(II) is a "soft" Lewis acid it is not suprising that its reactivity with the halide and SCN^- are in agreement with the polarizabilities of the nucleophiles.

The second order rate constants, (k_2), for the reaction of $[Pt(bpma)(OH_2)]^{2+}$ with various nucleophiles shows an order of nucleophilicity as: I^- > DMTU > TU > SCN^- > TMTU > Br^- > Cl^- which deviates from that reported by Pitteri *et al*[31] for $[Pt(SNS)Cl]^+$, SNS denotes 2,6-*bis*(methylthiomethyl)pyridine and in agreement with that of Belluco *et al* for $[Pt(py)_2Cl_2]$ systems.[32] In order to determine the ability of $[Pt(bpma)(OH_2)]^{2+}$ to discriminate between the nucleophiles, a Linear Free Energy Relationship (LFER) was determined. A plot of logk_2 against the nucleophilicity constants of the nucleophiles (n^0_{pt}) was plotted in **Figure 4.14**. The values of n^0_{pt} used for the plot were TU = 7.17, I^- = 3.04, Cl^- = 3.04, Br^- = 4.18, and for SCN^- = 5.75.[33]

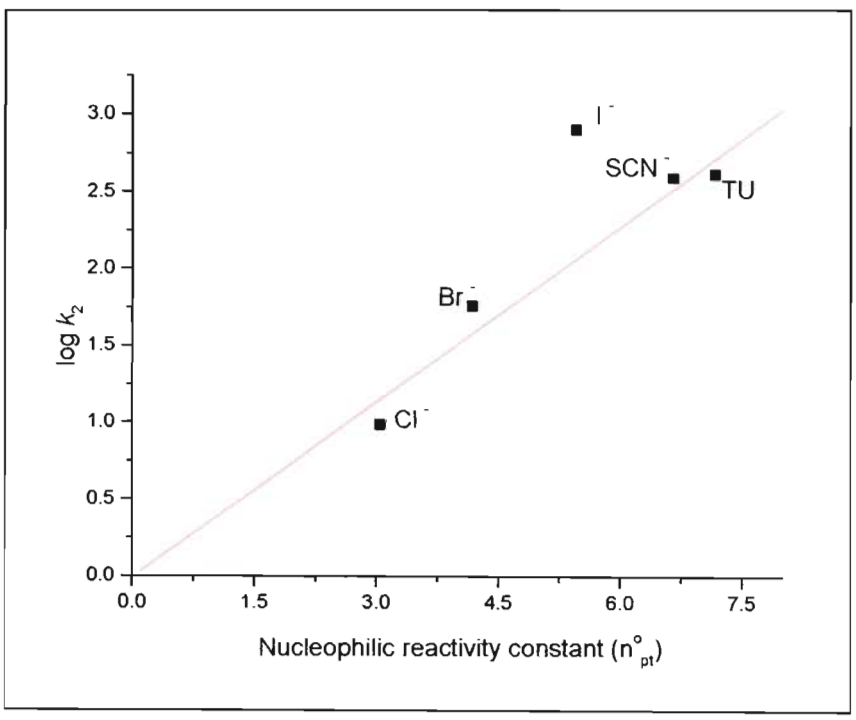

Figure 4.14 *Linear free energy relationship of $[Pt(bpma)(OH_2)]^{2+}$ with different nucleophiles.*

The plot obtained can be represented by equation (4.13), where s represents the nucleophilic discrimination factor. A straight-line indicates that the reactions of these nucleophiles with the platinum complex occur via the same mechanism.

$$\log k_2 = sn^{o}_{pt}(Y) + \text{constant} \qquad (4.13)$$

Since the points fall approximately on the straight line, this indicates that the reactions of these nucleophiles with the platinum complex occur via the same mechanism. From the slope of the graph the value of s for $[Pt(bpma)(OH_2)]^{2+}$ was obtained to be 0.38. This value which is dependent on the nature of the complex is less than that of the standard substrate *trans*-$[Pt(py)_2Cl_2]$ (s = 1.00).[34] This means that $[Pt(bpma)(OH_2)]^{2+}$ is less discriminating in reacting with different nucleophiles when compared to *trans*-$[Pt(py)_2Cl_2]$. The constant term is attributed to k_s, the rate constant for the attack by solvent. This term is not playing a role in these reactions since the concentration dependence studies had zero intercepts indicating the absence of the back reaction.

This kind of LFER plot has been reported in literature for other reactions.[35, 36] One of the reasons why nucleophiles such as TU have high reactivity towards a platinum centre is that it has a capacity to stabilize the five-coordinated transition state through metal-to-ligand π-interactions.[34]

The slight sensitivity of the reaction rates on the nature of the incoming ligands and the negative entropies of activation indicate that the reactions proceed via an associative mode of activation. There is very little difference in the enthalpy values. But a close look at the values reveals a trend which is more or less in line with the k_2 values.

In conclusion, the study has shown that it is possible to increase the reactivity of the Pt(II) metal centre through the introduction of the π-effect. This tuning of the metal complex does not change the substitution mechanism, which remains associative. The results show that $[Pd(bpma)(OH_2)]^{2+}$ is 10^3 times more reactive than $[Pt(bpma)(OH_2)]^{2+}$. The reactivity of the nucleophiles toward these complexes were found to follow the trend

DMTU > TU > TMTU for $[Pt(bpma)(OH_2)]^{2+}$ and DMTU ≈ TU > TMTU for $[Pd(bpma)(OH_2)]^{2+}$. This order has been attributed to the steric hindrance in the case of TMTU and the inductive effect in case of DMTU.

The reactivity of the other nucleophiles investigated, namely I^-, SCN^-, Br^- and Cl^- follows the order $I^- > SCN^- > Br^- > Cl^-$. This reactivity order depends on the polarizability of the incoming ligand. Iodine being the most polarized halide, reacts much faster than the other nucleophiles. The entropy values for $[Pt(bpma)(OH_2)]^{2+}$ are negative which confirm that the mechanism is associative as expected.

4.4 Kinetic Studies of the Monoaqua Ruthenium(II) Polypyridine Complexes

The pH titrations for $[Ru(terpy)(bipy)(OH_2)]^{2+}$ and $[Ru(terpy)(tmen)(OH_2)]^{2+}$ were carried out in aqueous solution over a pH range of 1-12. Since the initial pH was 1 ($HClO_4$) it meant that the ionic strength was μ = 0.1 M. The concentrations of the complexes were 8.42 x 10^{-5} M and 7.60 x 10^{-5} M for $[Ru(terpy)(bipy)(OH_2)]^{2+}$ and $[Ru(terpy)(tmen)(OH_2)]^{2+}$, respectively. These were titrated using an aqueous solution of NaOH as described in section **4.2.1** at 25 °C. The titration reactions of these complexes with NaOH can be represented by equation (4.14).

$$[Ru(terpy)(NN)(OH_2)]^{2+} + OH^- \underset{+H^+}{\overset{-H^+}{\rightleftharpoons}} [Ru(terpy)(NN)OH]^+ + H_2O \qquad (4.14)$$

NN = bipyridine or *N,N,N',N''*-tetramethylethylenediamine

Isosbetic points were observed upon titration, which is a clear indication that only two species were present in the solution (the hydroxo and the aqua species) and these species were in equilibrium as presented by equation (4.14). Reversibility of the titration was observed when a small amount of $HClO_4$ was added to the titrated solution.

The UV-Vis spectra representing the titration curves for $[Ru(terpy)(bipy)(OH_2)]^{2+}$ and $[Ru(terpy)(tmen)(OH_2)]^{2+}$ are given in **Figures 4.15 and 4.16** respectively. The insets are plots of absorbance versus pH at λ = 365 and λ = 360 nm. The pK_a curves were fitted through the points by using equation (3.1) (**section 3.10**).

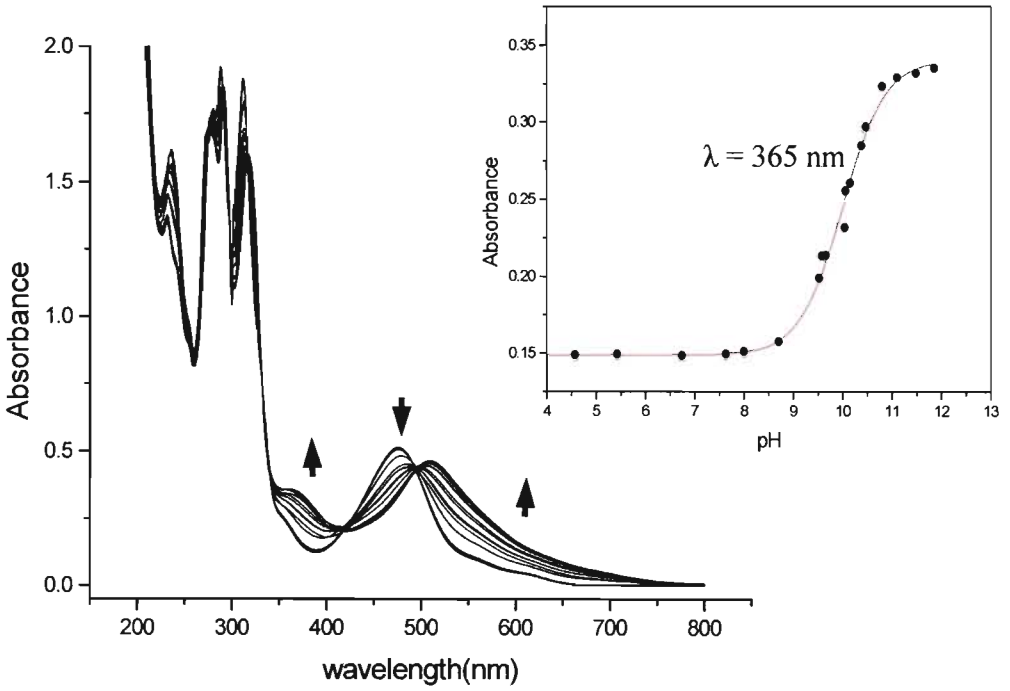

Figure 4.15 *UV-Vis spectra of* $[Ru(terpy)(bipy)(OH_2)]^{2+}$ *(8.42 x* 10^{-5} *M), in* μ *= 0.1 M* $(HClO_4)$*; pH range 2-12, T = 25 °C. Inset is the* pK_a *plot of absorbance versus pH at* λ *= 365 nm.*

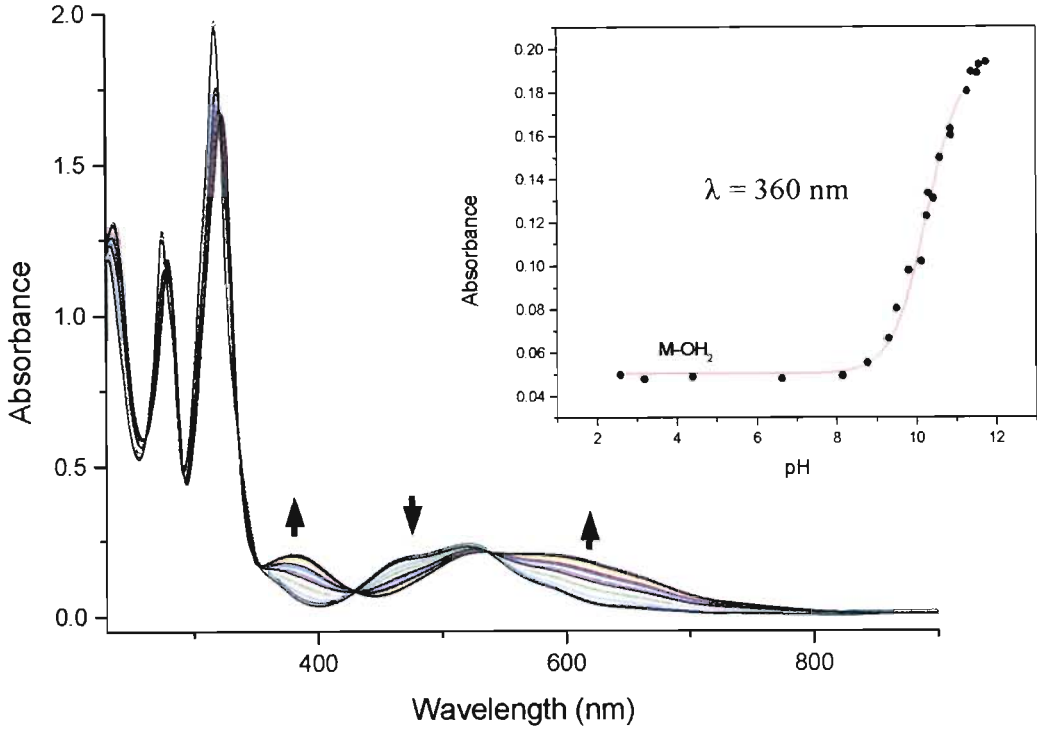

Figure 4.16 *UV-Vis spectra of* $[Ru(terpy)(tmen)(OH_2)]^{2+}$ *(8.39 x* 10^{-5} *M), in* μ *= 0.1 M* $(HClO_4)$*; pH range 2-12, T = 25 °C. Inset is the* pK_a *plot of absorbance versus pH at* λ *= 360 nm.*

The values of pK_a for the complexes were determined to be 9.99 ± 0.04 and 10.27 ± 0.04 for $[Ru(terpy)(bipy)(OH_2)]^{2+}$ and $[Ru(terpy)(tmen)(OH_2)]^{2+}$ respectively. These pK_a values agree with those reported in the literature of 9.7 for $[Ru(terpy)(bipy)(OH_2)]^{2+}$ and 10.2 for $[Ru(terpy)(tmen)(OH_2)]^{2+}$ obtained through an electrochemistry study.[37, 38, 39] From the pK_a values, it can be said that within pH 1-8, both complexes exist as pure aqua complexes. At pH's higher than 12, the complexes are entirely hydroxo species. As a result, substitution reactions of the coordinated water from these complexes were carried out within the pH range where the complexes were in the aqua form.

4.4.1 Substitution Reaction of $[Ru(terpy)(NN)(OH_2)]^{2+}$ (NN = 2,2"-bipyridine or *N, N, N', N'*-tetramethylethylenediamine) with CH_3CN, TU and DMTU

The substitution reaction of the coordinated water from $[Ru(terpy)(NN)(OH_2)]^{2+}$ (NN = 2,2'-bipyridine and *N, N, N', N"*-tetramethylethylenediamine) with the nucleophiles (Nu) denotes CH_3CN, DMTU, and TU were carried out in aqueous media of pH 4.0 ($HClO_4$), μ = 0.1 M. The ionic strength was adjusted using $NaClO_4$. The kinetic studies were monitored spectrophotometrically by taking repetitive UV-Vis scans as a function of time. These reactions can be represented by equation (4.15).

$$[Ru(terpy)(NN)(OH_2)]^{2+} + Nu \underset{k_{-2}}{\overset{k_2}{\rightleftharpoons}} [Ru(terpy)(NN)Nu]^{2+} + H_2O \quad (4.15)$$

The UV-Vis repetitive scans for the reactions of $[Ru(terpy)(bipy)(OH_2)]^{2+}$ and $[Ru(terpy)(tmen)(OH_2)]^{2+}$ with DMTU, TU and CH_3CN are given in **Figures 4.17 (a), (b) and (c)** and **Figures 4.18 (a), (b)** and **(c)** respectively. The Figures also show the corresponding kinetic traces, which were obtained by plotting absorbance versus time **(Insets)** at the specified wavelengths. After obtaining the wavelength of interest from the first scan the consecutive reactions at the other concentrations were monitored at this fixed wavelength.

The kinetic traces that were obtained were fitted using Origin 50 and were found to follow single exponentials which suggests that the substitution reactions were first-order in both the nucleophile and the ruthenium complex.

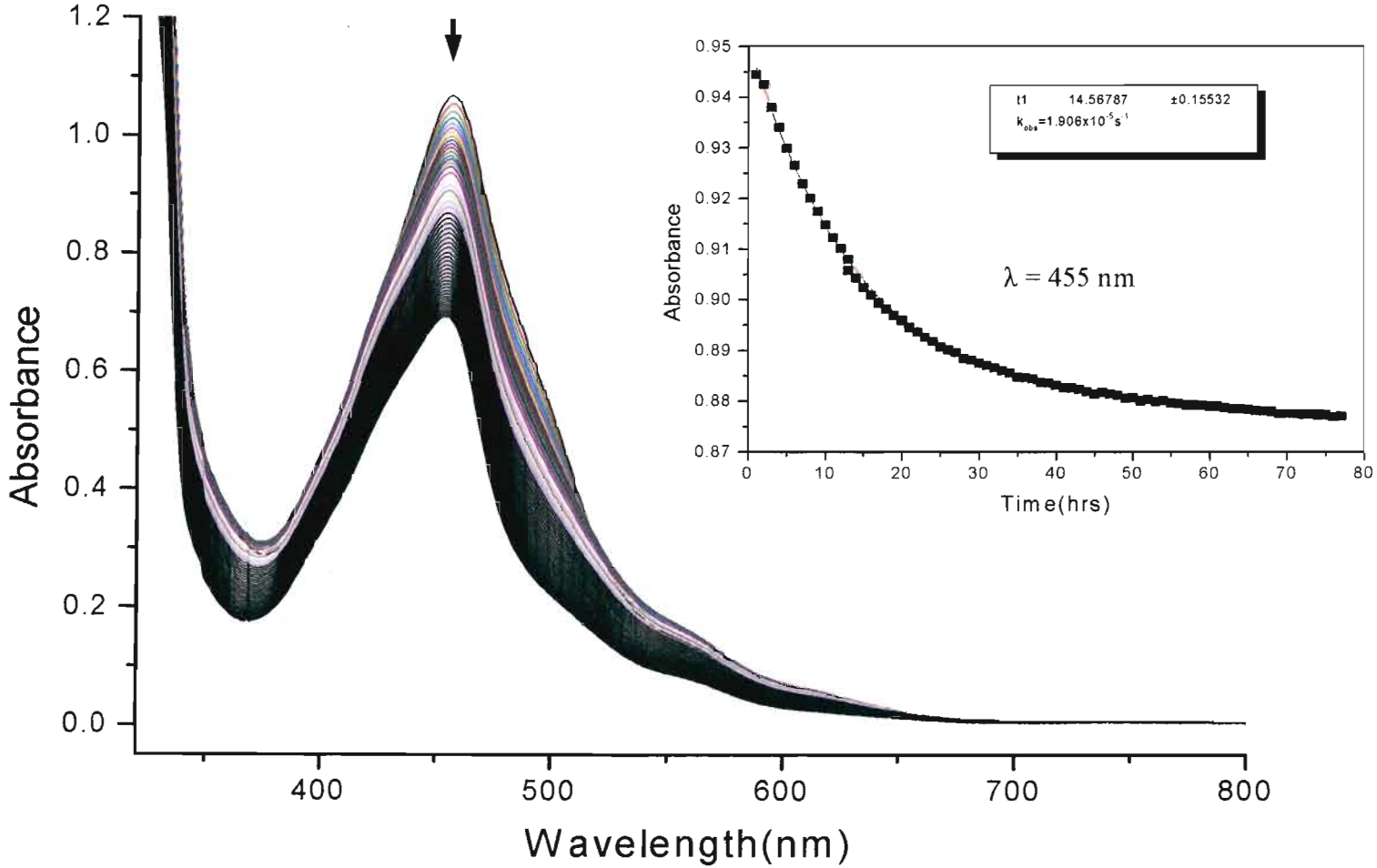

Figure 4.17(a) *UV-Vis spectra for the reaction of* $[Ru(terpy)(bipy)(OH_2)]^{2+}$ *(1.683 x* 10^{-4} *M) with DMTU in pH 4.0 (*$HClO_4$*) aqueous solution, T = 25 °C and* μ *= 0.1 M (*$NaClO_4$*).* ***Inset*** *is the corresponding kinetic plot for the reaction at* λ *= 455 nm.*

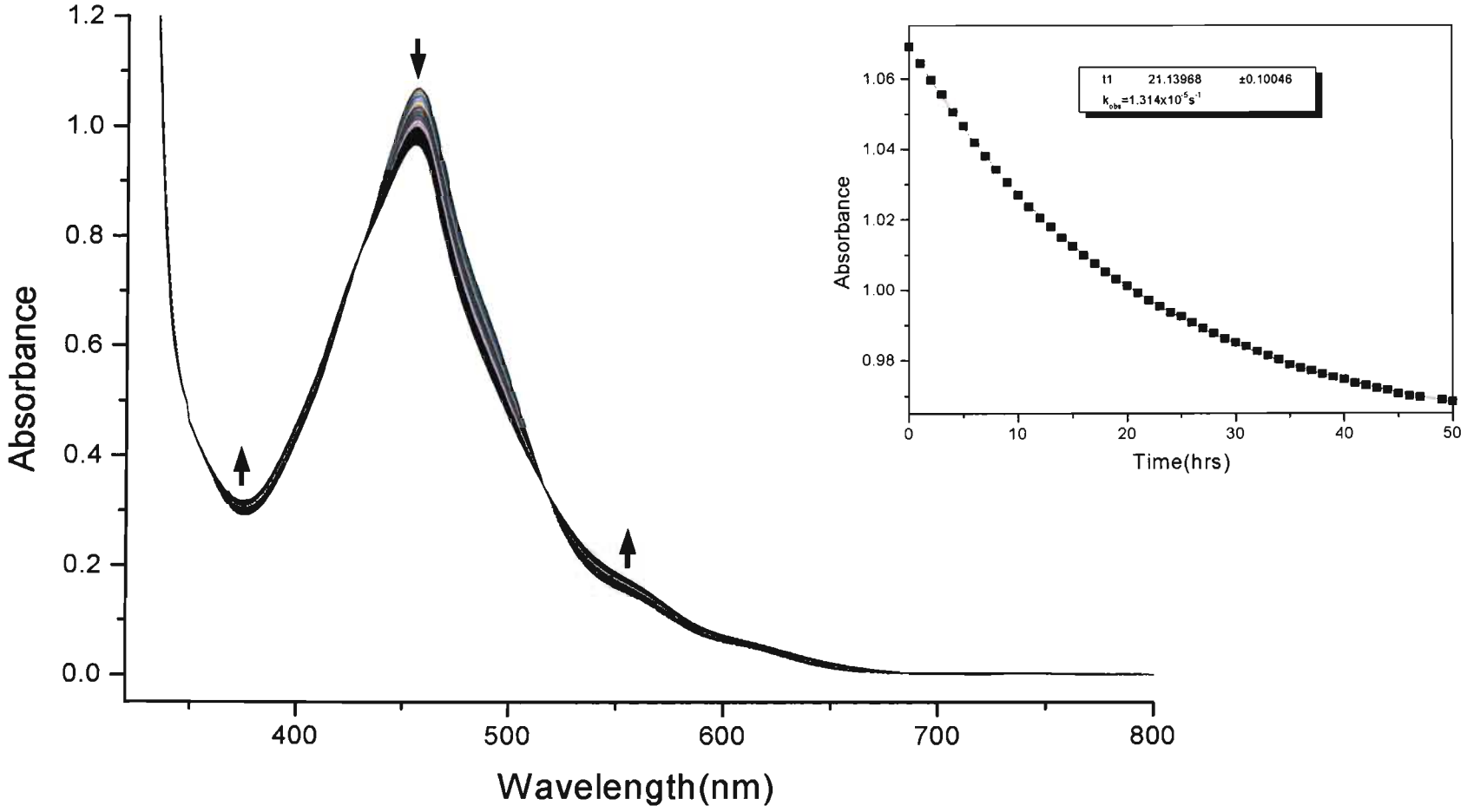

Figure 4.17(b) *UV-Vis spectra recorded for the reaction of* $[Ru(terpy)(bipy)(OH_2)]^{2+}$ *(1.683 x* 10^{-4} *M) with TU recorded in pH 4.0* ($HClO_4$) *aqueous solution,* $T = 25\ ^{o}C$ *and* $\mu = 0.1$ *M* ($NaClO_4$). ***Inset*** *is the corresponding kinetic plot for the reaction at* $\lambda = 458$ *nm.*

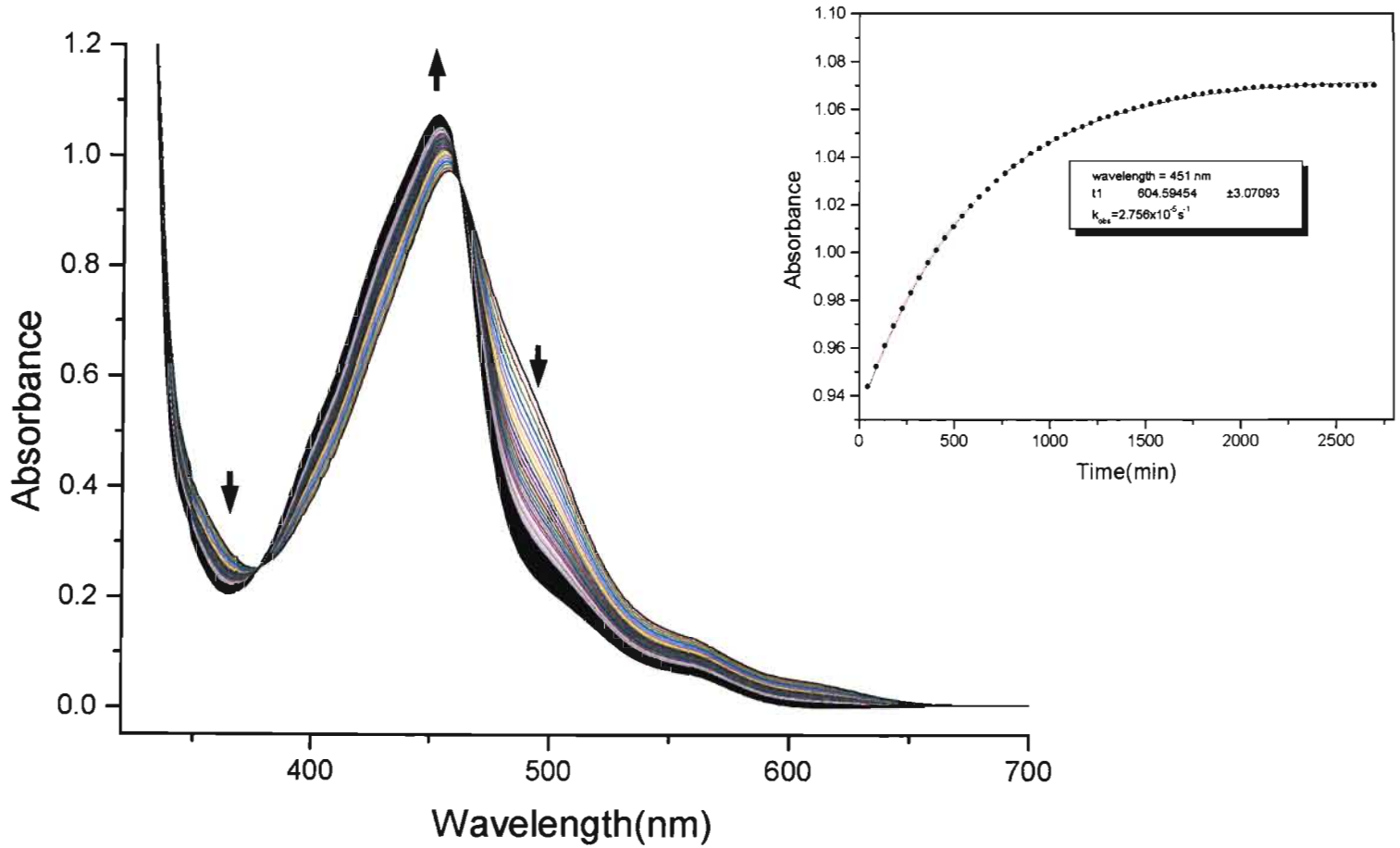

Figure 4.17(c) *UV-Vis spectra recorded for the reaction of* $[Ru(terpy)(bipy)(OH_2)]^{2+}$ *(1.683 x* 10^{-4} *M) with* CH_3CN *recorded in pH 4.0* ($HClO_4$) *aqueous solution, T = 25 °C and* μ *= 0.1 M* ($NaClO_4$). ***Inset*** *is the corresponding kinetic plot for the reaction at* λ *= 451 nm.*

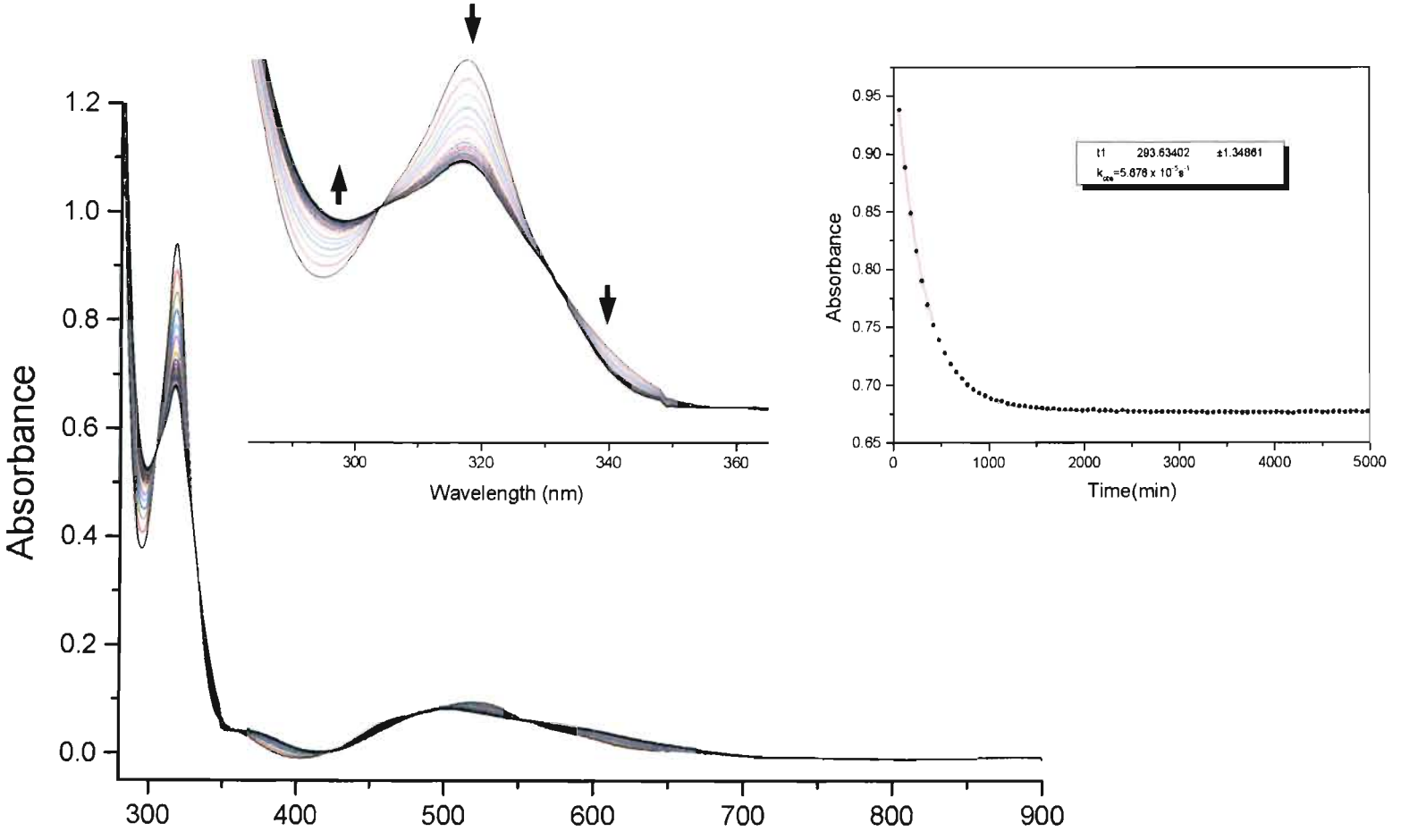

Figure 4.18(a) *UV-Vis spectra recorded for the reactions of* $[Ru(terpy)(tmen)(OH_2)]^{2+}$ *(8.39 x* 10^{-5} *M) with DMTU recorded in pH 4.0 (*$NaClO_4$*) aqueous solution, T = 25 °C.* ***Inset*** *is the corresponding kinetic plot for the reaction at* λ *= 317* nm.

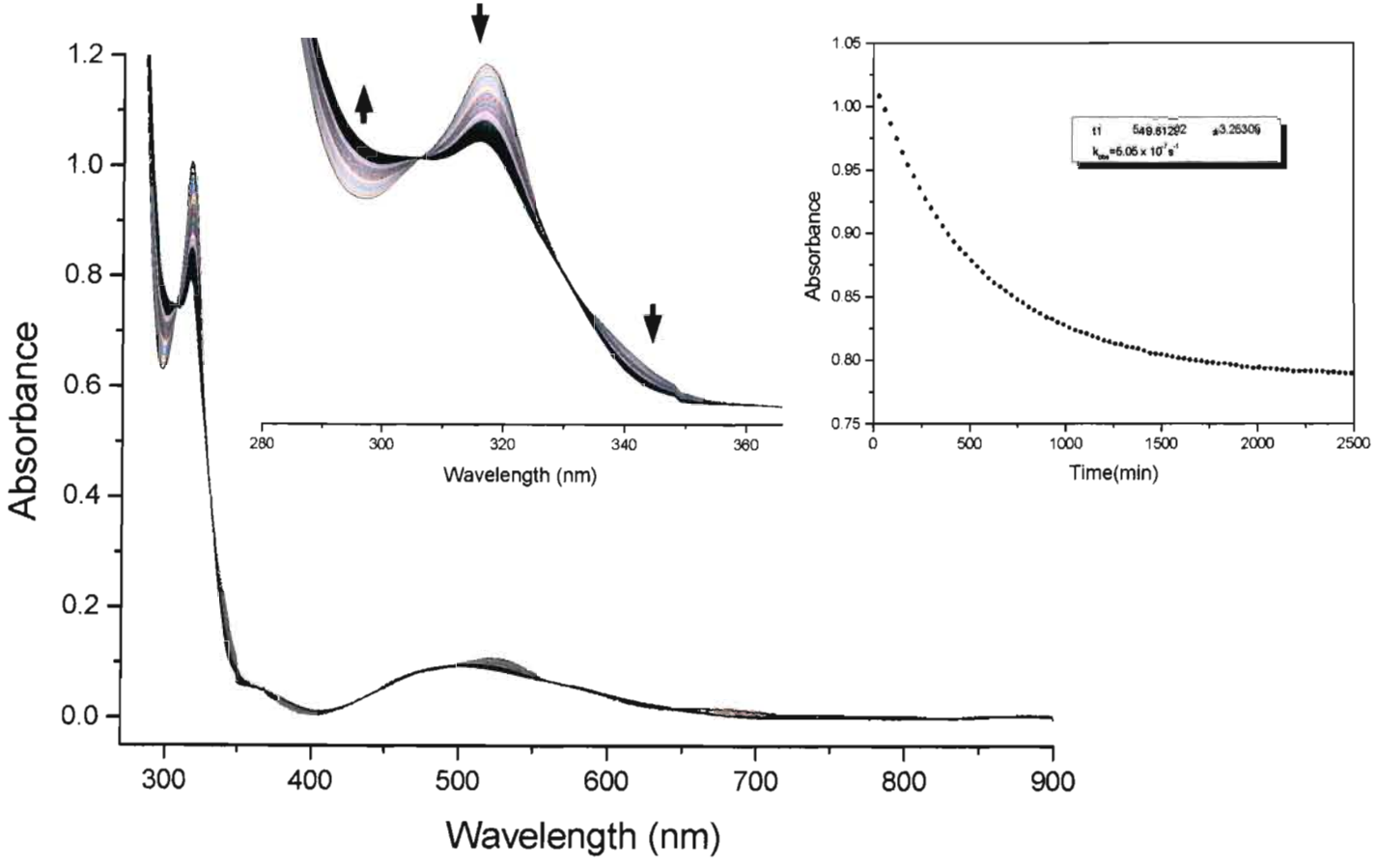

Figure 4.18(b) *UV-Vis spectra recorded for the reaction of* $[Ru(terpy)(tmen)(OH_2)]^{2+}$ *(8.39 x* 10^{-4} *M) with TU recorded in pH 4.0* ($HClO_4$) *aqueous solution,* $T = 25\ ^{o}C$ *and* $\mu = 0.1$ *M* ($NaClO_4$). ***Inset*** *is the corresponding kinetic plot for the reaction at* $\lambda = 317$ *nm.*

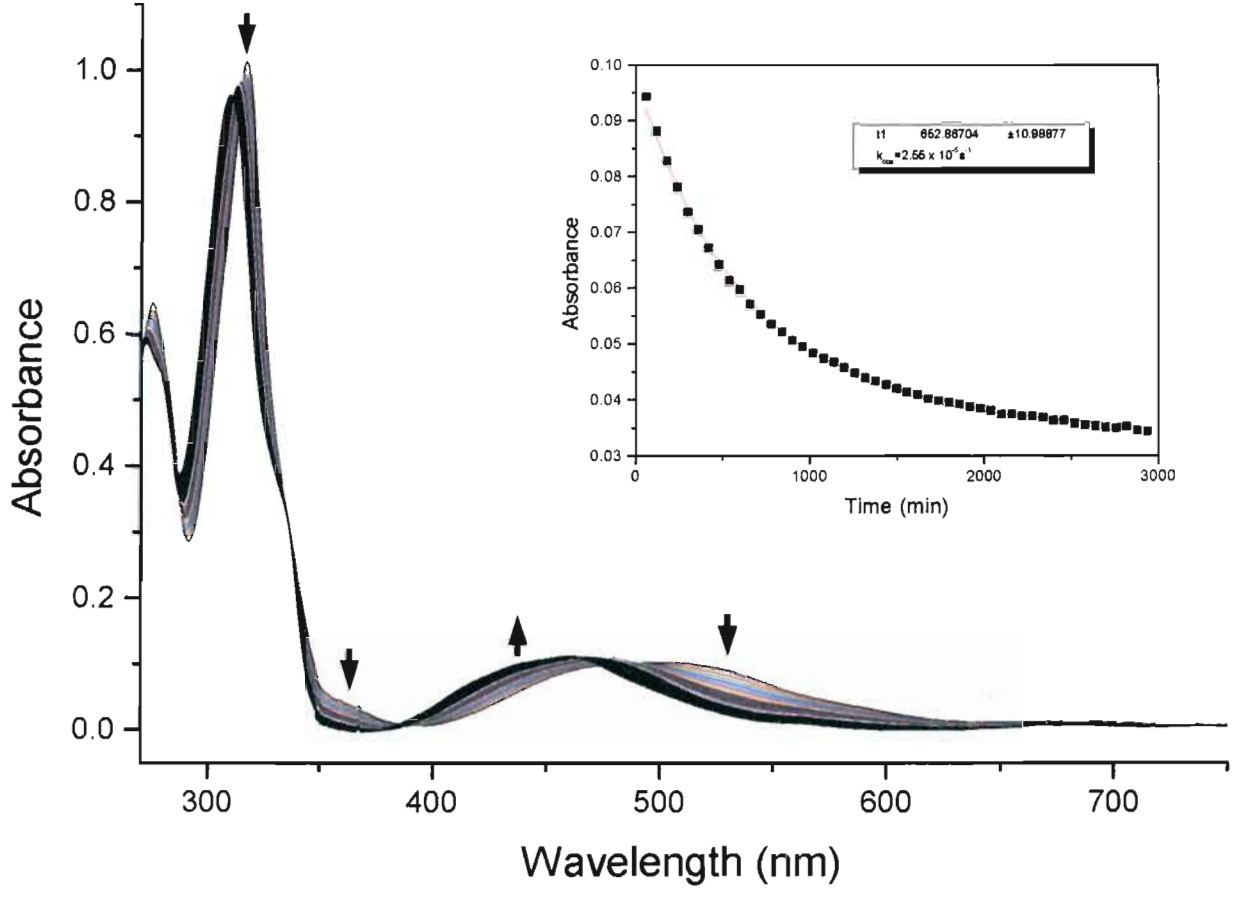

Figure 4.18(c) *UV-Vis spectra for the reaction of* $[Ru(terpy)(tmen)(OH_2)]^{2+}$ *(8.39 x* 10^{-5} *M) with* CH_3CN *recorded in pH 4.0* ($HClO_4$) *aqueous solution, T = 25* ^{o}C *and* μ *= 0.1 M* ($NaClO_4$). ***Inset*** *is the corresponding kinetic plot for the reaction at* λ *= 386 nm.*

Analysis of the kinetic data for $[Ru(terpy)(bipy)(OH_2)]^{2+}$ resulted in straight line graphs with zero intercepts when k_{obs} (average of four) was plotted versus the nucleophile concentration. Since the back substitution due to the solvent is absent, the linear dependence of k_{obs} on the concentration of the nucleophile can be expressed as:

$$k_{obs} = k_2[\text{nucleophile}] \qquad (4.16)$$

The graphs obtained for the two complexes are shown in **Figure 4.19 (a), (b)** and **(c)** for $[Ru(terpy)(bipy)(OH_2)]^{2+}$ and **Figure 4.20 (a), (b)** and **(c)** for $[Ru(terpy)(tmen)(OH_2)]^{2+}$. A non-zero intercept was obtained for the plot of k_{obs} versus [DMTU], [TU], and $[CH_3CN]$ for $[Ru(terpy)(tmen)(OH_2)]^{2+}$. Therefore in this case the backward reaction plays a role.

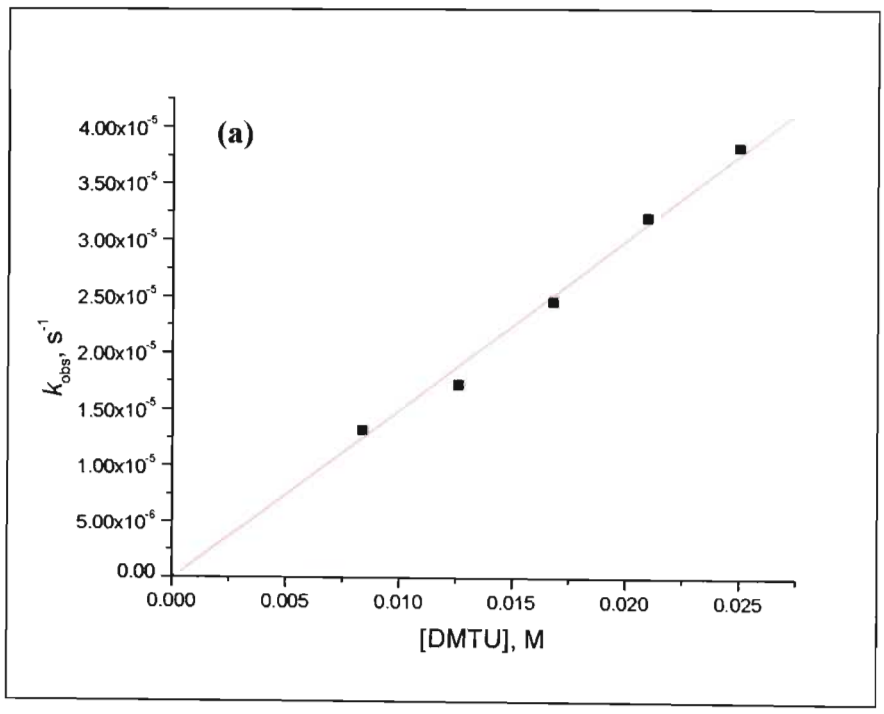

Figure 4.19 (a) *Plots of k_{obs} dependence on the concentration of DMTU $[Ru(terpy)(bipy)(OH_2)]^{2+}$ (1.683 x 10^{-4} M), pH = 4 ($HClO_4$), μ = 0.1 M ($NaClO_4$), T = 25 °C.*

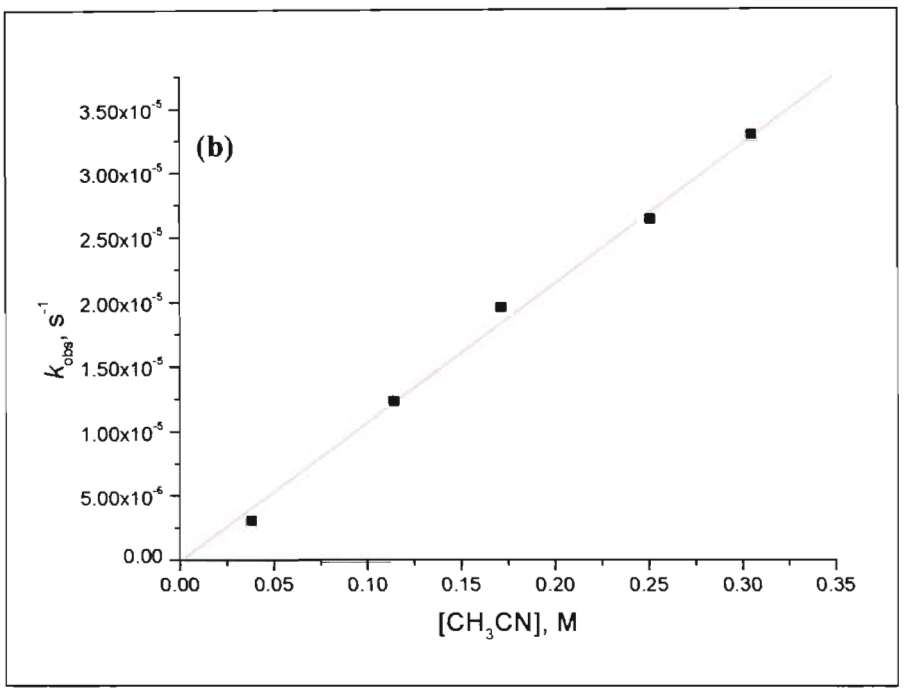

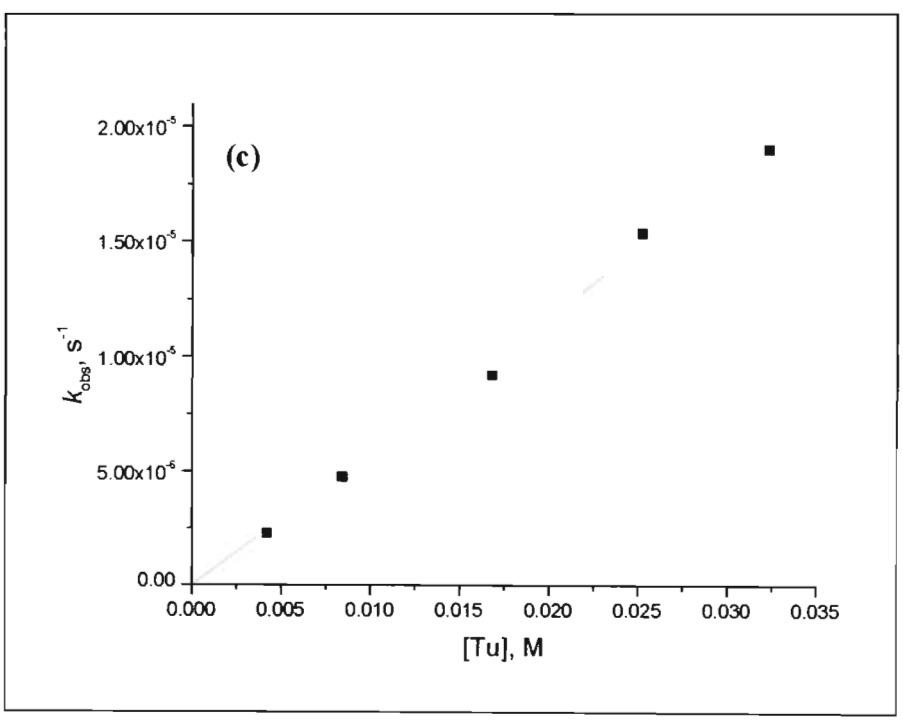

Figure 4.19 *Plots of k_{obs} dependence on the concentration of* **(b)** *CH_3CN and* **(c)** *TU $[Ru(terpy)(bipy)(OH_2)]^{2+}$ (1.683 x 10^{-4} M), pH = 4 ($HClO_4$), μ = 0.1 M ($NaClO_4$), T = 25 °C.*

involved the replacement of the ammonia ligand by isonicotinamide (isn) resulting in rate constants of lower values ($3.5 \times 10^{-3} - 5.0 \times 10^{-3}$).[44, 43] The other ligands used include: CO, N_2, Imn (Imidazole), py, OH, CN^-, SO_3^{2-}, imc (C-bound imidazole) whose specific rate constant ranged from 3×10^{-6} M^{-1} s^{-1} for CO to 60 M^{-1} s^{-1} for imc, when isn is used as the incoming ligand.[44]

Recently reactions involving the substitution of the water molecule from Ru(II) complexes has centred around bidentate and tridentate ligands.[45, 46] Studies involving polypyridyl complexes of ruthenium(II) have not resulted in a big difference in terms of rate constants, when compared to those of ammonia ligand. The largest increase in rate constant reported to date that involves the effect of the spectator ligand on the ruthenium(II) centre is by Huynh *et al.*[47] They observed a dramatic 1.9×10^7 rate increase in the substitution of water molecule by changing the spectator ligand (L_3) from terpy [$(5.9 \pm 0.1) \times 10^{-6}$ $M^{-1}s^{-1}$] to tris(pyrid-2-yl)methoxymethane (tppm) [$(1.1 \pm 0.) \times 10^2$ $M^{-1}s^{-1}$] in [$Ru(H_2O)(dpp)L_3$] complex. In another study they managed to increase the rate of substitution of water by 9.4×10^5 fold when DPMet {di(1-pyrazolyl)methane} (7.0×10^{-5} $M^{-1}s^{-1}$) was replaced with DPPro {(2,2-di(1-dipyrazolyl)propane} (66 $M^{-1}s^{-1}$) in the case of [$Ru(H_2O)(tpmm)L_2$] complex.[41] These "heteroscorpionate" ligands are shown under **Table 4.4.**

In this work the effect of the bidentate ligand on the reactivity of [$Ru(terpy)(NN)(OH_2)](ClO_4)_2$ was investigated by changing NN from bipy to tmen. The second order rate constants, (k_2), obtained are tabulated in **Table 4.4**. The k_2 value for $[Ru(terpy)(tmen)(OH_2)]^{2+}$ is 1.8 times bigger than for that of $[Ru(terpy)(bipy)(OH_2)]^{2+}$ when TU is used as the incoming nucleophile. When DMTU is used the factor becomes 1.5. In the case of CH_3CN there is no noticeable difference. This lack of sensitivity to the nature of the incoming ligand is an indication that there is a considerable degree of bond breaking in the transition state, suggesting that the substitution reaction must be going through a dissociative mechanism as reported in other similar systems.[41, 47] The slight reactivity difference between these two complexes can be explained in terms of structural differences. Looking at **Figure 4.21 (b)** tmen consists of methyl groups bonded to the

nitrogen. One would have expected, as in the case of the heteroscorpionate ligands (**Figure 4.21 (c)**), a hydrogen-oxygen interaction between the tmen methyl group and the oxygen of the leaving aqua group. Looking at the two structures, the interaction would be expected to be more effective in the case of tmen than bipy system because of the rigidity of the bipy ligand. The small difference in reactivity points to the fact that the expected interaction is either weak or absent.

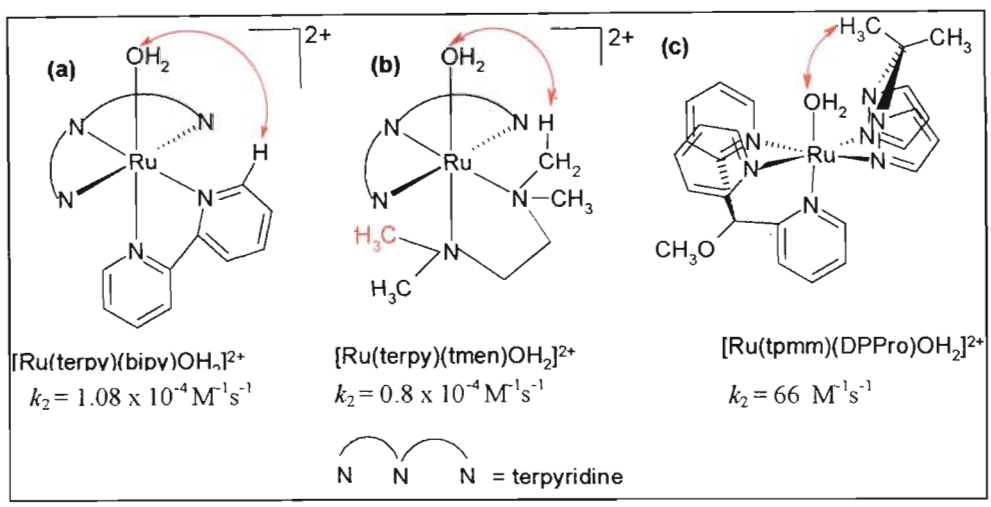

Figure 4.21 *Possible hydrogen-oxygen interaction in* **(a)** *$[Ru(terpy)(bipy)(OH_2)]^{2+}$*, **(b)** *$[Ru(terpy)(tmen)(OH_2)]^{2+}$ and* **(c)** *$[Ru(tpmm)(DPPro)(OH_2)]^{2+}$.*

The other possible reason for the small difference in reactivity is the presence of π-back bonding. In the bipy system, both the terpy as well as the bipy withdraw electron density from the metal centre, leaving ruthenium(II) more electrophilic. Given the dissociative nature of the reaction the metal-oxygen bond will be stronger in the $[Ru(terpy)(bipy)(OH_2)]^{2+}$ than in the $[Ru(terpy)(tmen)(OH_2)]^{2+}$. This is supported by the pK_a values of the two complexes. This same reasoning can be used to explain why the k_2 values involving polypyridyl complexes are in general smaller by a factor of 100 or more when compared to $[Ru(NH_3)_4L(OH_2)]$ complexes. The big difference of 1.9×10^7 for k_2 reported by Huynh *et al* involved replacement of terpy by tpmm. This did not only remove the back donation effect, but also increased the steric effect which is thought to be responsible for the high reactivity.[47]

One question that needs to be answered is why the k_2 values involving the terpy system as shown in **Table 4.4** are very similar in magnitude with the exception of $[Ru(terpy)(Me_2phen)(OH_2)]^{2+}$. The driving force behind the Me_2phen ligand is a steric effect introduced by the two methyl groups. The remaining complexes can be explained in terms of the terpy ligand. Taking the complexes investigated in this study it can be concluded that the withdrawing power of the terpy ligand through π-back donation is so strong that attaching any other ligands makes very little difference.

When comparing the reactivity of the incoming nucleophiles namely, DMTU, TU and CH_3CN towards the ruthenium centre, it is clear that the sulfur donors are better nucleophiles towards the Ru(II) centre than the nitrogen donor. The order of the reactivity of the nucleophiles towards the ruthenium center is: DMTU > TU > CH_3CN. The high reactivity of the DMTU can be explained to be due to the inductive effect of the methyl groups making it more nucleophilic. Since the reactivities of TU and DMTU, are different for the two complexes, this can be taken as an indication of the electrophilicity of the metal center, an additional proof that the π-back donation is playing a role in these substitution studies.

In conclusion, the study has managed to synthesize, characterize and compare the reactivity of $[Ru(terpy)(bipy)(OH_2)]^{2+}$ and $[Ru(terpy)(tmen)(OH_2)]^{2+}$. The slight difference in reactivity between the two complexes is due to the difference in π-back bonding effect. The investigation has also shown that sulfur donor ligands have a high affinity for ruthenium(II) metal and are better nucleophiles in this case compared to the nitrogen donors.

REFERENCES

1) K. J. Takeuchi, M.S. Thompson, D. W. Pipes and T. J. Meyer, *Inorg. Chem.*, **1984**, 23, 1845.

2) C. Ho and C. Che, *J. Chem. Soc., Dalton Trans.*, **1990**, 967.

3) T. Shi, J. Berglund, and L. I. Elding, *Inorg. Chem.*, **1996**, *35*, 3498.

4) D. L. Rabenstein, *J. Am. Chem. Soc.*, **1973**, *95*, 2797.

5) Applied Photophysics SX.18MV, Sequential Stopped-Flow ASVD Spectrofluorimeter, Software Manual. Applied Photophysics Ltd., Kingston Road, Leatherhead, UK.; Kinetic traces from the repetitive scans were analysed using Origin50 version 5.0 a data analysis and technical graphics software.

6) M. L. Tobe, Comprehensive Coordination Chemistry, Pergamon Press, **1987**, *1*, p. 313.

7) Ž. D. Bugarčić, G. Liehr and R. van Eldik, *J. Chem. Soc., Dalton Trans.*, **2002**, 951.

8) D. Jaganyi, A. Hofmann and R. van Eldik, *Angew. Chem., Int. Ed.*, **2001**, *40*, 1680.

9) M. Casumano, G. Guglielmo and V. Ricevuto, *Inorg. Chim. Acta*, 27, 197 (1978).

10) B. Pitteri, G. Marangoni, F. V. Viseutim, L. Cattalini and T. Bobbo, *Polyhedron*, **1998**, *17*, 475.

11) B. V. Petrović, M. I. Djuran and Ž. D. Bugarčić, *Met.-Based Drugs*, **1999**, *6*, 355.

12) G. Annibale, M. Brandolisio, Ž. D. Bugarčić and L. Cattalini, *Transition Met. Chem.*, **1998**, *23*, 715.

13) Ž. D. Burgarčič and B. V. Djordjević, *Monatsh. Chem.*, **1998**, 129, 1267.

14) R. G. Wilkins, *Kinetics and Mechanism of Reactions of Transition Metal Complexes*, New York, **1991**.

15) R.G. Wilkins, *Kinetics and Mechanism of Reactions of Transition Metal Complexes*, 2nd Edition, New York, **1991**, 240.

16) R.G. Wilkins, *Kinetics and Mechanism of Reactions of Transition Metal Complexes*, 2nd Edition New York, **1991**, 232.

17) F. Basolo and R. G. Pearson, *Mechanisms of Inorganic Reactions, A study of Metal Complexes in Solution*, 2nd, John Wiley and Sons, Inc., **1967**, 351, 406, 415.

18) F. A. Cotton, G. Wilkinson, *Advanced Inorganic Chemistry*, 5th Edition, John Wiley & Sons, New York, **1988,** 1297.

19) F. Basolo, J. Chatt, H. B. Gray, R. G. Pearson and B. L. Show, *J. Chem. Soc.*, **1961**, 2207.

20) D. Minniti, G. Alibrandi, M. L. Tobe and R. Romeo, *Inorg. Chem.*, **1987**, *26*, 3956.

21) G. Alibrandi, D. Minniti, L. M. Scolaro and R. Romeo, *J. Am. Chem. Soc.*, **1988**, *27*, 318.

22) U. Frey, L. Helm, A. E. Merbach and R. Romeo, *J. Am. Chem. Soc.*, **1989**, *111*, 8161.

23) M. Schmülling, A. D. Ryabov and R. van Eldik, *J. Chem. Soc., Dalton Trans.*, **1994**, 1257.

24) U. Frey, L. Helm, S. Elmorth, B. Moullet, L. I. Elding and A. E. Merbach, *Inorg. Chem.*, **1991**, *30*, 5033.

25) E. J. Breet and R. van Eldik, *Inorg. Chem.*, **1984**, *23*, 1865.

26) E. J. Breet, R. van Eldik, and H. Kelm, *Polyhedron.*, **1983**, *2*, 1181.

27) J. Berger, M. Kotowski, R. van Eldik, U. Frey, L. Helm and A. E. Merbach, *Inorg. Chem.*, **1989**, *28*, 3759.

28) A. Hofmann, D. Jaganyi, O. Q. Munro, G. Liehr, and R. van Eldik, Inorg. Chem., **2003**, 42, 1688.

29) B. Pitteri, G. Marangoni, L. Cattalini and T. Bobbo, *J. Chem. Soc., Dalton Trans.*, **1995**, 3853.

30) R. G. Pearson, *J. Am. Chem. Soc.*, **1963**, *85*, 3533.

31) L. Cattalini, G. Chessa, G. Marangoni, B. Pitteri, and E. Celon., *Inorg. Chem.*, **1989**, *28*, 1944.

32) U. Belluco, L. Cattalini, F. Basolo, R. G. Pearson, and A. Turco, *J. Am. Chem. Soc.*, **1965**, 241.

33) M. L. Tobe and J. Burgess, *Inorganic Reaction Mechanisms*, Addison Wesley Longman Limited, **1999,** 84.

34) B. Pitteri, L. Canovesa, G. Chessa, G. Marangoni and P. Uguagliati, *Polyhedron*, **1992**, *11*, 2363.

35) U. Belluco, L. Cattalini, F. Basolo, R.G. Pearson, A. Turco, *Ibid*, **1965**, *87*, 241.

36) R. G. Pearson, H. Sobel, J. Songstad, *J. Am. Chem. Soc.*, **1968**, *90*, 319.

37) A. Gerli, J. Reedjik, M. T. Lakin and A. L. Spek, *Inorg. Chem.*, **1995**, *34*, 1836.

38) N.Groveer, N. Gupta, P. Singh, and H. H. Thorp, *Inorg. Chem.*, **1992**, *31*, 2041.

39) N. Gupta, N. Grover, G. A. Neyahart, P. Singh, H. H. Thorp, *Inorg. Chem.*, **1993**, *32*, 310.

40) C. A. Bessel, J. A. Margarucci, J. H. Acquaye, R. S. Rubino, J. Crandall, A. J. Jircitano, and K. Takeuchi, *Inorg. Chem.*, **1993**, *32*, 5779.

41) M. H. V. Huynh, J. M. Lasker, M. Wetzler, B. Mort, L. F. Szcepura, L. M. Witham, J. M. Cintron, A. C. Marschilok, L. J. Ackerman, R. K. Castellano, D. L. Jameson, M. R. Churchill, A. J. Jircitanoand T. J. Takeuchi, *J. Am. Chem. Soc.*, **2001**, *123*, 8784.

42) I. Rapport, L. Helm, A. E. Merbach, P. Bernhard and A. Ludi, *Inorg. Chem.*, **1998**, *27*, 873.

43) L. Dozsa, J. E. Sutton and H. Taube, *Inorg. Chem.*, **1982**, *21*, 3997.

44) S. S. Isied and H. Taube, *Inorg. Chem.*, **1976**, *15*, 3071.

45) N. E. Davies, T. L. Mullins, *Aust. J. Chem.*, **1968**, *21*, 915.

46) L. R. Allen, P. P. Craft, B. Durham, and J. Walsh, *Inorg. Chem.*, **1987**, *26*, 53.

47) M. H. V. Huynh, J. Smyth, M. Welzler, B. Mort, P. K. Gong, L. M. Witham, D. L. Jameson, D. K. Geiger, J. M. Lasker, M. Charepoo, M. Gornikiewicz, J. M. Cintron, G. Imahori, R. R. Sanchez, A. C. Marschilok, L. M. Krajkowski, D. G. Churchill, M. R. Churchill, and T. J. Takeuchi, *Angew. Chem.*, **2001**, *113 (23)*, 4601.

APPENDIX A

NMR SPECTRA

APPENDIX A

NMR SPECTRA FOR SOME OF THE INVESTIGATED COMPLEXES

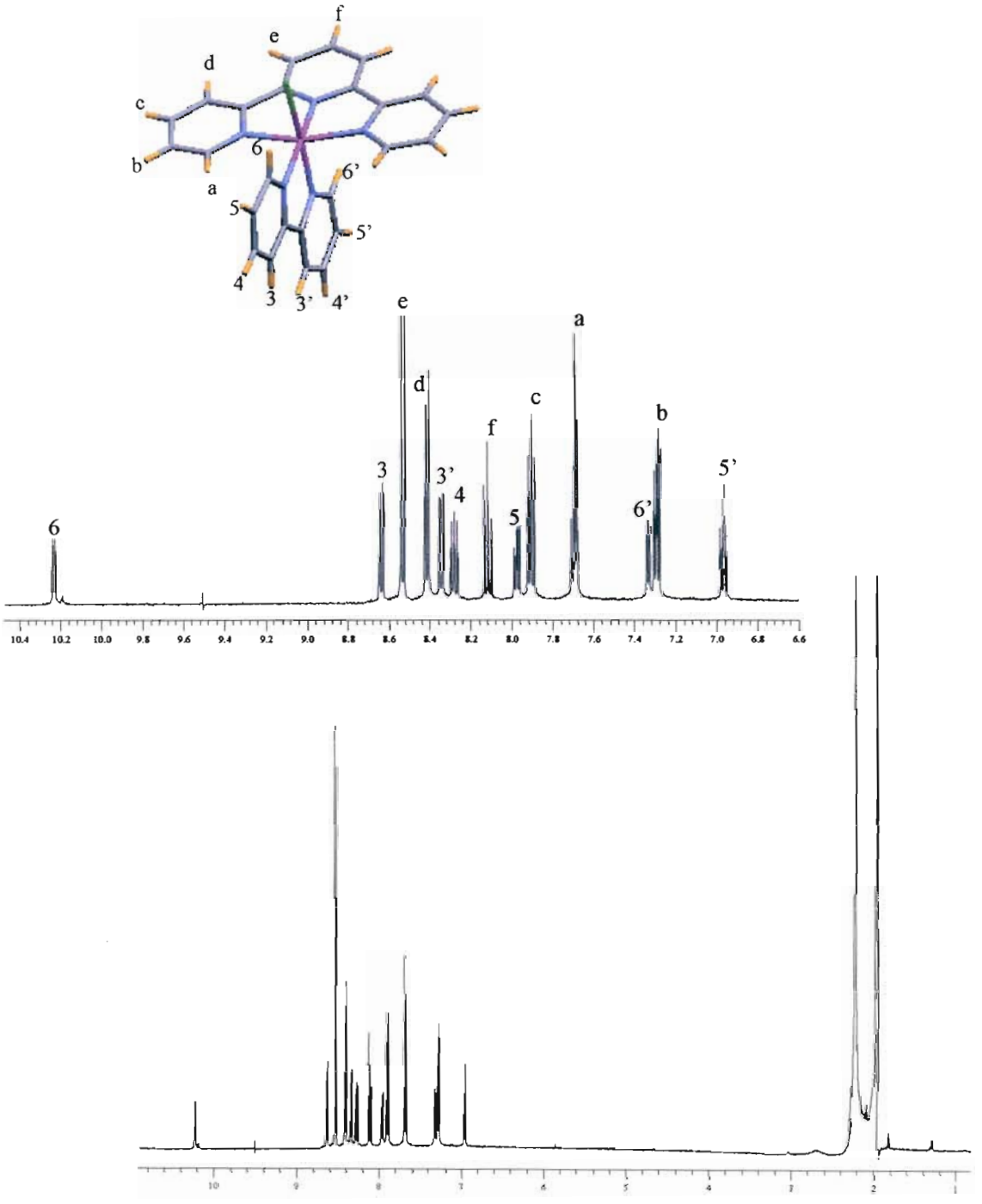

Figure A.1 *^{1}H-NMR spectrum of [Ru(terpy)(bipy)Cl]Cl in CD_3CN.*

^{1}H-NMR(CD_3CN[a], 500 MHz[b]): δ[c] 10.239 (d[d], $J_{6\text{-}5}$ = 5.541Hz, H6), 8.627 (d, $J_{3\text{-}4}$= 8.00 Hz, H3), 8.523 (d, $J_{e\text{-}f}$ = 8.00 Hz, He), 8.419 (d, $J_{d\text{-}c}$ = 8.00 Hz), 8.353 (d, $J_{3'\text{-}4'}$ = 8.00 Hz, H3'), 8.280 (m[e], $J_{4\text{-}5}$ = 8.00 Hz, H4), 8.118 (t[f], $J_{f\text{-}e}$= 8.00 Hz, Hf), 7.969 (m, $J_{5\text{-}4}$ = 8.312 Hz, H5), 7.705 (ddd[g], $J_{c\text{-}d}$ = 8.00 Hz, $J_{c\text{-}b}$ = 8.00Hz, Hc), 7.680 (d, $J_{a\text{-}b}$ = 5.541, Ha), 7.327 (d, $J_{6'\text{-}5'}$ = 4.926, H6'), 6.945 (m, $J_{b\text{-}a}$ = 5.541, $J_{b\text{-}c}$ = 8.00Hz, Hb).

The proton NMR of [Ru(terpy)(bipy)Cl]Cl consists of 14 resonances, 8 from the two nonequivalent bipyridine rings and the other 6 resonances are from the terpyridine. The splitting of the terpyridine is the same due to the fact that the terpyridine protons are all on the same plane.

From the spectrum, there is a doublet, which integrates for one proton at around 10.20 ppm. On the basis of Correlation Spectroscopy (COSY), this proton couples with the proton, which gave a triplet at around 8.0 ppm. The proton that gave a doublet at 10.20 ppm is assigned to proton 6 of the bipyridine, which is close to the chloride. As the result of the large diamagnetic anisotropy of the chloride the proton resonance downfield compared to the other bipyridine as well as the terpyridine protons.

The signal at 7.3 ppm for [Ru(terpy)(bipy)Cl]Cl is attributed to 6' of the bipyridine ring *trans* to the chloride ligands. The large upfield shift of this proton with respect to the other protons of the bipyridine is ascribed to the diamagnetic anisotropy of the adjacent terpyridine rings. The assignment of the other terpyridine and bipyridine signals follows from the COSY spectrum.

---

[a] CD_3CN (deuterated acetonitrile)
[b] MHz (mega Hertz)
[c] δ (chemical Shift in ppm)
[d] d (doublet)
[e] m (multiplet)
[f] t (triplet)
[g] ddd (doublet of a doublet of a doublet)

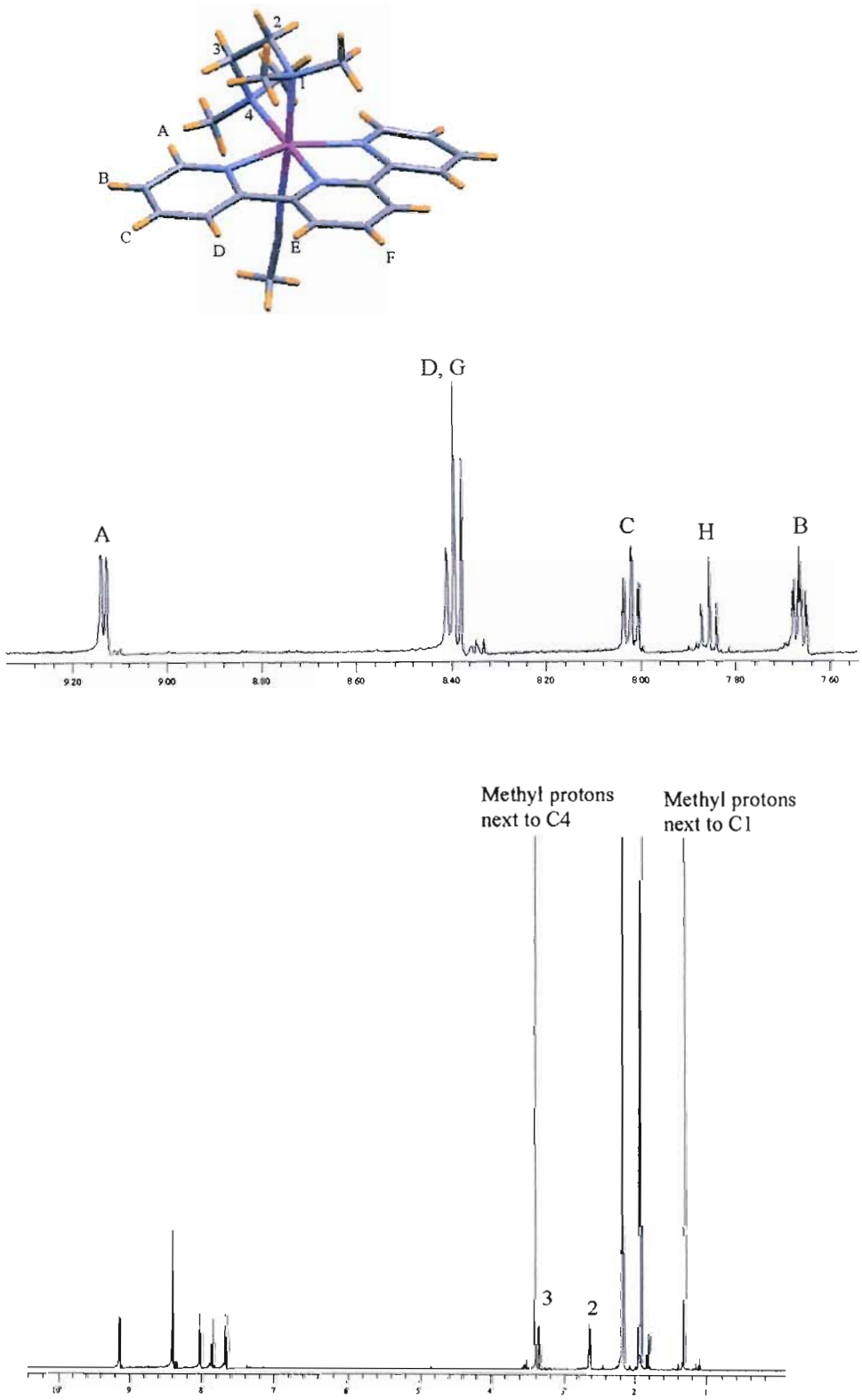

Figure A.2 *^{1}H-NMR spectrum of [Ru(terpy)(tmen)Cl]ClO_4 in CD_3CN.*

^{1}H-NMR(CD_3CN[a], 500 MHz[b]): δ[c] 9.128 (d[d], 2H, H_A), 8.395 (d, 4H, H_{G+D}), 8.019 (m[e], 2H, H_C), 7.856 (m, 1H, H_H), 7.667 (m, 2H, H_B), 3.416 (s[f], 6H, methyl protons next to C4), 3.280 (m, 2H, H_3), 2.620 (m, 2H, H_2), 1.329 (s, 6H, methyl protons next to C1).

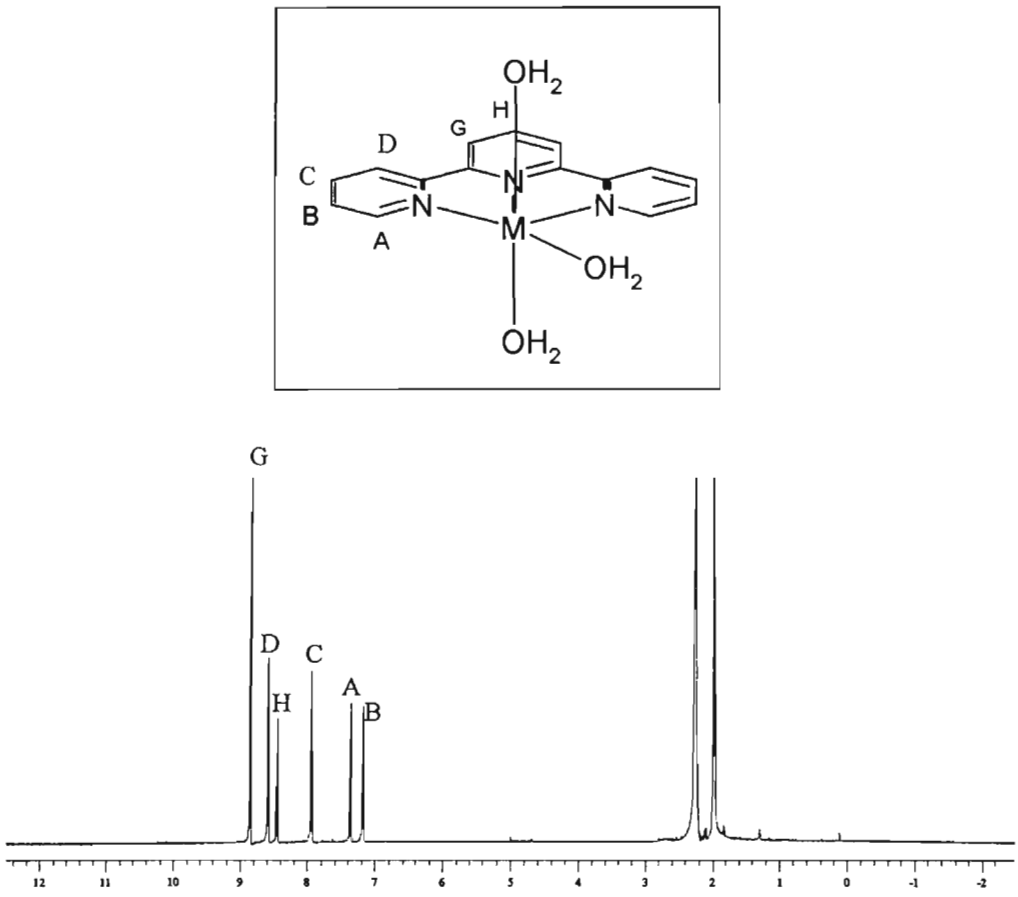

Figure A.3 *^{1}H-NMR spectrum of $[Ru(terpy)(OH_2)_3]^{2+}$ in CD_3CN.*

^{1}H-NMR(CD_3CN, 500 MHz): δ 8.826 (d, 2H, H_G), 8.572 (d, 2H, H_D), 8.442 (m, 1H, H_H), 7.933 (m, 2H, H_C), 7.355 (d, 2H, H_A), 7.177 (m, 2H, H_B).

[a] CD_3CN (deuterated acetonitrile)
[b] MHz (Mega Hertz)
[c] δ (chemical shift in ppm)
[d] d (doublet)
[e] m (multiplet)
[f] s (singlet)

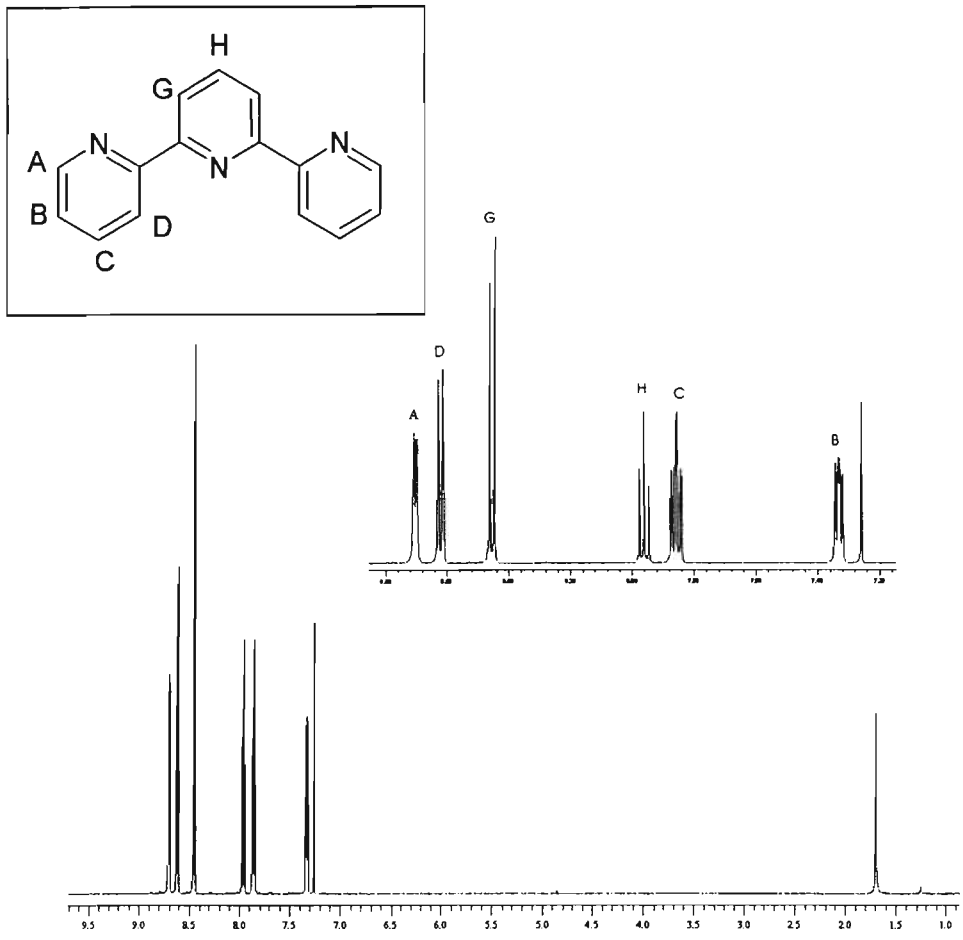

Figure A.4 *^{1}H-NMR spectrum of uncoordinated terpyridine (terpy) ligand in $CDCl_3$.*

^{1}H-NMR($CDCl_3$[a], 500 MHz[b]): δ 8.699 (d[c], 2H, H_A), 8.613 (d, 2H, H_D), 8.461 (d, 2H, H_G), 7.960 (m[d], 1H, H_H), 7.856 (m, 2H, H_C), 7.329 (m, 2H, H_B)

[a] $CDCl_3$ (deuterated chloroform)
[b] MHz (Mega Hertz)
[c] d (doublet)
[d] m (multiplet)

APPENDIX B

INFRARED SPECTRA

APPENDIX B

INFRARED SPECTRA FOR THE INVESTIGATED COMPLEXES

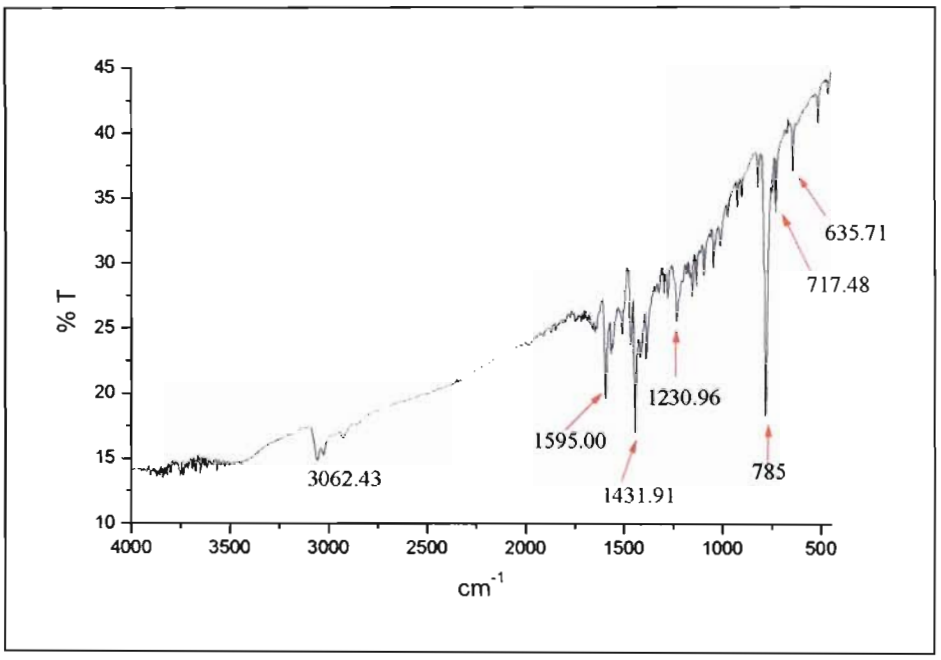

Figure B.1 *IR spectrum of [Ru(terpy)Cl_3].*

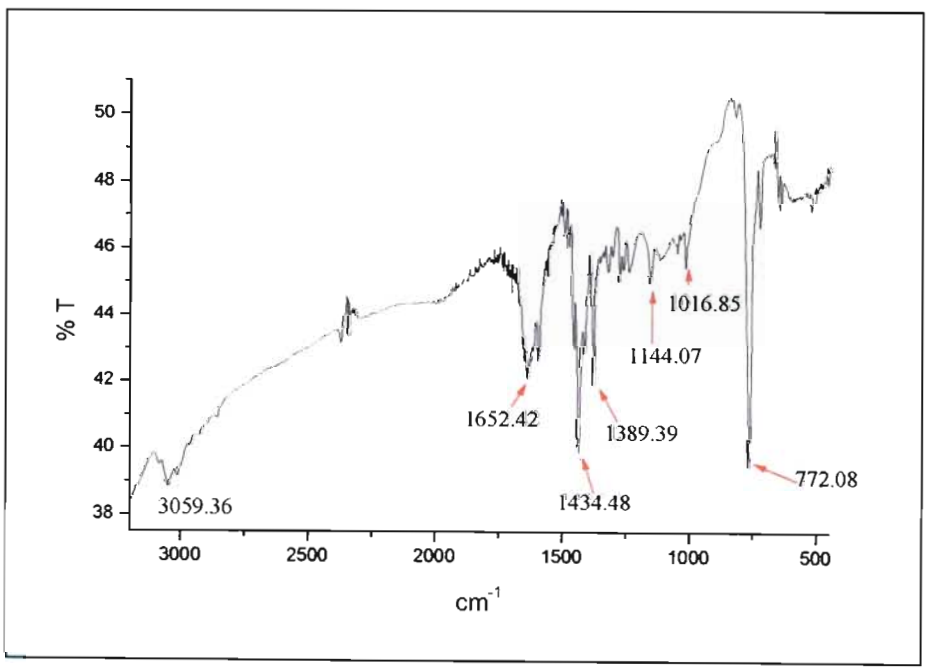

Figure B.2 *IR spectrum of [Ru(terpy)(bipy)Cl]Cl.*

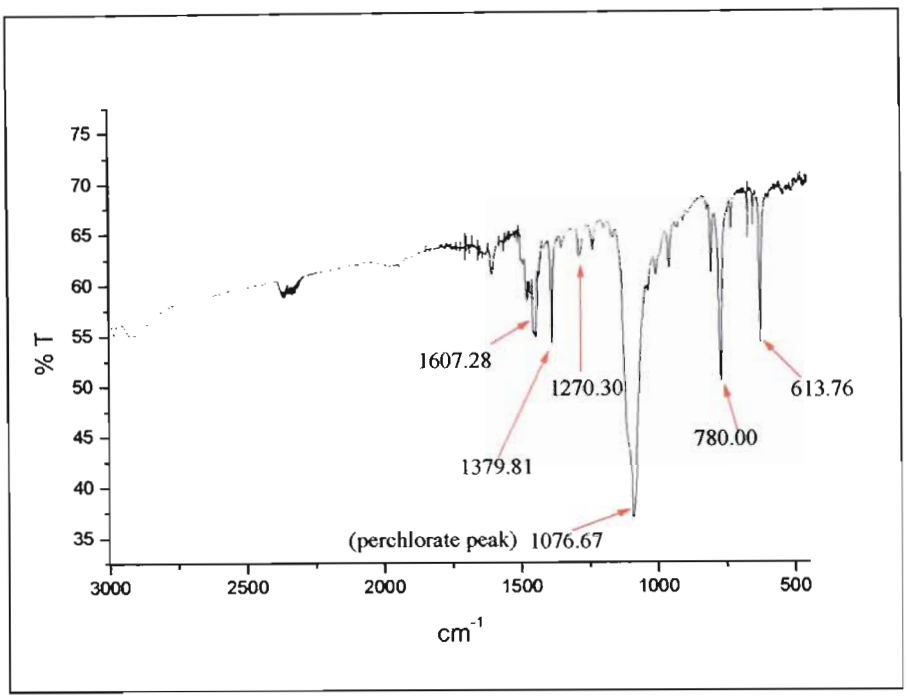

Figure B.3 *IR spectrum of [Ru(terpy)(tmen)Cl]ClO_4.*

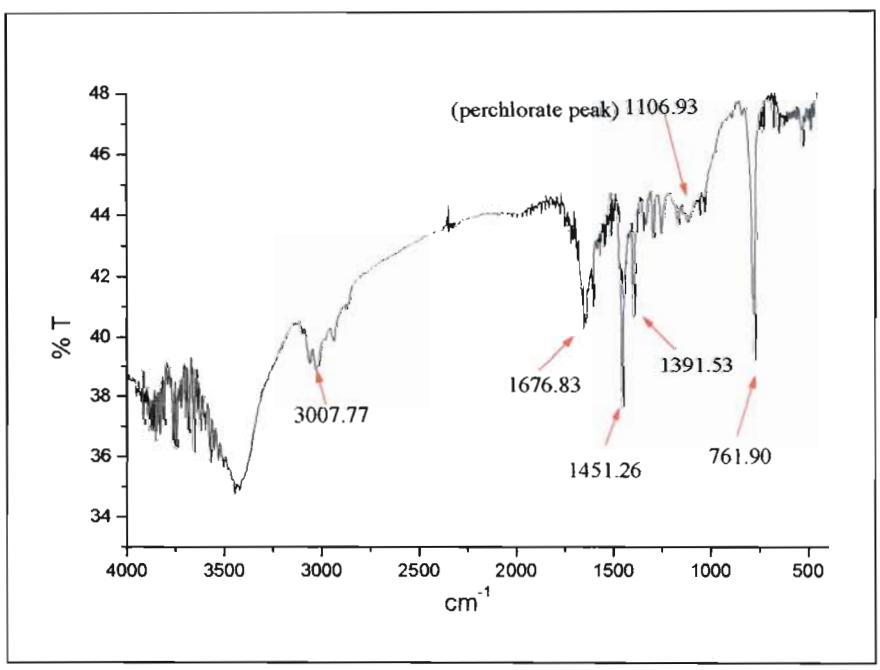

Figure B.4 *IR spectrum of crude [Ru(terpy)$(OH_2)_3$]$(ClO_4)_2$.*

APPENDIX C

X-RAY DATA

APPENDIX C

BOND ANGLES, DISTANCES FOR THE X-RAY STRUCTURES

Table C.1 *Atomic coordinates (x 10^4) and equivalent isotropic displacement parameters ($Å^2$ x 10^3) for [Ru(terpy)(bipy)Cl]ClO_4. U(eq) is defined as one third of the trace of the orthogonalized U^{ij} tensor.*

	x	y	z	U(eq)
Ru(1)	1459(1)	7580(1)	8065(1)	36(1)
N(1)	–590(4)	7544(3)	7140(3)	44(1)
N(1')	1679(4)	6849(3)	6614(3)	41(1)
N(2)	2851(5)	9159(3)	7972(3)	45(1)
N(3)	3490(4)	7647(3)	8808(3)	40(1)
N(4)	856(5)	6034(3)	8449(3)	41(1)
C(2')	556(6)	6790(4)	5804(4)	45(1)
C(3')	642(7)	6355(5)	4783(4)	60(1)
C(4')	1871(8)	5978(6)	4589(4)	67(2)
C(5')	2968(7)	5995(5)	5418(5)	61(1)
C(6')	2832(6)	6431(4)	6405(4)	50(1)
C(2)	–695(6)	7189(4)	6103(4)	45(1)
C(3)	–1929(7)	7229(5)	5401(5)	61(1)
C(4)	–3056(7)	7640(6)	5757(5)	71(2)
C(5)	–2933(7)	7996(6)	6791(5)	69(2)
C(6)	–1703(6)	7927(5)	7482(4)	57(1)
C(22)	4378(5)	9443(4)	8444(3)	45(1)
C(23)	5468(7)	10463(5)	8434(4)	59(1)
C(24)	5024(8)	11195(5)	7973(5)	71(2)
C(25)	3468(9)	10915(6)	7491(6)	76(2)
C(26)	2431(7)	9896(5)	7518(5)	61(1)
C(32)	4750(5)	8584(4)	8930(4)	44(1)
C(33)	6199(6)	8650(5)	9450(4)	55(1)
C(34)	6343(6)	7770(6)	9845(5)	64(2)
C(35)	5038(7)	6802(5)	9723(4)	60(1)
C(36)	3601(6)	6766(4)	9197(4)	45(1)
C(42)	2086(6)	5837(4)	8976(4)	45(1)

table continued..

C(43)	1906(7)	4829(5)	9275(4)	58(1)
C(44)	427(8)	4003(5)	9028(5)	66(2)
C(45)	–803(8)	4215(5)	8504(5)	63(2)
C(46)	–570(6)	5234(4)	8242(4)	49(1)
Cl(1)	844(1)	8402(1)	9675(1)	50(1)
Cl(2)	–4851(2)	5759(1)	2686(1)	57(1)
O(1)	–5459(8)	5565(7)	1624(4)	124(2)
O(2)	–3229(7)	6011(7)	2851(5)	133(3)
O(3)	–5195(9)	6692(5)	3236(5)	110(2)
O(4)	–5552(9)	4831(6)	3088(7)	132(3)

Table C.2 *Bond lengths [Å] and Bond angles [°] for [Ru(terpy)(bipy)Cl]ClO_4.*

Ru(1)–N(3)	1.956(4)
Ru(1)–N(1')	2.044(4)
Ru(1)–N(4)	2.069(4)
Ru(1)–N(2)	2.075(4)
Ru(1)–N(1)	2.086(4)
Ru(1)–Cl(1)	2.4149(17)
N(1)–C(6)	1.345(7)
N(1)–C(2)	1.352(6)
N(1')–C(6')	1.350(6)
N(1')–C(2')	1.364(6)
N(2)–C(26)	1.334(7)
N(2)–C(22)	1.360(6)
N(3)–C(36)	1.353(6)
N(3)–C(32)	1.355(6)
N(4)–C(46)	1.349(6)
N(4)–C(42)	1.360(6)
C(2')–C(3')	1.391(7)
C(2')–C(2)	1.452(7)
C(3')–C(4')	1.380(9)
C(4')–C(5')	1.385(9)
C(5')–C(6')	1.365(8)

table continued

C(2)–C(3)	1.389(7)
C(3)–C(4)	1.381(9)
C(4)–C(5)	1.347(9)
C(5)–C(6)	1.393(8)
C(22)–C(23)	1.387(7)
C(22)–C(32)	1.477(7)
C(23)–C(24)	1.342(9)
C(24)–C(25)	1.389(10)
C(25)–C(26)	1.372(8)
C(32)–C(33)	1.382(7)
C(33)–C(34)	1.364(9)
C(34)–C(35)	1.402(9)
C(35)–C(36)	1.388(7)
C(36)–C(42)	1.478(7)
C(42)–C(43)	1.391(7)
C(43)–C(44)	1.394(9)
C(44)–C(45)	1.370(9)
C(45)–C(46)	1.376(8)
Cl(2)–O(2)	1.395(6)
Cl(2)–O(1)	1.399(5)
Cl(2)–O(4)	1.410(6)
Cl(2)–O(3)	1.415(6)

N(3)–Ru(1)–N(1')	96.77(16)
N(3)–Ru(1)–N(4)	79.39(16)
N(1')–Ru(1)–N(4)	91.25(15)
N(3)–Ru(1)–N(2)	79.50(17)
N(1')–Ru(1)–N(2)	91.36(16)
N(4)–Ru(1)–N(2)	158.89(17)
N(3)–Ru(1)–N(1)	173.87(15)
N(1')–Ru(1)–N(1)	78.27(16)
N(4)–Ru(1)–N(1)	104.15(16)
N(2)–Ru(1)–N(1)	96.89(16)
N(3)–Ru(1)–Cl(1)	90.72(12)

table continued...

N(1')–Ru(1)–Cl(1)	172.43(11)
N(4)–Ru(1)–Cl(1)	89.04(11)
N(2)–Ru(1)–Cl(1)	91.08(12)
N(1)–Ru(1)–Cl(1)	94.32(12)
C(6)–N(1)–C(2)	119.1(4)
C(6)–N(1)–Ru(1)	125.8(3)
C(2)–N(1)–Ru(1)	114.9(3)
C(6')–N(1')–C(2')	118.6(4)
C(6')–N(1')–Ru(1)	125.3(3)
C(2')–N(1')–Ru(1)	116.1(3)
C(26)–N(2)–C(22)	118.1(4)
C(26)–N(2)–Ru(1)	128.3(4)
C(22)–N(2)–Ru(1)	113.6(3)
C(36)–N(3)–C(32)	121.6(4)
C(36)–N(3)–Ru(1)	119.4(3)
C(32)–N(3)–Ru(1)	119.0(3)
C(46)–N(4)–C(42)	118.3(4)
C(46)–N(4)–Ru(1)	128.0(3)
C(42)–N(4)–Ru(1)	113.7(3)
N(1')–C(2')–C(3')	120.5(5)
N(1')–C(2')–C(2)	114.9(4)
C(3')–C(2')–C(2)	124.6(5)
C(4')–C(3')–C(2')	119.7(5)
C(3')–C(4')–C(5')	119.4(5)
C(6')–C(5')–C(4')	118.6(5)
N(1')–C(6')–C(5')	123.1(5)
N(1)–C(2)–C(3)	120.4(5)
N(1)–C(2)–C(2')	115.4(4)
C(3)–C(2)–C(2')	124.2(5)
C(4)–C(3)–C(2)	120.2(5)
C(5)–C(4)–C(3)	118.8(5)
C(4)–C(5)–C(6)	120.0(6)
N(1)–C(6)–C(5)	121.4(5)
N(2)–C(22)–C(23)	120.7(5)
N(2)–C(22)–C(32)	114.9(4)
C(23)–C(22)–C(32)	124.4(5)

table continued..

C(24)–C(23)–C(22)	120.3(6)
C(23)–C(24)–C(25)	119.5(5)
C(26)–C(25)–C(24)	118.2(6)
N(2)–C(26)–C(25)	123.1(6)
N(3)–C(32)–C(33)	120.1(5)
N(3)–C(32)–C(22)	113.0(4)
C(33)–C(32)–C(22)	126.9(5)
C(34)–C(33)–C(32)	119.4(5)
C(33)–C(34)–C(35)	120.6(5)
C(36)–C(35)–C(34)	118.4(5)
N(3)–C(36)–C(35)	119.9(5)
N(3)–C(36)–C(42)	112.5(4)
C(35)–C(36)–C(42)	127.6(5)
N(4)–C(42)–C(43)	121.6(5)
N(4)–C(42)–C(36)	115.0(4)
C(43)–C(42)–C(36)	123.3(5)
C(42)–C(43)–C(44)	119.0(5)
C(45)–C(44)–C(43)	118.8(5)
C(44)–C(45)–C(46)	120.0(5)
N(4)–C(46)–C(45)	122.3(5)
O(2)–Cl(2)–O(1)	109.9(4)
O(2)–Cl(2)–O(4)	110.6(5)
O(1)–Cl(2)–O(4)	111.9(5)
O(2)–Cl(2)–O(3)	109.0(5)
O(1)–Cl(2)–O(3)	108.6(4)
O(4)–Cl(2)–O(3)	106.7(4)

Symmetry transformations used to generate equivalent atoms:

Table C.3 *Anisotropic displacement parameters ($Å^2$ x 10^3) for [Ru(terpy)(bipy)Cl]ClO_4. The anisotropic displacement factor exponent takes the form: $-2\pi^2[h^2a^{*2}U^{11} + ... + 2\,h\,k\,a^*\,b^*\,U^{12}]$.*

	U^{11}	U^{22}	U^{33}	U^{23}	U^{13}	U^{12}
Ru(1)	29(1)	39(1)	33(1)	6(1)	1(1)	4(1)
N(1)	31(2)	47(2)	43(2)	9(2)	0(2)	4(2)
N(1')	35(2)	42(2)	39(2)	9(2)	4(2)	4(2)
N(2)	43(2)	43(2)	41(2)	8(2)	4(2)	4(2)
N(3)	35(2)	44(2)	33(2)	4(2)	3(2)	8(2)
N(4)	40(2)	43(2)	31(2)	5(2)	3(2)	6(2)
C(2')	44(2)	45(2)	37(2)	10(2)	1(2)	3(2)
C(3')	63(3)	67(3)	39(3)	8(2)	1(2)	14(3)
C(4')	74(4)	75(4)	42(3)	1(3)	15(3)	19(3)
C(5')	56(3)	64(3)	60(3)	3(3)	16(3)	20(3)
C(6')	43(3)	54(3)	48(3)	8(2)	8(2)	12(2)
C(2)	40(2)	45(2)	42(2)	10(2)	–1(2)	4(2)
C(3)	52(3)	72(4)	50(3)	11(3)	–9(2)	15(3)
C(4)	48(3)	97(5)	64(4)	21(3)	–9(3)	27(3)
C(5)	46(3)	87(4)	76(4)	16(3)	6(3)	30(3)
C(6)	39(3)	76(4)	51(3)	8(3)	3(2)	19(2)
C(22)	39(2)	46(2)	36(2)	1(2)	6(2)	1(2)
C(23)	46(3)	56(3)	54(3)	2(2)	8(2)	–5(2)
C(24)	63(4)	56(3)	75(4)	17(3)	12(3)	–9(3)
C(25)	85(5)	59(4)	76(4)	28(3)	7(4)	11(3)
C(26)	54(3)	53(3)	67(3)	23(3)	–3(3)	4(2)
C(32)	33(2)	49(3)	40(2)	–2(2)	5(2)	5(2)
C(33)	33(2)	65(3)	51(3)	–2(2)	1(2)	8(2)
C(34)	38(3)	85(4)	60(3)	6(3)	–5(2)	20(3)
C(35)	54(3)	70(3)	55(3)	15(3)	0(2)	26(3)
C(36)	41(2)	54(3)	37(2)	8(2)	3(2)	17(2)
C(42)	49(3)	44(2)	39(2)	9(2)	7(2)	14(2)
C(43)	66(3)	58(3)	57(3)	22(3)	15(3)	23(3)
C(44)	80(4)	50(3)	66(4)	21(3)	19(3)	11(3)
C(45)	62(4)	49(3)	61(3)	12(3)	9(3)	–3(3)
C(46)	45(3)	48(3)	38(2)	4(2)	3(2)	1(2)

table continued..

Cl(1)	45(1)	53(1)	42(1)	1(1)	7(1)	7(1)
Cl(2)	56(1)	64(1)	48(1)	12(1)	5(1)	20(1)
O(1)	116(5)	198(7)	54(3)	21(4)	–5(3)	63(5)
O(2)	62(3)	214(8)	88(4)	–5(4)	13(3)	23(4)
O(3)	149(6)	82(4)	110(4)	20(3)	50(4)	47(4)
O(4)	124(5)	114(5)	188(7)	94(5)	38(5)	43(4)

Table C.4 *Hydrogen coordinates (x 10^4) and isotropic displacement parameters ($Å^2$ x 10^3) for [Ru(terpy)(bipy)Cl]ClO_4.*

	x	y	z	U(eq)
H(3')	–125	6318	4234	72
H(4')	1961	5714	3907	80
H(5')	3780	5716	5304	73
H(6')	3569	6441	6960	60
H(3)	–1997	6979	4689	74
H(4)	–3884	7670	5290	85
H(5)	–3670	8288	7044	83
H(6)	–1650	8151	8195	68
H(23)	6512	10640	8748	71
H(24)	5753	11884	7977	85
H(25)	3139	11405	7159	91
H(26)	1385	9711	7204	73
H(33)	7068	9289	9529	66
H(34)	7315	7812	10198	77
H(35)	5134	6199	9989	72
H(43)	2760	4708	9634	70
H(44)	279	3320	9215	79
H(45)	–1797	3671	8326	76
H(46)	–1426	5376	7910	58

Table C.5 *Torsion angles [°] for [Ru(terpy)(bipy)Cl]ClO_4.*

N(3)–Ru(1)–N(1)–C(6)	–143.5(13)
N(1')–Ru(1)–N(1)–C(6)	–179.8(5)
N(4)–Ru(1)–N(1)–C(6)	91.9(5)
N(2)–Ru(1)–N(1)–C(6)	–89.9(5)
Cl(1)–Ru(1)–N(1)–C(6)	1.8(4)
N(3)–Ru(1)–N(1)–C(2)	30.4(15)
N(1')–Ru(1)–N(1)–C(2)	–5.9(3)
N(4)–Ru(1)–N(1)–C(2)	–94.2(3)
N(2)–Ru(1)–N(1)–C(2)	84.1(4)
Cl(1)–Ru(1)–N(1)–C(2)	175.7(3)
N(3)–Ru(1)–N(1')–C(6')	8.9(4)
N(4)–Ru(1)–N(1')–C(6')	–70.5(4)
N(2)–Ru(1)–N(1')–C(6')	88.5(4)
N(1)–Ru(1)–N(1')–C(6')	–174.7(4)
Cl(1)–Ru(1)–N(1')–C(6')	–162.7(6)
N(3)–Ru(1)–N(1')–C(2')	–171.0(3)
N(4)–Ru(1)–N(1')–C(2')	109.5(3)
N(2)–Ru(1)–N(1')–C(2')	–91.4(3)
N(1)–Ru(1)–N(1')–C(2')	5.3(3)
Cl(1)–Ru(1)–N(1')–C(2')	17.4(11)
N(3)–Ru(1)–N(2)–C(26)	179.7(5)
N(1')–Ru(1)–N(2)–C(26)	83.1(5)
N(4)–Ru(1)–N(2)–C(26)	–179.9(5)
N(1)–Ru(1)–N(2)–C(26)	4.7(5)
Cl(1)–Ru(1)–N(2)–C(26)	–89.8(5)
N(3)–Ru(1)–N(2)–C(22)	–0.3(3)
N(1')–Ru(1)–N(2)–C(22)	–96.9(3)
N(4)–Ru(1)–N(2)–C(22)	0.1(6)
N(1)–Ru(1)–N(2)–C(22)	–175.3(3)
Cl(1)–Ru(1)–N(2)–C(22)	90.3(3)
N(1')–Ru(1)–N(3)–C(36)	–89.9(3)
N(4)–Ru(1)–N(3)–C(36)	0.1(3)
N(2)–Ru(1)–N(3)–C(36)	180.0(4)
N(1)–Ru(1)–N(3)–C(36)	–125.6(13)

table continued..

Cl(1)–Ru(1)–N(3)–C(36)	89.0(3)
N(1')–Ru(1)–N(3)–C(32)	90.8(3)
N(4)–Ru(1)–N(3)–C(32)	–179.2(4)
N(2)–Ru(1)–N(3)–C(32)	0.7(3)
N(1)–Ru(1)–N(3)–C(32)	55.1(15)
Cl(1)–Ru(1)–N(3)–C(32)	–90.3(3)
N(3)–Ru(1)–N(4)–C(46)	179.0(4)
N(1')–Ru(1)–N(4)–C(46)	–84.4(4)
N(2)–Ru(1)–N(4)–C(46)	178.6(4)
N(1)–Ru(1)–N(4)–C(46)	–6.2(4)
Cl(1)–Ru(1)–N(4)–C(46)	88.1(4)
N(3)–Ru(1)–N(4)–C(42)	–0.9(3)
N(1')–Ru(1)–N(4)–C(42)	95.8(3)
N(2)–Ru(1)–N(4)–C(42)	–1.3(6)
N(1)–Ru(1)–N(4)–C(42)	174.0(3)
Cl(1)–Ru(1)–N(4)–C(42)	–91.8(3)
C(6')–N(1')–C(2')–C(3')	–2.9(7)
Ru(1)–N(1')–C(2')–C(3')	177.1(4)
C(6')–N(1')–C(2')–C(2)	176.0(4)
Ru(1)–N(1')–C(2')–C(2)	–4.0(5)
N(1')–C(2')–C(3')–C(4')	0.2(8)
C(2)–C(2')–C(3')–C(4')	–178.6(5)
C(2')–C(3')–C(4')–C(5')	2.6(9)
C(3')–C(4')–C(5')–C(6')	–2.7(9)
C(2')–N(1')–C(6')–C(5')	2.9(8)
Ru(1)–N(1')–C(6')–C(5')	–177.1(4)
C(4')–C(5')–C(6')–N(1')	–0.1(9)
C(6)–N(1)–C(2)–C(3)	0.5(8)
Ru(1)–N(1)–C(2)–C(3)	–173.8(4)
C(6)–N(1)–C(2)–C(2')	179.9(4)
Ru(1)–N(1)–C(2)–C(2')	5.6(5)
N(1')–C(2')–C(2)–N(1)	–1.1(6)
C(3')–C(2')–C(2)–N(1)	177.7(5)
N(1')–C(2')–C(2)–C(3)	178.3(5)
C(3')–C(2')–C(2)–C(3)	–2.9(8)
N(1)–C(2)–C(3)–C(4)	0.4(8)

table continued...

C(2')–C(2)–C(3)–C(4)	–178.9(5)
C(2)–C(3)–C(4)–C(5)	–0.1(10)
C(3)–C(4)–C(5)–C(6)	–1.2(11)
C(2)–N(1)–C(6)–C(5)	–1.8(9)
Ru(1)–N(1)–C(6)–C(5)	171.9(5)
C(4)–C(5)–C(6)–N(1)	2.2(10)
C(26)–N(2)–C(22)–C(23)	–1.2(7)
Ru(1)–N(2)–C(22)–C(23)	178.7(4)
C(26)–N(2)–C(22)–C(32)	179.9(5)
Ru(1)–N(2)–C(22)–C(32)	–0.1(5)
N(2)–C(22)–C(23)–C(24)	1.3(8)
C(32)–C(22)–C(23)–C(24)	–180.0(5)
C(22)–C(23)–C(24)–C(25)	–1.1(10)
C(23)–C(24)–C(25)–C(26)	0.9(11)
C(22)–N(2)–C(26)–C(25)	1.1(9)
Ru(1)–N(2)–C(26)–C(25)	–178.9(5)
C(24)–C(25)–C(26)–N(2)	–0.9(11)
C(36)–N(3)–C(32)–C(33)	1.0(7)
Ru(1)–N(3)–C(32)–C(33)	–179.8(4)
C(36)–N(3)–C(32)–C(22)	179.8(4)
Ru(1)–N(3)–C(32)–C(22)	–0.9(5)
N(2)–C(22)–C(32)–N(3)	0.7(6)
C(23)–C(22)–C(32)–N(3)	–178.1(4)
N(2)–C(22)–C(32)–C(33)	179.4(5)
C(23)–C(22)–C(32)–C(33)	0.6(8)
N(3)–C(32)–C(33)–C(34)	–0.6(8)
C(22)–C(32)–C(33)–C(34)	–179.3(5)
C(32)–C(33)–C(34)–C(35)	0.3(9)
C(33)–C(34)–C(35)–C(36)	–0.3(9)
C(32)–N(3)–C(36)–C(35)	–1.0(7)
Ru(1)–N(3)–C(36)–C(35)	179.8(4)
C(32)–N(3)–C(36)–C(42)	179.9(4)
Ru(1)–N(3)–C(36)–C(42)	0.6(5)
C(34)–C(35)–C(36)–N(3)	0.6(8)
C(34)–C(35)–C(36)–C(42)	179.6(5)
C(46)–N(4)–C(42)–C(43)	1.7(7)

table continued..

Ru(1)–N(4)–C(42)–C(43)	–178.4(4)
C(46)–N(4)–C(42)–C(36)	–178.4(4)
Ru(1)–N(4)–C(42)–C(36)	1.5(5)
N(3)–C(36)–C(42)–N(4)	–1.4(6)
C(35)–C(36)–C(42)–N(4)	179.6(5)
N(3)–C(36)–C(42)–C(43)	178.5(4)
C(35)–C(36)–C(42)–C(43)	–0.6(8)
N(4)–C(42)–C(43)–C(44)	–0.1(8)
C(36)–C(42)–C(43)–C(44)	–179.9(5)
C(42)–C(43)–C(44)–C(45)	–0.4(9)
C(43)–C(44)–C(45)–C(46)	–0.7(9)
C(42)–N(4)–C(46)–C(45)	–2.9(7)
Ru(1)–N(4)–C(46)–C(45)	177.2(4)
C(44)–C(45)–C(46)–N(4)	2.4(9)

Symmetry transformations used to generate equivalent atoms:

Table C.6 *Atomic coordinates (x 10^4) and equivalent isotropic displacement parameters ($Å^2$ x 10^3) for [Ru(terpy)(tmen)(CH_3CN)](ClO_4)$_2$. U(eq) is defined as one third of the trace of the orthogonalized U^{ij} tensor.*

	x	y	z	U(eq)
C(1)	3329(2)	1452(6)	1265(3)	52(1)
C(1')	1673(3)	3547(10)	8747(4)	82(2)
C(2)	3053(2)	437(7)	1052(4)	61(2)
C(2')	1964(3)	4514(10)	8974(5)	90(3)
C(3')	2130(3)	4553(9)	9622(6)	96(3)
C(3)	2859(2)	427(8)	388(3)	65(2)
C(4)	2994(2)	1359(7)	-36(3)	52(1)
C(4')	2026(3)	3665(8)	10044(4)	77(2)
C(5)	3288(2)	2320(6)	207(3)	41(1)
C(5')	1733(2)	2674(7)	9813(4)	66(2)
C(6)	3456(2)	3244(6)	-237(3)	42(1)
C(6')	1552(2)	1761(7)	10245(3)	61(2)
C(7')	1683(3)	1613(9)	10935(4)	75(2)
C(7)	3330(2)	3387(7)	-923(3)	51(1)
C(8')	1444(3)	718(10)	11271(4)	82(2)
C(8)	3541(2)	4240(8)	-1286(3)	60(2)
C(9)	3885(2)	4999(6)	-950(2)	47(1)
C(9')	1139(3)	42(9)	10956(4)	80(2)
C(10')	1005(2)	174(7)	10293(3)	59(2)
C(10)	3997(2)	4844(5)	-271(2)	36(1)
C(11')	655(3)	-533(8)	9869(4)	68(2)
C(11)	4360(2)	5525(4)	148(2)	29(1)
C(12)	4632(2)	6333(5)	-131(2)	37(1)
C(12')	360(3)	-1327(8)	10117(4)	77(2)
C(13)	4980(2)	6908(5)	282(2)	34(1)
C(13')	48(3)	-1874(7)	9725(4)	86(2)
C(14')	4(3)	-1645(7)	9071(4)	78(2)
C(14)	5032(2)	6634(5)	953(2)	34(1)
C(15')	263(2)	-875(7)	8807(4)	64(2)
C(15)	4728(2)	5853(4)	1186(2)	31(1)

table continued...

C(16)	3952(2)	5402(6)	2268(3)	51(1)
C(16')	1064(3)	-421(8)	7748(4)	79(2)
C(17)	3519(2)	5732(7)	1892(3)	51(1)
C(17')	1492(3)	-745(9)	8116(4)	83(2)
C(18')	479(3)	1276(8)	7539(4)	79(2)
C(18)	3813(2)	3092(6)	2502(3)	55(2)
C(19')	1190(3)	1925(9)	7477(4)	82(2)
C(19)	4495(2)	3731(7)	2448(3)	52(2)
C(20')	1965(2)	-224(9)	9123(4)	82(2)
C(20)	3607(2)	6838(6)	879(3)	54(1)
C(21')	1403(3)	-1819(8)	9144(4)	79(2)
C(21)	3053(2)	5226(8)	885(4)	73(2)
C(22')	408(3)	3450(9)	8952(4)	74(2)
C(22)	4571(2)	1549(6)	1044(3)	45(1)
C(23')	136(4)	4597(12)	8952(6)	119(4)
C(23)	4897(3)	506(9)	1056(4)	86(3)
Cl(1)	694(1)	6026(2)	7489(1)	98(1)
Cl(2)	4316(1)	8967(1)	2514(1)	48(1)
Cl(3)	3995(1)	9879(2)	9402(1)	93(1)
Cl(4)	995(2)	5102(4)	591(2)	162(2)
N(1')	1553(2)	2580(6)	9169(3)	59(1)
N(1)	3451(1)	2404(4)	859(2)	39(1)
N(2')	1228(2)	1001(6)	9945(3)	55(1)
N(2)	3789(1)	3991(4)	70(2)	31(1)
N(3)	4396(1)	5272(4)	814(2)	26(1)
N(3')	612(2)	-279(5)	9210(3)	57(1)
N(4')	964(2)	1035(6)	7857(3)	64(1)
N(4)	4064(1)	3998(4)	2138(2)	33(1)
N(5')	1510(2)	-529(6)	8842(3)	71(2)
N(5)	3493(1)	5544(5)	1173(2)	44(1)
N(6)	4350(1)	2428(4)	1038(2)	30(1)
N(6')	664(2)	2586(6)	8972(3)	58(1)
O(1)	531(2)	6717(6)	8013(3)	94(2)
O(2)	522(2)	4706(6)	7438(4)	116(2)
O(3)	1122(3)	5969(8)	7562(4)	119(2)
O(4)	529(3)	6780(8)	6894(4)	138(3)
O(5)	4490(2)	10302(4)	2566(3)	79(2)

table continued....

O(6)	3855(2)	9029(6)	2417(3)	72(2)
O(7)	4441(2)	8309(5)	1972(3)	70(1)
O(8)	4475(2)	8264(7)	3107(3)	102(2)
O(9)	3959(3)	9544(11)	10098(4)	136(3)
O(10)	3588(3)	10212(13)	9002(6)	170(4)
O(11)	4118(3)	8736(9)	9079(5)	139(3)
O(12)	4253(3)	10870(7)	9367(4)	101(2)
O(13)	1389(5)	4699(17)	1020(8)	249(6)
O(14)	958(6)	6280(14)	951(7)	255(7)
O(15)	774(4)	4088(11)	655(5)	156(4)
O(16)	1090(4)	5437(13)	-78(6)	187(4)
Ru(01)	3927(1)	3916(1)	1044(1)	28(1)
Ru(02)	1078(1)	1084(1)	8960(1)	51(1)

Table C.7 *Bond lengths [Å] and angles [°] for [Ru(terpy)(tmen)(CH_3CN)](ClO_4)$_2$.*

C(1)-N(1)	1.361(8)
C(1)-C(2)	1.366(8)
C(1)-H(1)	0.9300
C(1')-C(2')	1.367(11)
C(1')-N(1')	1.391(10)
C(1')-H(1')	0.9300
C(2)-C(3)	1.398(9)
C(2)-H(2)	0.9300
C(2')-C(3')	1.348(13)
C(2')-H(2')	0.9300
C(3')-C(4')	1.319(13)
C(3')-H(3')	0.9300
C(3)-C(4)	1.388(10)
C(3)-H(3)	0.9300
C(4)-C(5)	1.377(7)
C(4)-H(4)	0.9300
C(4')-C(5')	1.390(10)
C(4')-H(4')	0.9300
C(5)-N(1)	1.356(6)
C(5)-C(6)	1.459(8)

table continued....

C(5')-N(1')	1.352(8)
C(5')-C(6')	1.457(11)
C(6)-N(2)	1.366(6)
C(6)-C(7)	1.403(7)
C(6')-N(2')	1.348(9)
C(6')-C(7')	1.414(10)
C(7')-C(8')	1.425(13)
C(7')-H(7')	0.9300
C(7)-C(8)	1.380(10)
C(7)-H(7)	0.9300
C(8')-C(9')	1.271(12)
C(8')-H(8')	0.9300
C(8)-C(9)	1.416(9)
C(8)-H(8)	0.9300
C(9)-C(10)	1.387(7)
C(9)-H(9)	0.9300
C(9')-C(10')	1.361(9)
C(9')-H(9')	0.9300
C(10')-N(2')	1.368(9)
C(10')-C(11')	1.479(10)
C(10)-N(2)	1.345(7)
C(10)-C(11)	1.490(7)
C(11')-N(3')	1.361(9)
C(11')-C(12')	1.391(11)
C(11)-N(3)	1.375(5)
C(11)-C(12)	1.379(7)
C(12)-C(13)	1.406(7)
C(12)-H(12)	0.9300
C(12')-C(13')	1.296(12)
C(12')-H(12')	0.9300
C(13)-C(14)	1.385(6)
C(13)-H(13)	0.9300
C(13')-C(14')	1.343(11)
C(13')-H(13')	0.9300
C(14')-C(15')	1.310(10)
C(14')-H(14')	0.9300
C(14)-C(15)	1.392(6)

table continued...

C(14)-H(14)	0.9300
C(15')-N(3')	1.408(9)
C(15')-H(15')	0.9300
C(15)-N(3)	1.333(6)
C(15)-H(15)	0.9300
C(16)-N(4)	1.479(7)
C(16)-C(17)	1.507(9)
C(16)-H(16A)	0.9700
C(16)-H(16B)	0.9700
C(16')-C(17')	1.486(12)
C(16')-N(4')	1.511(10)
C(16')-H(16C)	0.9700
C(16')-H(16D)	0.9700
C(17)-N(5)	1.475(7)
C(17)-H(17A)	0.9700
C(17)-H(17B)	0.9700
C(17')-N(5')	1.497(9)
C(17')-H(17C)	0.9700
C(17')-H(17D)	0.9700
C(18')-N(4')	1.601(10)
C(18')-H(18A)	0.9600
C(18')-H(18B)	0.9600
C(18')-H(18C)	0.9600
C(18)-N(4)	1.490(6)
C(18)-H(18D)	0.9600
C(18)-H(18E)	0.9600
C(18)-H(18F)	0.9600
C(19')-N(4')	1.451(9)
C(19')-H(19D)	0.9600
C(19')-H(19E)	0.9600
C(19')-H(19F)	0.9600
C(19)-N(4)	1.447(7)
C(19)-H(19A)	0.9600
C(19)-H(19B)	0.9600
C(19)-H(19C)	0.9600
C(20')-N(5')	1.506(9)
C(20')-H(20D)	0.9600

table continued...

C(20')-H(20E)	0.9600
C(20')-H(20F)	0.9600
C(20)-N(5)	1.494(8)
C(20)-H(20A)	0.9600
C(20)-H(20B)	0.9600
C(20)-H(20C)	0.9600
C(21')-N(5')	1.491(10)
C(21')-H(21A)	0.9600
C(21')-H(21B)	0.9600
C(21')-H(21C)	0.9600
C(21)-N(5)	1.469(7)
C(21)-H(21D)	0.9600
C(21)-H(21E)	0.9600
C(21)-H(21F)	0.9600
C(22')-N(6')	1.186(9)
C(22')-C(23')	1.439(12)
C(22)-N(6)	1.126(6)
C(22)-C(23)	1.471(8)
C(23')-H(23A)	0.9600
C(23')-H(23B)	0.9600
C(23')-H(23C)	0.9600
C(23)-H(23D)	0.9600
C(23)-H(23E)	0.9600
C(23)-H(23F)	0.9600
Cl(1)-O(3)	1.357(9)
Cl(1)-O(2)	1.423(7)
Cl(1)-O(1)	1.446(6)
Cl(1)-O(4)	1.454(8)
Cl(2)-O(7)	1.405(4)
Cl(2)-O(8)	1.423(6)
Cl(2)-O(5)	1.440(5)
Cl(2)-O(6)	1.460(5)
Cl(3)-O(12)	1.297(7)
Cl(3)-O(11)	1.405(7)
Cl(3)-O(10)	1.460(9)
Cl(3)-O(9)	1.487(8)
Cl(4)-O(15)	1.253(10)

table continued....

Cl(4)-O(14)	1.402(12)
Cl(4)-O(13)	1.469(15)
Cl(4)-O(16)	1.492(11)
N(1')-Ru(02)	2.123(6)
N(1)-Ru(01)	2.133(4)
N(2')-Ru(02)	1.998(5)
N(2)-Ru(01)	1.972(4)
N(3)-Ru(01)	2.132(4)
N(3')-Ru(02)	2.142(6)
N(4')-Ru(02)	2.230(6)
N(4)-Ru(01)	2.215(4)
N(5')-Ru(02)	2.160(6)
N(5)-Ru(01)	2.183(5)
N(6)-Ru(01)	2.010(4)
N(6')-Ru(02)	2.003(6)

N(1)-C(1)-C(2)	123.9(6)
N(1)-C(1)-H(1)	118.1
C(2)-C(1)-H(1)	118.1
C(2')-C(1')-N(1')	121.4(8)
C(2')-C(1')-H(1')	119.3
N(1')-C(1')-H(1')	119.3
C(1)-C(2)-C(3)	118.4(7)
C(1)-C(2)-H(2)	120.8
C(3)-C(2)-H(2)	120.8
C(3')-C(2')-C(1')	119.4(9)
C(3')-C(2')-H(2')	120.3
C(1')-C(2')-H(2')	120.3
C(4')-C(3')-C(2')	121.7(8)
C(4')-C(3')-H(3')	119.2
C(2')-C(3')-H(3')	119.2
C(4)-C(3)-C(2)	118.0(6)
C(4)-C(3)-H(3)	121.0
C(2)-C(3)-H(3)	121.0
C(5)-C(4)-C(3)	120.3(6)
C(5)-C(4)-H(4)	119.9
C(3)-C(4)-H(4)	119.9

table continued...

C(3')-C(4')-C(5')	118.9(8)
C(3')-C(4')-H(4')	120.5
C(5')-C(4')-H(4')	120.5
N(1)-C(5)-C(4)	121.8(6)
N(1)-C(5)-C(6)	117.1(4)
C(4)-C(5)-C(6)	121.0(5)
N(1')-C(5')-C(4')	122.4(8)
N(1')-C(5')-C(6')	113.7(6)
C(4')-C(5')-C(6')	123.4(7)
N(2)-C(6)-C(7)	118.6(5)
N(2)-C(6)-C(5)	113.4(4)
C(7)-C(6)-C(5)	127.9(5)
N(2')-C(6')-C(7')	118.4(7)
N(2')-C(6')-C(5')	115.3(6)
C(7')-C(6')-C(5')	126.3(7)
C(6')-C(7')-C(8')	117.0(7)
C(6')-C(7')-H(7')	121.5
C(8')-C(7')-H(7')	121.5
C(8)-C(7)-C(6)	121.3(6)
C(8)-C(7)-H(7)	119.4
C(6)-C(7)-H(7)	119.4
C(9')-C(8')-C(7')	121.0(7)
C(9')-C(8')-H(8')	119.5
C(7')-C(8')-H(8')	119.5
C(7)-C(8)-C(9)	118.5(6)
C(7)-C(8)-H(8)	120.8
C(9)-C(8)-H(8)	120.8
C(10)-C(9)-C(8)	118.7(6)
C(10)-C(9)-H(9)	120.7
C(8)-C(9)-H(9)	120.7
C(8')-C(9')-C(10')	123.0(9)
C(8')-C(9')-H(9')	118.5
C(10')-C(9')-H(9')	118.5
C(9')-C(10')-N(2')	118.2(7)
C(9')-C(10')-C(11')	128.6(8)
N(2')-C(10')-C(11')	113.1(6)
N(2)-C(10)-C(9)	121.6(5)

table continued...

N(2)-C(10)-C(11)	113.3(4)
C(9)-C(10)-C(11)	125.1(5)
N(3')-C(11')-C(12')	120.4(8)
N(3')-C(11')-C(10')	115.9(7)
C(12')-C(11')-C(10')	123.5(7)
N(3)-C(11)-C(12)	124.3(4)
N(3)-C(11)-C(10)	114.8(4)
C(12)-C(11)-C(10)	121.0(4)
C(11)-C(12)-C(13)	118.8(4)
C(11)-C(12)-H(12)	120.6
C(13)-C(12)-H(12)	120.6
C(13')-C(12')-C(11')	121.0(8)
C(13')-C(12')-H(12')	119.5
C(11')-C(12')-H(12')	119.5
C(14)-C(13)-C(12)	118.0(4)
C(14)-C(13)-H(13)	121.0
C(12)-C(13)-H(13)	121.0
C(12')-C(13')-C(14')	119.3(9)
C(12')-C(13')-H(13')	120.4
C(14')-C(13')-H(13')	120.4
C(15')-C(14')-C(13')	122.9(9)
C(15')-C(14')-H(14')	118.5
C(13')-C(14')-H(14')	118.5
C(13)-C(14)-C(15)	118.4(5)
C(13)-C(14)-H(14)	120.8
C(15)-C(14)-H(14)	120.8
C(14')-C(15')-N(3')	120.0(8)
C(14')-C(15')-H(15')	120.0
N(3')-C(15')-H(15')	120.0
N(3)-C(15)-C(14)	125.7(4)
N(3)-C(15)-H(15)	117.1
C(14)-C(15)-H(15)	117.1
N(4)-C(16)-C(17)	110.2(5)
N(4)-C(16)-H(16A)	109.6
C(17)-C(16)-H(16A)	109.6
N(4)-C(16)-H(16B)	109.6
C(17)-C(16)-H(16B)	109.6

table continued…

H(16A)-C(16)-H(16B)	108.1
C(17')-C(16')-N(4')	109.5(7)
C(17')-C(16')-H(16C)	109.8
N(4')-C(16')-H(16C)	109.8
C(17')-C(16')-H(16D)	109.8
N(4')-C(16')-H(16D)	109.8
H(16C)-C(16')-H(16D)	108.2
N(5)-C(17)-C(16)	112.3(4)
N(5)-C(17)-H(17A)	109.1
C(16)-C(17)-H(17A)	109.1
N(5)-C(17)-H(17B)	109.1
C(16)-C(17)-H(17B)	109.1
H(17A)-C(17)-H(17B)	107.9
C(16')-C(17')-N(5')	110.7(7)
C(16')-C(17')-H(17C)	109.5
N(5')-C(17')-H(17C)	109.5
C(16')-C(17')-H(17D)	109.5
N(5')-C(17')-H(17D)	109.5
H(17C)-C(17')-H(17D)	108.1
N(4')-C(18')-H(18A)	109.5
N(4')-C(18')-H(18B)	109.5
H(18A)-C(18')-H(18B)	109.5
N(4')-C(18')-H(18C)	109.5
H(18A)-C(18')-H(18C)	109.5
H(18B)-C(18')-H(18C)	109.5
N(4)-C(18)-H(18D)	109.5
N(4)-C(18)-H(18E)	109.5
H(18D)-C(18)-H(18E)	109.5
N(4)-C(18)-H(18F)	109.5
H(18D)-C(18)-H(18F)	109.5
H(18E)-C(18)-H(18F)	109.5
N(4')-C(19')-H(19D)	109.5
N(4')-C(19')-H(19E)	109.5
H(19D)-C(19')-H(19E)	109.5
N(4')-C(19')-H(19F)	109.5
H(19D)-C(19')-H(19F)	109.5
H(19E)-C(19')-H(19F)	109.5

table continued...

N(4)-C(19)-H(19A)	109.5
N(4)-C(19)-H(19B)	109.5
H(19A)-C(19)-H(19B)	109.5
N(4)-C(19)-H(19C)	109.5
H(19A)-C(19)-H(19C)	109.5
H(19B)-C(19)-H(19C)	109.5
N(5')-C(20')-H(20D)	109.5
N(5')-C(20')-H(20E)	109.5
H(20D)-C(20')-H(20E)	109.5
N(5')-C(20')-H(20F)	109.5
H(20D)-C(20')-H(20F)	109.5
H(20E)-C(20')-H(20F)	109.5
N(5)-C(20)-H(20A)	109.5
N(5)-C(20)-H(20B)	109.5
H(20A)-C(20)-H(20B)	109.5
N(5)-C(20)-H(20C)	109.5
H(20A)-C(20)-H(20C)	109.5
H(20B)-C(20)-H(20C)	109.5
N(5')-C(21')-H(21A)	109.5
N(5')-C(21')-H(21B)	109.5
H(21A)-C(21')-H(21B)	109.5
N(5')-C(21')-H(21C)	109.5
H(21A)-C(21')-H(21C)	109.5
H(21B)-C(21')-H(21C)	109.5
N(5)-C(21)-H(21D)	109.5
N(5)-C(21)-H(21E)	109.5
H(21D)-C(21)-H(21E)	109.5
N(5)-C(21)-H(21F)	109.5
H(21D)-C(21)-H(21F)	109.5
H(21E)-C(21)-H(21F)	109.5
N(6')-C(22')-C(23')	173.8(11)
N(6)-C(22)-C(23)	173.9(7)
C(22')-C(23')-H(23A)	109.5
C(22')-C(23')-H(23B)	109.5
H(23A)-C(23')-H(23B)	109.5
C(22')-C(23')-H(23C)	109.5
H(23A)-C(23')-H(23C)	109.5

table continued...

H(23B)-C(23')-H(23C)	109.5
C(22)-C(23)-H(23D)	109.5
C(22)-C(23)-H(23E)	109.5
H(23D)-C(23)-H(23E)	109.5
C(22)-C(23)-H(23F)	109.5
H(23D)-C(23)-H(23F)	109.5
H(23E)-C(23)-H(23F)	109.5
O(3)-Cl(1)-O(2)	110.0(5)
O(3)-Cl(1)-O(1)	114.9(5)
O(2)-Cl(1)-O(1)	108.1(5)
O(3)-Cl(1)-O(4)	109.6(6)
O(2)-Cl(1)-O(4)	109.6(5)
O(1)-Cl(1)-O(4)	104.5(4)
O(7)-Cl(2)-O(8)	109.7(4)
O(7)-Cl(2)-O(5)	109.4(3)
O(8)-Cl(2)-O(5)	108.2(4)
O(7)-Cl(2)-O(6)	109.1(3)
O(8)-Cl(2)-O(6)	110.4(4)
O(5)-Cl(2)-O(6)	110.0(3)
O(12)-Cl(3)-O(11)	111.2(5)
O(12)-Cl(3)-O(10)	108.2(6)
O(11)-Cl(3)-O(10)	102.3(7)
O(12)-Cl(3)-O(9)	112.1(6)
O(11)-Cl(3)-O(9)	110.0(7)
O(10)-Cl(3)-O(9)	112.7(6)
O(15)-Cl(4)-O(14)	121.4(10)
O(15)-Cl(4)-O(13)	99.3(9)
O(14)-Cl(4)-O(13)	93.1(11)
O(15)-Cl(4)-O(16)	118.8(8)
O(14)-Cl(4)-O(16)	110.2(9)
O(13)-Cl(4)-O(16)	109.0(10)
C(5')-N(1')-C(1')	116.2(6)
C(5')-N(1')-Ru(02)	114.9(5)
C(1')-N(1')-Ru(02)	128.6(5)
C(5)-N(1)-C(1)	117.2(5)
C(5)-N(1)-Ru(01)	111.4(4)
C(1)-N(1)-Ru(01)	130.9(4)

table continued...

C(6')-N(2')-C(10')	122.0(6)
C(6')-N(2')-Ru(02)	118.5(5)
C(10')-N(2')-Ru(02)	119.6(5)
C(10)-N(2)-C(6)	121.4(4)
C(10)-N(2)-Ru(01)	120.2(3)
C(6)-N(2)-Ru(01)	118.2(4)
C(15)-N(3)-C(11)	114.6(4)
C(15)-N(3)-Ru(01)	132.4(3)
C(11)-N(3)-Ru(01)	112.8(3)
C(11')-N(3')-C(15')	116.3(6)
C(11')-N(3')-Ru(02)	113.4(5)
C(15')-N(3')-Ru(02)	130.2(5)
C(19')-N(4')-C(16')	111.8(6)
C(19')-N(4')-C(18')	103.2(6)
C(16')-N(4')-C(18')	107.4(6)
C(19')-N(4')-Ru(02)	121.2(4)
C(16')-N(4')-Ru(02)	99.7(4)
C(18')-N(4')-Ru(02)	113.2(5)
C(19)-N(4)-C(16)	109.8(5)
C(19)-N(4)-C(18)	102.9(4)
C(16)-N(4)-C(18)	108.4(4)
C(19)-N(4)-Ru(01)	117.0(4)
C(16)-N(4)-Ru(01)	101.8(3)
C(18)-N(4)-Ru(01)	116.9(3)
C(21')-N(5')-C(17')	108.3(6)
C(21')-N(5')-C(20')	106.9(7)
C(17')-N(5')-C(20')	106.5(7)
C(21')-N(5')-Ru(02)	113.6(5)
C(17')-N(5')-Ru(02)	107.4(5)
C(20')-N(5')-Ru(02)	113.9(4)
C(21)-N(5)-C(17)	108.7(5)
C(21)-N(5)-C(20)	107.9(6)
C(17)-N(5)-C(20)	108.4(5)
C(21)-N(5)-Ru(01)	112.3(4)
C(17)-N(5)-Ru(01)	106.5(4)
C(20)-N(5)-Ru(01)	112.9(3)
C(22)-N(6)-Ru(01)	176.4(4)

table continued...

C(22')-N(6')-Ru(02)	176.8(6)
N(2)-Ru(01)-N(6)	93.48(15)
N(2)-Ru(01)-N(3)	78.51(15)
N(6)-Ru(01)-N(3)	88.02(14)
N(2)-Ru(01)-N(1)	79.29(17)
N(6)-Ru(01)-N(1)	86.64(16)
N(3)-Ru(01)-N(1)	156.79(16)
N(2)-Ru(01)-N(5)	93.10(17)
N(6)-Ru(01)-N(5)	173.36(17)
N(3)-Ru(01)-N(5)	92.46(16)
N(1)-Ru(01)-N(5)	95.42(17)
N(2)-Ru(01)-N(4)	175.45(15)
N(6)-Ru(01)-N(4)	90.69(16)
N(3)-Ru(01)-N(4)	99.84(14)
N(1)-Ru(01)-N(4)	102.80(16)
N(5)-Ru(01)-N(4)	82.70(17)
N(2')-Ru(02)-N(6')	93.9(2)
N(2')-Ru(02)-N(1')	77.3(2)
N(6')-Ru(02)-N(1')	85.8(2)
N(2')-Ru(02)-N(3')	78.1(2)
N(6')-Ru(02)-N(3')	88.9(2)
N(1')-Ru(02)-N(3')	154.4(2)
N(2')-Ru(02)-N(5')	91.7(2)
N(6')-Ru(02)-N(5')	174.4(2)
N(1')-Ru(02)-N(5')	95.4(2)
N(3')-Ru(02)-N(5')	92.3(3)
N(2')-Ru(02)-N(4')	174.2(2)
N(6')-Ru(02)-N(4')	91.8(2)
N(1')-Ru(02)-N(4')	102.2(2)
N(3')-Ru(02)-N(4')	103.0(2)
N(5')-Ru(02)-N(4')	82.6(2)

Symmetry transformations used to generate equivalent atoms:

Table C.8 *Anisotropic displacement parameters ($Å^2 x$ 10^3) for [Ru(terpy)(tmen)(CH_3CN)](ClO_4)$_2$. The anisotropic displacement factor exponent takes the form: $-2p^2[\, h^2 a^{*2} U^{11} + ... + 2\, h\, k\, a^*\, b^*\, U^{12}\,]$.*

	U^{11}	U^{22}	U^{33}	U^{23}	U^{13}	U^{12}
C(1)	52(3)	53(3)	55(3)	-15(3)	21(3)	-20(3)
C(1')	74(5)	96(6)	73(5)	-7(4)	3(4)	-27(4)
C(2)	53(4)	57(4)	68(4)	-7(3)	1(3)	-17(3)
C(2')	82(6)	103(6)	91(5)	-17(5)	29(5)	-39(5)
C(3')	88(6)	67(5)	123(6)	-21(5)	-10(5)	-25(5)
C(3)	36(3)	97(5)	58(4)	-13(3)	-6(3)	-15(3)
C(4)	31(2)	68(4)	57(3)	-14(3)	3(2)	-7(2)
C(4')	69(5)	60(4)	89(5)	-14(3)	-30(4)	-2(3)
C(5)	24(2)	55(3)	43(2)	-19(2)	0(2)	4(2)
C(5')	54(4)	65(4)	71(4)	-10(3)	-15(3)	2(3)
C(6)	33(2)	46(3)	42(2)	-6(2)	-2(2)	12(2)
C(6')	50(3)	73(4)	57(3)	-17(3)	-1(3)	15(3)
C(7')	67(4)	86(5)	65(4)	-22(4)	-6(3)	10(4)
C(7)	51(3)	64(4)	35(2)	-15(2)	-4(2)	16(3)
C(8')	98(6)	103(6)	39(3)	-9(3)	-4(3)	17(5)
C(8)	72(4)	73(4)	35(3)	-7(3)	5(3)	15(3)
C(9)	42(3)	67(4)	30(2)	-6(2)	5(2)	19(2)
C(9')	112(6)	76(5)	52(4)	4(3)	14(4)	1(4)
C(10')	64(4)	62(4)	50(3)	-3(3)	4(3)	15(3)
C(10)	35(2)	41(3)	31(2)	-2(2)	6(2)	10(2)
C(11')	69(4)	71(4)	67(4)	-7(3)	23(3)	8(3)
C(11)	43(2)	29(2)	18(2)	3(2)	10(2)	10(2)
C(12)	49(3)	38(2)	28(2)	5(2)	20(2)	6(2)
C(12')	103(6)	65(4)	70(4)	5(4)	38(4)	0(4)
C(13)	39(2)	32(2)	37(2)	5(2)	20(2)	-1(2)
C(13')	130(7)	48(4)	87(5)	-2(4)	33(5)	-8(4)
C(14')	95(6)	53(4)	91(5)	-13(4)	26(5)	-14(4)
C(14)	35(2)	34(2)	34(2)	1(2)	14(2)	-2(2)
C(15')	64(4)	50(4)	75(4)	3(3)	11(3)	0(3)
C(15)	37(2)	33(2)	25(2)	-7(2)	12(2)	-9(2)

table continued...

C(16)	70(4)	49(3)	37(3)	-10(2)	18(3)	-6(3)
C(16')	96(5)	85(4)	63(4)	-24(4)	36(4)	-22(4)
C(17)	37(3)	64(3)	55(3)	-17(3)	21(2)	10(2)
C(17')	109(6)	78(5)	68(4)	-25(4)	28(4)	1(4)
C(18')	87(5)	79(5)	66(4)	5(4)	0(4)	-29(4)
C(18)	80(4)	56(3)	35(3)	0(2)	24(3)	-30(3)
C(19')	96(6)	93(5)	61(4)	-22(4)	21(4)	-32(5)
C(19)	47(3)	73(4)	33(2)	11(3)	-6(2)	-11(3)
C(20')	44(3)	95(5)	106(6)	-25(5)	8(3)	34(3)
C(20)	62(4)	47(3)	51(3)	-10(2)	4(3)	20(3)
C(21')	96(6)	69(4)	78(5)	-10(4)	33(4)	23(4)
C(21)	37(3)	79(5)	99(5)	-39(4)	3(3)	4(3)
C(22')	78(5)	75(5)	73(5)	14(4)	27(4)	14(4)
C(22)	37(3)	59(3)	42(3)	27(2)	19(2)	19(2)
C(23')	119(8)	126(8)	122(8)	57(7)	53(7)	56(7)
C(23)	71(5)	98(6)	97(6)	46(5)	36(4)	60(5)
Cl(1)	134(2)	68(1)	93(2)	-24(1)	27(2)	3(1)
Cl(2)	52(1)	39(1)	53(1)	-18(1)	13(1)	-4(1)
Cl(3)	101(2)	78(1)	111(2)	10(1)	47(2)	15(1)
Cl(4)	244(5)	125(3)	132(3)	21(2)	73(3)	27(3)
N(1')	50(3)	66(3)	59(3)	-14(2)	9(2)	1(2)
N(1)	32(2)	43(2)	43(2)	-14(2)	9(2)	-4(2)
N(2')	48(3)	73(3)	44(2)	1(2)	6(2)	16(2)
N(2)	31(2)	32(2)	29(2)	-7(1)	3(1)	7(1)
N(3)	24(2)	27(2)	27(2)	5(1)	6(1)	4(1)
N(3')	66(3)	59(3)	47(3)	-3(2)	13(2)	1(2)
N(4')	60(3)	79(4)	55(3)	-14(3)	17(3)	-24(3)
N(4)	40(2)	35(2)	25(2)	2(2)	8(2)	-13(2)
N(5')	72(4)	66(3)	75(3)	-19(3)	13(3)	24(3)
N(5)	34(2)	52(2)	48(2)	-18(2)	14(2)	0(2)
N(6)	23(2)	34(2)	32(2)	3(2)	6(1)	-1(1)
N(6')	54(3)	72(3)	47(3)	3(2)	7(2)	4(2)
O(1)	100(4)	81(4)	108(4)	-22(3)	40(4)	-20(3)
O(2)	134(6)	73(4)	129(6)	-34(3)	-11(5)	-4(4)
O(3)	122(5)	133(6)	104(5)	-33(4)	25(5)	4(4)
O(4)	204(8)	109(5)	107(5)	-1(4)	42(5)	58(6)
O(5)	70(3)	34(2)	127(5)	-31(2)	3(3)	0(2)

table continued...

O(6)	44(2)	98(4)	77(3)	-23(3)	16(2)	-5(2)
O(7)	80(3)	56(3)	83(3)	-32(2)	45(3)	-12(2)
O(8)	137(6)	93(4)	75(3)	3(3)	16(4)	59(4)
O(9)	122(6)	192(8)	99(5)	-5(5)	33(4)	-24(6)
O(10)	99(5)	214(10)	187(8)	45(8)	-9(5)	41(6)
O(11)	103(6)	133(6)	186(8)	-62(6)	37(6)	16(4)
O(12)	109(5)	87(4)	115(5)	-24(4)	44(4)	-4(4)
O(13)	241(10)	243(12)	242(11)	61(11)	-23(9)	-8(9)
O(14)	386(17)	187(8)	187(10)	-77(8)	33(11)	10(9)
O(15)	201(9)	159(7)	119(7)	9(5)	64(6)	-32(7)
O(16)	224(11)	200(10)	151(7)	18(6)	73(7)	-22(9)
Ru(01)	24(1)	36(1)	25(1)	-4(1)	7(1)	0(1)
Ru(02)	48(1)	58(1)	48(1)	-6(1)	7(1)	1(1)

Table C.9 *Hydrogen coordinates (x 10^4) and isotropic displacement parameters ($Å^2$x 10^3) for [Ru(terpy)(tmen)(CH_3CN)](ClO_4)$_2$.*

	x	y	z	U(eq)
H(1)	3440	1495	1713	62
H(1')	1553	3535	8302	98
H(2)	2995	-230	1341	73
H(2')	2045	5140	8683	108
H(3')	2324	5224	9775	115
H(3)	2647	-187	235	78
H(4)	2884	1335	-485	63
H(4')	2146	3701	10489	93
H(7')	1914	2080	11159	89
H(7)	3100	2898	-1136	62
H(8')	1512	628	11728	98
H(8)	3460	4315	-1742	72
H(9)	4032	5588	-1180	56
H(9')	1002	-571	11189	96
H(12)	4586	6494	-584	44
H(12')	388	-1467	10571	92
H(13)	5170	7457	110	41
H(13')	-144	-2420	9894	104
H(14')	-219	-2051	8794	94
H(14)	5264	6964	1241	40
H(15')	215	-723	8353	76
H(15)	4759	5726	1641	37
H(16A)	4159	6005	2133	61
H(16B)	3954	5525	2738	61
H(16C)	855	-990	7901	94
H(16D)	1055	-587	7279	94
H(17A)	3311	5162	2049	61
H(17B)	3451	6656	1979	61
H(17C)	1701	-180	7958	100
H(17D)	1560	-1673	8035	100
H(18A)	409	744	7146	118
H(18B)	435	2208	7430	118

table continued...

H(18C)	301	1020	7852	118
H(18D)	3904	2182	2461	83
H(18E)	3518	3169	2318	83
H(18F)	3855	3341	2960	83
H(19D)	1471	2075	7714	123
H(19E)	1043	2766	7411	123
H(19F)	1206	1525	7056	123
H(19A)	4669	4494	2395	78
H(19B)	4600	2960	2245	78
H(19C)	4503	3559	2911	78
H(20D)	1994	-117	9594	123
H(20E)	2049	589	8930	123
H(20F)	2141	-950	9024	123
H(20A)	3584	6740	409	81
H(20B)	3892	7076	1065	81
H(20C)	3418	7531	975	81
H(21A)	1591	-2509	9044	119
H(21B)	1117	-2063	8967	119
H(21C)	1431	-1715	9615	119
H(21D)	2879	6006	902	109
H(21E)	2952	4512	1132	109
H(21F)	3040	4952	433	109
H(23A)	190	5025	9377	178
H(23B)	-154	4312	8861	178
H(23C)	189	5219	8617	178
H(23D)	5113	635	1435	129
H(23E)	5021	565	661	129
H(23F)	4771	-362	1079	129

Table C.10 *Atomic coordinates (x 10^4) and equivalent isotropic displacement parameters ($Å^2$x 10^3) for [Ru(terpy)$_2$](ClO$_4$)$_2$. U(eq) is defined as one third of the trace of the orthogonalized U^{ij} tensor.*

	x	y	z	U(eq)
C(1)	460(4)	9150(2)	2453(2)	13(1)
C(2)	-851(4)	9436(2)	2712(2)	16(1)
C(3)	-1124(4)	9301(2)	3427(2)	18(1)
C(4)	-92(4)	8848(2)	3883(2)	16(1)
C(5)	1194(4)	8550(2)	3600(2)	11(1)
C(6)	2299(4)	8012(2)	4034(2)	11(1)
C(7)	2212(4)	7631(2)	4763(2)	14(1)
C(8)	3335(4)	7073(2)	5069(2)	15(1)
C(9)	4559(4)	6926(2)	4652(2)	14(1)
C(10)	4618(4)	7355(2)	3927(2)	11(1)
C(11)	5830(4)	7324(2)	3401(2)	12(1)
C(12)	7167(4)	6944(2)	3581(2)	18(1)
C(13)	8260(4)	6980(3)	3050(2)	26(1)
C(14)	7969(4)	7387(3)	2350(2)	23(1)
C(15)	6628(4)	7760(2)	2193(2)	15(1)
C(16)	2388(4)	6582(2)	2916(2)	13(1)
C(17)	1765(4)	5986(2)	2749(2)	17(1)
C(18)	1475(4)	6154(2)	2060(2)	17(1)
C(19)	1828(4)	6912(2)	1544(2)	15(1)
C(20)	2462(3)	7479(2)	1741(2)	11(1)
C(21)	2855(3)	8305(2)	1237(2)	12(1)
C(22)	2666(4)	8626(2)	518(2)	14(1)
C(23)	2985(4)	9452(2)	137(2)	17(1)
C(24)	3530(4)	9933(2)	473(2)	14(1)
C(25)	3730(4)	9574(2)	1185(2)	13(1)
C(26)	4314(4)	9957(2)	1626(2)	12(1)
C(27)	4843(4)	10752(2)	1360(2)	16(1)
C(28)	5435(4)	11053(2)	1809(2)	16(1)
C(29)	5457(4)	10569(2)	2522(2)	15(1)
C(30)	4885(4)	9794(2)	2768(2)	12(1)

table continued..

C(31)	333(4)	14206(2)	2362(2)	14(1)
C(32)	-966(4)	14498(2)	2621(2)	19(1)
C(33)	-1253(4)	14315(2)	3346(2)	22(1)
C(34)	-241(4)	13823(2)	3794(2)	16(1)
C(35)	1035(4)	13527(2)	3512(2)	12(1)
C(36)	2138(4)	12973(2)	3936(2)	12(1)
C(37)	2053(4)	12587(2)	4672(2)	14(1)
C(38)	3176(4)	12031(2)	4969(2)	14(1)
C(39)	4403(4)	11892(2)	4553(2)	13(1)
C(40)	4469(4)	12321(2)	3830(2)	11(1)
C(41)	5690(4)	12316(2)	3298(2)	12(1)
C(42)	7032(4)	11954(2)	3480(2)	16(1)
C(43)	8131(4)	12020(2)	2944(2)	20(1)
C(44)	7845(4)	12445(2)	2244(2)	20(1)
C(45)	6489(4)	12795(2)	2096(2)	15(1)
C(50)	2265(4)	11591(2)	2760(2)	14(1)
C(51)	1632(4)	11015(2)	2568(2)	16(1)
C(52)	1317(4)	11228(2)	1866(2)	19(1)
C(53)	1598(4)	12010(2)	1388(2)	17(1)
C(54)	2212(4)	12567(2)	1616(2)	13(1)
C(55)	2562(4)	13423(2)	1138(2)	14(1)
C(56)	2207(4)	13825(2)	446(2)	21(1)
C(57)	2607(5)	14635(2)	89(2)	25(1)
C(58)	3306(4)	15042(2)	418(2)	20(1)
C(59)	3615(4)	14625(2)	1115(2)	13(1)
C(60)	4270(3)	14958(2)	1575(2)	13(1)
C(61)	4901(4)	15724(2)	1332(2)	17(1)
C(62)	5467(4)	15993(2)	1812(2)	16(1)
C(63)	5400(4)	15501(2)	2517(2)	17(1)
C(64)	4776(4)	14745(2)	2734(2)	13(1)
N(1)	1477(3)	8732(2)	2881(1)	11(1)
N(2)	3492(3)	7860(2)	3635(1)	10(1)
N(3)	5556(3)	7740(2)	2702(1)	11(1)
N(4)	2725(3)	7323(2)	2428(2)	12(1)
N(5)	3399(3)	8772(2)	1549(1)	11(1)
N(6)	4318(3)	9483(2)	2334(1)	11(1)
N(7)	1341(3)	13746(2)	2788(2)	13(1)

table continued..

N(8)	3340(3)	12831(2)	3538(2)	11(1)
N(9)	5410(3)	12742(2)	2608(2)	12(1)
N(10)	2545(3)	12361(2)	2299(2)	12(1)
N(11)	3231(3)	13825(2)	1461(2)	11(1)
N(12)	4216(3)	14464(2)	2283(2)	11(1)
Ru(1)	3516(1)	8319(1)	2587(1)	10(1)
Ru(2)	3368(1)	13325(1)	2494(1)	10(1)
Cl(1)	2645(1)	9828(1)	4536(1)	23(1)
Cl(2)	2630(1)	14758(1)	4557(1)	21(1)
Cl(3)	3530(1)	12201(1)	-401(1)	20(1)
Cl(4)	-1217(1)	12815(1)	270(1)	26(1)
O(1S)	5942(3)	10031(2)	4149(1)	21(1)
O(2S)	5917(3)	15054(2)	4137(1)	23(1)
O(3S)	78(3)	16208(2)	4512(1)	25(1)
O(4S)	-103(3)	11177(2)	4397(1)	26(1)
O(5S)	5454(3)	12933(2)	458(1)	25(1)
O(6S)	-378(3)	9801(2)	926(2)	33(1)
O(7S)	649(3)	11334(2)	-119(2)	36(1)
O(8S)	1015(3)	13775(2)	-1038(2)	38(1)

Table C.11 *Bond lengths [Å] and Bond angles [°] for* $[Ru(terpy)_2](ClO_4)_2$.

C(1)-N(1)	1.342(4)
C(1)-C(2)	1.389(5)
C(2)-C(3)	1.375(5)
C(3)-C(4)	1.397(5)
C(4)-C(5)	1.397(5)
C(5)-N(1)	1.373(4)
C(5)-C(6)	1.464(5)
C(6)-N(2)	1.358(4)
C(6)-C(7)	1.383(4)
C(7)-C(8)	1.388(5)
C(8)-C(9)	1.399(5)
C(9)-C(10)	1.385(4)
C(10)-N(2)	1.346(4)
C(10)-C(11)	1.474(5)
C(11)-N(3)	1.382(4)
C(11)-C(12)	1.385(5)
C(12)-C(13)	1.387(5)
C(13)-C(14)	1.386(6)
C(14)-C(15)	1.376(5)
C(15)-N(3)	1.348(4)
C(16)-N(4)	1.345(4)
C(16)-C(17)	1.382(5)
C(17)-C(18)	1.374(5)
C(18)-C(19)	1.391(5)
C(19)-C(20)	1.382(5)
C(20)-N(4)	1.366(4)
C(20)-C(21)	1.476(5)
C(21)-N(5)	1.346(4)
C(21)-C(22)	1.386(5)
C(22)-C(23)	1.392(5)
C(23)-C(24)	1.402(5)
C(24)-C(25)	1.379(5)
C(25)-N(5)	1.357(4)
C(25)-C(26)	1.458(5)

table continued..

C(26)-N(6)	1.374(4)
C(26)-C(27)	1.397(5)
C(27)-C(28)	1.383(5)
C(28)-C(29)	1.389(5)
C(29)-C(30)	1.386(5)
C(30)-N(6)	1.358(4)
C(31)-N(7)	1.351(4)
C(31)-C(32)	1.384(5)
C(32)-C(33)	1.385(5)
C(33)-C(34)	1.392(5)
C(34)-C(35)	1.387(5)
C(35)-N(7)	1.377(4)
C(35)-C(36)	1.463(5)
C(36)-N(8)	1.358(4)
C(36)-C(37)	1.396(5)
C(37)-C(38)	1.383(5)
C(38)-C(39)	1.395(5)
C(39)-C(40)	1.382(5)
C(40)-N(8)	1.351(4)
C(40)-C(41)	1.481(5)
C(41)-N(9)	1.370(4)
C(41)-C(42)	1.383(5)
C(42)-C(43)	1.391(5)
C(43)-C(44)	1.389(5)
C(44)-C(45)	1.376(5)
C(45)-N(9)	1.349(4)
C(50)-N(10)	1.348(4)
C(50)-C(51)	1.388(5)
C(51)-C(52)	1.396(5)
C(52)-C(53)	1.376(5)
C(53)-C(54)	1.393(5)
C(54)-N(10)	1.367(4)
C(54)-C(55)	1.486(5)
C(55)-N(11)	1.344(4)
C(55)-C(56)	1.390(5)
C(56)-C(57)	1.385(5)
C(57)-C(58)	1.377(5)

table continued..

C(58)-C(59)	1.388(5)
C(59)-N(11)	1.364(4)
C(59)-C(60)	1.470(5)
C(60)-N(12)	1.381(4)
C(60)-C(61)	1.399(5)
C(61)-C(62)	1.388(5)
C(62)-C(63)	1.374(5)
C(63)-C(64)	1.384(5)
C(64)-N(12)	1.347(4)
N(1)-Ru(1)	2.067(3)
N(2)-Ru(1)	1.981(3)
N(3)-Ru(1)	2.068(3)
N(4)-Ru(1)	2.064(3)
N(5)-Ru(1)	1.975(3)
N(6)-Ru(1)	2.073(3)
N(7)-Ru(2)	2.063(3)
N(8)-Ru(2)	1.975(3)
N(9)-Ru(2)	2.071(3)
N(10)-Ru(2)	2.065(3)
N(11)-Ru(2)	1.972(3)
N(12)-Ru(2)	2.068(3)

N(1)-C(1)-C(2)	122.0(3)
C(3)-C(2)-C(1)	119.7(3)
C(2)-C(3)-C(4)	119.0(3)
C(5)-C(4)-C(3)	119.2(3)
N(1)-C(5)-C(4)	120.8(3)
N(1)-C(5)-C(6)	115.5(3)
C(4)-C(5)-C(6)	123.7(3)
N(2)-C(6)-C(7)	119.7(3)
N(2)-C(6)-C(5)	112.5(3)
C(7)-C(6)-C(5)	127.7(3)
C(6)-C(7)-C(8)	118.8(3)
C(7)-C(8)-C(9)	120.8(3)
C(10)-C(9)-C(8)	118.0(3)
N(2)-C(10)-C(9)	120.4(3)
N(2)-C(10)-C(11)	113.0(3)

table continued..

C(9)-C(10)-C(11)	126.6(3)
N(3)-C(11)-C(12)	121.5(3)
N(3)-C(11)-C(10)	114.9(3)
C(12)-C(11)-C(10)	123.6(3)
C(11)-C(12)-C(13)	119.5(3)
C(14)-C(13)-C(12)	118.6(4)
C(15)-C(14)-C(13)	120.2(4)
N(3)-C(15)-C(14)	122.1(3)
N(4)-C(16)-C(17)	122.5(3)
C(18)-C(17)-C(16)	119.0(3)
C(17)-C(18)-C(19)	119.6(3)
C(20)-C(19)-C(18)	118.7(3)
N(4)-C(20)-C(19)	121.9(3)
N(4)-C(20)-C(21)	115.2(3)
C(19)-C(20)-C(21)	122.9(3)
N(5)-C(21)-C(22)	120.4(3)
N(5)-C(21)-C(20)	112.8(3)
C(22)-C(21)-C(20)	126.7(3)
C(21)-C(22)-C(23)	118.6(3)
C(22)-C(23)-C(24)	120.2(3)
C(25)-C(24)-C(23)	118.7(3)
N(5)-C(25)-C(24)	120.2(3)
N(5)-C(25)-C(26)	112.6(3)
C(24)-C(25)-C(26)	127.2(3)
N(6)-C(26)-C(27)	121.0(3)
N(6)-C(26)-C(25)	115.6(3)
C(27)-C(26)-C(25)	123.3(3)
C(28)-C(27)-C(26)	119.6(3)
C(27)-C(28)-C(29)	119.4(3)
C(30)-C(29)-C(28)	119.2(3)
N(6)-C(30)-C(29)	122.3(3)
N(7)-C(31)-C(32)	122.7(3)
C(31)-C(32)-C(33)	119.0(4)
C(32)-C(33)-C(34)	118.9(3)
C(35)-C(34)-C(33)	120.1(3)
N(7)-C(35)-C(34)	120.5(3)
N(7)-C(35)-C(36)	115.0(3)

table continued..

C(34)-C(35)-C(36)	124.4(3)
N(8)-C(36)-C(37)	119.6(3)
N(8)-C(36)-C(35)	113.3(3)
C(37)-C(36)-C(35)	127.1(3)
C(38)-C(37)-C(36)	118.2(3)
C(37)-C(38)-C(39)	121.4(3)
C(40)-C(39)-C(38)	118.3(3)
N(8)-C(40)-C(39)	120.1(3)
N(8)-C(40)-C(41)	112.3(3)
C(39)-C(40)-C(41)	127.5(3)
N(9)-C(41)-C(42)	122.1(3)
N(9)-C(41)-C(40)	114.8(3)
C(42)-C(41)-C(40)	123.0(3)
C(41)-C(42)-C(43)	118.9(3)
C(44)-C(43)-C(42)	119.0(3)
C(45)-C(44)-C(43)	119.4(3)
N(9)-C(45)-C(44)	122.5(3)
N(10)-C(50)-C(51)	122.4(3)
C(50)-C(51)-C(52)	118.9(3)
C(53)-C(52)-C(51)	119.4(3)
C(52)-C(53)-C(54)	119.0(3)
N(10)-C(54)-C(53)	122.0(3)
N(10)-C(54)-C(55)	115.0(3)
C(53)-C(54)-C(55)	122.9(3)
N(11)-C(55)-C(56)	120.6(3)
N(11)-C(55)-C(54)	112.4(3)
C(56)-C(55)-C(54)	126.9(3)
C(57)-C(56)-C(55)	118.4(3)
C(58)-C(57)-C(56)	120.9(4)
C(57)-C(58)-C(59)	118.9(3)
N(11)-C(59)-C(58)	119.9(3)
N(11)-C(59)-C(60)	112.3(3)
C(58)-C(59)-C(60)	127.7(3)
N(12)-C(60)-C(61)	121.0(3)
N(12)-C(60)-C(59)	115.3(3)
C(61)-C(60)-C(59)	123.7(3)
C(62)-C(61)-C(60)	119.4(3)

table continued..

C(63)-C(62)-C(61)	119.4(3)
C(62)-C(63)-C(64)	119.3(3)
N(12)-C(64)-C(63)	122.9(3)
C(1)-N(1)-C(5)	119.1(3)
C(1)-N(1)-Ru(1)	127.4(2)
C(5)-N(1)-Ru(1)	113.5(2)
C(10)-N(2)-C(6)	122.2(3)
C(10)-N(2)-Ru(1)	118.7(2)
C(6)-N(2)-Ru(1)	118.9(2)
C(15)-N(3)-C(11)	118.2(3)
C(15)-N(3)-Ru(1)	128.2(2)
C(11)-N(3)-Ru(1)	113.5(2)
C(16)-N(4)-C(20)	118.3(3)
C(16)-N(4)-Ru(1)	128.0(2)
C(20)-N(4)-Ru(1)	113.6(2)
C(21)-N(5)-C(25)	121.8(3)
C(21)-N(5)-Ru(1)	118.8(2)
C(25)-N(5)-Ru(1)	119.0(2)
C(30)-N(6)-C(26)	118.5(3)
C(30)-N(6)-Ru(1)	128.0(2)
C(26)-N(6)-Ru(1)	113.4(2)
C(31)-N(7)-C(35)	118.6(3)
C(31)-N(7)-Ru(2)	127.9(2)
C(35)-N(7)-Ru(2)	113.5(2)
C(40)-N(8)-C(36)	122.2(3)
C(40)-N(8)-Ru(2)	119.3(2)
C(36)-N(8)-Ru(2)	118.3(2)
C(45)-N(9)-C(41)	118.0(3)
C(45)-N(9)-Ru(2)	127.7(2)
C(41)-N(9)-Ru(2)	114.1(2)
C(50)-N(10)-C(54)	118.2(3)
C(50)-N(10)-Ru(2)	128.2(2)
C(54)-N(10)-Ru(2)	113.5(2)
C(55)-N(11)-C(59)	121.3(3)
C(55)-N(11)-Ru(2)	118.9(2)
C(59)-N(11)-Ru(2)	119.0(2)
C(64)-N(12)-C(60)	118.0(3)

table continued..

C(64)-N(12)-Ru(2)	128.5(2)
C(60)-N(12)-Ru(2)	113.4(2)
N(5)-Ru(1)-N(2)	176.07(11)
N(5)-Ru(1)-N(4)	79.38(12)
N(2)-Ru(1)-N(4)	98.64(12)
N(5)-Ru(1)-N(1)	97.42(12)
N(2)-Ru(1)-N(1)	79.12(12)
N(4)-Ru(1)-N(1)	89.67(11)
N(5)-Ru(1)-N(3)	104.17(12)
N(2)-Ru(1)-N(3)	79.30(12)
N(4)-Ru(1)-N(3)	94.23(11)
N(1)-Ru(1)-N(3)	158.41(11)
N(5)-Ru(1)-N(6)	78.99(11)
N(2)-Ru(1)-N(6)	103.04(11)
N(4)-Ru(1)-N(6)	158.32(11)
N(1)-Ru(1)-N(6)	94.62(11)
N(3)-Ru(1)-N(6)	89.56(12)
N(11)-Ru(2)-N(8)	175.49(12)
N(11)-Ru(2)-N(7)	96.19(12)
N(8)-Ru(2)-N(7)	79.58(12)
N(11)-Ru(2)-N(10)	79.34(12)
N(8)-Ru(2)-N(10)	98.96(12)
N(7)-Ru(2)-N(10)	89.58(12)
N(11)-Ru(2)-N(12)	79.44(12)
N(8)-Ru(2)-N(12)	102.36(12)
N(7)-Ru(2)-N(12)	94.83(11)
N(10)-Ru(2)-N(12)	158.67(11)
N(11)-Ru(2)-N(9)	105.36(12)
N(8)-Ru(2)-N(9)	78.91(12)
N(7)-Ru(2)-N(9)	158.42(11)
N(10)-Ru(2)-N(9)	95.47(11)
N(12)-Ru(2)-N(9)	88.05(12)

Symmetry transformations used to generate equivalent atoms:

Table C.12 *Anisotropic displacement parameters ($Å^2 x\ 10^3$) for $[Ru(terpy)_2](ClO_4)_2$. The anisotropic displacement factor exponent takes the form: $-2\pi^2[h^2a^{*2}U^{11} + ... + 2\ h\ k\ a^*\ b^*\ U^{12}]$*

	U^{11}	U^{22}	U^{33}	U^{23}	U^{13}	U^{12}
C(1)	12(2)	14(2)	12(2)	-1(1)	0(1)	0(1)
C(2)	12(2)	16(2)	18(2)	-2(1)	-4(1)	3(1)
C(3)	13(2)	16(2)	20(2)	-2(1)	5(1)	2(1)
C(4)	14(2)	16(2)	14(2)	-4(1)	3(1)	1(1)
C(5)	12(2)	10(2)	12(2)	-3(1)	2(1)	-3(1)
C(6)	13(2)	7(2)	10(2)	-2(1)	1(1)	-1(1)
C(7)	14(2)	16(2)	10(2)	-4(1)	0(1)	-3(1)
C(8)	17(2)	15(2)	11(2)	-1(1)	-1(1)	-3(1)
C(9)	17(2)	11(2)	13(2)	-2(1)	-4(1)	0(1)
C(10)	15(2)	10(2)	9(2)	-3(1)	-2(1)	-2(1)
C(11)	13(2)	12(2)	11(2)	-5(1)	-1(1)	0(1)
C(12)	16(2)	17(2)	18(2)	-5(1)	-4(1)	3(1)
C(13)	17(2)	33(2)	26(2)	-13(2)	0(2)	7(2)
C(14)	15(2)	32(2)	21(2)	-12(2)	4(2)	4(2)
C(15)	15(2)	18(2)	12(2)	-6(1)	1(1)	0(1)
C(16)	14(2)	10(2)	11(2)	0(1)	-1(1)	0(1)
C(17)	19(2)	11(2)	19(2)	-3(1)	-3(2)	-1(1)
C(18)	17(2)	11(2)	23(2)	-6(1)	-2(2)	-2(1)
C(19)	13(2)	16(2)	18(2)	-7(1)	-5(1)	1(1)
C(20)	8(2)	14(2)	13(2)	-7(1)	1(1)	-1(1)
C(21)	9(2)	13(2)	16(2)	-7(1)	1(1)	-2(1)
C(22)	9(2)	19(2)	14(2)	-7(1)	-1(1)	-2(1)
C(23)	17(2)	22(2)	9(2)	-2(1)	-2(1)	-2(1)
C(24)	11(2)	13(2)	14(2)	0(1)	2(1)	-2(1)
C(25)	11(2)	12(2)	13(2)	-2(1)	1(1)	-2(1)
C(26)	12(2)	12(2)	9(2)	-1(1)	-1(1)	-1(1)
C(27)	20(2)	14(2)	13(2)	-3(1)	0(1)	-4(1)
C(28)	20(2)	12(2)	17(2)	-5(1)	-2(2)	-3(1)
C(29)	18(2)	13(2)	17(2)	-8(1)	-3(1)	-2(1)
C(30)	15(2)	16(2)	8(2)	-7(1)	-2(1)	1(1)

table continued..

C(31)	15(2)	12(2)	15(2)	-3(1)	-1(1)	0(1)
C(32)	15(2)	16(2)	22(2)	-2(2)	0(2)	-1(1)
C(33)	16(2)	17(2)	26(2)	-3(2)	4(2)	1(2)
C(34)	14(2)	17(2)	17(2)	-5(1)	5(1)	-3(1)
C(35)	15(2)	10(2)	11(2)	-2(1)	2(1)	-3(1)
C(36)	15(2)	10(2)	12(2)	-4(1)	1(1)	0(1)
C(37)	14(2)	13(2)	13(2)	-3(1)	4(1)	-3(1)
C(38)	18(2)	11(2)	11(2)	0(1)	1(1)	-3(1)
C(39)	14(2)	13(2)	14(2)	-6(1)	-1(1)	0(1)
C(40)	13(2)	10(2)	12(2)	-5(1)	-1(1)	1(1)
C(41)	15(2)	7(2)	12(2)	-3(1)	0(1)	1(1)
C(42)	18(2)	18(2)	14(2)	-7(1)	-2(1)	0(1)
C(43)	12(2)	25(2)	21(2)	-5(2)	-3(2)	4(2)
C(44)	17(2)	24(2)	18(2)	-9(2)	5(2)	-4(2)
C(45)	17(2)	15(2)	14(2)	-7(1)	4(1)	-1(1)
C(50)	12(2)	14(2)	16(2)	-5(1)	2(1)	0(1)
C(51)	13(2)	14(2)	20(2)	-5(1)	3(1)	-4(1)
C(52)	16(2)	18(2)	26(2)	-13(2)	2(2)	-3(1)
C(53)	17(2)	19(2)	17(2)	-10(1)	-2(1)	-3(1)
C(54)	13(2)	14(2)	12(2)	-4(1)	0(1)	1(1)
C(55)	14(2)	13(2)	15(2)	-5(1)	-1(1)	0(1)
C(56)	20(2)	24(2)	21(2)	-10(2)	-6(2)	-1(2)
C(57)	36(2)	21(2)	14(2)	-1(2)	-6(2)	0(2)
C(58)	22(2)	16(2)	17(2)	-2(1)	-1(2)	0(2)
C(59)	12(2)	13(2)	12(2)	-4(1)	4(1)	0(1)
C(60)	8(2)	12(2)	15(2)	-3(1)	5(1)	1(1)
C(61)	20(2)	13(2)	15(2)	-2(1)	4(1)	-3(1)
C(62)	14(2)	11(2)	21(2)	-4(1)	6(1)	-3(1)
C(63)	13(2)	17(2)	22(2)	-10(2)	1(1)	0(1)
C(64)	14(2)	13(2)	12(2)	-4(1)	2(1)	1(1)
N(1)	13(1)	7(1)	10(1)	-1(1)	2(1)	-1(1)
N(2)	11(1)	10(1)	10(1)	-4(1)	3(1)	-2(1)
N(3)	14(1)	11(1)	9(1)	-3(1)	0(1)	-1(1)
N(4)	11(1)	11(1)	13(1)	-3(1)	1(1)	0(1)
N(5)	13(1)	8(1)	10(1)	-1(1)	-2(1)	-1(1)
N(6)	11(1)	11(1)	11(1)	-4(1)	-1(1)	-1(1)
N(7)	12(1)	9(1)	15(1)	-3(1)	2(1)	-2(1)

table continued...

N(8)	13(1)	5(1)	12(1)	-2(1)	1(1)	0(1)
N(9)	14(1)	11(1)	11(1)	-4(1)	1(1)	-1(1)
N(10)	11(1)	10(1)	14(1)	-4(1)	1(1)	0(1)
N(11)	11(1)	12(1)	11(1)	-5(1)	1(1)	0(1)
N(12)	11(1)	10(1)	11(1)	-3(1)	1(1)	1(1)
Ru(1)	11(1)	9(1)	8(1)	-2(1)	0(1)	-1(1)
Ru(2)	11(1)	9(1)	10(1)	-2(1)	1(1)	-1(1)
Cl(1)	18(1)	25(1)	25(1)	-9(1)	-3(1)	-1(1)
Cl(2)	17(1)	23(1)	20(1)	-2(1)	-3(1)	1(1)
Cl(3)	22(1)	20(1)	16(1)	-2(1)	0(1)	-4(1)
Cl(4)	20(1)	38(1)	23(1)	-14(1)	-5(1)	1(1)
O(1S)	22(1)	24(1)	16(1)	-6(1)	3(1)	0(1)
O(2S)	24(2)	26(2)	18(1)	-6(1)	6(1)	-2(1)
O(3S)	23(2)	21(1)	26(2)	-4(1)	1(1)	2(1)
O(4S)	27(2)	25(2)	22(1)	-3(1)	-2(1)	4(1)
O(5S)	26(2)	25(2)	23(1)	-7(1)	-3(1)	-4(1)
O(6S)	32(2)	47(2)	16(1)	-7(1)	-6(1)	3(1)
O(7S)	26(2)	31(2)	56(2)	-17(2)	-10(2)	-5(1)
O(8S)	36(2)	49(2)	26(2)	-6(2)	-12(1)	-9(2)

Table C.13 *Hydrogen coordinates (x 10^4) and isotropic displacement parameters ($Å^2$x 10^3) for $[Ru(terpy)_2](ClO_4)_2$.*

	x	y	z	U(eq)
H(1)	642	9253	1957	16
H(2)	-1554	9725	2397	20
H(3)	-2003	9512	3609	22
H(4)	-263	8743	4379	19
H(7)	1399	7748	5050	16
H(8)	3271	6789	5568	18
H(9)	5326	6542	4859	17
H(12)	7334	6661	4065	21
H(13)	9188	6732	3163	31

table continued..

H(14)	8697	7409	1977	27
H(15)	6451	8041	1710	18
H(16)	2586	6463	3393	16
H(17)	1540	5468	3106	21
H(18)	1036	5755	1937	20
H(19)	1637	7037	1065	18
H(22)	2327	8289	291	17
H(23)	2832	9690	-352	21
H(24)	3757	10496	216	17
H(27)	4796	11085	873	19
H(28)	5824	11585	1631	20
H(29)	5858	10767	2838	18
H(30)	4890	9469	3258	15
H(31)	525	14333	1864	17
H(32)	-1651	14820	2305	23
H(33)	-2127	14523	3536	26
H(34)	-423	13690	4293	20
H(37)	1244	12705	4962	17
H(38)	3110	11737	5466	17
H(39)	5173	11512	4761	16
H(42)	7201	11665	3962	19
H(43)	9064	11779	3056	25
H(44)	8580	12493	1870	23
H(45)	6306	13084	1616	18
H(50)	2510	11437	3234	17
H(51)	1418	10485	2908	19
H(52)	911	10836	1720	22
H(53)	1378	12168	910	20
H(56)	1703	13550	222	25
H(57)	2395	14913	-389	30
H(58)	3572	15599	171	24
H(61)	4942	16057	843	20
H(62)	5896	16512	1655	19
H(63)	5778	15678	2852	20
H(64)	4740	14409	3222	16

Table C.14 *Torsion angles [°] for $[Ru(terpy)_2](ClO_4)_2$.*

N(1)-C(1)-C(2)-C(3)	0.7(5)
C(1)-C(2)-C(3)-C(4)	-2.4(5)
C(2)-C(3)-C(4)-C(5)	0.5(5)
C(3)-C(4)-C(5)-N(1)	3.1(5)
C(3)-C(4)-C(5)-C(6)	-174.9(3)
N(1)-C(5)-C(6)-N(2)	6.7(4)
C(4)-C(5)-C(6)-N(2)	-175.3(3)
N(1)-C(5)-C(6)-C(7)	-169.6(3)
C(4)-C(5)-C(6)-C(7)	8.4(5)
N(2)-C(6)-C(7)-C(8)	-2.3(5)
C(5)-C(6)-C(7)-C(8)	173.7(3)
C(6)-C(7)-C(8)-C(9)	2.6(5)
C(7)-C(8)-C(9)-C(10)	0.4(5)
C(8)-C(9)-C(10)-N(2)	-3.9(5)
C(8)-C(9)-C(10)-C(11)	176.6(3)
N(2)-C(10)-C(11)-N(3)	-6.4(4)
C(9)-C(10)-C(11)-N(3)	173.1(3)
N(2)-C(10)-C(11)-C(12)	170.9(3)
C(9)-C(10)-C(11)-C(12)	-9.5(5)
N(3)-C(11)-C(12)-C(13)	0.1(5)
C(10)-C(11)-C(12)-C(13)	-177.1(3)
C(11)-C(12)-C(13)-C(14)	-1.1(6)
C(12)-C(13)-C(14)-C(15)	1.3(6)
C(13)-C(14)-C(15)-N(3)	-0.6(6)
N(4)-C(16)-C(17)-C(18)	0.0(5)
C(16)-C(17)-C(18)-C(19)	0.8(5)
C(17)-C(18)-C(19)-C(20)	-0.2(5)
C(18)-C(19)-C(20)-N(4)	-1.2(5)
C(18)-C(19)-C(20)-C(21)	-179.0(3)
N(4)-C(20)-C(21)-N(5)	-0.7(4)
C(19)-C(20)-C(21)-N(5)	177.2(3)
N(4)-C(20)-C(21)-C(22)	-178.2(3)
C(19)-C(20)-C(21)-C(22)	-0.4(5)
N(5)-C(21)-C(22)-C(23)	-3.1(5)
C(20)-C(21)-C(22)-C(23)	174.2(3)

table continued..

C(21)-C(22)-C(23)-C(24)	2.2(5)
C(22)-C(23)-C(24)-C(25)	-0.5(5)
C(23)-C(24)-C(25)-N(5)	-0.2(5)
C(23)-C(24)-C(25)-C(26)	178.4(3)
N(5)-C(25)-C(26)-N(6)	-5.3(4)
C(24)-C(25)-C(26)-N(6)	176.0(3)
N(5)-C(25)-C(26)-C(27)	174.6(3)
C(24)-C(25)-C(26)-C(27)	-4.1(6)
N(6)-C(26)-C(27)-C(28)	2.7(5)
C(25)-C(26)-C(27)-C(28)	-177.2(3)
C(26)-C(27)-C(28)-C(29)	-1.9(6)
C(27)-C(28)-C(29)-C(30)	0.1(5)
C(28)-C(29)-C(30)-N(6)	0.9(5)
N(7)-C(31)-C(32)-C(33)	0.0(5)
C(31)-C(32)-C(33)-C(34)	-1.8(5)
C(32)-C(33)-C(34)-C(35)	0.3(5)
C(33)-C(34)-C(35)-N(7)	2.9(5)
C(33)-C(34)-C(35)-C(36)	-176.9(3)
N(7)-C(35)-C(36)-N(8)	5.7(4)
C(34)-C(35)-C(36)-N(8)	-174.5(3)
N(7)-C(35)-C(36)-C(37)	-173.1(3)
C(34)-C(35)-C(36)-C(37)	6.7(6)
N(8)-C(36)-C(37)-C(38)	-3.7(5)
C(35)-C(36)-C(37)-C(38)	175.0(3)
C(36)-C(37)-C(38)-C(39)	3.8(5)
C(37)-C(38)-C(39)-C(40)	-0.5(5)
C(38)-C(39)-C(40)-N(8)	-2.9(5)
C(38)-C(39)-C(40)-C(41)	175.6(3)
N(8)-C(40)-C(41)-N(9)	-7.0(4)
C(39)-C(40)-C(41)-N(9)	174.4(3)
N(8)-C(40)-C(41)-C(42)	169.4(3)
C(39)-C(40)-C(41)-C(42)	-9.2(5)
N(9)-C(41)-C(42)-C(43)	-0.4(5)
C(40)-C(41)-C(42)-C(43)	-176.6(3)
C(41)-C(42)-C(43)-C(44)	-0.3(5)
C(42)-C(43)-C(44)-C(45)	0.5(6)

table continued…

C(43)-C(44)-C(45)-N(9)	-0.1(6)
N(10)-C(50)-C(51)-C(52)	2.2(5)
C(50)-C(51)-C(52)-C(53)	-2.0(5)
C(51)-C(52)-C(53)-C(54)	0.9(5)
C(52)-C(53)-C(54)-N(10)	0.1(5)
C(52)-C(53)-C(54)-C(55)	179.7(3)
N(10)-C(54)-C(55)-N(11)	3.8(4)
C(53)-C(54)-C(55)-N(11)	-175.8(3)
N(10)-C(54)-C(55)-C(56)	-172.8(4)
C(53)-C(54)-C(55)-C(56)	7.6(6)
N(11)-C(55)-C(56)-C(57)	2.4(6)
C(54)-C(55)-C(56)-C(57)	178.7(4)
C(55)-C(56)-C(57)-C(58)	-1.7(6)
C(56)-C(57)-C(58)-C(59)	0.4(6)
C(57)-C(58)-C(59)-N(11)	0.3(6)
C(57)-C(58)-C(59)-C(60)	-176.1(4)
N(11)-C(59)-C(60)-N(12)	-8.1(4)
C(58)-C(59)-C(60)-N(12)	168.5(3)
N(11)-C(59)-C(60)-C(61)	172.5(3)
C(58)-C(59)-C(60)-C(61)	-10.9(6)
N(12)-C(60)-C(61)-C(62)	-0.7(5)
C(59)-C(60)-C(61)-C(62)	178.7(3)
C(60)-C(61)-C(62)-C(63)	0.2(5)
C(61)-C(62)-C(63)-C(64)	0.3(5)
C(62)-C(63)-C(64)-N(12)	-0.3(5)
C(2)-C(1)-N(1)-C(5)	2.8(5)
C(2)-C(1)-N(1)-Ru(1)	-176.3(2)
C(4)-C(5)-N(1)-C(1)	-4.7(5)
C(6)-C(5)-N(1)-C(1)	173.4(3)
C(4)-C(5)-N(1)-Ru(1)	174.5(3)
C(6)-C(5)-N(1)-Ru(1)	-7.4(3)
C(9)-C(10)-N(2)-C(6)	4.3(5)
C(11)-C(10)-N(2)-C(6)	-176.2(3)
C(9)-C(10)-N(2)-Ru(1)	-170.7(2)
C(11)-C(10)-N(2)-Ru(1)	8.9(4)
C(7)-C(6)-N(2)-C(10)	-1.1(5)

table continued..

C(5)-C(6)-N(2)-C(10)	-177.7(3)
C(7)-C(6)-N(2)-Ru(1)	173.9(2)
C(5)-C(6)-N(2)-Ru(1)	-2.7(4)
C(14)-C(15)-N(3)-C(11)	-0.3(5)
C(14)-C(15)-N(3)-Ru(1)	175.7(3)
C(12)-C(11)-N(3)-C(15)	0.6(5)
C(10)-C(11)-N(3)-C(15)	178.0(3)
C(12)-C(11)-N(3)-Ru(1)	-176.0(3)
C(10)-C(11)-N(3)-Ru(1)	1.4(4)
C(17)-C(16)-N(4)-C(20)	-1.3(5)
C(17)-C(16)-N(4)-Ru(1)	175.1(3)
C(19)-C(20)-N(4)-C(16)	2.0(5)
C(21)-C(20)-N(4)-C(16)	179.8(3)
C(19)-C(20)-N(4)-Ru(1)	-174.9(3)
C(21)-C(20)-N(4)-Ru(1)	2.9(4)
C(22)-C(21)-N(5)-C(25)	2.5(5)
C(20)-C(21)-N(5)-C(25)	-175.2(3)
C(22)-C(21)-N(5)-Ru(1)	175.6(3)
C(20)-C(21)-N(5)-Ru(1)	-2.1(4)
C(24)-C(25)-N(5)-C(21)	-0.7(5)
C(26)-C(25)-N(5)-C(21)	-179.5(3)
C(24)-C(25)-N(5)-Ru(1)	-173.9(3)
C(26)-C(25)-N(5)-Ru(1)	7.3(4)
C(29)-C(30)-N(6)-C(26)	0.0(5)
C(29)-C(30)-N(6)-Ru(1)	176.4(3)
C(27)-C(26)-N(6)-C(30)	-1.8(5)
C(25)-C(26)-N(6)-C(30)	178.1(3)
C(27)-C(26)-N(6)-Ru(1)	-178.8(3)
C(25)-C(26)-N(6)-Ru(1)	1.1(4)
C(32)-C(31)-N(7)-C(35)	3.2(5)
C(32)-C(31)-N(7)-Ru(2)	-175.9(3)
C(34)-C(35)-N(7)-C(31)	-4.6(5)
C(36)-C(35)-N(7)-C(31)	175.2(3)
C(34)-C(35)-N(7)-Ru(2)	174.6(3)
C(36)-C(35)-N(7)-Ru(2)	-5.6(3)
C(39)-C(40)-N(8)-C(36)	3.0(5)

table continued..

C(41)-C(40)-N(8)-C(36)	-175.7(3)
C(39)-C(40)-N(8)-Ru(2)	-172.4(2)
C(41)-C(40)-N(8)-Ru(2)	8.9(4)
C(37)-C(36)-N(8)-C(40)	0.4(5)
C(35)-C(36)-N(8)-C(40)	-178.5(3)
C(37)-C(36)-N(8)-Ru(2)	175.9(2)
C(35)-C(36)-N(8)-Ru(2)	-3.0(4)
C(44)-C(45)-N(9)-C(41)	-0.5(5)
C(44)-C(45)-N(9)-Ru(2)	173.5(3)
C(42)-C(41)-N(9)-C(45)	0.8(5)
C(40)-C(41)-N(9)-C(45)	177.2(3)
C(42)-C(41)-N(9)-Ru(2)	-174.1(3)
C(40)-C(41)-N(9)-Ru(2)	2.4(3)
C(51)-C(50)-N(10)-C(54)	-1.2(5)
C(51)-C(50)-N(10)-Ru(2)	176.2(3)
C(53)-C(54)-N(10)-C(50)	0.0(5)
C(55)-C(54)-N(10)-C(50)	-179.5(3)
C(53)-C(54)-N(10)-Ru(2)	-177.8(3)
C(55)-C(54)-N(10)-Ru(2)	2.7(4)
C(56)-C(55)-N(11)-C(59)	-1.8(5)
C(54)-C(55)-N(11)-C(59)	-178.6(3)
C(56)-C(55)-N(11)-Ru(2)	167.8(3)
C(54)-C(55)-N(11)-Ru(2)	-9.0(4)
C(58)-C(59)-N(11)-C(55)	0.4(5)
C(60)-C(59)-N(11)-C(55)	177.3(3)
C(58)-C(59)-N(11)-Ru(2)	-169.2(3)
C(60)-C(59)-N(11)-Ru(2)	7.7(4)
C(63)-C(64)-N(12)-C(60)	-0.2(5)
C(63)-C(64)-N(12)-Ru(2)	175.5(3)
C(61)-C(60)-N(12)-C(64)	0.7(5)
C(59)-C(60)-N(12)-C(64)	-178.7(3)
C(61)-C(60)-N(12)-Ru(2)	-175.6(3)
C(59)-C(60)-N(12)-Ru(2)	5.0(4)
C(21)-N(5)-Ru(1)-N(2)	-57.2(17)
C(25)-N(5)-Ru(1)-N(2)	116.2(16)
C(21)-N(5)-Ru(1)-N(4)	2.9(2)

table continued..

C(25)-N(5)-Ru(1)-N(4)	176.2(3)
C(21)-N(5)-Ru(1)-N(1)	-85.4(3)
C(25)-N(5)-Ru(1)-N(1)	88.0(3)
C(21)-N(5)-Ru(1)-N(3)	94.6(3)
C(25)-N(5)-Ru(1)-N(3)	-92.1(3)
C(21)-N(5)-Ru(1)-N(6)	-178.7(3)
C(25)-N(5)-Ru(1)-N(6)	-5.3(2)
C(10)-N(2)-Ru(1)-N(5)	145.7(15)
C(6)-N(2)-Ru(1)-N(5)	-29.4(17)
C(10)-N(2)-Ru(1)-N(4)	86.3(2)
C(6)-N(2)-Ru(1)-N(4)	-88.9(2)
C(10)-N(2)-Ru(1)-N(1)	174.2(3)
C(6)-N(2)-Ru(1)-N(1)	-0.9(2)
C(10)-N(2)-Ru(1)-N(3)	-6.5(2)
C(6)-N(2)-Ru(1)-N(3)	178.4(3)
C(10)-N(2)-Ru(1)-N(6)	-93.5(2)
C(6)-N(2)-Ru(1)-N(6)	91.4(2)
C(16)-N(4)-Ru(1)-N(5)	-179.6(3)
C(20)-N(4)-Ru(1)-N(5)	-3.1(2)
C(16)-N(4)-Ru(1)-N(2)	-3.1(3)
C(20)-N(4)-Ru(1)-N(2)	173.5(2)
C(16)-N(4)-Ru(1)-N(1)	-82.0(3)
C(20)-N(4)-Ru(1)-N(1)	94.5(2)
C(16)-N(4)-Ru(1)-N(3)	76.7(3)
C(20)-N(4)-Ru(1)-N(3)	-106.7(2)
C(16)-N(4)-Ru(1)-N(6)	176.3(3)
C(20)-N(4)-Ru(1)-N(6)	-7.2(4)
C(1)-N(1)-Ru(1)-N(5)	1.8(3)
C(5)-N(1)-Ru(1)-N(5)	-177.3(2)
C(1)-N(1)-Ru(1)-N(2)	-176.3(3)
C(5)-N(1)-Ru(1)-N(2)	4.6(2)
C(1)-N(1)-Ru(1)-N(4)	-77.4(3)
C(5)-N(1)-Ru(1)-N(4)	103.4(2)
C(1)-N(1)-Ru(1)-N(3)	-178.1(3)
C(5)-N(1)-Ru(1)-N(3)	2.7(4)
C(1)-N(1)-Ru(1)-N(6)	81.3(3)

table continued...

C(5)-N(1)-Ru(1)-N(6)	-97.9(2)
C(15)-N(3)-Ru(1)-N(5)	8.1(3)
C(11)-N(3)-Ru(1)-N(5)	-175.7(2)
C(15)-N(3)-Ru(1)-N(2)	-173.8(3)
C(11)-N(3)-Ru(1)-N(2)	2.4(2)
C(15)-N(3)-Ru(1)-N(4)	88.2(3)
C(11)-N(3)-Ru(1)-N(4)	-95.6(2)
C(15)-N(3)-Ru(1)-N(1)	-171.9(3)
C(11)-N(3)-Ru(1)-N(1)	4.3(4)
C(15)-N(3)-Ru(1)-N(6)	-70.4(3)
C(11)-N(3)-Ru(1)-N(6)	105.8(2)
C(30)-N(6)-Ru(1)-N(5)	-174.6(3)
C(26)-N(6)-Ru(1)-N(5)	2.0(2)
C(30)-N(6)-Ru(1)-N(2)	8.8(3)
C(26)-N(6)-Ru(1)-N(2)	-174.5(2)
C(30)-N(6)-Ru(1)-N(4)	-170.5(3)
C(26)-N(6)-Ru(1)-N(4)	6.2(4)
C(30)-N(6)-Ru(1)-N(1)	88.7(3)
C(26)-N(6)-Ru(1)-N(1)	-94.6(2)
C(30)-N(6)-Ru(1)-N(3)	-70.1(3)
C(26)-N(6)-Ru(1)-N(3)	106.6(2)
C(55)-N(11)-Ru(2)-N(8)	-60.0(15)
C(59)-N(11)-Ru(2)-N(8)	109.8(14)
C(55)-N(11)-Ru(2)-N(7)	-80.1(3)
C(59)-N(11)-Ru(2)-N(7)	89.7(3)
C(55)-N(11)-Ru(2)-N(10)	8.3(3)
C(59)-N(11)-Ru(2)-N(10)	178.1(3)
C(55)-N(11)-Ru(2)-N(12)	-173.9(3)
C(59)-N(11)-Ru(2)-N(12)	-4.1(2)
C(55)-N(11)-Ru(2)-N(9)	101.1(3)
C(59)-N(11)-Ru(2)-N(9)	-89.1(3)
C(40)-N(8)-Ru(2)-N(11)	155.4(13)
C(36)-N(8)-Ru(2)-N(11)	-20.3(15)
C(40)-N(8)-Ru(2)-N(7)	175.7(3)
C(36)-N(8)-Ru(2)-N(7)	0.1(2)
C(40)-N(8)-Ru(2)-N(10)	87.8(3)

table continued…

C(36)-N(8)-Ru(2)-N(10)	-87.8(2)
C(40)-N(8)-Ru(2)-N(12)	-91.6(2)
C(36)-N(8)-Ru(2)-N(12)	92.8(3)
C(40)-N(8)-Ru(2)-N(9)	-6.1(2)
C(36)-N(8)-Ru(2)-N(9)	178.3(3)
C(31)-N(7)-Ru(2)-N(11)	0.6(3)
C(35)-N(7)-Ru(2)-N(11)	-178.5(2)
C(31)-N(7)-Ru(2)-N(8)	-177.8(3)
C(35)-N(7)-Ru(2)-N(8)	3.1(2)
C(31)-N(7)-Ru(2)-N(10)	-78.6(3)
C(35)-N(7)-Ru(2)-N(10)	102.3(2)
C(31)-N(7)-Ru(2)-N(12)	80.5(3)
C(35)-N(7)-Ru(2)-N(12)	-98.6(2)
C(31)-N(7)-Ru(2)-N(9)	177.4(3)
C(35)-N(7)-Ru(2)-N(9)	-1.7(4)
C(50)-N(10)-Ru(2)-N(11)	176.8(3)
C(54)-N(10)-Ru(2)-N(11)	-5.6(2)
C(50)-N(10)-Ru(2)-N(8)	-7.4(3)
C(54)-N(10)-Ru(2)-N(8)	170.1(2)
C(50)-N(10)-Ru(2)-N(7)	-86.8(3)
C(54)-N(10)-Ru(2)-N(7)	90.8(2)
C(50)-N(10)-Ru(2)-N(12)	170.9(3)
C(54)-N(10)-Ru(2)-N(12)	-11.5(5)
C(50)-N(10)-Ru(2)-N(9)	72.2(3)
C(54)-N(10)-Ru(2)-N(9)	-110.3(2)
C(64)-N(12)-Ru(2)-N(11)	-176.6(3)
C(60)-N(12)-Ru(2)-N(11)	-0.7(2)
C(64)-N(12)-Ru(2)-N(8)	7.7(3)
C(60)-N(12)-Ru(2)-N(8)	-176.5(2)
C(64)-N(12)-Ru(2)-N(7)	88.0(3)
C(60)-N(12)-Ru(2)-N(7)	-96.1(2)
C(64)-N(12)-Ru(2)-N(10)	-170.6(3)
C(60)-N(12)-Ru(2)-N(10)	5.2(4)
C(64)-N(12)-Ru(2)-N(9)	-70.5(3)
C(60)-N(12)-Ru(2)-N(9)	105.3(2)
C(45)-N(9)-Ru(2)-N(11)	8.9(3)

table continued..

C(41)-N(9)-Ru(2)-N(11)	-176.8(2)
C(45)-N(9)-Ru(2)-N(8)	-172.6(3)
C(41)-N(9)-Ru(2)-N(8)	1.7(2)
C(45)-N(9)-Ru(2)-N(7)	-167.9(3)
C(41)-N(9)-Ru(2)-N(7)	6.4(4)
C(45)-N(9)-Ru(2)-N(10)	89.3(3)
C(41)-N(9)-Ru(2)-N(10)	-96.4(2)
C(45)-N(9)-Ru(2)-N(12)	-69.6(3)
C(41)-N(9)-Ru(2)-N(12)	104.7(2)

Symmetry transformations used to generate equivalent atoms:

APPENDIX D

KINETIC GRAPHS

APPENDIX D

UV-VISIBLE KINETIC SCANS FOR THE REACTIONS OF $[Pt(bpma)(OH_2)]^{2+}$ WITH THIOLS

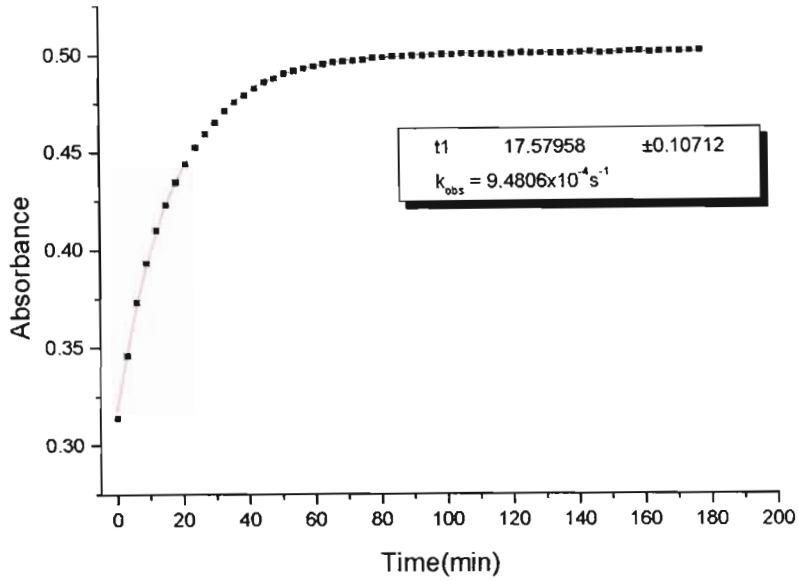

Figure D.1 *Typical UV-Visible kinetic trace for the reaction of* $[Pt(bpma)(OH_2)]^{2+}$ *(4.94 x* 10^{-5} *M) with L-cysteine (5.14 x* 10^{-3} *M).*

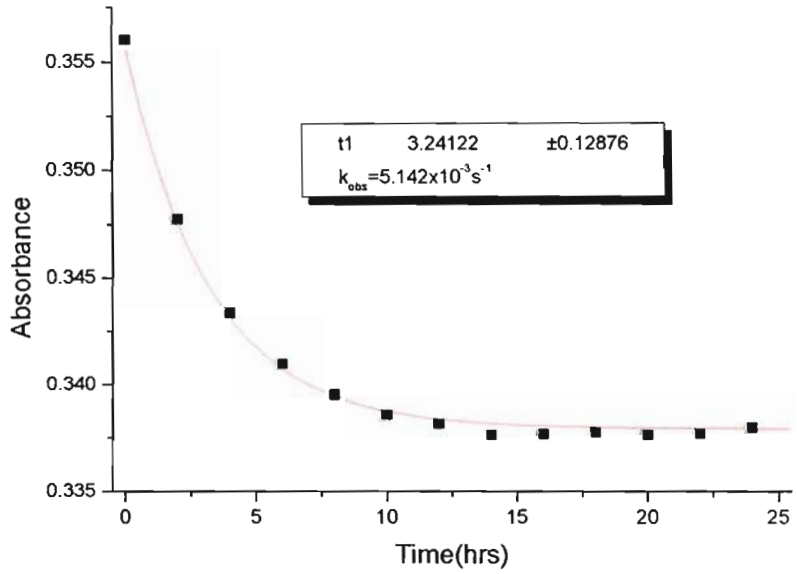

Figure D.2 *Typical UV-Visible kinetic trace for the reaction of* $[Pt(bpma)(OH_2)]^{2+}$ *(4.94 x* 10^{-5} *M) with DL-penicillamine(7.70 x* 10^{-3} *M).*

KINETIC TRIALS FOR THE REACTIONS OF $[Pt(bpma)(OH_2)]^{2+}$ WITH NUCLEOPHILES, NaBr, NaCl, NaI, NaSCN, AND TMTU CARRIED AT 25 °C

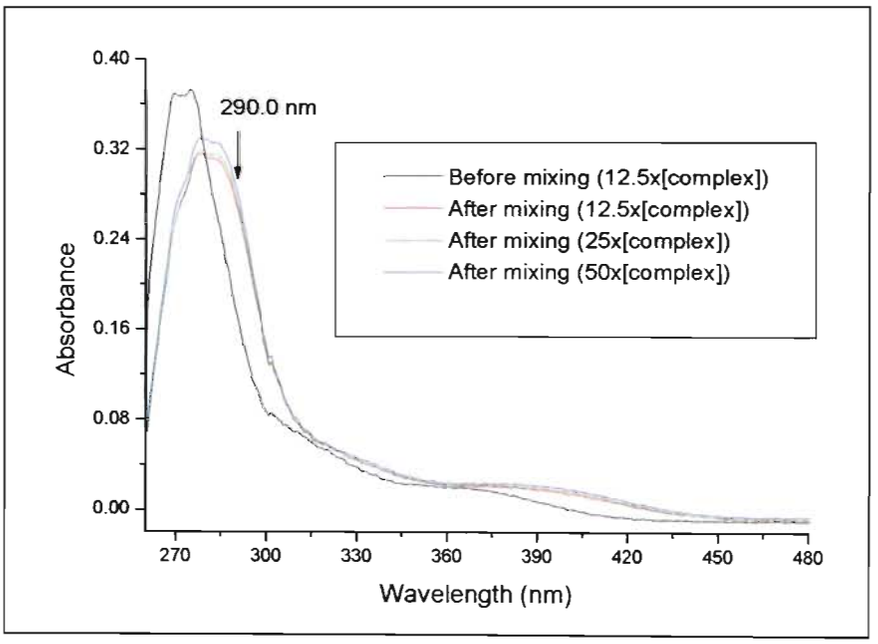

Figure D.3 *Kinetic trials for the reactions of $[Pt(bpma)(OH_2)]^{2+}$ (5.0×10^{-5} M) with NaBr.*

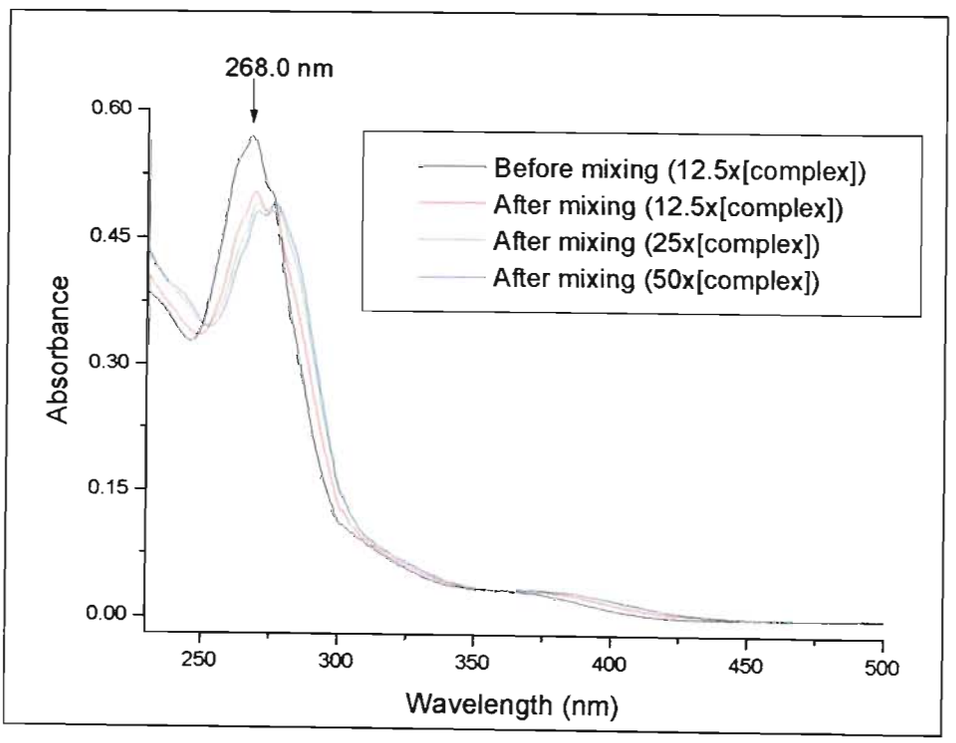

Figure D.4 *Kinetic trials for the reactions of $[Pt(bpma)(OH_2)]^{2+}$ (5.0×10^{-5} M) with NaCl.*

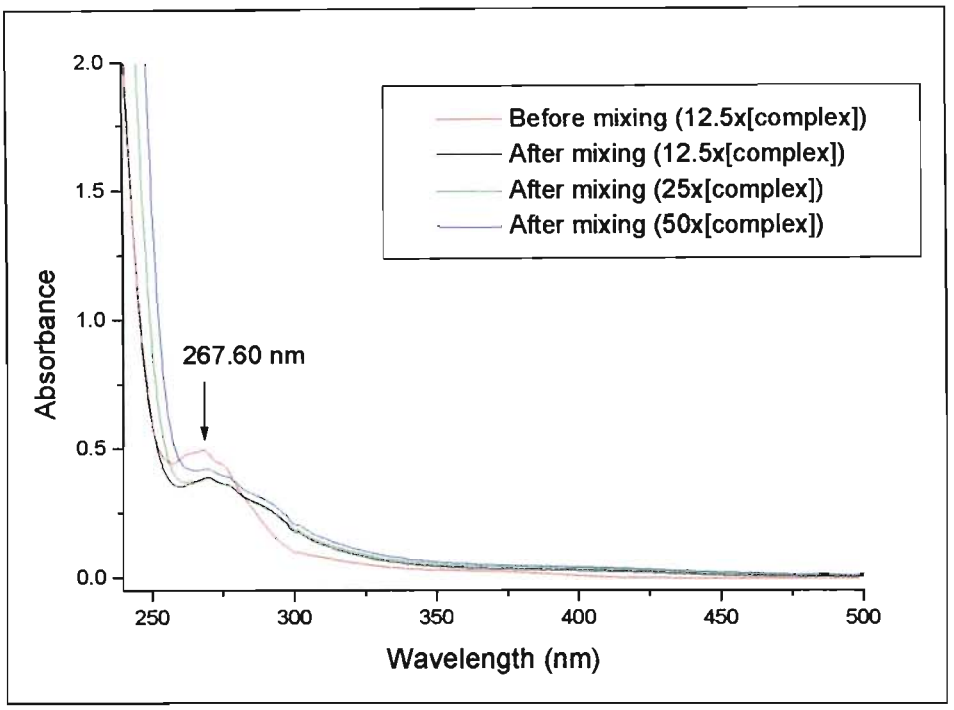

Figure D.5 *Kinetic trials for the reactions of* $[Pt(bpma)(OH_2)]^{2+}$ *(5.0 x* 10^{-5} *M) with NaI.*

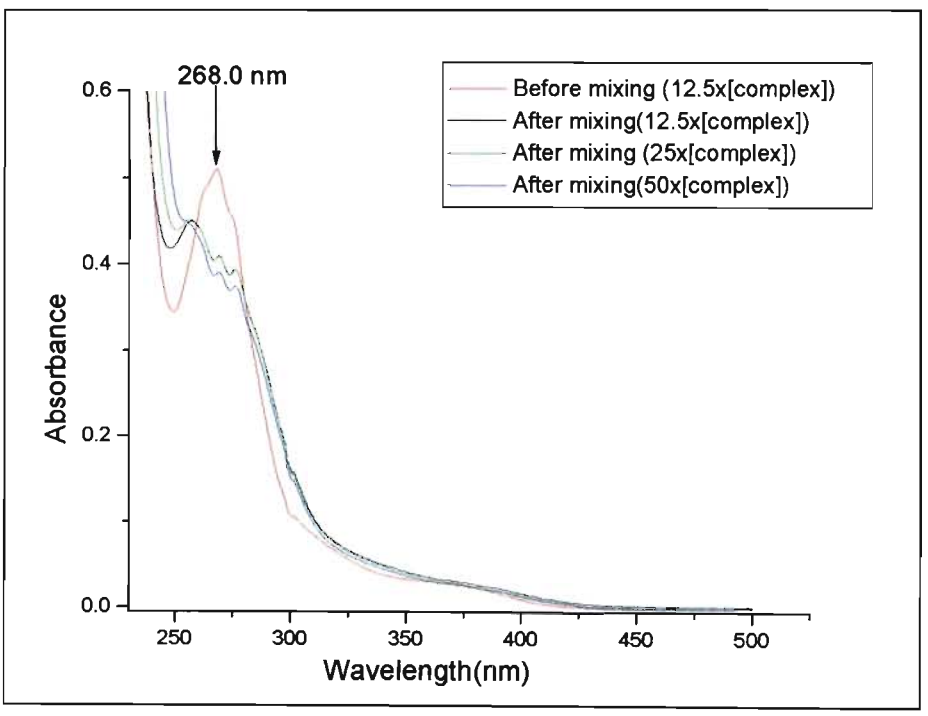

Figure D.6 *Kinetic trials for the reactions of* $[Pt(bpma)(OH_2)]^{2+}$ *(5.0 x* 10^{-5} *M) with NaSCN.*

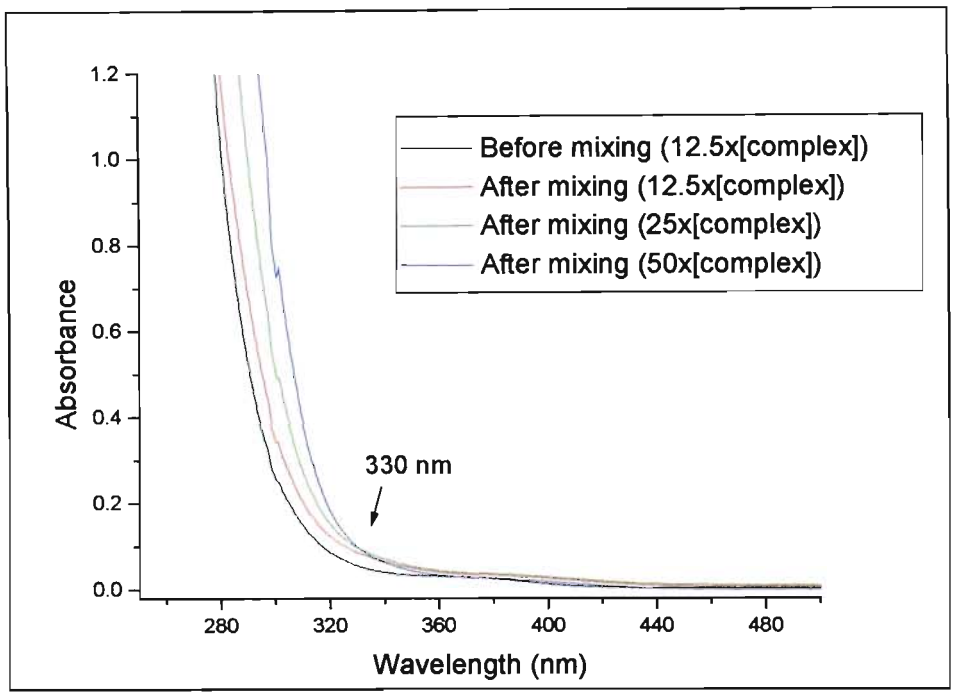

Figure D.7 *Kinetic trials for the reactions of $[Pt(bpma)(OH_2)]^{2+}$ (5.0×10^{-5} M) with TMTU.*

PLOTS OBTAINED FOR TEMPERATURE DEPENDENCE STUDIES FOR THE REACTIONS OF $[Pt(bpma)(OH_2)]^{2+}$ WITH NON-THIOLS NUCLEOPHILES

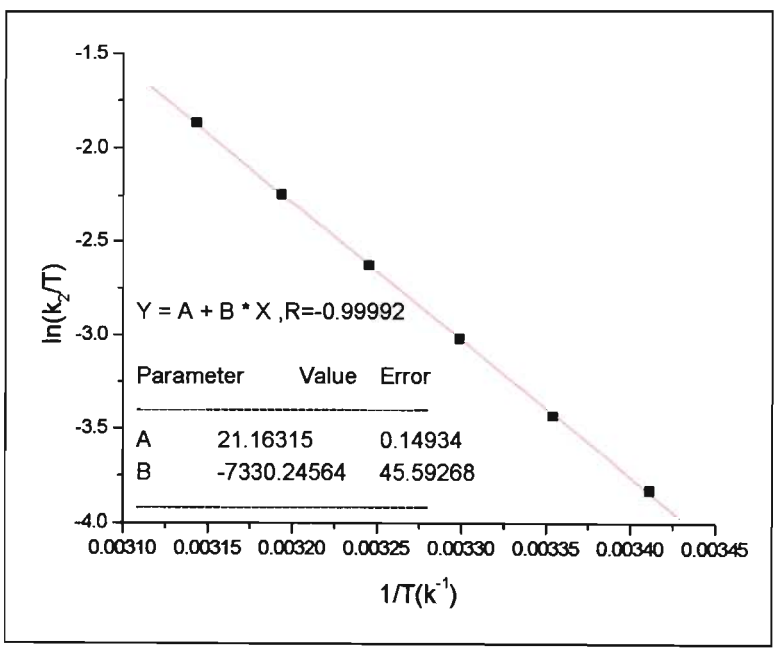

Figure D.8 *Temperature Dependence plot for the reactions of $[Pt(bpma)(OH_2)]^{2+}$ (5.0×10^{-5} M) with NaCl.*

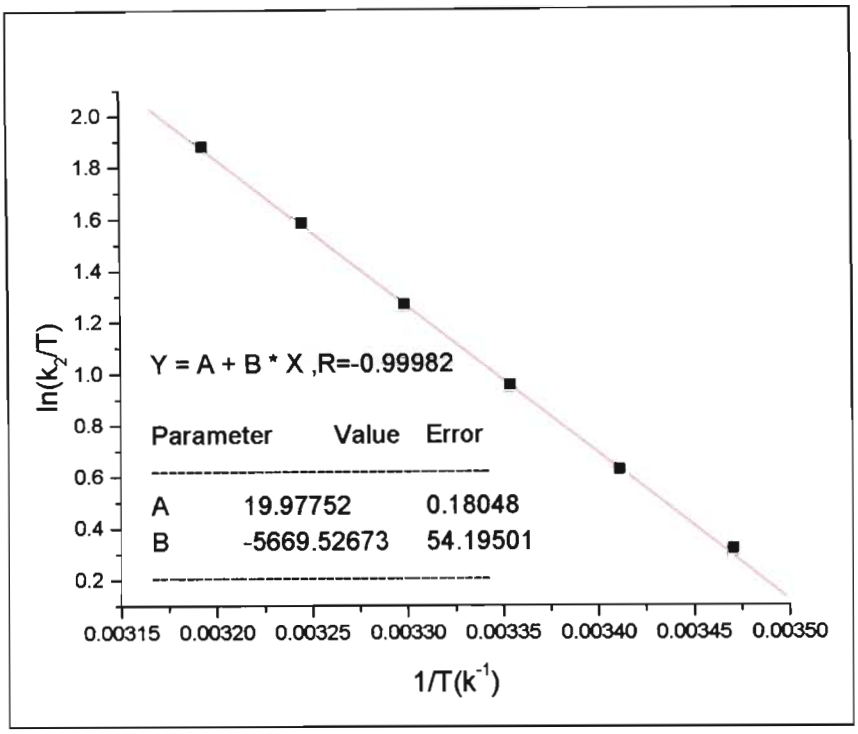

Figure D.9 *Temperature Dependence plot for the reactions of* $[Pt(bpma)(OH_2)]^{2+}$ *(5.0 x* 10^{-5} *M) with NaI.*

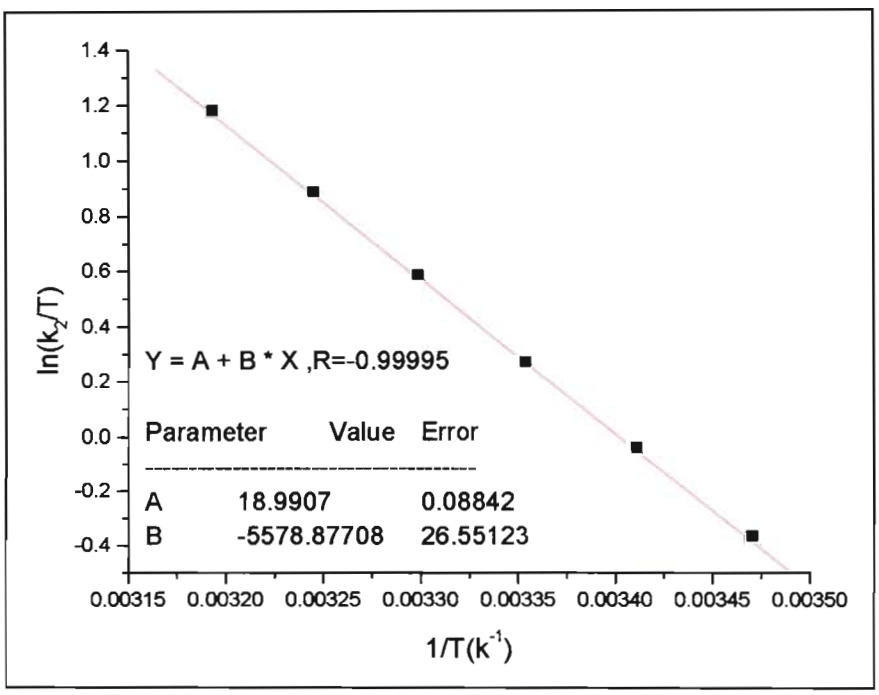

Figure D.10 *Temperature Dependence plot for the reactions of* $[Pt(bpma)(OH_2)]^{2+}$ *(5.0 x* 10^{-5} *M) with NaSCN.*

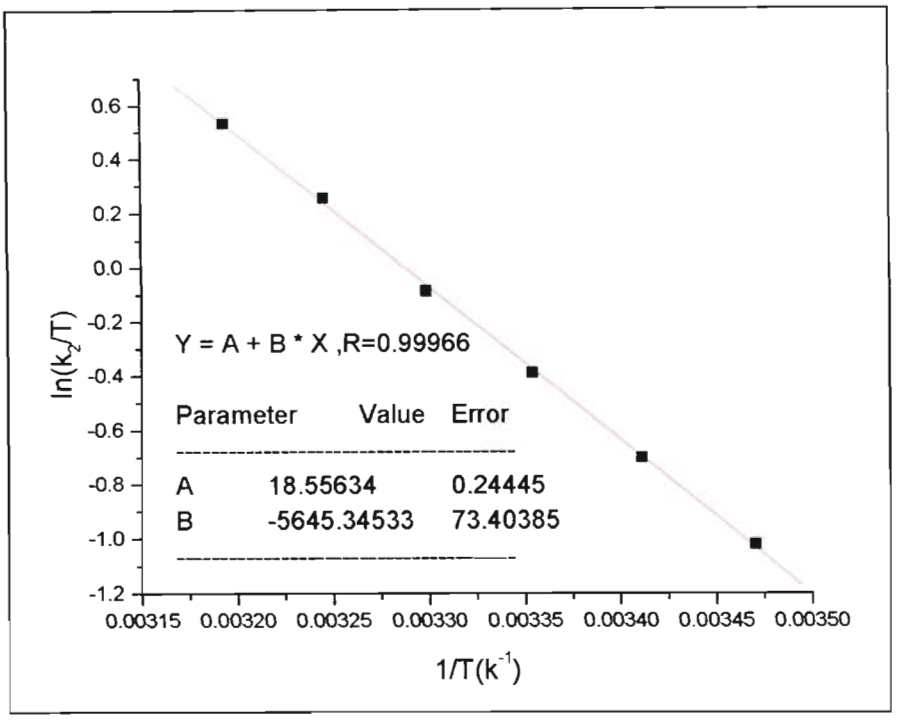

Figure D.11 *Temperature Dependence plot for the reactions of* $[Pt(bpma)(OH_2)]^{2+}$ *(5.0 x* 10^{-5} *M) with TMTU.*

KINETIC TRIALS FOR THE REACTIONS OF $[Pd(bpma)(OH_2)]^{2+}$ WITH DMTU AND TMTU CARRIED AT 25°C

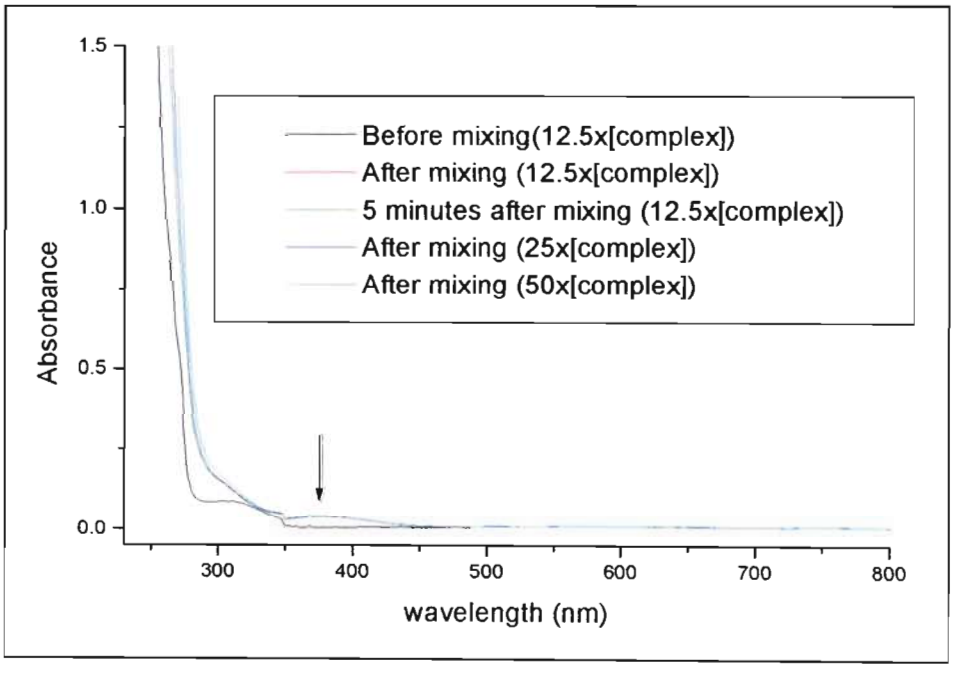

Figure D.12 *UV-Vis scans for the reactions of* $[Pd(bpma)(OH_2)]^{2+}$ *(4.62 x* 10^{-4} *M) with TU.*

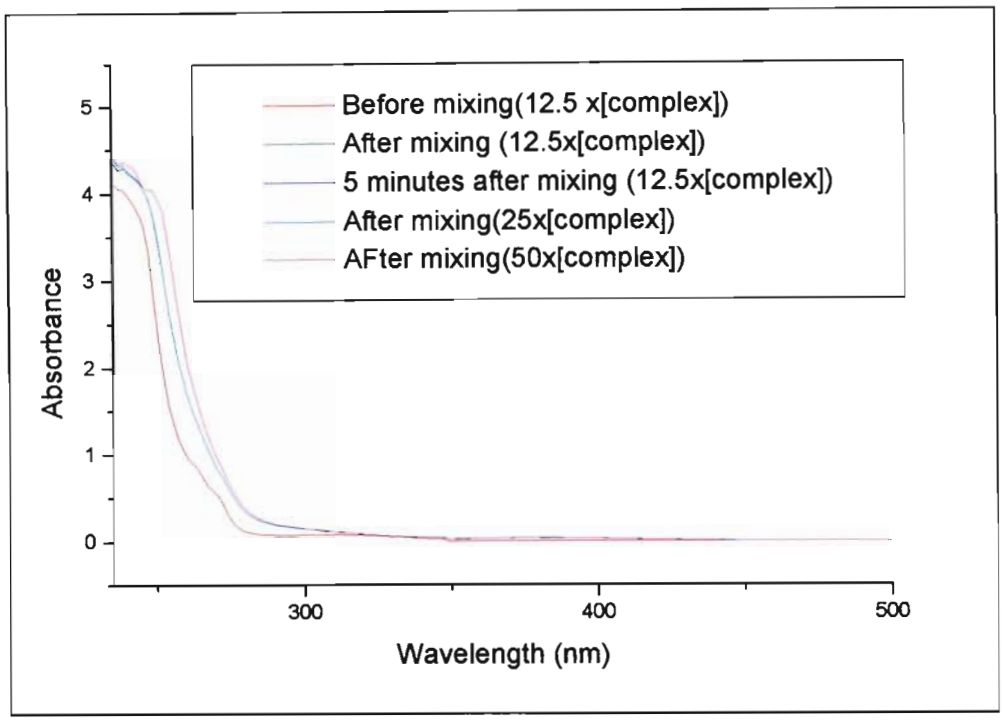

Figure D.13 *UV-Vis scans for the reactions of* $[Pd(bpma)(OH_2)]^{2+}$ *(4.62 x* 10^{-4} *M) with DMTU.*

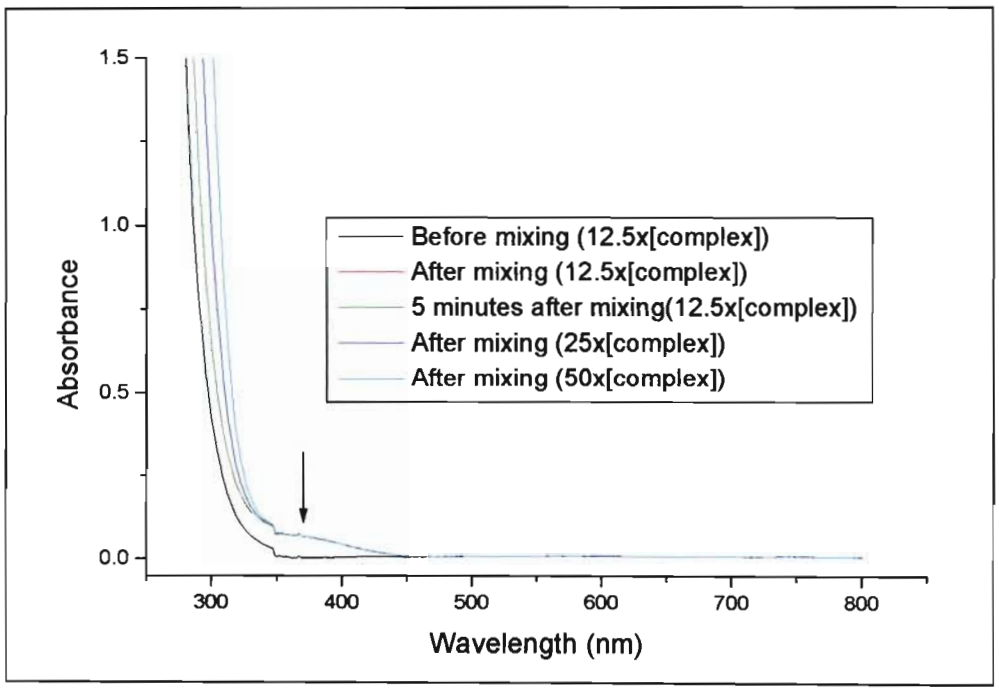

Figure D.14 *UV-Vis scans for the reactions of* $[Pd(bpma)(OH_2)]^{2+}$ *(4.62 x* 10^{-4} *M) with TMTU.*

APPENDIX E

OTHER COMPLEXES SYNTHESIZED

APPENDIX E

RESULTS AND DISCUSSION FOR THE OTHER COMPLEXES SYNTHESIZED

An attempt was made to synthesize complexes of the type $[Ru(terpy)(OH_2)_3]^{2+}$. The primary aim of synthesizing this complex was to determine whether all three water molecules from the complex are substituted simultaneously, or whether the two axial water molecules (denoted by (a) in **Figure E.1)** are substituted first before the water molecule (b).

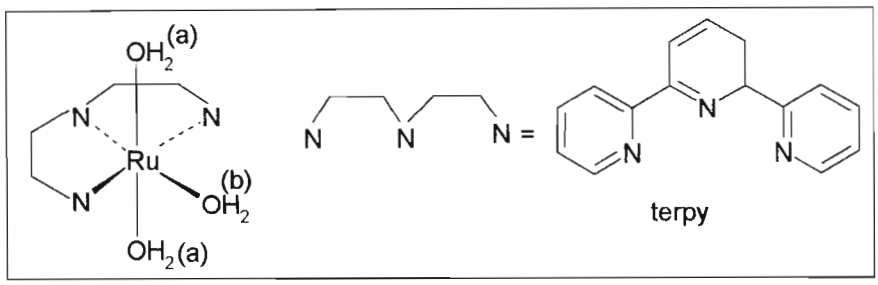

Figure E.1 *Proposed structure for* $[Ru(terpy)(OH_2)_3]^{2+}$.

Synthesis of this complex was attempted following two different routes. The first route involved the removal of the chloride ions from the metal chloride using $AgClO_4$ to form $[Ru(ClO_4)_3.3H_2O]$ which was then reacted with an equivalent amount of terpyridine in aqueous ethanol solution to afford $[Ru(terpy)(OH_2)_3]^{2+}$. The second route involved the removal of the chloride ions from $[Ru(terpy)Cl_3]$ using $AgClO_4$ in aqueous ethanol solution. The desired product was not isolated from either of these routes due to the difficulty in getting the complex to precipitate out of the aqueous solution.

A NMR spectrum of the crude $[Ru(terpy)(OH_2)_3]^{2+}$ product formed by following the first route was recorded in acetonitrile. Since acetonitrile is a strong coordinating solvent, it was expected that if the desired product did form, three acetonitrile molecules would replace the three water molecules in the coordination sphere to form

$[Ru(terpy)(CH_3CN)_3]^{2+}$. However, the main interest was to investigate if the terpy did bind to the metal.

It was expected that if the terpyridine did coordinate to the metal centre, there would be a shift in the resonances of the protons. When comparing the ^{1}H-NMR spectrum of this complex with the ^{1}H-NMR spectrum of the uncoordinated terpyridine ligand given in **Figure A.4**, **APPENDIX A**. It is clear that the signals due to the ^{1}H-NMR terpyridine protons are all present and they have shifted downfield compared to those of the uncoordinated terpyridine. This is an indication that the terpyridine ligand did coordinate to the metal.

An attempt was made to grow single crystals suitable for X-ray analysis from the crude by slow evaporation of the acetonitrile complex solution with diethyl ether. No single crystals were obtained for the complex isolated using the first route. Analysis of the X-ray data collected for the single crystal of the complex isolated following the second route, showed that the complex formed from this route was $[Ru(terpy)_2]^{2+}$. An ORTEP diagram representing the cation X-ray structure of $[Ru(terpy)_2]^{2+}$ is given in **Figure E.2**.

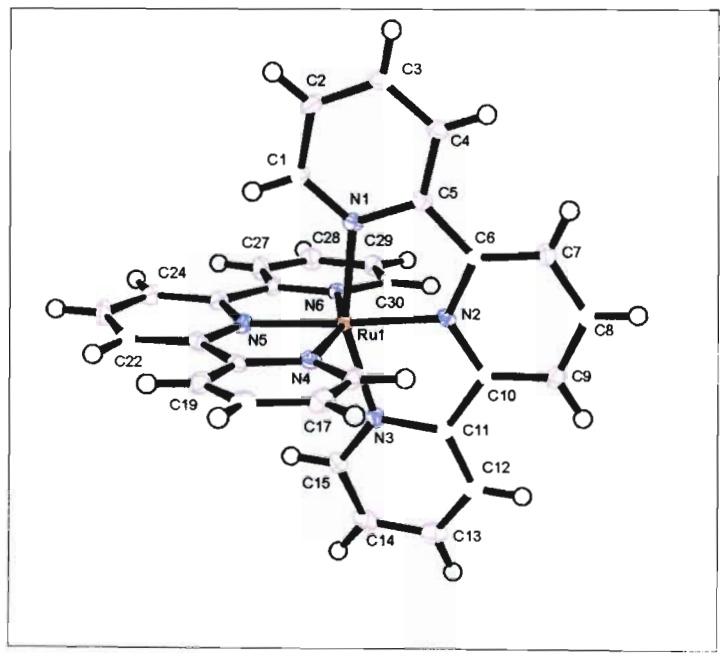

Figure E.2 *ORTEP diagram representing the X-ray structure of the cation in* $[Ru(terpy)_2](ClO_4)_2$.

APPENDIX F

A COPY OF THE MANUSCRIPT TO BE PUBLISHED

APPENDIX F

A COPY OF THE MANUSCRIPT TO BE PUBLISHED

AUTHOR'S PROOF
(Spare Set-Please Retain)

Transition Metal Chemistry 28: 00–00, 2003.

Substitution of $[Pt(terpy)H_2O]^{2+}$ and $[Pt(bpma)H_2O]^{2+}$ with thiols in acidic aqueous solution (terpy = 2,2′:6′2″-terpyridine); (bpma = bis(2-pyridylmethyl)amine)

Deogratius Jaganyi* and Felicia Tiba
School of Chemical and Physical Sciences, University of Natal, Private Bag X01, Scottsville, Pietermaritzburg 3201, South Africa

Received 07 February 2003; accepted 03 March 2003

Abstract

The substitution behaviour of $[Pt(terpy)H_2O]^{2+}$ and $[Pt(bpma)H_2O]^{2+}$, where terpy is 2,2′:6′2″-terpyridine and bpma is bis(2-pyridylmethyl)amine, was studied as a function of entering thiol concentration and temperature. The reactions between the Pt-complexes and DL-penicillamine, L-cysteine and glutathione were carried out in a 0.10 mol dm^{-3} aqueous $HClO_4$ medium using stopped-flow and conventional u.v.–vis spectrophotometry. The observed pseudo-first-order rate constants for the substitutions are given by $k_{obs} = k_2[thiol] + k_{-2}$. The k_{-2} term represents the reverse solvolysis. This was found to be zero for Pt^{II}(terpy) which was the most reactive complex. The second-order rate constants, k_2, for the three thiols varied between 0.107 ± 0.001 and 0.517 ± 0.025 M^{-1} s^{-1} for Pt^{II}(bpma) and 10.7 ± 0.7–711.9 ± 18.3 M^{-1} s^{-1} for Pt^{II}(terpy), whereas glutathione was found to be the strongest nucleophile. An analysis of the activation parameters, $\Delta H^{\ddagger}$ and $\Delta S^{\ddagger}$, clearly shows that the substitution process is associative in nature.

Introduction

Platinum amine co-ordination has fascinated chemists for more than a century [1, 2]. Early research provided the basis for modern mechanistic inorganic chemistry [3], offering a better understanding with regards to ligand exchange and the kinetics for different ligands and different geometries. The wealth of data from these studies resulted in the development of the useful rule, the *trans*-effect. The serendipitous discovery by Rosenberg in the 1960s of the inhibition of cell division by Pt complexes [4], renewed interest in platinum research because of its biological and medical potential. Since then over 3000 cisplatin analogues have been tested [5] for biological activity, but with only 28 platinum compounds entering clinical trials [6] and most of these encountering difficulties. Other metal compounds [7] have also been tested *in vivo* but cisplatin, *cis*-$[PtCl_2(NH_3)_2]$, has shown by far the best results.

The cystostatic effect of cisplatin is generally accepted to be through co-ordination with DNA in the cell nucleus, the major adduct being an intrastrand cross-link between N7 atoms of two adjacent guanine(G) residues [8, 9]. Its reactions in other regions, *e.g.* serum proteins, causes undesired side effects. The most common side effects include kidney and gastro-intestinal toxicity. These can be attributed to the inhibition of enzymes through co-ordination of the metal platinum to sulfhydryl(thiol) groups in proteins [10, 11].

The high affinity of platinum compounds for sulfur atoms and the biological importance of some of these complexes has attracted much interest among chemists, biochemists, biologists and medical researchers. Questions such as 'why does cisplatin get to guanine-N7 with competing S-donor ligands available in the cell?' have been asked. The early papers focused on the negative phenomena resulting from the interactions between Pt-metal with sulfur-containing biomolecules. These include aspects such as resistance and toxicity in the antitumor treatment [12]. However, in search of an answer to the above question, sulfur-containing compounds are currently under investigation as 'protecting agents' to ameliorate the side effects of platinum therapy [13]. These include compounds such as glutathione, cysteine, penicillamine, *S*-2-(3-(aminopropyl)amino)ethylphosphorothioic acid, sodium diethyldithiocarbamate and WR-2721 which is already registered in a number of European countries [14]. The protective nature of these compounds is thought to involve prevention or reversal of Pt-S adducts in proteins. Recent work from the groups of Reedijk and Sadler involving Pt-amines with sulfur-containing ligands and nucleobases has shown that these compounds, including the protecting agents, may be involved in platinum cancer therapy as reaction intermediates when the Pt-complex is en route to form the ultimate Pt-GG chelate [15].

Kinetic studies on substitutions of $[Pt(dien)Cl]^+$, $[Pt(dien)(GSMe)]^+$, *cis*-$[Pt(Cl_2(NH_3)_2)]$ and *cis*-$[Pt(NH_3)_2(GSMe)_2]^{2+}$ with sulfur-bonding protective agents have

* Author for correspondence

Journal : TMCH MS Code : 3696 PIPS No. : 81240234 ☐ TYPESET ☑ DISK ☐ LE ☑ CP Dispatch : 3-6-2003 Pages : 6

been reported [16]. The general interest in the interaction of platinum complexes with nucleophilic sulfur compounds [17, 18], and the fact that the reactivity of square planar platinum(II) complexes has been shown to be tuneable using steric as well as electronic effects [19, 20], has prompted the current study. The objective was to investigate the substitutions of $[Pt(bpma)H_2O]^{2+}$ with sulfur donor ligands and to compare its reactivity with that of $[Pt(terpy)H_2O]^{2+}$.

The structures of $[Pt(bpma)H_2O]^{2+}$ and $[Pt(terpy)H_2O]^{2+}$, and the thiols used, are shown in Chart 1. The summary of acid dissociation constants for cysteine and penicillamine is given in the literature [17]. At pH = 1.0, where the kinetic parameters were determined, all nucleophiles were fully protonated. Therefore all the other reaction pathways were neglected since their contribution to the overall kinetics would be < 5%. The pH of 1 also ensured that the complexes were in the aqua form since their pK_a values have been reported to be 5.30 ± 0.03 for $[Pt(bpma)H_2O]^{2+}$ and 4.42 ± 0.05 for $[Pt(terpy)H_2O]^{2+}$ [19].

Experimental

Synthesis and solutions

The ligands 2,2':6'2"-terpyridine (terpy) and bis(2-pyridylmethyl)amine (pbma) were purchased from Aldrich. All other chemicals used were of the highest purity and were used as received. [Pt(bis(2-pyridylmethyl)amine)-OH]ClO_4 and [Pt(terpyridine)(OH_2)][BF_4]$_2$ were prepared according to literature procedures [19, 21]. Microanalyses and ^{1}H-n.m.r. spectra agreed well with the data already reported.

Deionized millipore H_2O (MODULAB H_2O purification system) was used throughout the experiments. Since the perchlorate ion is a non-coordinating ion to Pt-metal [22], complex solutions including glutathione, L-cysteine and DL-penicillamine (all from Aldrich) were prepared by dissolving known quantities in 0.1 M $HClO_4$ (Merck) shortly before use. This insured that the complex was in its aqua form and that its ionic strength was 0.1 M.

Instrumentation and measurements

The purity of the complexes was checked using n.m.r. spectroscopy (Bruker Avance DPX 300) and a Carlo Erba Elemental Analyser 1106. U.v.–vis spectra were recorded using 1.0 or 0.80 cm Tendum quartz Suprasil cells with a CARY 100 u.v.–vis spectrophotometer equipped with a cell compartment thermostated by a Varian Peltier temperature programmer: accuracy ± 0.05 °C. Kinetic measurements for fast reactions were monitored using an SX.18MV (Applied Photophysics) Stopped-flow spectrophotometer coupled to an on-line data analysis system. The temperature of the instrument was controlled to within ± 0.1 °C.

Kinetic measurements

The ligand substitutions were performed under pseudo-first order conditions with the concentration of the nucleophiles in at least a 10-fold excess over that of the metal complexes. The substitution kinetics for fast reactions were followed using an Applied Photophysics SX.18MV Stopped-flow ASVD instrument. The wavelengths at which the measurements were performed were predetermined spectrophotometrically by recording the spectral change of the complex and ligand solutions over the 200–500 nm range. The wavelengths used in case of $[Pt(terpy)(H_2O)]^{2+}$ were 340, 341 and 240 nm with respect to DL-penicillamine, L-cysteine and glutathione. The reaction between $[Pt(bpma)(H_2O)]^{2+}$ and glutathione was followed at 240 nm. Slow reactions involving $[Pt(bpma)H_2O]^{2+}$ with L-cysteine and DL-penicillamine were monitored spectrophotometrically at 300 and 266 nm respectively using a CARY 100 UV/Vis spectrophotometer. All reactions were followed for at least six half-lives.

For all the reactions, the spectra had well defined isosbestic points, from that of the starting aqua complexes $[Pt(terpy)(H_2O)]^{2+}$ or $[Pt(bpma)(H_2O)]^{2+}$, to that of the substituted products $[Pt(terpy)(SR)]^+$ or $[Pt(bpma)(SR)]^+$. A representative spectrum is shown as Figure 1. This clearly indicates that the reactions that were investigated involved the displacement of the water molecule by the thiol.

Pseudo-first order rate constants, k_{obs}, were calculated from the single-exponential kinetic traces, by on-line non-linear least-square fit [23] of experimental data:

$$A_t = A_\infty + (A_o - A_\infty)\exp(-k_{obs}t) \qquad (1)$$

where A_o, A_t and A_∞ represent absorbance of the reaction mixture initially, at time t and at the end of the

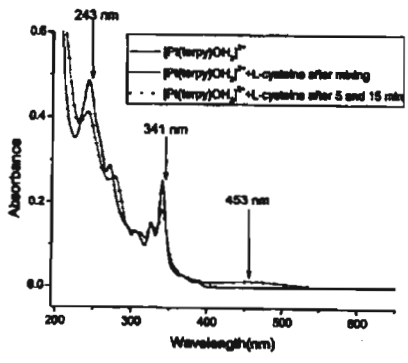

Fig. 1. U.v.–vis scans for the reaction between $[Pt(terpy)OH_2]^{2+}$ and L-cysteine recorded before mixing, after mixing and 5 min after mixing.

reaction respectively. The activation parameters $\Delta H^{\ddagger}$ and $\Delta S^{\ddagger}$ were determined from temperature studies of k_{obs} over the 20–40 °C range.

Results and discussion

The kinetic traces for the substitutions of the co-ordinated H_2O by thiols in aqueous media followed single exponentials, suggesting that the substitutions are first-order in both the thiols and platinum(II) complexes. The analysis of the kinetic data shows that the pseudo-first order rate constants, k_{obs}, obtained from an average of six kinetic runs for the fast reactions and four for the slow reactions, are linearly dependent upon thiol concentration, according to the two-term rate law:

$$k_{obs} = k_2[\text{thiol}] + k_{-2} \qquad (2)$$

which is usual for nucleophilic substitution at planar d^8 metal complexes [24], where k_2 denotes a second-order rate constant. Linear plots with non-zero intercepts were obtained by plotting k_{obs} values of $[Pt(terpy)H_2O]^{2+}$ *versus* the thiol concentrations (Figure 2). Plots involving k_{obs} of $[Pt(bpma)H_2O]^{2+}$ showed small but noticeable intercepts; an indication that $k_{-2} \approx 0$. This means

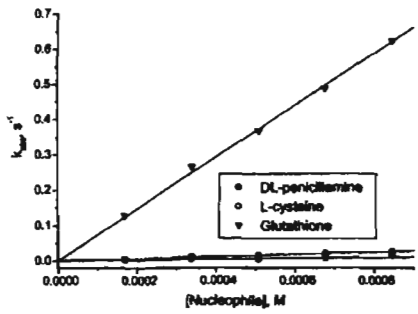

Fig. 2. Dependence of k_{obs} on the concentration of incoming thiol at 25 °C: $[Pt^{II}(terpy)H_2O] = 4.96 \times 10^{-5}$ M; pH 1.0 ($HClO_4$).

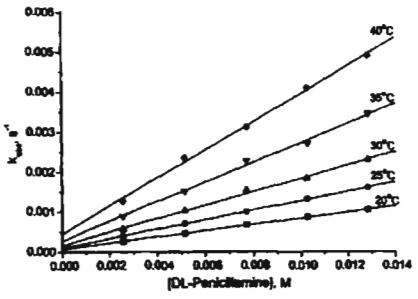

Fig. 3. Plots of observed pseudo-first order rate constants k_{obs} *versus* [DL-penicillamine] for the reaction between $[Pt^{II}(bpma)H_2O]$ and DL-penicillamine at different temperatures; experimental conditions: $[Pt^{II}] = 4.94 \times 10^{-5}$ M, pH 1.0 ($HClO_4$).

that the back reaction for these reactions is negligible, implying that substitution of the attached thiol by a water molecule is not effective. Representative plots of $[Pt(pbma)H_2O]^{2+}$ are shown in Figure 3. The values of k_2, obtained by least-square analysis, are summarized in Table 1 along with the associated activation parameters, $\Delta H^{\ddagger}$ and $\Delta S^{\ddagger}$, which were calculated from the temperature dependence of the rate constants. Additional information relating to the pseudo-first order plots including temperature dependence graphs are given in Figures 4 and 5.

The study has managed to compare the reactivity of the two platinum(II) complexes. The comparison is seen clearly from Table 1, in which the corresponding reactivity of $[Pt(bpma)H_2O]^{2+}$ is compared with that of Pt(terpy); the latter complex reacts 10^2–10^3 faster with the same thiols. The difference in the rate of substitution is a reflection of the individual complex structures. The major reason for the enhanced reactivity of $[Pt(terpy)H_2O]^{2+}$ can be attributed to extensive conjugation of the aromatic system around the metal [19]. Hence, the flow of electron density away from the d_{xz} metal orbital into the aromatic antibonding π^* orbitals due to the π-back donation is more widely spread in the case of $[Pt(terpy)H_2O]^{2+}$ than in $[Pt(bpma)H_2O]^{2+}$. This increases the electrophilicity of the metal centre by making

Table 1. Rate constants and activation parameters for substitution reactions of $[Pt(terp)H_2O]^{2+}$ and $[Pt(bpma)H_2O]^{2+}$ with thiols at pH 1.0 ($HClO_4$)

Complex + Thiol	k_2^{298} ($M^{-1}s^{-1}$)	k_{-2}^{298} (s^{-1})	$\Delta H_2^{\ddagger}$ (kJ mol^{-1})	$\Delta S_2^{\ddagger}$ (JK^{-1} mol^{-1})	K (M)
$[Pt(terpy)H_2O]^{2+}$					
DL-Penicillamine	10.7 ± 0.7		42.3 ± 2.3	−83.1 ± 7.7	
L-Cysteine	29.7 ± 0.2		23.7 ± 0.9	−143.2 ± 3.0	
L-Glutathione	711.9 ± 18.3		17.5 ± 0.8	−131.9 ± 2.6	
$[Pt(bpma)H_2O]^{2+}$					
DL-Penicillamine	$(1.07 \pm 0.01) \times 10^{-1}$	$(9.88 \pm 1.25) \times 10^{-5}$	52.8 ± 1.6	−85.9 ± 5.2	1083
L-Cysteine	$(1.25 \pm 0.03) \times 10^{-1}$	$(4.17 \pm 0.39) \times 10^{-4}$	43.8 ± 1.2	−115.1 ± 4.0	300
L-Glutathione	$(5.17 \pm 0.25) \times 10^{-1}$	$(4.15 \pm 0.21) \times 10^{-4}$	30.6 ± 2.5	−140.8 ± 8.3	1246

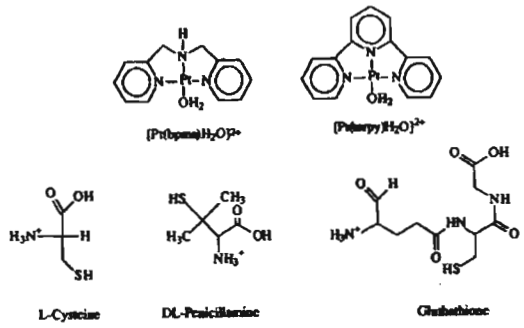

Fig. 4. Plots of pseudo-first order rate constants, k_{obs} *versus* [thiol] for reactions between $[Pt^{II}(bpma)H_2O]$ and (a) glutathione and (b) L-cysteine at different temperatures. Experimental conditions: $[Pt^{II}] = 4.94 \times 10^{-5}$ M, pH 1.0 ($HClO_4$).

it more positive, resulting in easier attack by the incoming nucleophile. In addition, $[Pt(terpy)H_2O]^{2+}$ is likely to stabilize the trigonal–bipyramidal transition state much better than $[Pt(bpma)H_2O]^{2+}$, through the delocalization of the negative charge facilitating new bond formation. The high lability of the metal-terpy system has also been reported in $[Pd(terpy)Cl]^+$ [25] and $[Pt(terpy)Cl]^+$ [26, 27]. The effect is similar to that of $[Pt(terpy)H_2O]^{2+}$ and has been described as being due to the electronic communication between the aromatic system and the metal d_{xz} orbital.

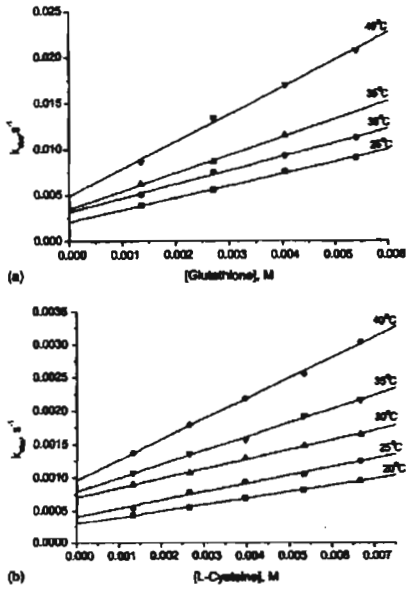

Fig. 5. Eyring plots used to determine the activation parameters for (a) $[Pt^{II}(terpy)H_2O]$ and (b) $[Pt^{II}(bpma)H_2O]$ with the named thiols.

Comparison between $[Pt(terpy)H_2O]^{2+}$ and $[Pt(bpma)H_2O]^{2+}$ with $[Pd(terpy)H_2O]^{2+}$ and $[Pd(bpma)H_2O]^{2+}$ shows that in changing the spectator ligand from (bpma) to (terpy), the reactivity increased by a factor of 10^2–10^3 for platinum(II) metal but only by a factor of 5–8 for palladium(II) metal when the same nucleophiles are used [17]. This difference in reactivity points to the fact that the aromatic terpy ligand increases the lability of the platinum(II) metal more than palladium(II) metal. This is because of the fact that platinum metal is a softer centre than the palladium metal and, as a result, it is more sensitive to the electronic communication between the metal and the co-planar aromatic conjugation system.

The second order rate constants, k_2, for $[Pt(terpy)H_2O]^{2+}$ listed in Table 1 are similar to ones reported by Bugarčić [18]. Looking at the two complexes investigated, the order of reactivity of the thiols is also the same, glutathione being the most reactive while DL-penicillamine is the least. This trend can be accounted for in terms of anchimeric and steric effects. Based on the structures of the nucleophiles one would expect glutathione to be the least reactive because of its bulkiness, however its unexpected reactivity points to the existence of an anchimeric effect. This feature probably arises from hydrogen bonding between the incoming thiol and the leaving water molecule during the transition state, with a net reduction in the activation energy of substitution. This neighbouring group participation has been observed by other researchers [27, 28] and is a phenomenon well known in organic reactions [29]. The lower reactivity of DL-penicillamine can be linked to the presence of the two methyl groups attached to the α-carbon centre causing steric hindrance.

The stability constants ($K = k_2/k_{-2}$) for the Pt(bpma) complex listed in Table 1 indicate that the thiol products are very stable. The large and negative values of $\Delta S^{\ddagger}$ for

the forward reactions support the operation of an associative substitution mechanism.

In conclusion, the results of this study demonstrate that sulfur-containing biomolecules have a high affinity for platinum(II) complexes. The reactivity of the complexes depends on the extent of π-conjugation of the spectator and on the size, bulk and solvation of the entering nucleophile. Since the reactions were carried out at pH 1, it would be interesting to expand the study to a wider pH including one closer to the physiological value.

Acknowledgements

The authors gratefully acknowledge financial support from the University of Natal and the South African National Research Foundation. We are also grateful to the Alexander von Humboldt Foundation for the donation of the u.v.–vis spectrophotometer.

References

1. F.A. Cotton, G. Wilkinson, C.A. Murillo and M. Bochmann, *Advanced Inorganic Chemistry*, 6th edit., Wiley, New York, 1999, p. 1075.
2. F.R. Hartley, *The Chemistry of Platinum and Palladium*, Applied Science Publishers, Essex, 1973.
3. F. Basolo and R.G. Pearson, *Mechanisms of Inorganic Reactions*, Wiley, New York, 1967, p. 351; M. Tobe and J. Burgess, *Inorganic Reaction Mechanisms*, Longman, New York, 1999, p. 70; F. Basolo, J. Chatt, H.B. Gray, R.G. Pearson and L.B. Shaw, *J. Chem. Soc.*, 2207 (1961); J.D. Atwood, *Inorganic and Organometallic Reaction Mechanisms*, 2nd edit., Wiley-VCH, New York, 1997, p. 43; M.C. Lim and R.B. Martin, *J. Inorg. Nucl. Chem.*, 38, 1911 (1976).
4. B. Rosenberg, L. Van Camp and T. Krigas, *Nature*, 205, 698 (1965).
5. R.B. Weiss and M.C. Christian, *Drugs*, 46, 360 (1993).
6. D. Lebwohl and R. Canetta, *Eur. J. Cancer*, 34, 1522 (1998).
7. B.K. Keppler, *New J. Chem.*, 14, 389 (1990); B.K. Keppler (ed.); I. Haiduc and C. Silvestru, *Coord. Chem. Rev.*, 99, 253 (1990); I. Haiduc and C. Silvestru, *Coord. Chem. Rev.*, 99, 253 (1990); P. Köpf-Maier and H. Köpf, *Chem. Rev.*, 87, 1137 (1987).
8. D.B. Zamble and S.J. Lippard, *Trends Biochem. Sci.*, 20, 435 (1995).
9. J. Reedijk, *Chem. Commun.*, 801 (1996).
10. B.J. Corden, *Inorg. Chim. Acta*, 137, 125 (1987).
11. R.F. Borch and M.E. Pleasants, *Proc. Natl. Acad. Sci. USA*, 76, 6611 (1979).
12. R.B. Martin, in B. Lippert (ed.), *Cisplatin Chemistry and Biochemistry of Leading Anticancer Drugs*, Wiley-VCH, Zürich, 1999, p. 183; J. Reedijk, *Chem. Rev.*, 99, 2499 (1999); E.R. Jamieson and S.J. Lippard, *Chem. Rev.*, 99, 2467 (1999); E.L.M. Lempers and J. Reedijk, *Adv. Inorg. Chem.*, 37, 175 (1991).
13. J.M. Yuhas and F. Calo, *Cancer Treat. Rep.*, 64, 57 (1980); S.B. Howell and R. Taetle, *Cancer Treat. Rep.*, 64, 611 (1980).
14. A.E.C. Korst, C.M. Eekink, J.B. Vermorken and W.J.F. van der Vijgh, *Eur. J. Cancer*, 33, 1425 (1997).
15. S.S.G.E. van Boom and J. Reedijk, *J. Chem. Soc., Chem. Commun.*, 1397 (1993); K.J. Barnham, Z. Guo and P.J. Sadler, *J. Chem. Soc., Dalton Trans.*, 2867 (1996); J.M. Teuben, S.S.G.E. van Boom and J. Reedijk, *J. Chem. Soc., Dalton Trans.*, 3979 (1997); Y. Chen, Z. Guo, P. del S. Murdoch, E. Zang and P.J. Sadler, *J. Chem. Soc., Dalton Trans.*, 1503 (1998).
16. J.M. Teuben, M.R. i Zabri and J. Reedijk, *J. Chem. Soc., Dalton Trans.*, 369 (2000); K. Lemma, S.K.C. Elmroth and L.I. Elding, *J. Chem. Soc., Dalton Trans.*, 1281 (2002).
17. Ž.D. Bugarčić, G. Liehr and R. van Eldik, *J. Chem. Soc., Dalton Trans.*, 951 (2002).
18. Ž.D. Bugarčić, G. Liehr and R. van Eldik, *J. Chem. Soc., Dalton Trans.*, 2825 (2002).
19. D. Jaganyi, A. Hofmann and R. van Eldik, *Angew. Chem., Int. Ed.*, 40, 1680 (2001).
20. R. Romeo, M.R. Plutino, M Scolaro, S. Stoccro and G. Minghetti, *Inorg. Chem.*, 39, 4749 (2000); M.R. Plutino, L.M. Scolaro, R. Romeo and A. Grassi, *Inorg. Chem.*, 39, 2712 (2000).
21. G. Annibale, P. Bergamini, V. Bertolasi, M. Cattabriga, A. Lazzaro, A. Marchi and G. Vertuani, *J. Chem. Soc., Dalton Trans.*, 3877 (1999).
22. T.G. Appleton, J.R. Hall, S.F. Ralph and C.S.M. Thompson, *Inorg. Chem.*, 23, 3521 (1984).
23. Applied Photophysics SX.18MV, Sequential Stopped-Flow ASVD Spectrofluorimeter, Software Manual. Applied Photophysics Ltd., Kingston Road, Leatherhead, UK; Kinetic traces from the repetitive scans was analysed using Origin50 version 5.0 a data analysis and technical graphics software.
24. M.L. Tobe, *Comprehensive Coordination Chemistry*, Pergamon Press, 1987. Vol. 1, chap 7. p. 313.
25. M. Cusumano, G. Guglielmo and V. Ricevuto, *Inorg. Chim. Acta*, 27, 197 (1978).
26. B. Pitteri, G. Marangoni, F.V. Visentin, L. Cattalini and T. Bobbo, *Polyhedron*, 17, 475 (1998); B.V. Petrović, M.I. Djuran and Ž.D. Bugarčić, *Met.-Based Drugs*, 6, 355 (1999).
27. G. Annibale, M. Brandolisio, Ž.D. Bugarčić and L. Cattalini, *Trans. Met. Chem.*, 23, 715 (1998).
28. Ž.D. Bugarčić, D. Ilic and M.I. Djuran, *Austr. J. Chem.*, 54, 237 (2001); T. Shi and L.I. Elding, *Inorg. Chem.*, 35, 735 (1996); T. Shi and L.I. Elding, *Inorg. Chem.*, 36, 528 (1997); Ž.D. Bugarčić and B.V. Djordjević, *Monatsh. Chem.*, 129, 1267 (1998).
29. R.G. Wilkins, *Kinetics and Mechanism of Reactions of Transition Metal Complexes*, 2nd edit., Verlag, Berlin, 1991, p. 300.

TMCH 5605